A TECHNIQUE FOR SIMULTANEOUS DETERMINATION OF THERMAL CONDUCTIVITY & MOISTURE CONTENT OF GRANULAR MATERIALS

By

Kamlesh Gopal Gupta

A Thesis Submitted to the School of Graduate Studies

of the University of Ottawa in Partial Fulfillment

of the Requirements for the Degree of

Doctor of Philosophy

in

Mechanical Engineering

Ottawa, Canada

March, 1974

ACKNOWLEDGEMENT

I would like to express my deepest appreciation and gratitude to Dr. M.J. Laubitz and Dr. A. Feingold, for their guidance and continued encouragement throughout the course of this investigation. I am most grateful to Dr. Feingold for suggesting the topic, for his contribution in the preparation of this dissertation, as well as for doing his utmost in providing the continued financial assistance. I am also indebted to Dr. Laubitz for his enthusiastic support, many stimulating discussions, unlimited patience, and for authorizing the use of various instruments in the High Temperature Physics Section of the National Research Council of Canada.

Thanks are also due to Dr. C.M. Mitchell of the Department of Energy, Mines, and Resources; Dr. P.J. Williams of Carleton University; Mr. N.S. Verma of the University of Ottawa; and Dr. T.M. Dauphinee of the National Research Council of Canada, for their help and advice in certain phases of the work presented in this thesis. Thanks to Mrs. D. Champion-Demers for her expert typing of the thesis.

The financial support from the Department of Mechanical Engineering, University of Ottawa, and from the National Research Council of Canada, grant number SH9-COT, is gratefully acknowledged.

ABSTRACT

A technique has been developed for simultaneous determination of thermal conductivity and distribution of moisture content in a specimen of granular material. Also, the effect of the variation of moisture content on thermal conductivity of the specimen has been studied. A distinct feature of this technique is that moisture distribution is determined nondestructively, thus, allowing the use of a single specimen for a whole set of experiments at various moisture contents. This eliminates the otherwise inevitable variation in the intrinsic conductivity of specimens. In particular, it allows the study of the effect of the variation of moisture content on thermal conductivity of a particular specimen at low overall moisture contents, which otherwise would not be possible.

Local values of the thermal conductivity along the thickness of the specimen of 20-30 Ottawa sand have been obtained, rather than a single value of the overall thermal conductivity. The variation of the overall moisture content in the specimen has been obtained by measuring the local values of the moisture content along the thickness of the specimen. An analysis has been developed to evaluate the distribution of moisture under isothermal conditions of the specimen, and it is shown how this analysis could be employed to evaluate the local values of the moisture contents under gradient conditions, that is, the test conditions. The knowledge of conductivity and moisture content at several locations in the specimen on

a one-to-one basis at different mean temperatures and different overall moisture contents of the specimen, enabled us to produce a general correlation of conductivity with moisture and temperature of the granular material.

An attempt has been made to develop a theoretical expression to predict the conductivity of moist sand. The evaluation of conductivities using transient heat conduction method has also been attempted. Conductivity values obtained by these two methods, as well as those resulting from previously published theories of other authors have been compared with our own steady-state results.

TABLE OF CONTENTS

LIST OF FIGURES

LIST OF TABLES

NOMENCLATURE

A	area of cross-section [m^2]
B	a parameter [page 24]
C	a parameter [page 24]
c	specific heat [mW-sec/g-K]
CD	a parameter [page 33]
d	distance [m]
H	moisture content by volume
I	current [A]
L	latent heat [W-h/g]
ℓ	length
M	moisture content by weight
M(x)	local moisture content
<M>	overall moisture content
P	porosity
p	pressure [kg/m^2]
Q	amount of heat
q	rate of heat flow [mW]
R	resistance [Ω]
r	potentiometer reading
r	radius
T	temperature [deg. C]
t	time [sec]
V	volume [cm^3]
V	voltage [V]
W	weight [g]
w	uncertainty

Greek symbols:

α	diffusivity [m^2/sec]
γ	Euler's constant
δ	error
δT	temperature difference
ΔT	temperature difference

ΔV	voltage difference
Δx	thickness
ϵ	small difference
λ	coefficient of thermal conductivity [mW/m-K]
μ	coefficient of diffusion [m^2/h]
ρ	density [g/cm^3]
τ	time

Subscripts:

a	air
cal	calibrated value
f	fluid
i	initial
o	isothermal condition
p	porous
q	gradient conditions
s	solid
sat	saturated
w	water
x	unknown
1	upper part of the specimen
2	lower part of the specimen

Chapter I

INTRODUCTION

Thermal conductivity is an important property of materials, whether homogeneous or consisting of well-defined mixtures. Knowledge of thermal conductivity is useful not only to the workers in the field of basic sciences, but also, and perhaps primarily, to those in applied sciences. It is the needs of the latter that led among other things to the research into the thermal conductivity of granular materials. Among engineering endeavors which would benefit from a reliable method of evaluating this property are: (a) design of foundations for buildings, highways, tunnels, towers, canals, dams, refrigerated spaces, etc., (b) determination of heat transfer from underground steam, water, or oil pipes, electrical cables, etc., (c) construction of earth reservoirs for storage of industrial fluids, (d) development of granular or porous insulating materials, (e) reduction of viscosity of heavy oils by underground heating to enhance their flow towards oil wells.

The study of heat transmission in granular materials has attracted the attention of scientists from the very beginning of this century, since the realisation of the importance of these materials in

the development of various branches of applied science, such as soil science, mechanical engineering, chemical engineering, and building materials science. Many attempts have since been made to obtain formulae that express thermal conductivity in terms of various parameters, namely, volume fraction, size, and conductivities of the constituent phases.

Several formulae have been proposed for two-phase granular materials consisting of a solid and a gaseous (or a liquid) phase. The following list without claiming completeness may serve as a representative sample: Lord Rayleigh (1892) for a cubical array of uniform spheres, Maxwell (1904) for a random distribution of solid spheres in a continuous medium, Burgers (1919) for a cubical arrangement of arbitrary ellipsoids, Russell (1935) for a cubical array of cubes, De Vries (1952a) for soil, Woodside and Cliffe (1959) for a cubical array of spheres, Laubitz (1959) for powders, Brailsford and Major (1964) for a random distribution of solid spheres which are far enough apart so as not to interact mutually, Cheng and Vachon (1969a) for powders. These formulae have been tested against experimental data for certain particular cases and have been accepted as being able to predict thermal conductivity with a reasonable degree of accuracy.

Theoretical investigation of thermal conductivity of multiphase media is complex and has been attempted in a few simple cases

only. Brailsford and Major (1964) extended their model for the two-phase media to determine the conductivity of a system of three or more phases. Cheng and Vachon (1969b) also extended their two-phase model to a three-phase one.

The above formulae are applicable in cases when the interstices between the solid grains are either occupied by a gaseous phase or completely filled by a liquid phase. They are not to be used for materials partially filled by liquid (unsaturated granular materials).

Theoretical investigation of thermal conductivity of unsaturated granular material is complicated, because of the changes in the heat-flow mechanism in it. Heat in presence of moisture is transferred not only by simple conduction, convection, and radiation, but also by two other means: latent heat is transferred by diffusion of water vapor and sensible heat is transferred by movement of liquid water in the interstices between the grains of the solid phase. Formulation of thermal conductivity of moist granular material was attempted by Gemant (1950), De Vries (1952b), Krischer and Esdorn (1956), Joy (1957), Woodside and Cliffe (1959), etc.

The understanding of the moisture-flow mechanism in moist granular materials under temperature gradient is a prerequisite for the understanding of heat-flow mechanism in such a case. Various hypotheses have been proposed in the past in an effort to create a simplified model representing the flow of the moisture. These hypotheses are

discussed under a separate heading in Appendix G. Based on these moisture-flow mechanisms, attempts have also been made to evaluate the contribution of moisture to the overall heat transfer processes (Appendix H).

Despite the growing need for accurate thermal conductivity determination and better understanding of the heat and moisture-flow mechanisms in granular materials, nothing conclusive has unfortunately been proposed so far. There is, as yet, no general agreement regarding the most appropriate method to determine accurately the thermal conductivity of moist granular materials, nor is there any reliable theory to predict the same.

It is for these reasons, that this project was undertaken with the idea of proposing a new experimental technique for simultaneous determination of thermal conductivity and moisture content of granular materials, and with a hope of suggesting a way to correlate thermal conductivity with moisture and temperature.

But what is so unique about simultaneous determination? The answer to this question is, that despite its advantages, it was never attempted before. What was done in such cases before is that on completion of thermal conductivity tests, moisture contents were determined by removal of discrete samples at various space intervals across the thickness of the specimens, and by consequent drying of these samples until they reach a constant weight. A new specimen had

to be prepared for each test. Differences thus obtained in different tests for various moisture contents and temperatures could conceivably be at least partly due to intrinsic differences between the specimens. In other words, even if the moisture and temperature conditions were kept unchanged, differences could be expected in the outcome of the tests, since no one material can be said to be truly reproducible; indeed each sample may be said to have its own unique thermal conductivity. These inherent differences are usually small for homogeneous materials, but in granular materials not completely saturated with moisture, these could be surprisingly large.

The chief virtue of the proposed method of simultaneous determination lies in the fact that, unlike in other methods (e.g. Woodside and Cliffe, 1959), the moisture distribution is determined nondestructively, thus, allowing the use of a single specimen for a whole set of experiments at various moisture contents and temperatures. This, by eliminating the otherwise inherent variation in the intrinsic conductivity of the specimen, could greatly improve the precision with which one can determine the effect of the variation of moisture content and temperature on the thermal conductivity of a particular specimen.

The possibility of the water freezing being of vital importance in the case of moist materials used at relatively low temperatures, the experiments were performed throughout a temperature interval striding the freezing point. A range from -15 to 20 deg. C was chosen.

The overall moisture content was varied in various experiments from zero to five per cent by weight.

A steady state method is said to be unsuitable for determining the thermal conductivity of moist granular materials (Joy, 1957; Pratt, 1969; etc.). The moisture starts redistributing itself as soon as the specimen is subjected to a temperature gradient. It is transferred in the direction from hot to cold by a process of vapor diffusion, setting up a moisture gradient in the opposite direction. Because of this gradient, the liquid starts moving from the colder side towards the warmer. Under steady state conditions, a dynamic equilibrium is thought to establish itself between these two opposing processes, and a new moisture distribution takes place in the material (Bouyoucos, 1915; Taylor and Cavazza, 1954; Philip and De Vries, 1957). The thermal conductivity of a specimen measured under such a condition is some sort of an average value for a non-uniform moisture distribution. This value is quite different from the value of thermal conductivity which would be obtained with a uniform average distribution of moisture in the specimen. The reduction in the applied temperature gradient would reduce this problem substantially, but there is a limit to this because too small a gradient would be detrimental to the accuracy of all experimental results.

A transient heat flow method, which requires considerably shorter test-time -- of the order of only a few minutes as compared to several hours needed in a steady state method, produces only a small temperature rise. The redistribution of moisture in such a case is much less significant than in a steady state method. But the problem with a transient heat flow method is that it does not give a very accurate value of thermal conductivity.

In short, the steady state method gives some sort of an average value of thermal conductivity because of a considerable degree of redistribution of moistere. And a transient method, though not completely immune to this problem, gives a better value of thermal conductivity as far as moisture is concerned, but the method itself is not considered very reliable as far as the overall accuracy is considered. A solution to this dilemma is suggested in the proposed technique which resorts to a steady state method for accuracy of measurement and measures local thermal conductivity and moisture content at several different places along the thickness of the specimen in order to eliminate the problem of *some sort of an average value of thermal conductivity*. Several values of thermal conductivity corresponding to different local moisture contents, rather than just one value of the overall conductivity, are thus obtained. This enables us to observe the variation of thermal conductivity with moisture within a single specimen.

The thermal conductivity, in this proposed procedure, was measured by the standard guarded hot-plate technique, according to the ASTM specifications (1963) with such modifications as are further described in Chapter II, Section 3.

The distribution of the moisture content of the specimen was obtained from the measurements of the self-heating response of copper wires embedded in it (Chapter II, Section 4). This response, the temperature-rise versus time curve, was found to be quite sensitive to the amount of moisture surrounding the wire. One of the parameters describing this response was chosen as a scale to indicate the amount of moisture present around the wire. This particular parameter was first calibrated at each temperature and moisture content under isothermal conditions, and was then used to measure the moisture under temperature gradient conditions, that is, test conditions.

Going back to the transient method, the self-heating response of an electric-current carrying wire can, under ideal conditions, be analytically correlated with the conductivity of the specimen (Appendix F). Doubts exist as to the applicability of this procedure in our specific experimental situation, mainly due to the possible but unknown influence that such functions as moisture migration under test or contact resistance, have on the response of the wires. However, an attempt has been made to evaluate the conductivity in this manner and the results have been compared with those obtained

using the steady state method. The comparison, in fact, was not good. For reasons just stated, it is believed that the steady state results correspond more nearly to the reality.

An attempt has also been made to develop a new model to predict the thermal conductivity of our moist granular material. This has been compared with our experimental results.

Now a few words about the style of presentation of the work. For a better readability of the presentation, the whole of it is divided into two main parts. The first part contains an explanation of the methodology, a brief description of the actual operation and of the specimen material, and a summary, analysis and discussion of results. The second part, presented in form of appendices, besides dealing with more cumbersome details related to the topics dealt with in the first part, includes also other relevant material such as a simplified model, a discussion of the transient method of conductivity determination, a description of moisture and heat flow mechanisms, etc.

It should perhaps be mentioned that a report on the early progress of this investigation has been presented at the XII International Conference on Thermal Conductivity held in Birmingham, Alabama in September of 1972.

Chapter II

DESCRIPTION OF THE METHOD

1. GENERAL

Determination of the thermal conductivity of any homogeneous material by means of a steady state method requires a sample of the material to be subjected to a temperature gradient. In one variant of this method, a measurable amount of heat is made to flow unidirectionally through the specimen of known dimensions, and the resulting temperature difference across the specimen is measured when the system has attained the state of a steady heat flow. The thermal conductivity of the specimen is then calculated from the well-known steady-state one-dimensional Fourier's heat conduction equation.

Macroscopically, a moist granular material could be considered to be homogeneous, as long as the moisture is uniformly distributed in it. This, however, is not generally the case, and, what is more, the moisture redistributes itself when the material is subjected to a temperature gradient in the process of the determination of the conductivity of that material. The conductivity, measured as described

above, would provide some kind of an average value for the particular moist material and for the particular distribution of the moisture which prevailed during the experiment.

The thermal conductivity of granular materials is known to increase with their moisture content. However, the rate of increase of conductivity with moisture is larger at low moisture contents than at high moisture contents. In a material with a certain initial moisture distribution, the hotter region loses moisture to the colder one, when the material is subjected to a temperature gradient, although the total moisture content does not change. The thermal conductivity of the hotter region decreases, however, by an amount greater than the increase in conductivity of the colder region. Thus, the overall conductivity of the material, which is the quantity measured, is less than if the moisture were uniformly distributed. This effect is greater the more uneven the moisture distribution. And therefore, the measured overall conductivity of the material gives no direct indication of what are the local conductivity values corresponding to local moisture content in any given layer of the material.

In order, therefore, to evaluate correctly the dependence of thermal conductivity on moisture content of a granular material it was thought necessary to determine the exact variation of moisture content as well as that of conductivity in the specimen by obtaining several local values of the two along the thickness of the specimen.

The knowledge of conductivity and moisture content at several locations in the specimen on a one-to-one basis at different mean temperatures and different overall moisture contents of the specimen, enabled us to produce a general correlation of conductivity with moisture and temperature of the granular material.

2. SPECIMEN CONTAINER

The basic experimental equipment adapted here for this investigation is a standard research unit built by the Dynatech Corporation of Cambridge, Massachusetts. The operation of this unit is described in Appendix A.

The unit, in its original form, was designed to test solid or cellular materials, like building materials, plastics, rubbers, glasses, fibrous insulations, foams, etc., but not granular materials. The change from solid or cellular material to granular material to be tested in this unit not only necessitated use of a container to hold the granular material, but substantially changed the measurement technique involved. A watertight cell had to be constructed and equipped with provisions for injecting an accurately measured quantity of moisture into it. The implementation of the special feature of this project, namely the performance of the tests for measuring the moisture distribution and thermal conductivity of the specimen simultaneously and thus rendering the tests non-destructive, required some special features to be included in the design of the container. The modification of the unit thus amounted to a re-design of the entire test stack assembly.

The specimen test-section of the unit was replaced by a suitably designed watertight cell having built-in facilities for the measurement of temperature and moisture. The main factors that governed the design of the cell were:

(1) the adherance to the specifications laid down by the ASTM;

(2) the need to preserve the geometry of the granular specimen;

(3) the ability to vary the moisture content of the specimen;

(4) the necessity to maintain a chosen moisture content over repeated temperature cycles;

(5) the need to allow for a small volumetric change of the specimen under different thermal conditions;

(6) the importance of proper contact between the specimen and the temperature and moisture measuring sensors; and

(7) the fulfillment of the condition that the flow of heat through the central test-section of the specimen should be unidirectional.

The sketch of the cell is shown in Fig. 1. The available space in the Dynatech unit provided for a cylindrical specimen of 20.32 cm diameter and the specifications laid down by the ASTM(1963) allowed for a maximum thickness of about 3.4 cm for such a specimen. The outside radial wall of the cell was made of stainless steel and was attached to the bottom copper plate which forms an isothermal region in that place.

The granular sample was poured into the container to the height of 3.4 cm. The container was gently tapped from time to time to ensure compaction. The sample was then covered by the main and guard heater assembly. The 20.32 cm diameter specimen could be viewed as consisting of two portions. The central 10.16 cm diameter cylindrical portion

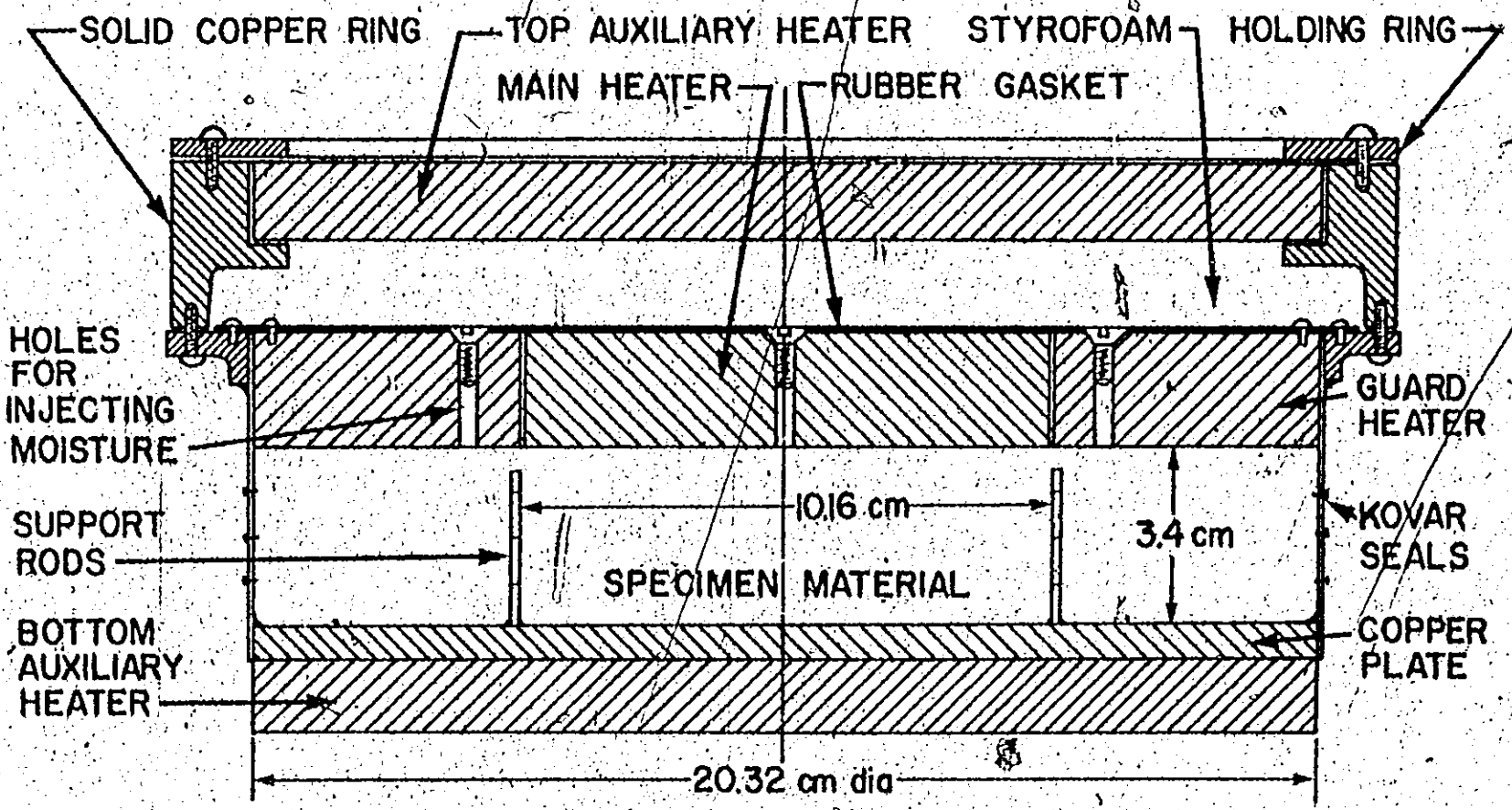

FIG. 1 DESIGN OF THE CELL

under the main heater forms the actual sample with respect to which the measurements were taken, and the surrounding remaining portion under the annular guard heater acts as a thermal guard ring.

To minimize the effect of relatively high conductance of the radial wall of the cell on the heat flow pattern in the guard ring, the top of the wall was connected by a solid coppper ring to another heater (— a top auxiliary heater). The function of this heater, besides supplying heat to the stainless steel wall, was to prevent the upward heat losses from the main heater. As the central section of the main and guard heater assembly was guarded by the top auxiliary heater and on the side by the guard heater and the stainless steel container, the heat generated in it flowed through the specimen establishing a temperature gradient along its path.

The circumferential space between the main heater and the container wall was sealed with a rubber gasket making the cell watertight. This rubber joint allows also for a slight freedom of movement of the main and guard heater assembly in the vertical direction. A few symmetrically placed holes in the main heater allowed the required amount of moisture to be injected through them, subsequent to which they were kept sealed.

It is useful to determine the local values of moisture content and temperature at as many locations as possible in the specimen along its thickness, for an accurate mapping of these distributions. The number of sensors to be used for the determination of these local values was

a compromise between the desire to obtain an accurate picture of these distributions, and the necessity of minimizing the disturbing effect that the sensors themselves have on these distributions. For a specimen as small as ours, three sensors seemed to represent a reasonable compromise.

Three annealed and varnished copper wires, 0.0254 cm in diameter (30 gauge), were stretched diametrically through the specimen at equal vertical spacings. These copper wires have sufficiently stable and reproducible resistance-temperature characteristics to be used as resistance thermometers in the temperature range from 20 to 320 K. These three copper wires were used, both for temperature and moisture measurement in the specimen at their respective levels. These wires pass through *Kovar* seals fixed in the wall. In order to reduce the sag of the wires, two supporting bakelite rods were provided on the perimeter of the main test-section of the specimen, as shown in Fig. 1. These rods are located just outside the heat-metering area to reduce the error resulting from any possible distortion of the heat flow pattern. On one hand these bakelite rods helped fix and maintain the distance between the copper wires; and on the other, they also provided support to the potential leads used for measuring the potential drop across the length of the wires within the main test-section. The potential leads were soldered to each of the three copper wires at the border of 10.16 cm main test-section, and were wound around the bakelite rods a few times before coming out of the cell through the Kovar seals.

3. MEASUREMENT OF THERMAL CONDUCTIVITY

3.1 FUNDAMENTALS:

In principle the thermal conductivity of the specimen was obtained using a steady-state one-dimensional Fourier's heat conduction equation

$$q = \lambda A \frac{\Delta T}{\Delta x}, \tag{1}$$

from which

$$\lambda = \frac{\Delta x}{A} \frac{q}{\Delta T} = \frac{\Delta x}{A} \frac{q}{T_H - T_L}, \tag{2}$$

where q is the net amount of heat flowing per unit time perpendicular to the cross-sectional area of the specimen, [mW],

λ is the coefficient of thermal conductivity, [mW/m-K],

A is the area of cross-section of the specimen, [m^2],

T_H and T_L are temperatures of any two isothermal planes in the specimen, $T_H > T_L$, [deg.C],

$\Delta T = T_H - T_L$, is the temperature difference between these two isothermal planes, and

Δx denotes the distance between them, [m].

The local values of the conductivity were obtained with the use of Eq.(2). The cross-sectional area was fixed by the dimensions of the specimen and the distances between the consecutive temperature sensing wires were fixed once for all by the separation of the copper wires embedded in the specimen. Their values are

$$A = 8.107\ (10^{-3})\ m^2, \tag{3}$$

$$\Delta x = 8.763\ (10^{-3})\ m. \tag{4}$$

The total heat, q, released by the main heater was made to flow through the sample, as explained in the previous section, establishing a temperature gradient across the specimen-thickness of the order of one to two degrees Kelvin per centimeter. The d.c. power input to the main heater was determined directly by the voltage and current measurements to an accuracy of at least four significant figures. The temperature differences, ΔT, were obtained from the temperature measurements of the consecutive sensors and were modified, before their use in Eq.(2), as explained in the next section.

For the temperature measurement, a current small enough to cause negligible self-heating (0.03 A) was passed through each of the three copper wires and the resistance of the 10.16 cm lengths of the wires inside the central test-section was accurately measured to six significant figures. The resistances of these wires in turn were used to calculate their respective absolute temperatures to five significant figures using the temperature-resistance relationship given in Dauphinee and Preston-Thomas (1954). This relationship is shown to be linear in the range from 80 to 340 K.

The copper-resistance technique has distinct advantages over the use of the thermocouples for temperature measurements. The copper wires give a radial average value of the temperature at their particular levels, as compared to the point temperatures obtained by thermocouples, which in granular materials may accidently vary somewhat even when measured at the same level. The use of the same sensors for temperature and

moisture content measurements not only minimizes disturbance in the specimen due to their very presence, but also gives the results that pertain to the identical sections of the specimen which may not be the case if separate sensors were used.

3.2 MODIFIED TEMPERATURE DIFFERENCE:

Despite taking all the precautions, necessary for a valid use of Eq.(2), there are generally some error-causing features present in the apparatus which prevent a straightforward use of Fourier heat conduction equation for calculating the thermal conductivity of the specimen to a sufficient degree of accuracy. The necessity of working in a temperature range away from room temperature and the lack of a perfect guard and perfect insulation give rise to heat sinks and sources in any multi-component experimental system. These undesirable heat sinks and sources make the heat flow pattern in the experimental test-section of the specimen two or three dimensional. The determination of temperature difference, ΔT, to be used in Eq.(2) for the conductivity calculation was virtually impossible under these conditions. Considerable ingenuity had to be exercised to simplify the problem so that some plausible analysis could yield accurate values of ΔT and therefore of λ.

In the first place the use of cylindrical symmetry had reduced the heat-flow pattern to two dimensions. As the most important step, we reduced the influence of the auxiliary heat sources and sinks in the following manner.

First, the temperature differences were measured with only incidental heat flowing through the specimen when no heat flowed from the main heater. These temperature differences will be denoted by ΔT_o, and the condition under which they were measured will be referred to as *Isothermal Condition*.

Then the temperature differences were measured when the specimen was subjected to both the still present incidental heat flow and the heat flow from the main heater. These temperature differences will be denoted by ΔT_q and the test condition will be referred to as *Gradient Condition*.

By the principle of superposition of heat flows, the effect of the incidental heat flow on the temperature difference in the specimen was eliminated by taking the difference of the above two measurements to give a correct ΔT. That is, the value of ΔT used in Eq.(2) is

$$\Delta T = \Delta T_q - \Delta T_o . \qquad (5)$$

This approach is virtually indispensible for accurate λ measurements (Laubitz and McElory, 1971). It depends on the principle of superposition of heat flows, which is valid if the temperature changes due to the specimen heater are small, so that the effect of temperature on the conductivities of all the components of the system can be ignored. In practice, this means that ΔT should not exceed 10 to 20 K, and of course the smaller it is the better, provided that the precision of the measurement itself is not a problem. In our case ΔT was less than

5 K, which was acceptable from both points of views.

Coming back to the discussion of ΔT_o, the relationship between ΔT_o and T was found to be almost linear. Straight lines, later referred to as *Base Lines* were fitted between the experimental points by the least square method (see Appendix D, Section 2).

By calculating the conductivity using a steady-state method one of course ignores any intrinsic variation of conductivity of a material within the narrow range of temperature drop between two neighboring measurement points. For tests on low conducting materials using the guarded hot plate method, this temperature drop is suggested to run between 20 to 30 K (Tye, 1968). In order to improve the accuracy of the variation of conductivity with temperature of our specimen, we reduced this temperature drop to about 1 to 2 K.

4. DETERMINATION OF MOISTURE DISTRIBUTION

4.1 PRINCIPLE:

The distribution of the moisture content of the specimen was obtained from the measurements of the effects of *self-heating* of copper wires embedded in it. The resistance of these wires is a direct function of their temperature (Dauphinee and Preston-Thomas, 1954); and their temperature in turn is a function of the properties of the surrounding medium (Carslaw and Jaeger, 1959). To obtain the moisture distribution of the specimen, a d.c. current was passed through each of the three wires and the change in voltage over their central portion, contained within the main test-section, was recorded as a function of time. This response was first calibrated at each temperature and overall moisture content under isothermal conditions, and was then used to measure the moisture distribution within the specimen under temperature gradient conditions. The whole process is explained below.

When an electric current is passed through a thin wire embedded in any material, the temperature of the wire and consequently of the surrounding material would rise as the time increases. The rate of rise of temperature is governed by the ability of the material to conduct heat away from the wire, which in case of granular material mixed with water depends not only upon the temperature of this material but also on its moisture content. This temperature rise is a function of the rise in resistance of the wire, as mentioned above, which in turn is

proportional to the change in voltage, ΔV, across the two measuring points on the wire. A typical self-heating curve, showing the variation of ΔV with time t, is drawn in Fig. 2. This curve, when plotted on ΔV — ℓnt coordinates was found to be representable by a straight line, as is done in Fig. 3. The equation of this line is

$$\Delta V = B\, \ell nt + C, \qquad (6)$$

where B and C are slope and intercept, respectively, of the line.

For readers' convenience, an analytical derivation of an equation of an ideal line heat source and its transformation into a form similar to one given in Eq.(6) is given in Appendix B. Also shown in the same appendix is the theoretical dependence of the parameters B and C on the properties of the surrounding medium.

The parameters B and C are constant for a particular self-heating curve. But their value varies with different curves taken under different surrounding conditions. These parameters were found to be quite sensitive to moisture content and temperature of the material surrounding the wire. Parameter C was found to vary consistently with temperature and moisture content of the surrounding material, and hence it was chosen to be used as a scale to indicate the amount of moisture present around the wire.

It now seems necessary to explain the meaning of the terms *Local Moisture Content*, $M(x)$, and *Overall Moisture Content*, $\langle M \rangle$, which will

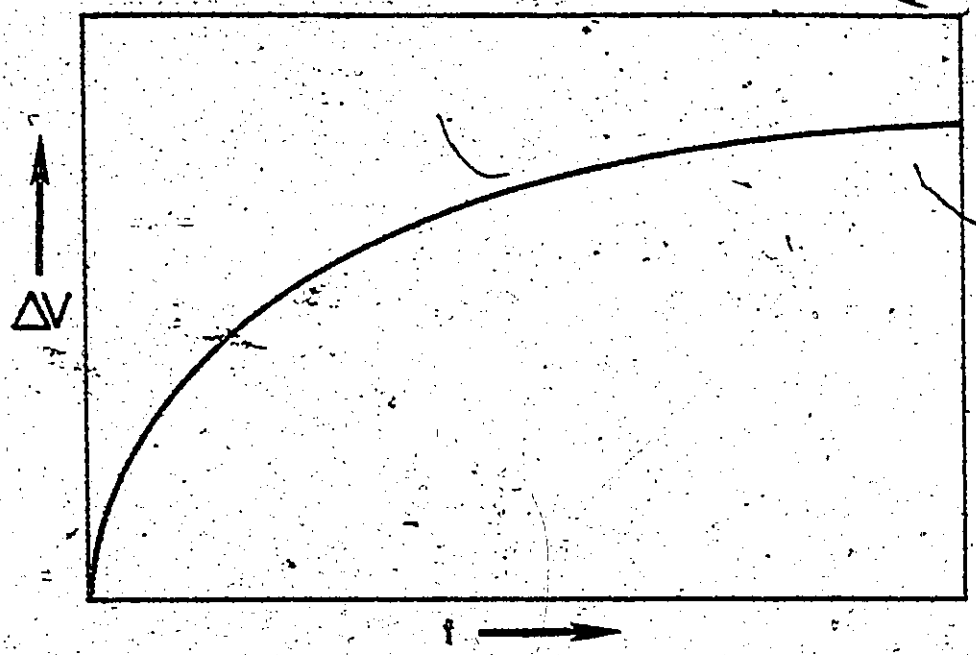

FIG. 2. SELF-HEATING RESPONSE ON ΔV-t COORDINATES.

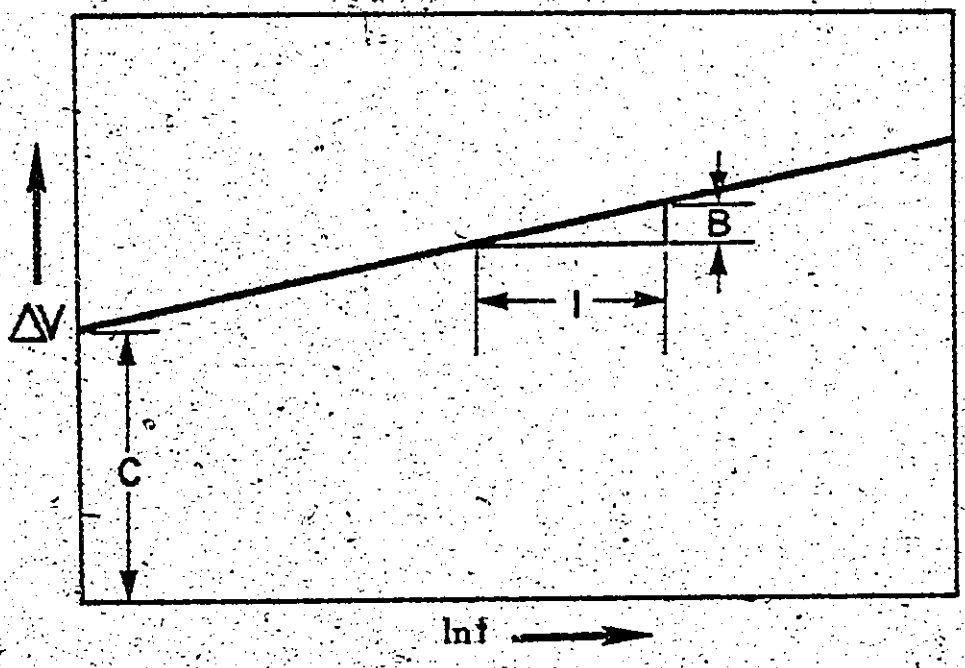

FIG. 3 SELF-HEATING RESPONSE ON ΔV-lnt COORDINATES

be used henceforth. The overall moisture content is the total amount of moisture present in the specimen expressed as a percentage of the total weight of granular material, whereas the local moisture content is the percentage of water in the material in the immediate vicinity of the wire. Figure 4 represents a cross-section of one of our wires with a ring of surrounding material deemed to influence the temperature rise in this wire due to a combined effect of the current flow and heat transfer. The diameter of the material mainly influencing the wire temperature can be considered so small that the moisture content variation within the ring between points A and B may be assumed to be linear. Thus, the expression *local moisture content* refers to the moisture content prevalent at the level of the center of the wire. (Of course, similar things may be said of the temperature of the material as well.)

A known percentage of moisture was injected into the specimen. The specimen was held under a moderately high and uniform temperature of about 40 deg. C for a duration long enough for the moisture in the specimen to distribute itself in a manner compatible with this temperature. In order to perform moisture calibration tests on the specimen, the specimen was brought down to a desired level of the isothermal temperature in the temperature range of our interest. A d.c. current of about 2 A, sufficient to cause a moderate self-heating of the copper wires, was passed through each of the three wires, and the change in voltage, ΔV, over their central 10.16 cm portion was recorded as a function of time,

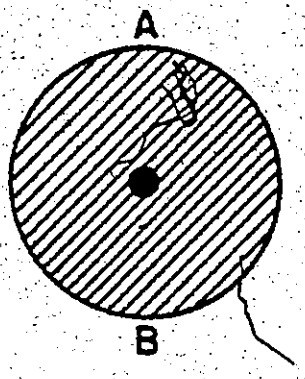

FIG. 4 CROSS-SECTION OF A WIRE WITH A RING OF SURROUNDING MATERIAL

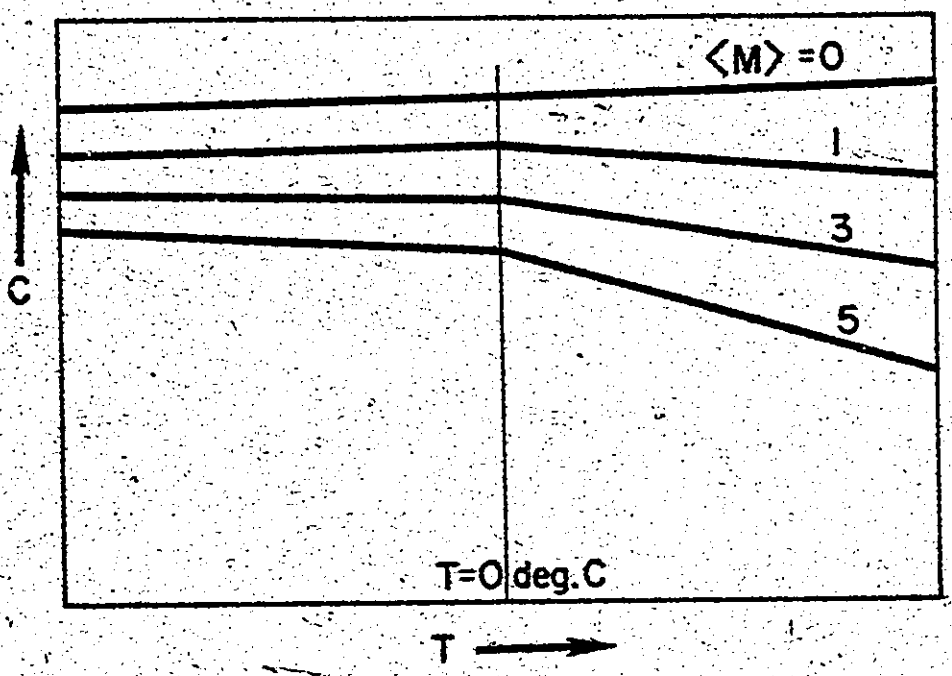

FIG. 5 SCHEMATIC DIAGRAM OF C VERSUS T & M

the shape of curves being of the form shown in Fig. 2. The values of the parameter C, described above, for the three copper wires, were obtained. Variation of C with temperature was obtained by varying the isothermal temperature of the specimen while the overall moisture content was held constant. Similar tests were performed for different known overall moisture contents. Thus, a whole set of values of C for each of the three copper wires was obtained as a function of T and <M>. The results were plotted in C - T coordinates and points relating to the same <M> were connected by lines, as shown schematically in Fig.5. It was found that each of these lines was composed of two very nearly straight segments joining at a point corresponding to T = 0 deg. C. In fact, best straight segments were drawn through the experimentally obtained points in the manner described above. Three such plots were obtained, one for each of the three copper wires of the specimen.

If the values of the local moisture contents could now be assigned to the lines drawn in these three plots, drawn under isothermal conditions of the specimen, then these plots could be used to evaluate the unknown values of M(x) for a different condition of the specimen provided the respective values of C and T were made available. Specifically, under temperature gradient condition — in which redistribution of the moisture takes place in the specimen — the new distribution of the overall moisture content could be obtained with the help of these plots. This is based on the fact that the value of C depends on the local values of moisture content and temperature (as explained in

the description of Fig.4), whatever they may be due to, and irrespectively of the overall condition, isothermal or gradient, of the specimen.

Originally it was thought that heating the specimen and maintaining it at a high level of temperature after injecting a known amount of moisture into it, would help moisture distribute itself uniformly in the specimen. It was thought that capillary forces in the granular specimen, discussed in Chapter IV, would become strong enough to spread the moisture uniformly after a prolonged heating of the specimen. If this were true, then at every isothermal temperature of the specimen, a uniform condition of moisture in the specimen would have prevailed, that is, the percentage of moisture at each of the three levels in the specimen would have been the same and would have been equal to the known overall percentage of moisture injected into the specimen. Or, in other words, the values of $\langle M \rangle$ in the three plots, discussed above, would be the same as $M(x)$, rendering these three plots ready for direct use as moisture calibration curves.

Unfortunately, this was found not to be the case (see Chapter V, Section 2). The moisture did not distribute itself uniformly within the specimen, even after a prolonged heating at high temperature. The moisture also remained non-uniformly distributed in the specimen during the tests under isothermal conditions which took place after the initial heating and cooling as required. Therefore, an analysis had to be

developed to evaluate the distribution of moisture under isothermal conditions, and a functional relationship was produced to express $M(x)$ in terms of C and T. This analysis is shown in the following section. This relationship was then employed to evaluate $M(x)$ under temperature gradient conditions with the help of the corresponding measured values of C and T, in the manner already explained.

4.2 ANALYSIS:

In order to obtain a dependence of local moisture content, $M(x)$, on parameter C and temperature T, under isothermal conditions of the specimen, let us first analyse the moisture distribution for a particular isothermal temperature and a particular overall moisture content, $\langle M \rangle$.

Considering a nonuniform moisture distribution along the thickness of the specimen, let us assume that this distribution can be represented by a polynomial

$$M(x) = A_o + A_1 x + A_2 x^2 + \ldots , \qquad (7)$$

where x is a variable distance from the central plane of the specimen. The central plane of the specimen coincides in Fig.6 with the middle copper wire. As the three copper wires divide the specimen thickness into four equal parts, let one quarter of the specimen thickness be denoted by unity, as shown in Fig. 6. The local moisture content at the three levels (for the three copper wires) could be written as

$$M(1) = A_o + A_1 + A_2 + \ldots , \qquad (8)$$

$$M(0) = A_o , \qquad (9)$$

$$M(-1) = A_o - A_1 + A_2 + \ldots \qquad (10)$$

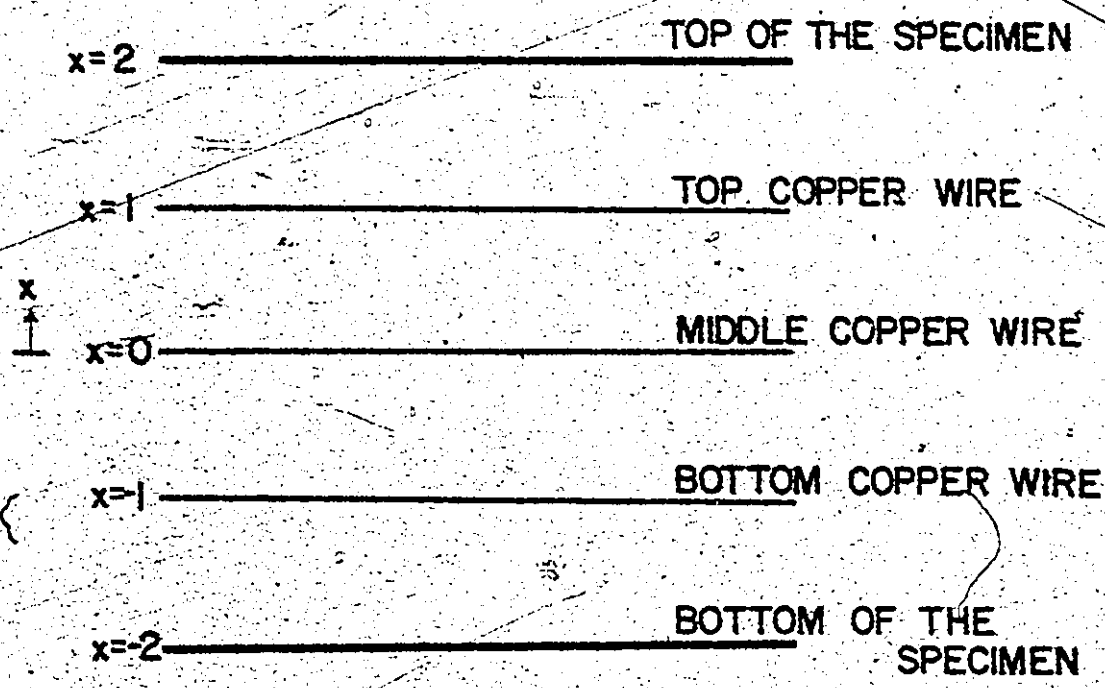

FIG.6 LOCATION OF THE WIRES IN THE SPECIMEN

The number of copper wires in our experimental unit has restricted the number of terms in Eq.(7) to represent $M(x)$ to three. If we had, e.g., five equidistant wires, we could produce a system of five linear equations with five unknown coefficients, A_o, A_1, A_2, A_3, and A_4. Upon the evaluation of, in our case, three unknowns A_o, A_1, and A_2, the moisture distribution in the specimen could be approximated by properly fitted curves for the particular values of T and $\langle M \rangle$. With only three terms in Eq.(7) this approximation could not be very precise, but this is the best we can do without an increase in the number of wires which as we recall is undesirable.

The overall moisture content in the specimen could be obtained by integrating Eq.(7) within proper limits.

$$\langle M \rangle = \frac{1}{4} \int_{-2}^{2} M(x)\, dx, \tag{11}$$

Substituting the expression for $M(x)$ from Eq.(7) into Eq.(11),

$$\langle M \rangle = \frac{1}{4} \int_{-2}^{2} (A_o + A_1 x + A_2 x^2)\, dx. \tag{12}$$

On integration,

$$\langle M \rangle = A_o + \frac{4}{3} A_2 . \tag{13}$$

In order to determine the unknowns A_o, A_1, and A_2 in Eq.(7), the use is made of the values of C, obtained for the three copper wires under isothermal conditions of the specimen, as a function of the known values of T and $\langle M \rangle$ and an unknown value of $M(x)$. Symbolically,

$$C = C[T, \langle M \rangle, M(x)] \tag{14}$$

and

$$C = C(x), \text{ for } T = \text{const. and } \langle M \rangle = \text{const.} \tag{15}$$

Now, the dependence of $C(x)$ on $M(x)$ is assumed to be representable in the following form:

$$\frac{C(x)}{CD(x)} = 1 - b\,M(x)^n - d\,M(x)^{2n} \tag{16}$$

where $CD(x)$, (D for dry), is the value of $C(x)$ at $\langle M \rangle = 0$, that is, for the dry specimen, and b, d, and n are unknown positive constants. Since the values of the ratio $C(x)/CD(x)$ are calculable for $x = 1$, $x = 0$, and $x = -1$, from the plots of C versus T and $\langle M \rangle$, as explained in the previous section, Eq.(16) is a quadratic equation in $M(x)^n$. Therefore, Eq.(16) could be solved for $M(x)$ as

$$M(x) = \left[\frac{-b \pm \sqrt{b^2 - 4d[C(x)/CD(x) - 1]}}{2d}\right]^{1/n}. \tag{17}$$

Since, b and d are positive constants and $C(x)/CD(x)$ is less than unity, consideration of only the positive square root gives us the positive value of $M(x)$. Rewriting Eq.(17) for $x = 1$, $x = 0$, and $x = -1$, we have

$$M(1) = \{(-b + \sqrt{b^2 - 4d[C(1)/CD(1) - 1]})/2d\}^{1/n}, \tag{18}$$

$$M(0) = \{(-b + \sqrt{b^2 - 4d[C(0)/CD(0) - 1]})/2d\}^{1/n}, \tag{19}$$

$$M(-1) = \{(-b + \sqrt{b^2 - 4d[C(-1)/CD(-1) - 1]})/2d\}^{1/n}. \tag{20}$$

Comparing Eqs.(8), (9), and (10) with Eqs.(18), (19), and (20), respectively, and solving for parameters A_o, A_1, and A_2, we get

$$A_o = \{ (-b + \sqrt{b^2 - 4d[\, C(0)/CD(0) - 1]}\,)/2d\}^{1/n} , \qquad (21)$$

$$A_1 = \tfrac{1}{2}\{(-b + \sqrt{b^2 - 4d[\, C(1)/CD(1) - 1]}\,)/2d\}^{1/n}$$

$$- \tfrac{1}{2}\{(-b + \sqrt{b^2 - 4d[C(-1)/CD(-1) - 1]}\,)/2d\}^{1/n} , \qquad (22)$$

$$A_2 = \tfrac{1}{2}\{(-b + \sqrt{b^2 - 4d[\, C(1)/CD(1) - 1]}\,)/2d\}^{1/n}$$

$$+ \tfrac{1}{2}\{(-b + \sqrt{b^2 - 4d[C(-1)/CD(-1) - 1]}\,)/2d\}^{1/n}$$

$$- \{ (-b + \sqrt{b^2 - 4d[\, C(0)/CD(0) - 1]}\,)/2d\}^{1/n} . \qquad (23)$$

Substituting the values of A_o and A_2 into Eq.(13), the overall moisture content in the specimen is expressed as

$$\langle M \rangle = \tfrac{2}{3}\{(-b + \sqrt{b^2 - 4d[\, C(1)/CD(1) - 1]}\,)/2d\}^{1/n}$$

$$+ \tfrac{2}{3}\{(-b + \sqrt{b^2 - 4d[C(-1)/CD(-1) - 1]}\,)/2d\}^{1/n}$$

$$- \tfrac{1}{3}\{(-b + \sqrt{b^2 - 4d[\, C(0)/CD(0) - 1]}\,)/2d\}^{1/n} . \qquad (24)$$

In this equation, only b, d, and n are unknown. As mentioned earlier, the values of $C(x)/CD(x)$ can be obtained from experiments on the three copper wires under isothermal conditions of the specimen, at various temperatures and at various overall moisture contents. With these, $\langle M \rangle$ could be calculated from Eq.(24), provided b, d, and n were known. But the actual value of $\langle M \rangle$ is known. This allows us to determine the values of b, d, and n by trial and error in such a way, that

$$\delta = \sum_{i=1}^{m} \varepsilon_i^{\,2} \qquad \text{is a minimum,} \qquad (25)$$

where m is the total number of known overall moisture contents, which in our case is three, and ε_1, ε_2, and ε_3 are the three differences between the known and the calculated values of $\langle M \rangle$ for the three moisture contents.

Having obtained the values of b, d, and n for a particular isothermal temperature, the whole procedure is repeated for other isothermal temperatures. On completion of these calculations, a set of b, d, and n would be obtained at various temperatures. This set of values could be used to express these three parameters as a function of temperature.

Having done this, Eq.(17) becomes ready to be used to determine the local moisture content at any value of T and $\langle M \rangle$, provided the corresponding values of parameters $C(x)$ and $CD(x)$ are known.

Because we only had three wires, the curve fitting procedure is open to criticism as to the accuracy with which the resulting curve represents the actual moisture distribution at all levels.

Similar procedure could be applied with suitable modification to a larger number of measuring stations, rendering hopefully a more accurately fitted curve.

Chapter III

DETAILS OF THE EXPERIMENTAL SET UP AND ITS OPERATION

1. RESISTANCE MEASURING CIRCUIT

As mentioned earlier, the temperature of the specimen at three different levels was deduced from the resistances of the copper wires embedded in it, which in fact were obtained by passing a weak current (0.03 A) through them. On the other hand, the signal generated due to self-heating of these copper wires was used to obtain moisture distribution. For this latter part a relatively large current (2 A) was passed through each of the three copper wires and their change in resistance was recorded as a function of time. Thus, both, temperature and moisture measurement required a precise determination of the resistance of the copper wires under different conditions.

In order to minimize the errors in our evaluation of thermal conductivity as a function of temperature, a low temperature gradient was used (about 1 K/cm), consequently the temperature had to be measured to an accuracy of about 0.005 K, and the resistance, in turn, to about 5 part per million. The current that was passed through the copper wires

being of the order of 0.03 A, measurement of the voltage had to have a precision of about 0.2 μV.

In the case of moisture-measurement, the self-heating response of the wires was to be measured with the precision of about 10 μV in 200-mV, that is, about 5 in 10^5.

Conventional direct-current resistance measurements are generally made either with a bridge or by potentiometric methods. Either procedure has its own advantages as well as definite limitations. The Wheatstone bridge technique offers high degree of precision, but the use of this technique was not open to us, because of the requirement that the resistance measured be that of the central portion of the probe wire only, and not of its whole length. Though the bridge-measurement is independent of the fluctuation in the current flowing through the bridge, it is certainly affected by the resistance of the lead wires. Thus, Wheatstone bridge should not be used whenever lead resistance is significant as compared to the resistance to be measured. An attempt to avoid the use of potential leads would tend to introduce errors in the resistance of the bridge wires which would then have to pass through the thermal guard portion of the specimen. This would have only replaced one undesirable factor by another.

A potentiometric technique is completely free from any effect of potential or current lead resistances. Its main disadvantage is that it requires a current stability which should at least be as good as

the resolution required in the measurement. When this resolution approaches one part per million, the corresponding current stability is often difficult if not impossible to achieve; since it is affected by both the drift of the supply unit and lead resistance variations. The lead resistances concerned are those in the current circuit where they may constitute an appreciable portion of the total circuit resistance. Such stabilities were feasible for the low currents necessary for the temperature measurement, but were not readily available at 2 A level required for the moisture determination.

It was, therefore, decided to use a *d.c. chopper technique* (Dauphinee, 1953; Dauphinee and Mooser, 1955; Dauphinee and Preston-Thomas, 1958) which combines the inherent insensitivity to current fluctuations of the bridge with the ability to employ potential leads of the potentiometer.

The unknown resistance is connected in series with a known standard resistance in a current-supplying circuit to ensure current equality through the two resistances. The electromotive forces developed across the two resistances can be compared accurately using the d.c. chopper technique without making any direct electrical connection between them. Though, in practice, these two electromotive forces can be compared by means of any intermediate electromotive force usually in form of some manually adjusted measuring instrument such as a potentiometer and a null indicator as shown in Fig. 1, this would, as already mentioned,

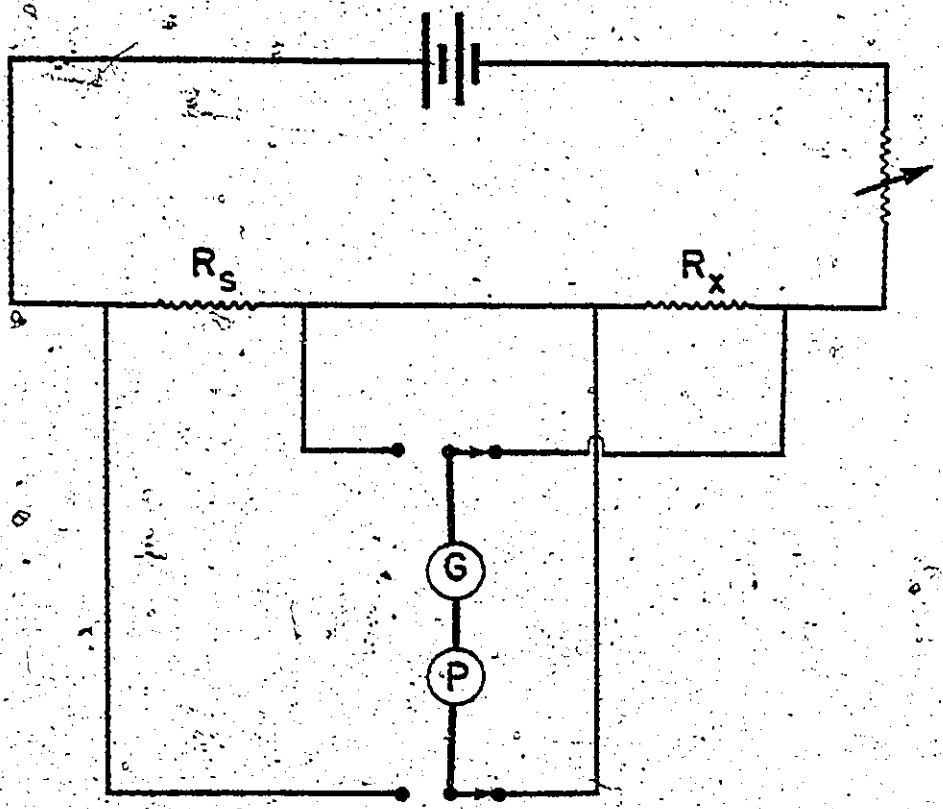

FIG. 1 POTENTIOMETRIC CIRCUIT

require considerable voltage or current stability and sufficient time for the comparison to be made. Such a method would, therefore, be fundamentally unsuited for any measurement where either one or both the electromotive forces are varying quantities. In the d.c. chopper technique the effective period of comparison is reduced to a few hundredths of a second eliminating the need of the stability of the current source. This reduction in time period is accomplished by replacing manually adjusted intermediate electromotive force in Fig. 1 by the voltage across a large condenser and by replacing the manual switching mechanism by a mechanically driven three-section double pole chopper. The circuit is schematically shown in Fig. 2. The condenser is connected between the continuously revolving contacts which are of the brake-before-make type.

The basic circuit for chopper is shown in Fig. 3. Operation of the chopper connects the condenser first to electromotive force 1 causing it to charge to voltage e_1. The chopper contacts now open, and then close on the other side, connecting the condenser with the same polarity to electromotive force 2 through the galvanometer G. If e_1 is equal to e_2 the total electromotive force around the loop is zero and no current flows. However, if e_1 is not equal to e_2, the condenser charges or discharges through the galvanometer until it has the value e_2. The condenser is then transferred back to electromotive force 1, and the whole process is repeated several times a second. The net result of the inequality between e_1 and e_2 is that a series of current pulses pass

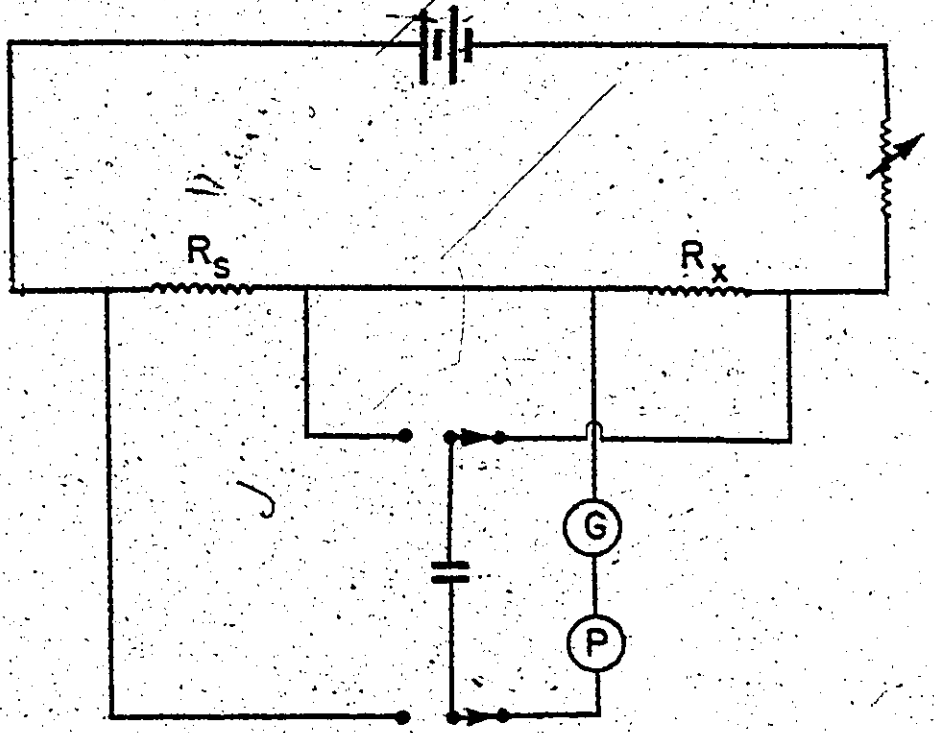

FIG. 2 POTENTIOMETRIC MEASUREMENTS WITH A CHOPPER

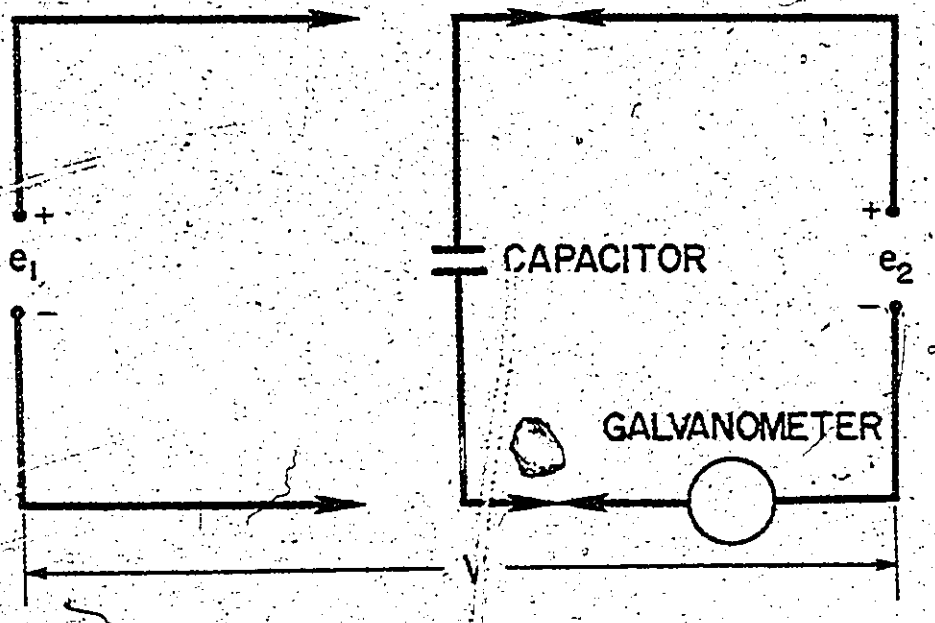

FIG. 3 BASIC CHOPPER CIRCUIT

through the galvanometer making its pointer remain stationary at a certain position. The galvanometer thus acts as a null detector. At balance, there is no current flowing in any of the potential leads and the resistance of these leads is completely eliminated from the result essential for true potentiometric comparisons.

In our case, measurements were made through the use of this technique to better than 0.1 μV. The circuit diagram shown in Fig. 4 is capable of measuring the resistance of the copper wires at low current levels, as well as recording the change in balance due to heating of the copper wires at high current levels.

The two facts, one — that the absence of flow of current in potential leads at balance renders measurements independent of the lead resistance, and the other — that the flow of the same current through standard and unknown resistances avoids the necessity of very high current stability, allowed this technique to enjoy the advantages of both the potentiometric and bridge methods.

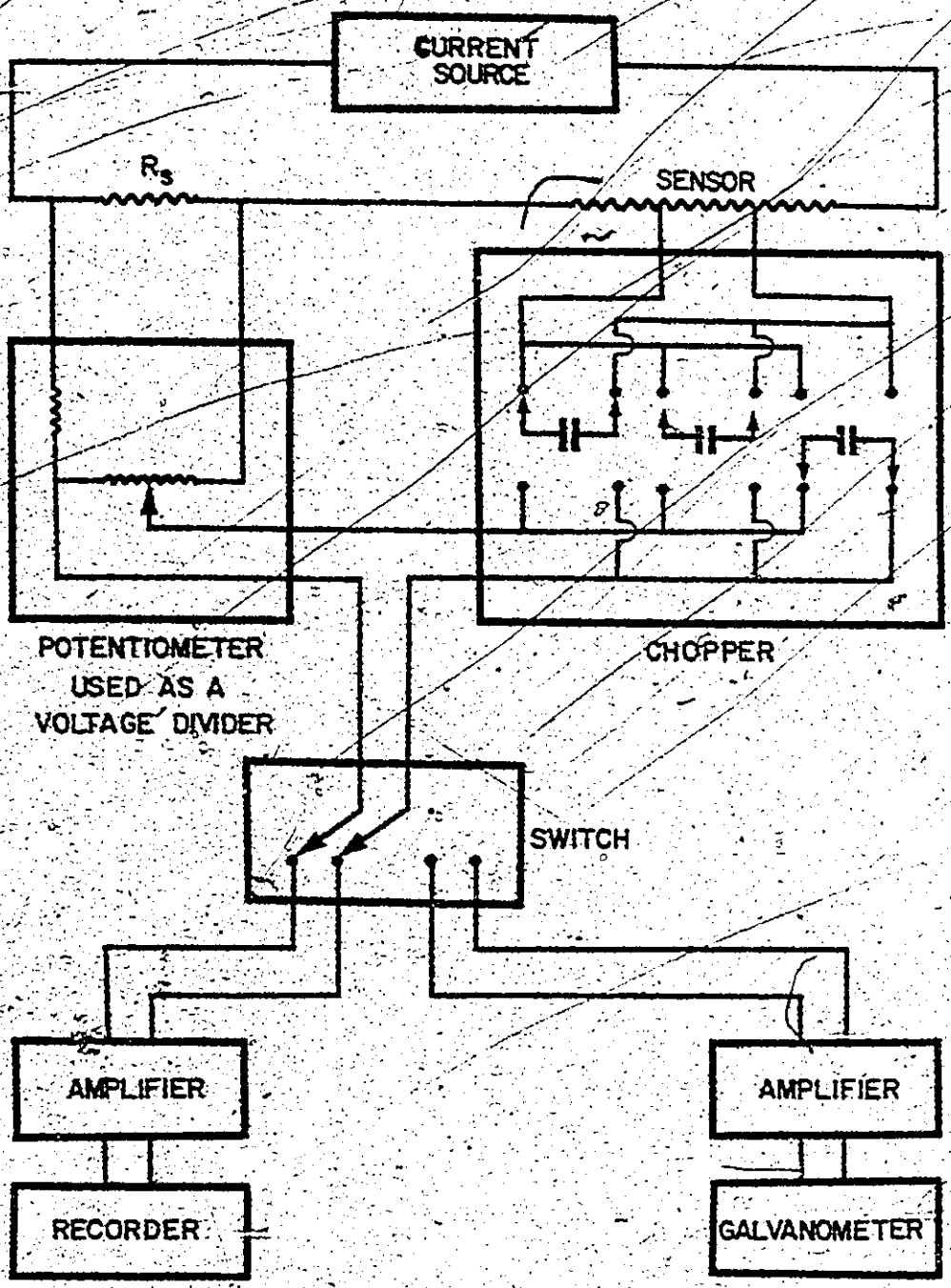

FIG. 4 CIRCUIT DIAGRAM FOR R & ΔR MEASUREMENTS

2. INSTRUMENTATION

The following functions had to be performed by appropriate instruments:

(1) The supply of a measurable quantity of heat flowing unidirectionally through the specimen;

(2) The achievement and maintenance of a desired level of temperature in the specimen;

(3) The measurement of the resistance of the sensors at the low level of currents, and the recording of the change in resistance of these sensors at a relatively high level of currents.

Various types of instruments and circuits were employed to perform these basic functions. They are described in detail in Appendix C under two categories; the first consisting of what was available to us as an integral part of the basic experimental unit, and the second consisting of what had to be designed and manufactured to complete the experimental set-up for simultaneous temperature and moisture measurement. The salient features of the instruments and circuits from both the categories are described here in this section.

The main heater, which is the central portion of the heater assembly lying on the top of the specimen, supplied a measurable heat flow which was produced by the d.c. power being dissipated in the main heater resistance. The voltage and current to the main heater were supplied by a power supply having an output voltage regulated to 0.015

per cent or 1 mV (whichever is greater for load variations from zero to full load) and an output current regulated to 0.1 per cent or 10 mA (whichever is greater). The load current and voltage were measured potentiometrically.

The guard heater, which is the remaining portion of the heater assembly, is separated from the main heater by a narrow gap. The guard heater was operated at the same temperature as the main heater to eliminate the radial heat flow to and from the main heater. The thermal balance of the order of 0.025 deg. C was maintained by the use of a zero-differential proportional controller. This controller operates on an unbalance signal produced by a differential thermocouple whose junctions alternate between the main and the guard heater surface.

The upward heat flow from the main heater was prevented by maintaining the temperature of the top auxiliary heater, placed on the top of the main heater and separated from it by a gap filled with Styrofoam, at the level of the main heater temperature. This heater was accurately matched in temperature to the main heater by means of an automatic heater control.

A coolant from a refrigerating unit, circulating in the experimental unit, was used to control the isothermal temperature of the specimen. For gradient tests, this coolant was used to set the cold-side temperature of the specimen. The temperature of the coolant was maintained at a set temperature to an accuracy of ±0.05 deg. C.

Temperatures were monitored at three levels in the experimental section of the unit by six thermocouples. Copper-constantan thermocouples were employed for this purpose. These thermocouples are good for measurement between -190 and 400 deg. C. The thermocouple junctions were connected at the desired temperature sensing locations, and the thermocouple wires were made to pass through 0.032 in. O.D. ceramic insulators, accommodated in the specially cut grooves on the surfaces of the heaters. In this manner they came out of the heaters along isothermal planes reducing the conduction heat losses always encountered in thermocouple leads. The wires were then connected to the thermocouple terminals on the base plate. After exiting from the insulators, the thermocouple wires were covered with glass silk sleeving for their protection.

The reference junctions of the thermocouples have to be maintained at a definite temperature. The most common reference temperature is 0 deg. C since this temperature is easy to achieve by using an equilibrium mixture of pure ice and distilled water at the atmospheric pressure. Referring each of the several thermocouples individually to the ice-point, as shown in Fig. 5, may introduce large errors in temperature differences unless a large volume of distilled ice-water mixture is used and each wire is immersed individually to a considerable depth. At least five inches are considered adequate for this purpose (Tye and Hurley, 1967). This problem can be avoided by the use of an isothermal junction block where each thermocouple is referenced to a copper block

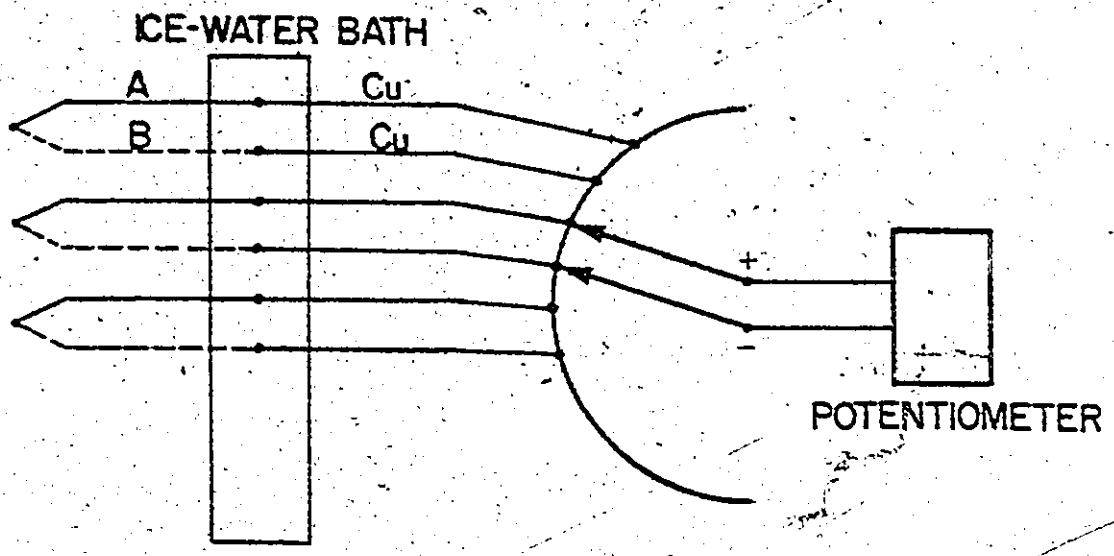

FIG. 5 THERMOCOUPLES WITH INDIVIDUAL ICE-POINTS

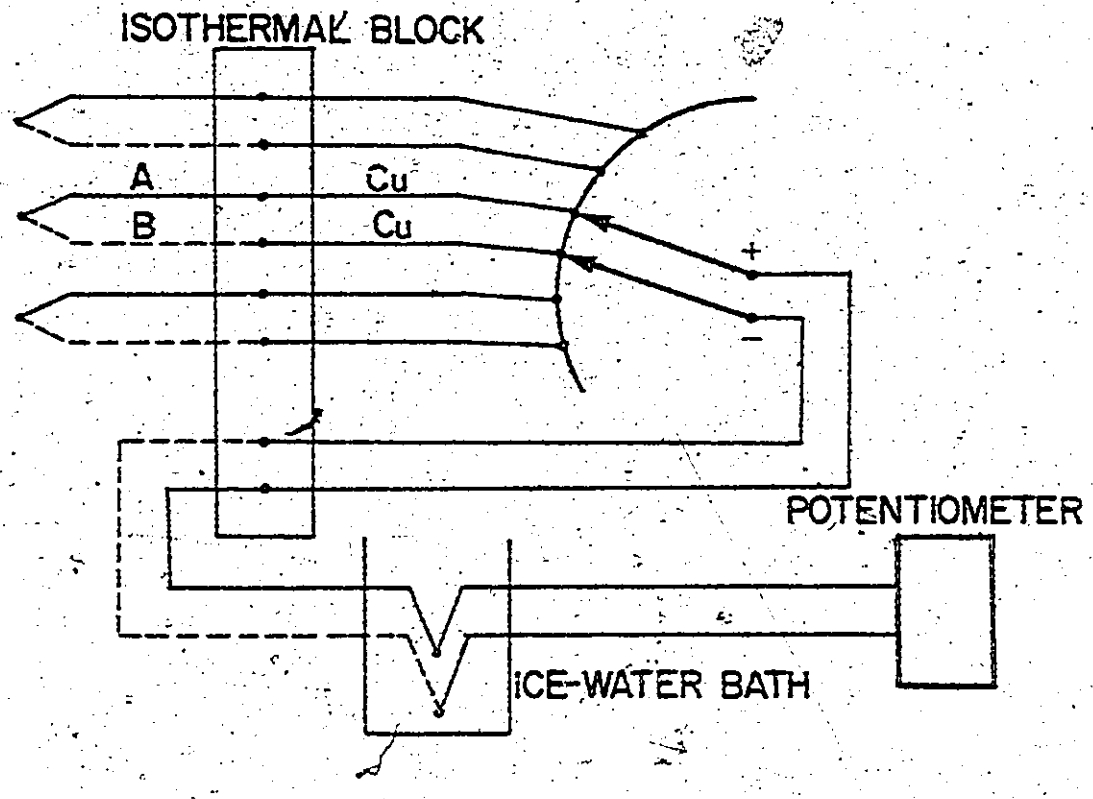

FIG. 6 THERMOCOUPLES WITH A COMMON ICE-POINT

before connecting it to a multi-point switch as shown in Fig. 6. From the output of the switch a pair of copper wires is run back to the isothermal junction block and from there an original metal pair is run to an ice-water bath before being connected to a potentiometer. This method is said to yield extremely reliable results (Tye and Hurley, 1967) and was adopted in this investigation.

The thermoelectric electromotive forces were measured by a potentiometer with a resolution of ± μV, which was quite sufficient for the purpose, since accuracy in the absolute value of the temperature was not of much importance here. What was important was an accurate determination of the temperature difference. This was achieved here by employing pre-calibrated thermocouples in an arrangement shown in Fig. 6.

Ice water bath preparation and maintenance require great care. Ice made from distilled water should be finely crushed and washed also with distilled water. After washing, the liquid should be drained and replaced by a fresh one. As the ice melts, new mixture has to be prepared in replacement. Any deviation from these procedures is apt to affect the correct measurement of the absolute value of a temperature because of a possibly incorrect reference point. Even though our interest here is in the evaluation of temperature differences at different measuring points rather than in the exact knowledge of various individual temperatures, all the above-mentioned precautions had constantly been taken.

A schematic diagram of the circuit, capable of measuring the resistance of the copper wires at low current levels and recording the change in resistance due to the heating of these copper wires at high current levels, was shown in Fig. 4. The details of the same circuit are now shown in Fig. 7.

The two levels of current requirements, that is, 0.03 A for resistance measurement, and 2 A for self-heating of copper wires, were met by a d.c. power supply. This supply has a voltage regulation of 5 mV and a current regulation of 0.01 per cent plus 250 μA. The influence of thermal electromotive forces, usually present in any circuit, was reduced in our case by the use of a reversing switch. The generation of transients during the reversal of the current was avoided by the introduction of a shorting resistance and a shorting switch in the current circuit.

The two fixed resistances, 0.1 Ω and 0.01 Ω, used for supplying a standard voltage in the potentiometer circuit and for calibrating the potentiometer, respectively, were calibrated before use at the Division of Physics, National Research Council of Canada, Ottawa. The potentiometer in the measuring circuit was used only as a voltage divider. The voltage across the fixed resistance of 0.1 Ω was divided by the potentiometer in such a way that it was equal to the voltage across the copper wires within six digit accuracy.

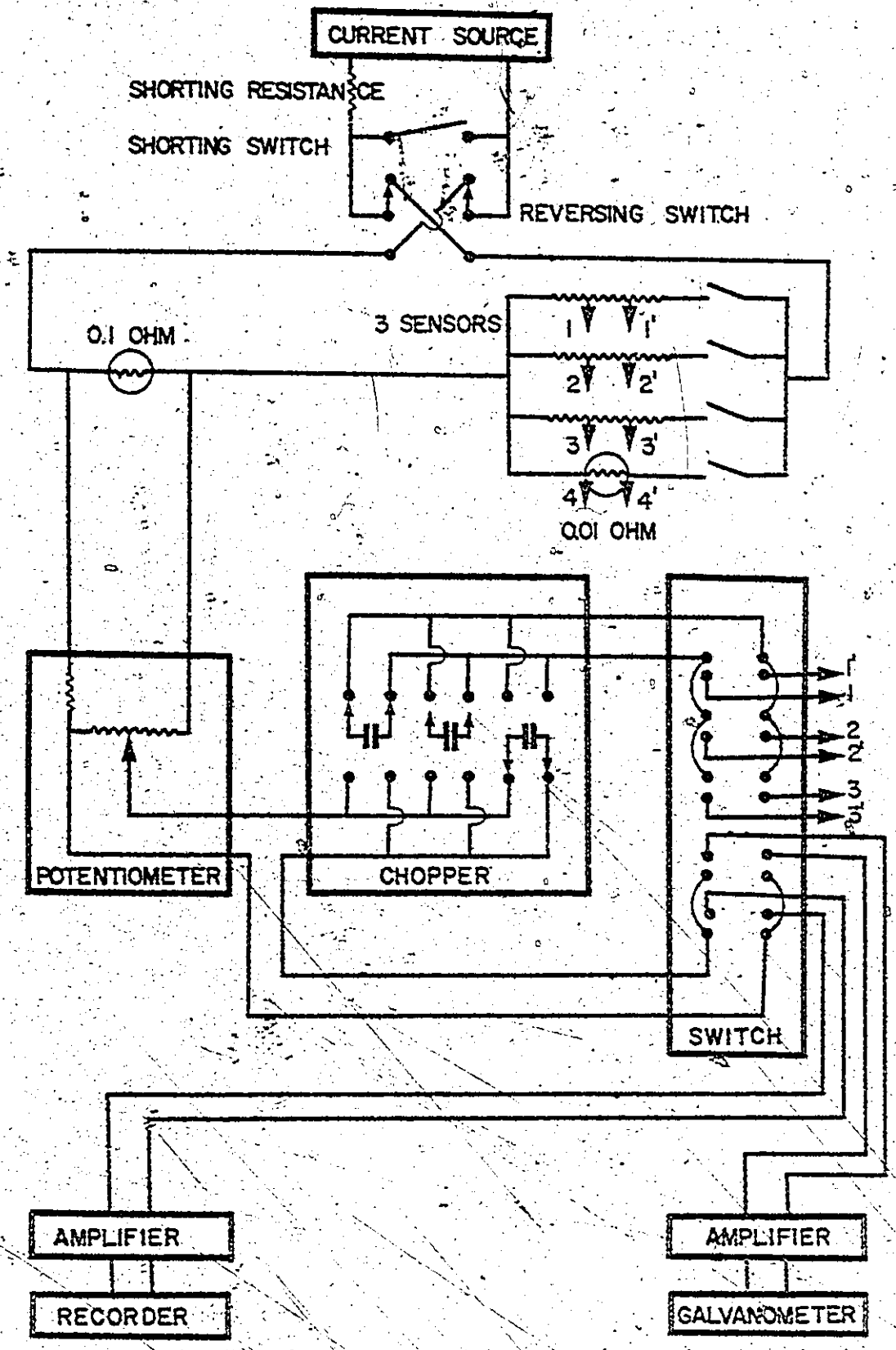

FIG. 7 DETAILS OF THE R & ΔR MEASURING CIRCUIT

The chopper, used in the circuit for comparing an unknown voltage with a known voltage without making a direct contact between the two sides, has three pairs of contact arms made of a gold-silver alloy and the contacts of solid gold blocks to reduce thermal electromotive forces to a minimum of 0.1 μV.

The functioning of this device has been explained in the previous section, and it is clear that at any given time it is necessary that at least one pair of poles be in contact with one of the electromotive force circuits while not being simultaneously in contact with the other. Theoretically, two sections having contact angles from 0° to 180 degrees could be sufficient for this purpose, as shown in Fig. 8a. But in practice, in order to avoid short circuit, they have to be separated by some angle as shown in Fig. 8b. This would unfortunately leave the circuit open during the period of separation decreasing the sensitivity. The minimum number of sections is, therefore three in order to eliminate the problem of short circuiting and to provide continuous transfer of electric charge from one circuit to the other. The overlaps provide what is known as the *make-before-brake contacts*. The three pairs of contact arms of the chopper in our particular model were adjusted to give contact angles of 140 degrees with 20 degrees of overlap as shown in Fig. 8c.

The contact arms are activated by a common camshaft, which was driven mechanically by a small motor at a certain speed. In almost all practical circuits there are a few microvolts, often considerably more,

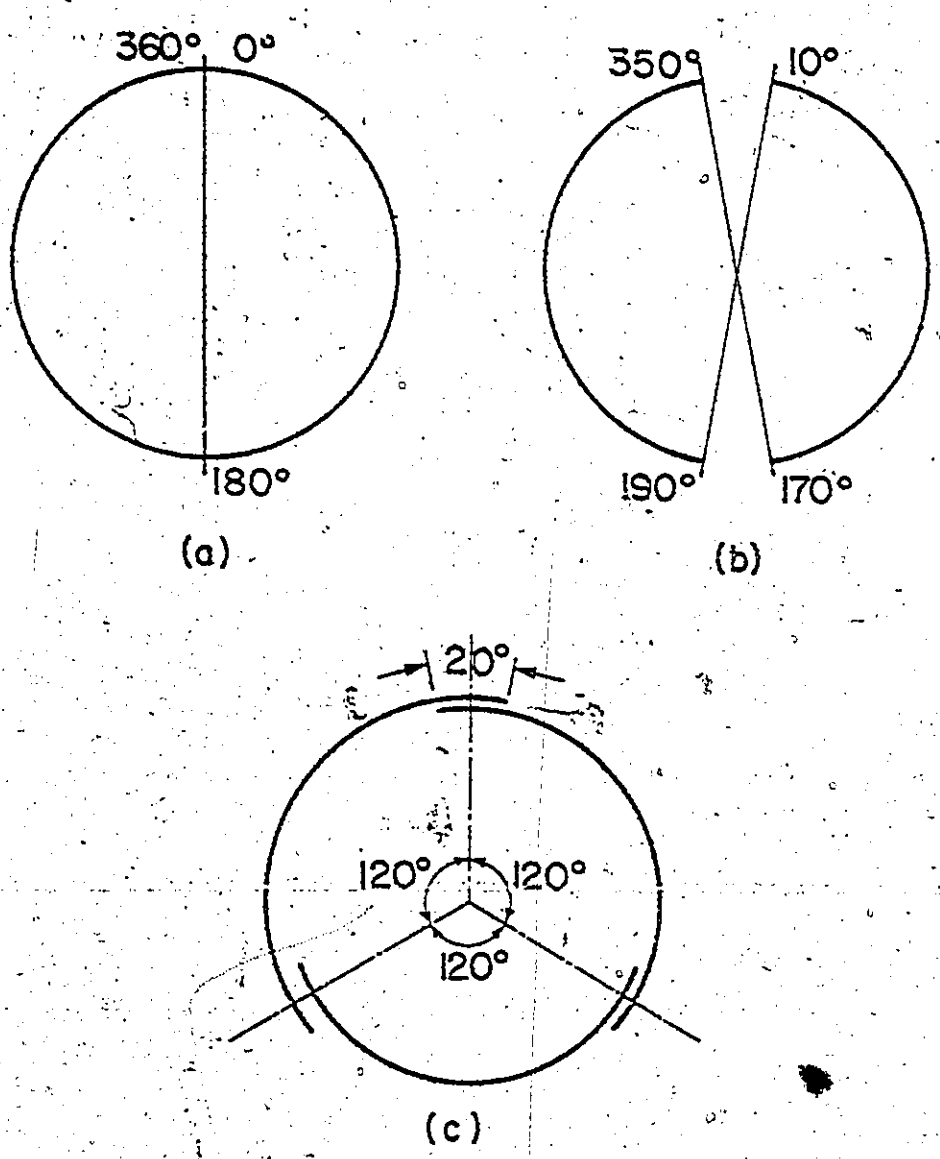

FIG. 8 CHOPPER-ARM CONTACT ANGLES

of a.c. main's frequency pickup. A chopper driven synchronously with the main may effectively rectify this pickup, while a nonsynchronous chopper gives beats with main's frequency or its harmonics. It has been suggested (Dauphinee, 1953) that the effect of a.c. pickup can be practically eliminated by using mechanically driven choppers at a frequency of 37.5 cps. The cam-shaft and a shaft of a constant speed d.c. motor were connected by an *O-ring* through pulleys. The mounting of the motor on the base plate was such that the distance between the two pulleys could be varied in order to achieve the desired speed of the chopper. Finer adjustments in the chopper speed were also made by varying the speed of the motor. The motor-speed was controlled by a variable voltage transformer (Variac) included in the circuit shown in Fig. 9. A constant voltage transformer, 95-130P/115 S, was used as a constant voltage supply. Variac has voltage regulation from 0 to 115 V. Another transformer with 115P/25 S was also used in the circuit as shown in Fig. 9. By manoeuvering the Variac as well as the distance between the two pulleys, a desired frequency of the copper was obtained to avoid beats in the galvanometer. The whole chopper assembly was enclosed in an electrically grounded chamber to protect the chopper from picking up extraneous signals.

A galvanometer, preceded by a photocell galvanometer amplifier, capable of amplifying d.c. signals of nanovolt and nanoampere levels, was used to function as a null detector in the potentiometric circuit. The amplifier was mounted in such a position that it was not subjected to vibration and was connected to a source capable of supplying up to

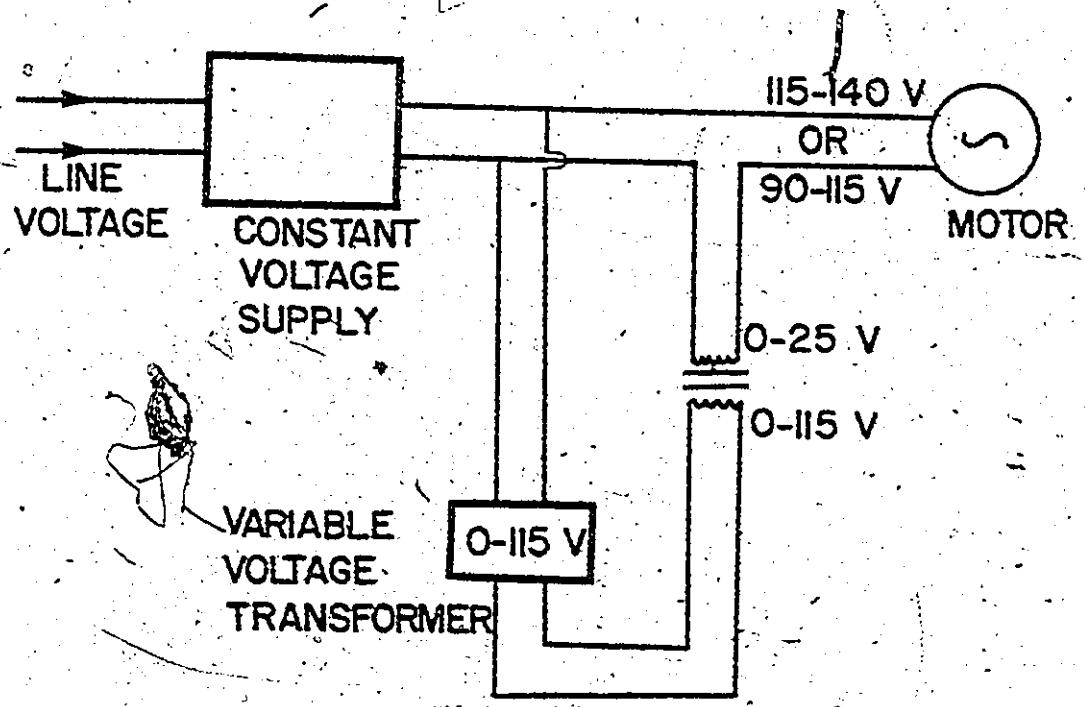

FIG. 9 SPEED-CONTROL CIRCUIT FOR CHOPPER-MOTOR

3 A at 6 V.

A strip chart recorder, preceded by an amplifier, was used in the circuit to record the increase in voltage due to self heating of copper wires. The zero mark of the recorder was adjusted to lie on the center of the chart.

The thermal electromotive forces of the circuit were reduced by the use of a low thermal switch, low thermal solder, and high purity connecting wires. The low thermal switch generates no more than 0.01 μV thermal electromotive forces. Considerable thermal electromotive forces may be generated in the circuit at the junction of two or more dissimilar metals, depending on the type of metals and the difference of temperature to which they are subjected. A conventional lead-tin solder has 3 μV/K of thermal electromotive forces versus copper. To minimize this, a special low thermal solder, cadmium-tin alloy, was used which has thermal electromotive forces versus copper of less than 0.3 μV/K. A high purity copper wire originating from one lot was used to connect various instruments. Low thermal interconnecting insulated wires, 20 gauge solid copper conductors were selected. These wires are untinned to avoid thermoelectric effects and were twisted together to minimize magnetic field pickup. They were covered with a woven copper shield to eliminate electrostatic effects. An insulating sleeve separated the shield from the conductors. The shields in the various parts of the circuit were all connected to the ground. This kind of a cable is thought to be essential for the transmission of d.c. signals whose integrity must be maintained down to the nanovolt level.

3. EXPERIMENTATION

3.1 PLAN:

The experiments were conducted on the specimen with varying moisture content ranging from 0 to 5 per cent by weight over a temperature range from -15 to 20 deg. C. The overall moisture contents chosen for the experiments were: 0 per cent, that is, the dry specimen; 1 per cent; 3 per cent; and 5 per cent. For each moisture content at least eight tests were performed, varying the temperature in steps of about 5 degrees. Two kinds of tests, namely isothermal and gradient, were performed at each combination of temperature and moisture contents.

3.2 ASSEMBLING OF EQUIPMENT AND SAMPLE PREPARATION:

The preliminary work for the actual experiments involved putting together the test-stack assembly and instrumenting it. The bottom auxiliary heater and the cell were put on the top of the bottom heat sink, as shown in Fig. 10. The base plate, to which the bottom heat sink is attached, has terminals for connecting copper-constantan thermocouple wires and heater wires. These terminals are internally connected to a multijunction selector switch in a remotely located control panel. They are also connected to another terminal at the back of the control panel from where further connections could be made to external signal monitoring system if so desired. These internally connected thermocouple wires, besides being used to carry the thermocouple outputs from the test stack assembly to the control panel, were also used for the following additional purpose. The current and potential leads of the three copper wires were

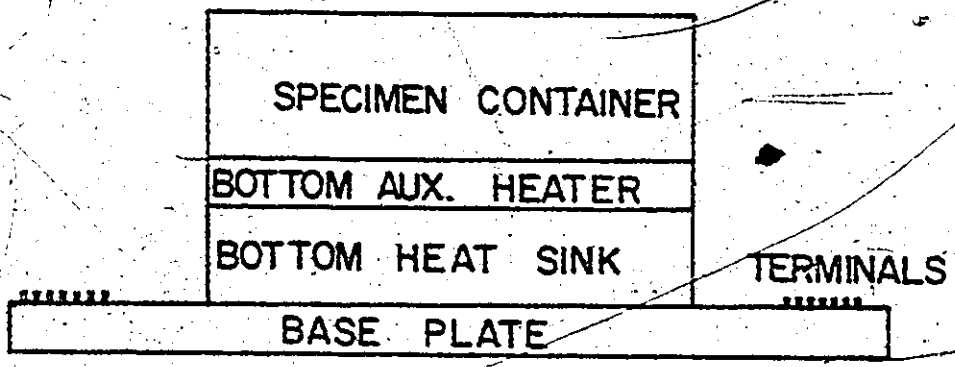

FIG. 10 ASSEMBLY OF THE TEST-STACK

connected to the copper wires of these thermocouple terminals, and the other ends of these terminals on the back of the control panel were connected to the appropriate current-supplying and voltage-measuring circuits.

Before filling the cell with the specimen material, it was necessary to perform an additional experiment. The cell was filled with ice so that the ice-point resistance of each of the three copper wires could be measured. These ice-point resistances were necessary for the evaluation of temperatures of the three wires, since the relation used for the purpose gives the temperature of copper wire as a function of a ratio of a resistance at unknown temperature to a resistance at ice-point. The cell was filled with crushed ice and the pores were saturated with distilled water. This mixture of crushed ice and distilled water served as an appropriate ice-point for these wires. The resistance of the three copper wires was measured as a function of current flowing through them so that the desired values of the resistances could be extrapolated for no flow of current through them. The process of resistance measurement is explained later in Section 3.5.

After having determined the resistance of the copper wires at ice-point the cell was emptied, dried, and then filled with a known volume of water to the height of 3.4 cm in order to determine the exact volume of the cell. Subsequent to this the cell was again emptied, dried, and filled with dry granular material. To make sure that such material was indeed completely dry, it was heated in an oven at 105 deg. C for several days. While the cell was being filled, it was gently tapped so that the material

could settle down, thus ensuring compaction. During the process of filling the cell with the material, care was taken not to disturb the wires through tapping or otherwise. Appropriate temporary supports were provided for this purpose. Having filled the cell to the required height with the granular material in the densest possible manner, these temporary supports were removed and the top of the cell was covered by the main heater assembly. The main heater assembly was fastened to the cell-top by peripheral screws. A rubber seal on the top of the main heater assembly covered the space between the heater and the cell-wall and thus made the cell watertight.

Figure 11 shows the complete test-stack assembly. The solid copper ring and the top auxiliary heater were connected together by a holding ring, and the space under the heater was filled with Styrofoam. This assembly was placed on the cell and held tight to it by means of circumferential screws. Figure 12 shows a photograph of the test-stack assembly.

There are three vertical rods on the base plate which support two horizontal plates. Of these two plates, the one on the top could be fixed on the three rods anywhere along their height by means of three screws. The lower plate, to which the top heat sink is attached, is connected to the top plate by means of a long screw, which can make it slide up or down using the three rods as guides. The purpose of this arrangement is to allow to exercise a desired degree of pressure by rotating the long screw by hand. On the one hand some pressure is

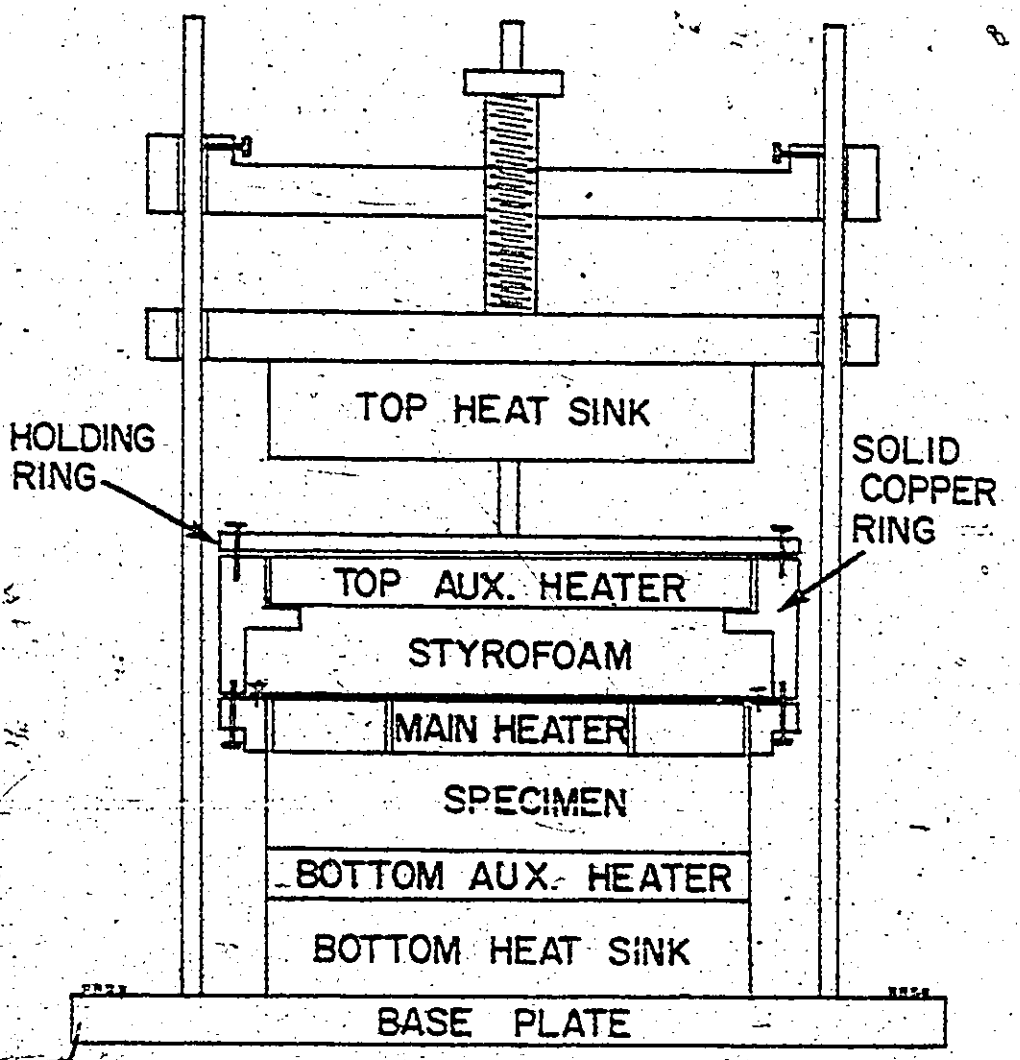

FIG. II SCHEMATIC DIAGRAM OF THE TEST-STACK ASSEMBLY

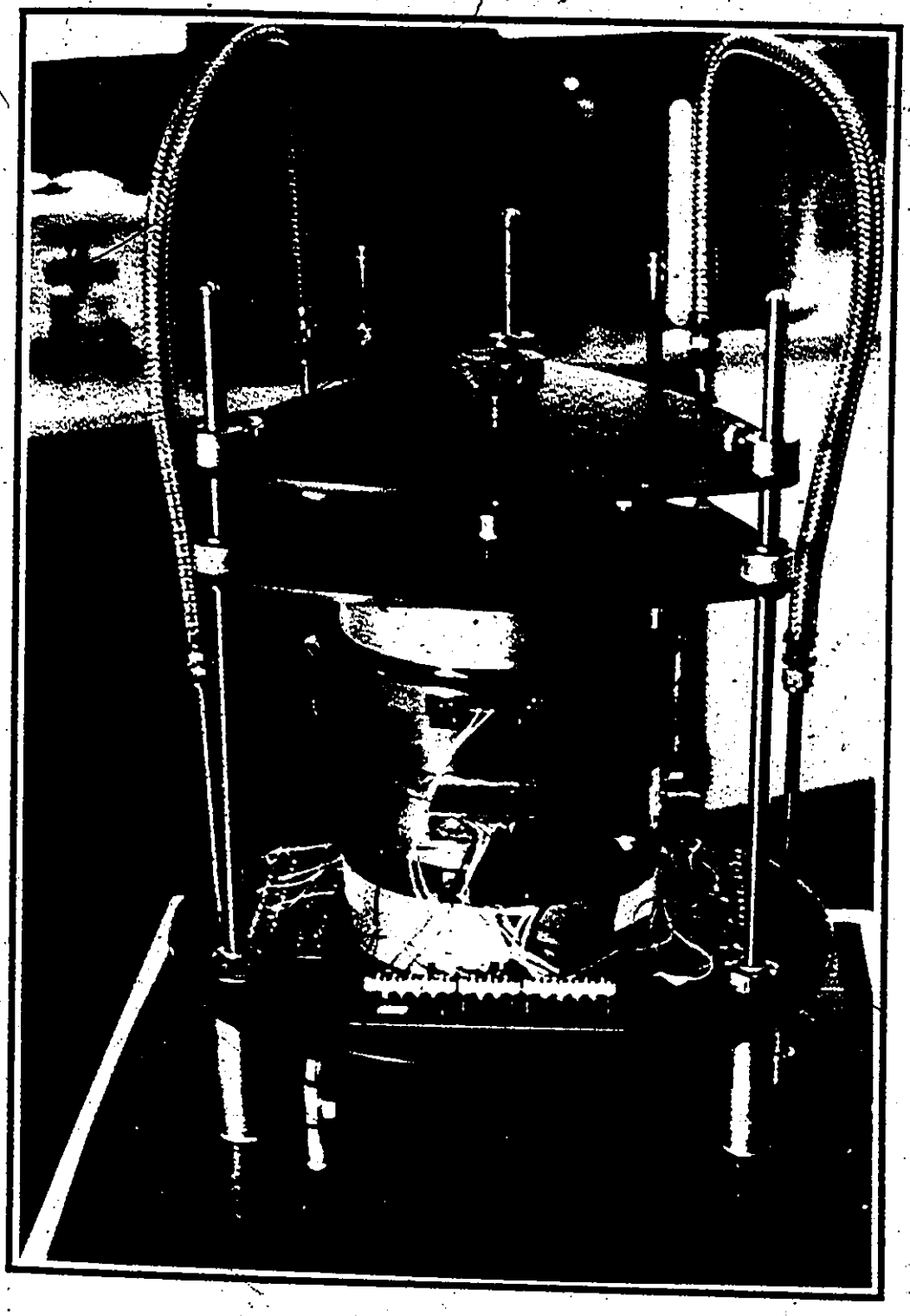

FIG. 12 OUR TEST-STACK ASSEMBLY

needed to ensure good contact, but on the other — excessive pressure would unduly compact the material.

Appropriate connections were made for supplying and measuring power to the main heater and to the controllers of the guard heater and the top auxiliary heater.

Figure 13 represents the wiring diagram for the test stack assembly. Six thermocouples were installed at three different levels in the experimental section of the unit for temperature monitoring. These three levels are: bottom of the top auxiliary heater, top of the main and guard heater assembly, and top of the bottom auxiliary heater. The purpose of temperature monitoring was two-fold. First, it was used to check from time to time whether a condition of steady state was being maintained in the system. In the second place, it helped us match the temperatures of the guard and the top auxiliary heaters to the level of the main heater temperature. All these thermocouples were accurately calibrated before installation.

It is important to understand that the purpose of this calibration is not merely to determine the general level of deviation of the thermocouple reading from the true temperature, but rather to know this deviation at different temperatures. We were really interested only in temperature differences rather than in the absolute values. Thus, if all the measured values differred from the true ones by the same amount, this would be of little concern to us. Unfortunately, the deviations do vary with the temperature and proper calibration is therefore necessary.

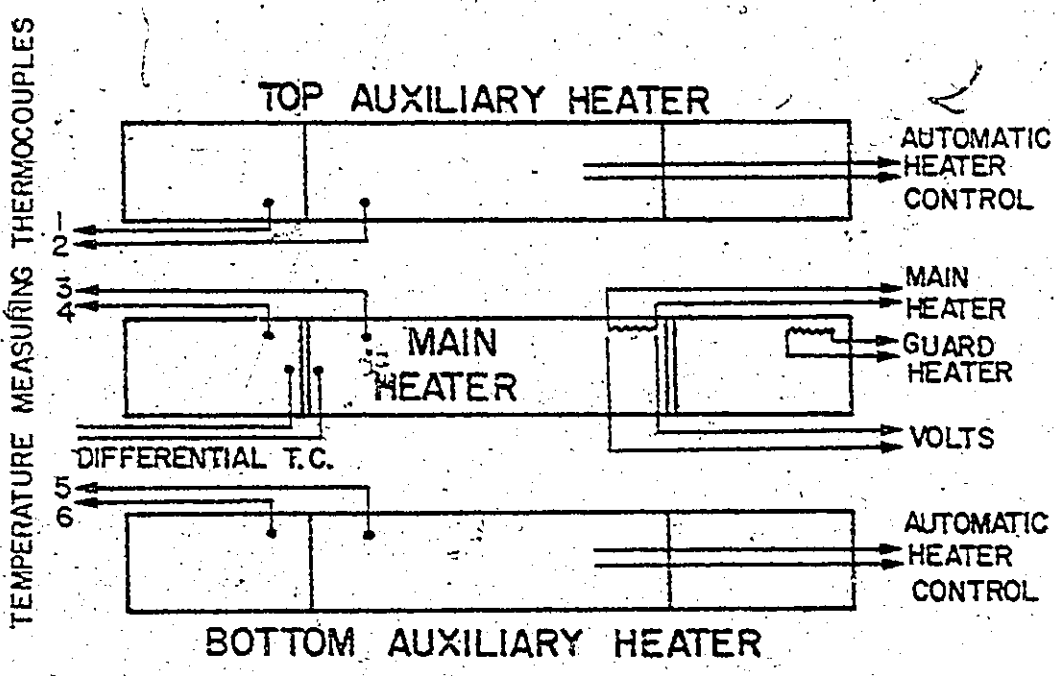

FIG. 13 WIRING DIAGRAM FOR THE TEST-STACK ASSEMBLY

The test-stack assembly was surrounded by Styrofoam pieces which were cut to size to fill tightly the space around it as shown in Fig. 14. The cooling shroud was then slid on to this from the top. Several bags of activated Silica-Gel were placed in different locations and the whole assembly was then covered with a pyrex bell jar resting on the base. The pyrex bell jar was insulated from outside using Armflex insulation in order to minimize any heat transfer through it. Bags of Silica-Gel were also placed under the base of the unit which contains all the electrical connections. The base was made airtight and then covered with insulation. Activated Silica-Gel absorbs atmospheric water vapor.

Pipe connections were made to the refrigerating unit to carry cooling fluid to and from that unit. The fluid flows through the top and bottom heat sinks and the shroud.

3.3 ISOTHERMAL TESTS:

To perform a test under isothermal condition at a temperature anywhere between -15 to 20 deg. C the desired temperature of the specimen was achieved by controlling the temperature of the cooling fluid. The temperature of the bath of the refrigerating unit was maintained 2 to 4 degrees lower than the desired temperature of the specimen since the fluid temperature increases on its way to the test unit by approximately that much. No power was supplied to any of the heaters in the test stack assembly. The temperature of the test-stack assembly was monitored by six thermocouples from day to day, and also several times in the course

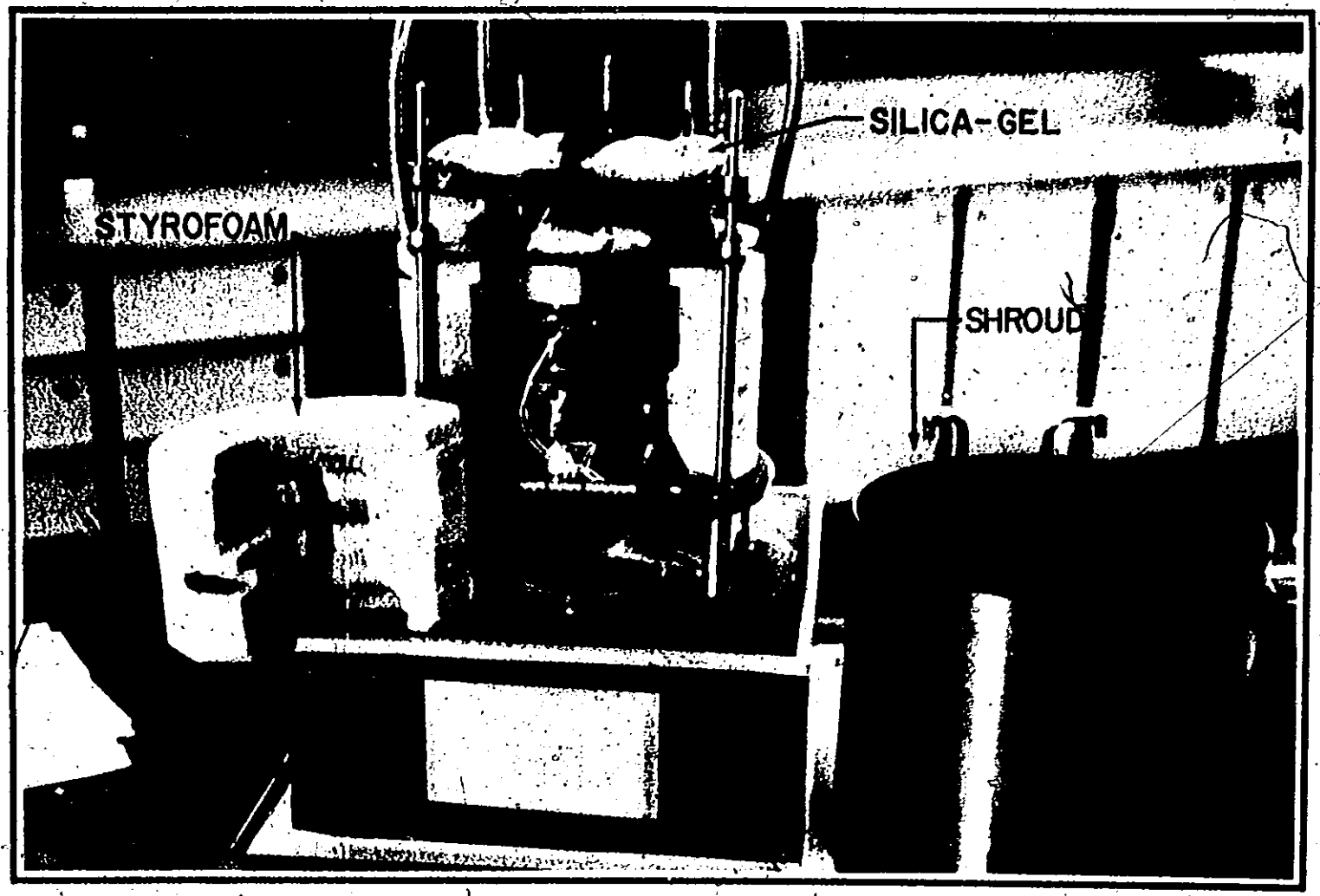

FIG. 14 STYROFOAM INSULATION, SILICA-GEL BAGS, COOLING SHROUD, AND THE TEST-STACK ASSEMBLY

of each day. It took anywhere between two to four days to achieve steady state heat flow in the test section, depending on the initial temperature of the unit as well as on the value of the desired temperature. The unit was taken to be under steady state condition when the fluctuation in the thermocouple temperatures was not more than one fortieth of a degree per day.

When the steady state condition was reached, the resistance of the three copper wires was measured, and their self-heating response recorded. The details of these measurements are described later in Sections 3.5 and 3.6.

3.4 GRADIENT TESTS:

On completion of isothermal tests, the various heat sources and sinks were adjusted to give a desired temperature gradient. The desired temperature difference across a 3.4-cm specimen was anywhere between three to five degrees. The mean temperature of the specimen was controlled by the temperature of the cooling fluid. The temperature of the fluid bath of the refrigerating unit was maintained at a temperature somewhere between 5 to 10 degrees lower than the desired mean temperature of the specimen. The heat from the main heater created temperature gradient across the specimen. The voltage and the current to the main heater were adjusted to give a temperature gradient of about one to two degrees per centimeter.

The guard and the top auxiliary heater were accurately matched in temperature to the main heater section. As was explained in Section 2

of this chapter, the guard heater was automatically matched to the main heater by a zero-differential proportional controller. If the temperatures monitored by the thermocouples still indicated a difference in the temperature of the two heaters, then the zero-differential proportional controller was accordingly biased. The top auxiliary heater was matched manually by observing the temperature difference between the auxiliary and the main heater. These temperatures were matched to an accuracy of better than one tenth of a degree.

The resistance of the three copper wires was measured and their self-heating response recorded after a steady-state condition had reached . The time required for the unit to come to steady state in this case was about twice as much as in the case of isothermal condition. This was so because a considerable amount of time was required to match the three temperatures. The current and voltage supplied to the main heater were accurately measured.

3.5 RESISTANCE MEASUREMENT:

The potentiometer in the measuring circuit had to be calibrated before it was ready for resistance measurement. A standard of known resistance R_s was incorporated in the circuit as shown in Fig. 15a. A small current of 0.03 A was passed through the circuit and the potentiometer reading r_s corresponding to R_s was noted. This served as a calibration of the potentiometer for resistance measurement. Now, if r_x is the potentiometer reading corresponding to any unknown resistance R_x

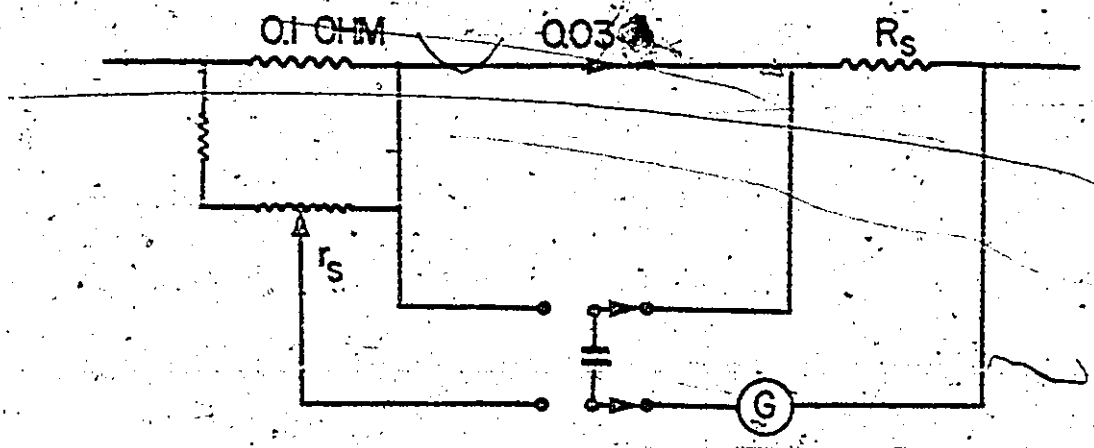

(a) CIRCUIT WITH STANDARD RESISTANCE

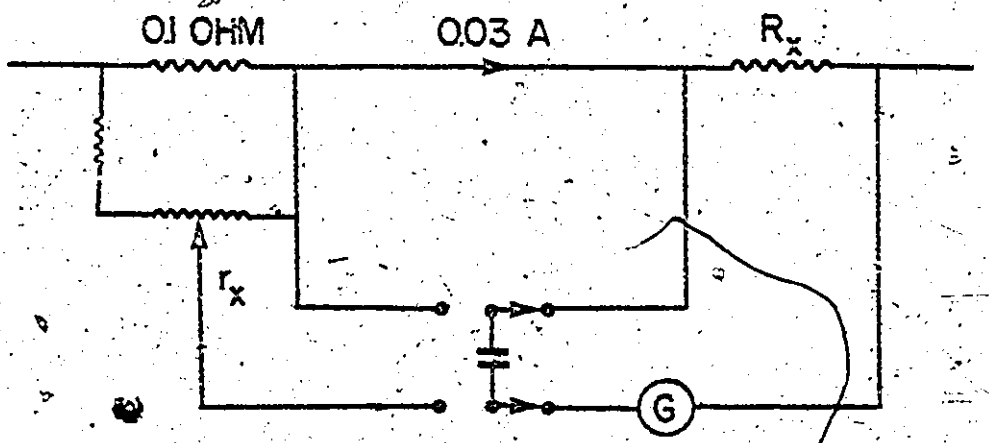

(b) CIRCUIT WITH UNKNOWN RESISTANCE

FIG. 15 POTENTIOMETER CALIBRATION

(Fig. 15b), then R_x is obtained by

$$R_x = r_x R_s / r_s \qquad (1)$$

In our case R_s was 0.0099974 Ω and r_s was 52328.

Hence,

$$R_x = 1.9105\ (10^{-7}) r_x . \qquad (2)$$

For measurement of the unknown resistance of the copper wires, the current supply was adjusted to given 0.83 A. The chopper-motor was switched on and the speed of the chopper was adjusted to about 37.5 cps, by checking the speed with a stroboscope.

One of the three copper wires was connected to the current supplying circuit by means of a switch. Then the switch connecting the galvanometer to the circuit was depressed. The dials of the potentiometer were adjusted to give a null point on the galvanometer. The null point corresponded to the position on the galvanometer scale which did not change upon the reversal of the current. The reversal of the current was necessary to eliminate the effect of the thermal electromotive forces in the circuit. The potentiometer reading at the final null balance was noted and was used to calculate the resistance, and further, the temperature of the copper wire. The procedure was repeated for the other two copper wires.

3.6 SELF-HEATING RESPONSE MEASUREMENT:

The current used for self-heating of the copper wires was 2 A. This was found to be large enough to provide a sufficient self-heating response

without an undue disturbance of moisture distribution by unnecessary local heating of the granular material. The copper wires were heated, one at a time, for a period of sixty seconds.

The current supply was set on a constant voltage mode when 0.03 A were required, and on a constant current mode when the magnitude was 2 A. A sufficient time of about 30 minutes was allowed to elapse between two consecutive heating experiments to ensure that the sample and the wires were able to return to their initial temperatures. Initially, a small amount of current, namely 0.03 A, was allowed to pass through the circuit and the potentiometer was adjusted to give a null on the galvanometer. This procedure was identical to that of the resistance measurement described earlier. The motor, turning the chart on the recorder, was turned on, and was adjusted to give the chart-speed of six inches per minute. The null point was recorded on the chart in form of a straight line in the center of the chart as shown in Fig. 16a. Since the null point was obtained when the potential drop across the sensor, V_x, equals that across the potentiometer as shown in Fig. 16b, the straight line in Fig. 16a represents V_x to a certain scale. Its magnitude was unimportant for our purpose. After a few seconds, the circuit current was suddenly increased to 2 A. A generation of heat in the sensor due to this large current increased the temperature of the surrounding medium as well as that of the sensor material itself, which in turn increased the resistance of the sensor according to the relation

$$R_{xx} = R_x(1 + a\,\delta T), \tag{3}$$

$$R_{xx} = R_x + \Delta R_x. \tag{4}$$

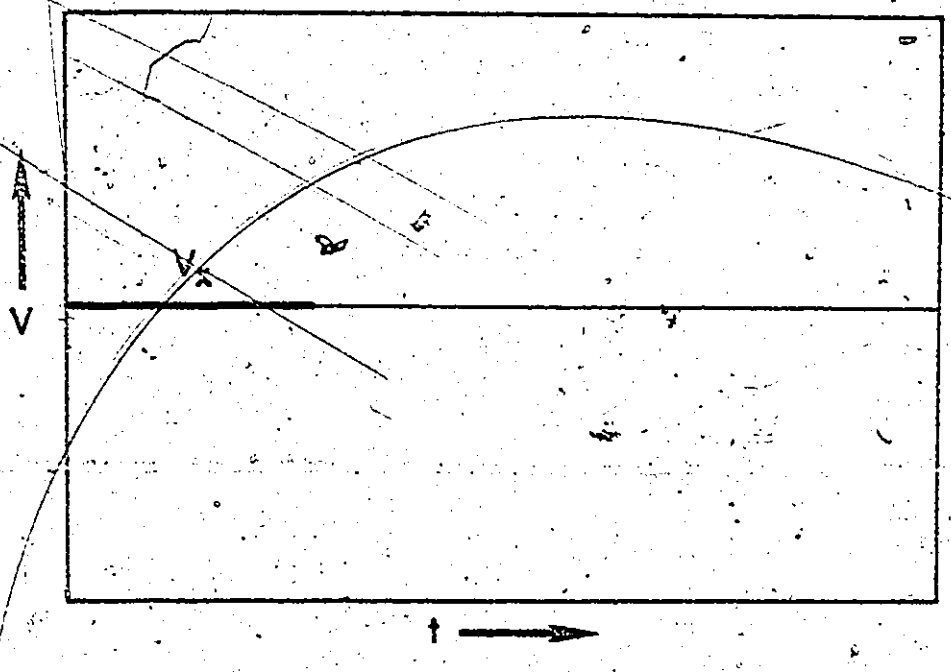

(a) V_x RECORDING

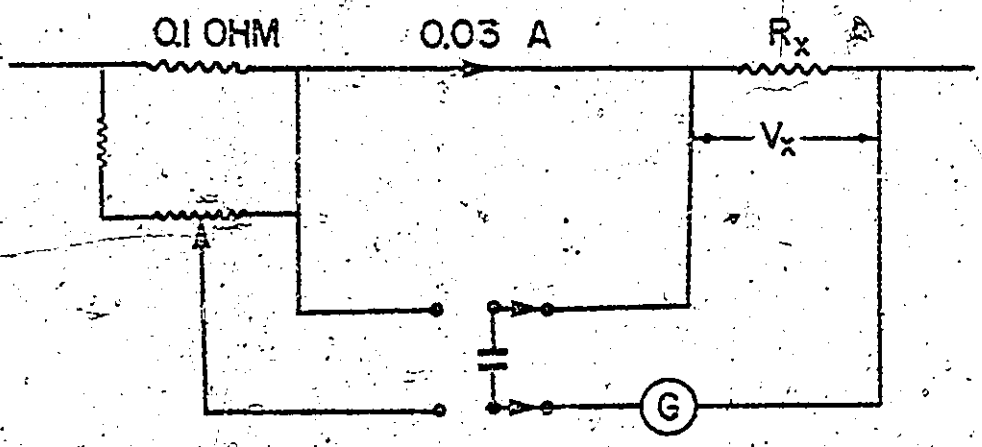

(b) V_x MEASURING

FIG. 16 NULL-POINT RECORDING

where R_x is the original resistance,

R_{xx} is the new resistance,

a is a temperature coefficient of resistance $= 4(10^{-3})$ (deg. C)$^{-1}$,

δT is the temperature change, and

$\Delta R_x = R_x a\, \delta T$ is the change in resistance.

Consequently, the voltage drop across the sensor increased and the galvanometer no longer remained at the null. The increase in voltage due to the increase in the resistance was recorded on the chart as a function of time as shown in Fig. 17a. The increase in voltage ΔV_x is equal to $I\, \Delta R_x$, where I is a preset value of 2 A, shown in Fig. 17b. Because of the possibility of a change in the magnitude of the heating current between one experiment and another, every self-heating curve was calibrated at the end of the 60-second period. This was accomplished by making a known change in the potentiometer setting, Δr_{cal}, and recording the corresponding deviation, ΔV_{cal}, on the chart, as shown in Fig. 17a. Since, the current remains unchanged for ΔV_x and ΔV_{cal}, we have

$$\Delta V_x = \Delta R_x\, \Delta V_{cal}/\Delta R_{cal} \qquad (5)$$

Thus, values of ΔV_x versus t for a particular self-heating response are obtained from the curve similar to one shown in Fig. 15a. Relation between ΔV_x and δT could now be obtained as follows:

$$\Delta R_x = R_x a\, \delta T \quad \text{, from Eqs.(3) and (4)} \qquad (6)$$

$$\Delta R_x = \Delta R_{cal} \Delta V_x/\Delta V_{cal} \text{, from Eq.(5)} \qquad (7)$$

Equating (6) and (7), and simplifying,

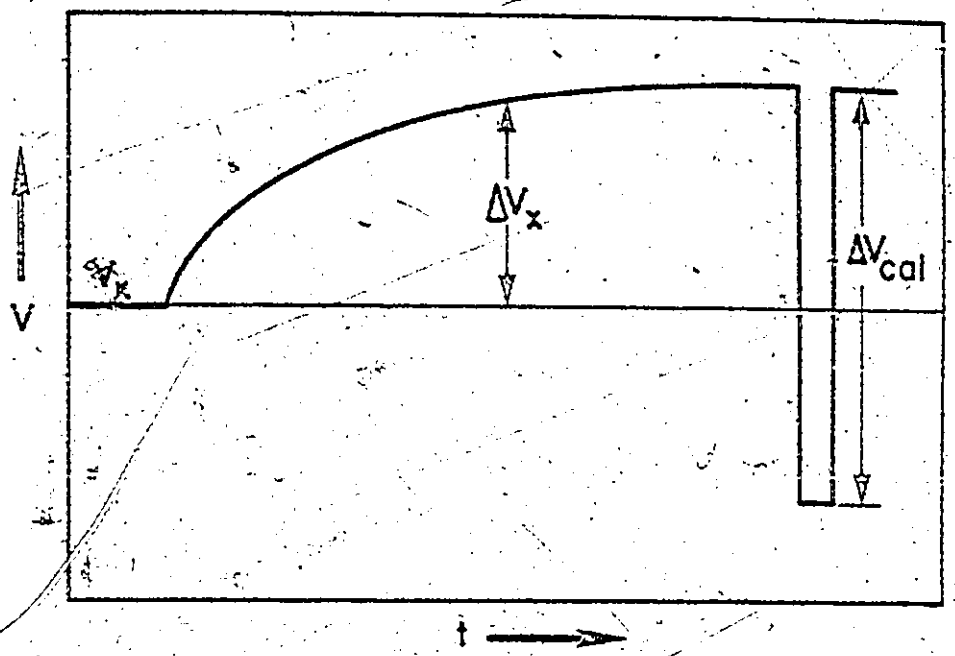

(a) ΔV_x RECORDING

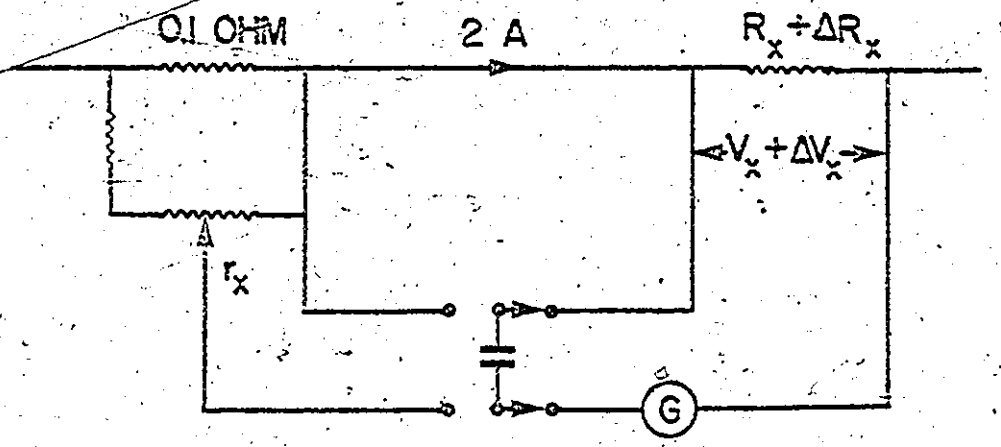

(b) ΔV_x MEASURING

FIG. 17 RECORDING OF A SELF-HEATING RESPONSE

$$\delta T = (\Delta R_{cal}/R_x)(\Delta V_x/a\Delta V_{cal}) . \quad (8)$$

But, $\Delta R_{cal}/R_x = \Delta r_{cal}/r_x$, from Eq.(2)

Therefore, $$\delta T = (\Delta r_{cal}/a\, r_x \Delta V_{cal})\Delta V_x . \quad (9)$$

Substituting the value of a and dropping the subscript x, we have

$$\delta T = (250\, \Delta r_{cal}/r\, \Delta V_{cal})\Delta V . \quad (10)$$

Thus, the increase in temperature of a sensor due to self-heating could also be obtained experimentally as a function of ΔV, and in turn, as a function of time t.

3.7 MOISTURE INJECTION:

After a set of experiments with the dry specimen was over the test stack assembly was completely uncovered by removing the bell jar, the shroud, and the Styrofoam. The top heat sink was raised and the top auxiliary heater assembly removed from the top of the cell. The cell was now ready for moisture injection.

For moisture content of 1 per cent by weight, the total weight of the moisture to be injected was 19.71 g (19.71 cm^3). For 3 and 5 per cent, the respective volumes of water were 59.13 and 98.55 cm^3. There are three holes in the main heater assembly through which moisture was injected using a syringe as shown in Fig. 18. Equal amounts were injected through each of the three holes which were unscrewed one at a time.

After the desired amount of water was injected into the cell, the test stack assembly was again put together and covered with Styrofoam,

the shroud, and the bell jar, as before. The temperature of the assembly was raised to about 40 deg. C, and it remained at that level for two to three weeks. The resistance and the self-heating response of the copper wires were checked from day to day. When the specimen was observed to have reached a steady state with respect to the moisture and temperature distribution within it, the required tests were performed again as before.

FIG. 18a /SPECIMEN-CONTAINER AND SYRINGE

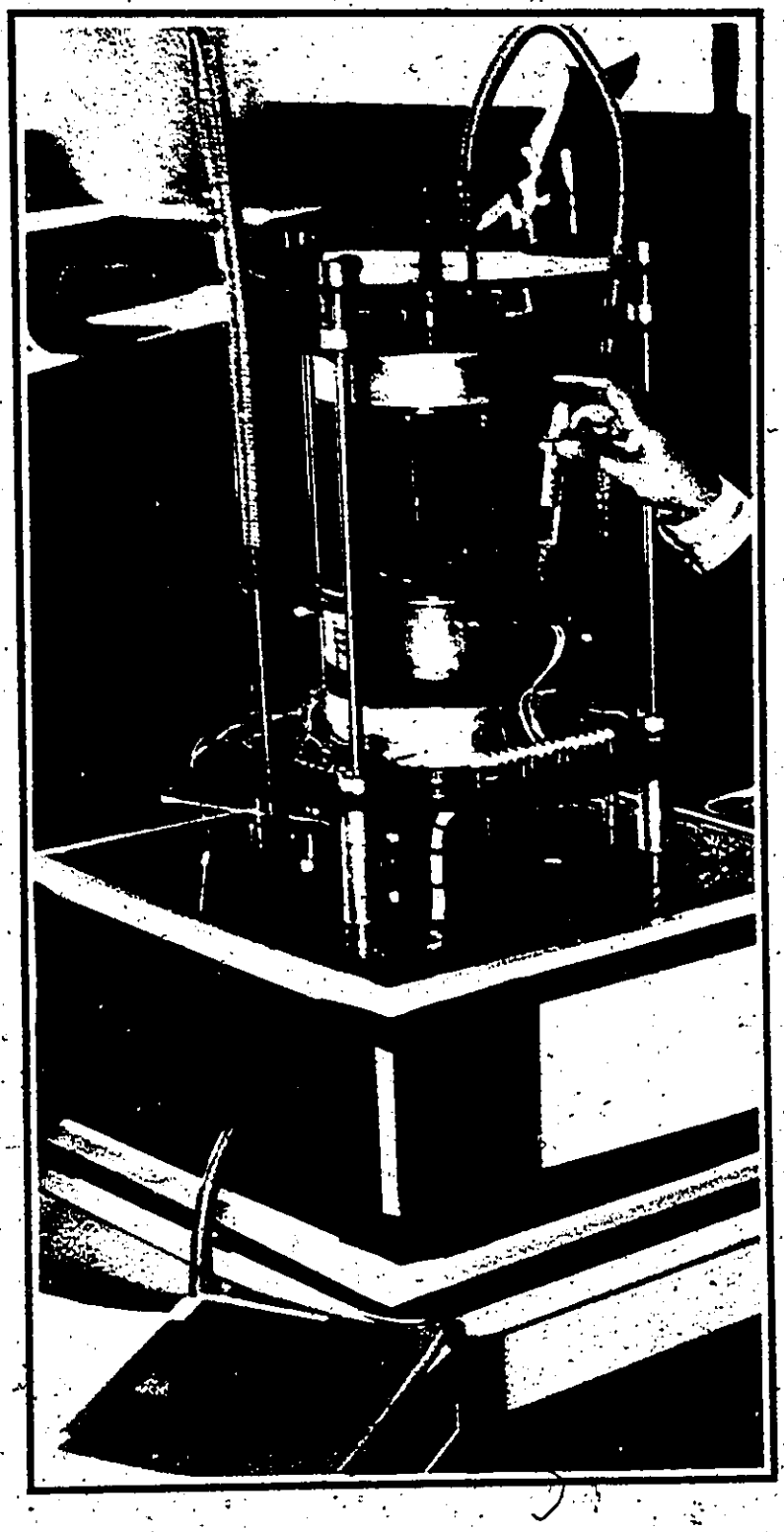

FIG. 18b MOISTURE INJECTION INTO THE SPECIMEN

Chapter IV

SPECIMEN MATERIAL

1. CHOICE OF SPECIMEN MATERIAL

In order to be able to compare our results with others, available in the literature and to facilitate an analytical study of the heat-flow mechanism involved, we had to choose a specimen material of standard description and simple geometry. A graded quartz sand from the Ottawa river (in the State of Illinois), commonly known as *20-30 Ottawa sand* was found to be suitable for this purpose.

Graded quartz sand is considered to be as good a standard in case of granular materials as is, for example, high purity copper in metals. Many investigators, for example Kersten (1949) and Woodside and Cliffe (1959), have used this sand as a specimen in their experiments in an attempt to correlate the thermal conductivity of granular materials with moisture content and temperature. The Ottawa sand particles, which are quite close to uniform spheres in shape, facilitated consideration of a simplified model to study the heat-flow mechanism.

The thermal conductivity of granular materials is known to be strongly dependent on density and grain size, besides being a function of moisture content and temperature (Kersten, 1949). Therefore, a detailed knowledge of these properties of the sand is essential in making the presentation of the results of experimentation complete, meaningful, and useful.

2. STRUCTURE AND MINERAL COMPOSITION

Quartz (silicon dioxide, also known as silica) can exist in many different forms. Of these, two main forms are amorphous or glassy and crystalline. These two forms differ radically in their behavior. The thermal conductivity of amorphous quartz is low at low temperature and increases with the temperature, whereas that of crystals is high and decreases with increasing temperature. To illustrate this, Table 1 gives the thermal conductivity of quartz (SiO_2) in amorphous (glassy) and crystalline phase, the latter for conduction normal and parallel to the main crystallographic axis. These values are taken from Jakob (1958).

TABLE 1

Comparison between the conductivities of fused and crystalline quartz

Temperature (deg. C)	λ (W/m-K)		
	Quartz Glass (Fused Silica)	Quartz Crystal	
		Normal to axis	Parallel to axis
- 255			692
- 200	0.93	40	100
- 100	1.56	17	35
0	1.90	10	19
100	2.08	7	12
200	2.25		

The figures in this table are striking. At -200 deg. C the crystal conducts the heat 40 to 100 times better than the glass, and at 100 deg. C still 3 to 5 times better, depending upon the orientation of the heat flow with respect to the crystal axis. Thus, the structure of the quartz seems to dominate its thermal conductivity value very strongly. And therefore, it is necessary to know whether our sand is amorphous or crystalline.

A sample of our Ottawa sand was sent to the Department of Energy, Mines and Resources of Canada, in Ottawa, for examination. There a detailed analysis on this sample was carried out by Dr. C.M. Mitchell of Physical Metallurgy Division, using X-ray diffraction technique, which is at present considered to be the most powerful method of elucidating structure.

The experiments with X-rays constitute a search for signs of an orderly packing of atoms and ions within the structure of a particle. If a beam of X-rays of suitable wavelength (say between 1 and 2 angstron units, this unit being 10^{-8} cm) from an X-ray tube fitted with a pin-hole collimator system impinges upon a small fragment of solid material, each of the constituent atoms is disturbed by the radiation, and the result is a number of scattered radiations, one from each disturbed particle. If the material has a lattice structure, i.e. an orderly repetitive pattern of particles, there may be directions in which the weak waves from each of a particular series of regularly spaced particles reinforce each other to produce a relatively powerful scattered beam. Such reinforcement is

not achieved unless the piece of material is presented to the incident beam at a particular angle. Hence, if one places the piece of material at the center of a cylindrical strip of photograph film, fires the X-rays at it along one of the radii through a gap in the film, and then turns the material about in all possible directions, each time the angle of incidence suits a particular set of atoms there will be a more or less powerful scattered beam emerging in a direction which amounts to reflection at planes in which those atoms are found to lie. The end result is a pattern of lines on the developed film, the positions of which indicate the angles of reflection of the X-rays, exponents of the art can specify the structures of quite complicated crystals, including most of the known minerals (Cullity, 1967).

With the help of the technique just described it was concluded that the material is all crystalline. Amorphous silica, having no regular structure, does not have diffraction pattern but gives diffuse lines. Such diffuse lines were not observed, hence no sign of amorphous silica. Negligibly small amounts of impurities present in the material were identified as those due to compounds of Fe, Ca, K, Ti, and Na. The α-Quartz SiO_2 was identified as the major constituent of the material. This analysis also confirmed the mineral composition of the material suggested by its supplier: SiO_2 – 99.756 per cent, Fe_2O_2 – 0.020, Al_2O_3 – 0.080, TiO_2 – 0.014, CaO – 0.040, MgO – 0.020, other – 0.070.

3. PARTICLE SHAPE AND SIZE CHARACTERISTICS

Normally, particles are divided into five different groups (Lambe and Whitman, 1969), namely, angular, subangular, subrounded, rounded, and well rounded, as shown in Fig. 1. The particles of our Ottawa sand fall into the category of *well rounded*. It could be observed from Fig. 2, which is an enlarged photograph of several sand particles randomly chosen from the specimen material, that these particles are nearly spherical in shape.

The average diameter of the particles shown in Fig. 2 is about 0,8 mm. But what is important to know is not the size of that or other individual particles, it is the size distribution of the sample that matters. The usual and most practical method of analysing a sample of sand in order to find the proportions in which the grains of each size are present, is by sifting it through a series of sieves, beginning with the one having the largest aperture. The sample is passed successively through the sieves, and the separated material is weighed. Each weight is divided by the total weight of the sample in order to turn it into a percentage. For a visual presentation of these values, a diagram is usually constructed on a semi-logarithmic scale, in which the percentage weight of all that has passed through each sieve is plotted against the size of the sieve aperture.

The grain size analysis on a sample of our Ottawa sand was carried out by Mr. N.S. Verma of Civil Engineering Department at the University

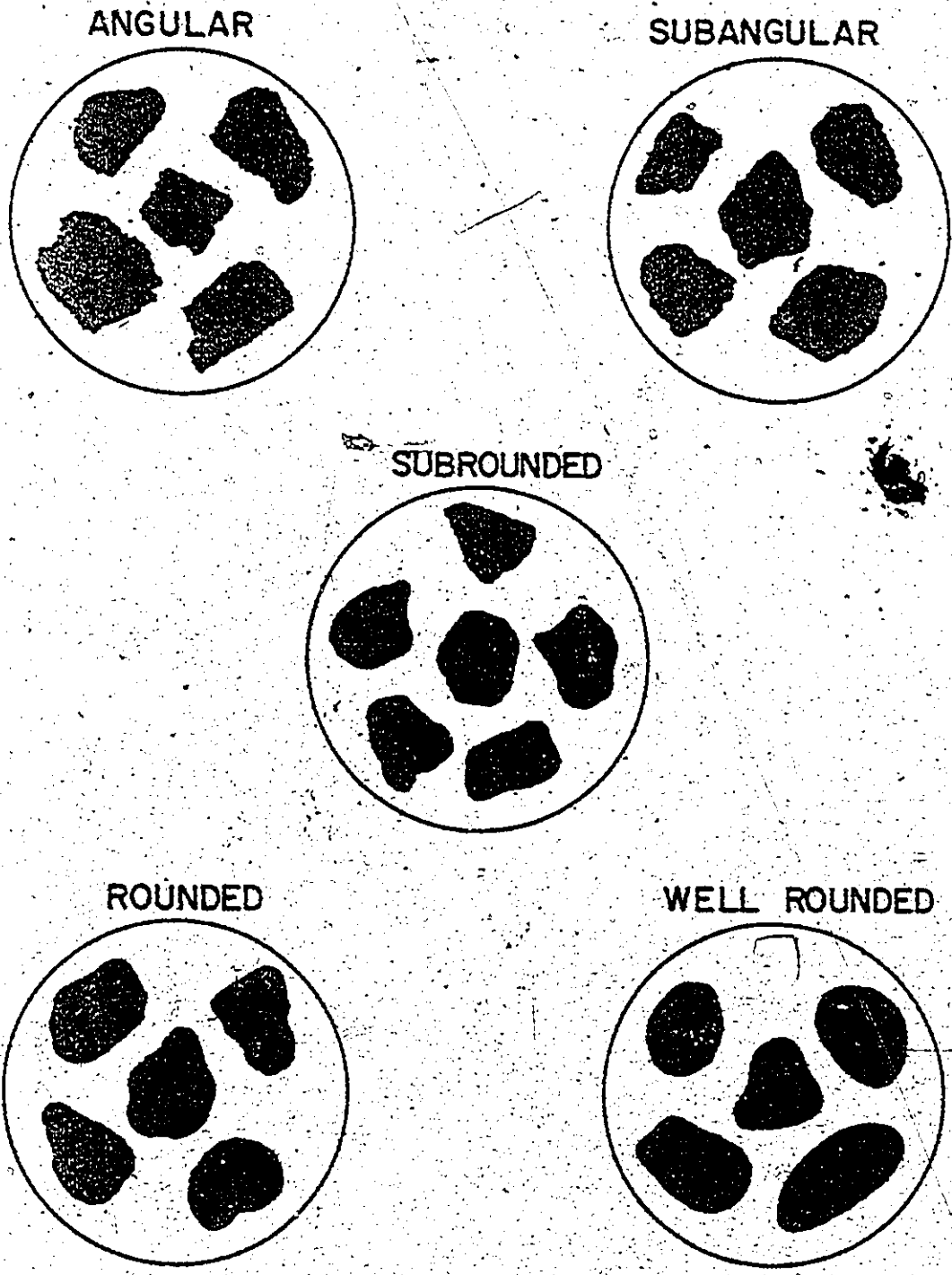

FIG. 1 DEGREE OF PARTICLE ROUNDNESS

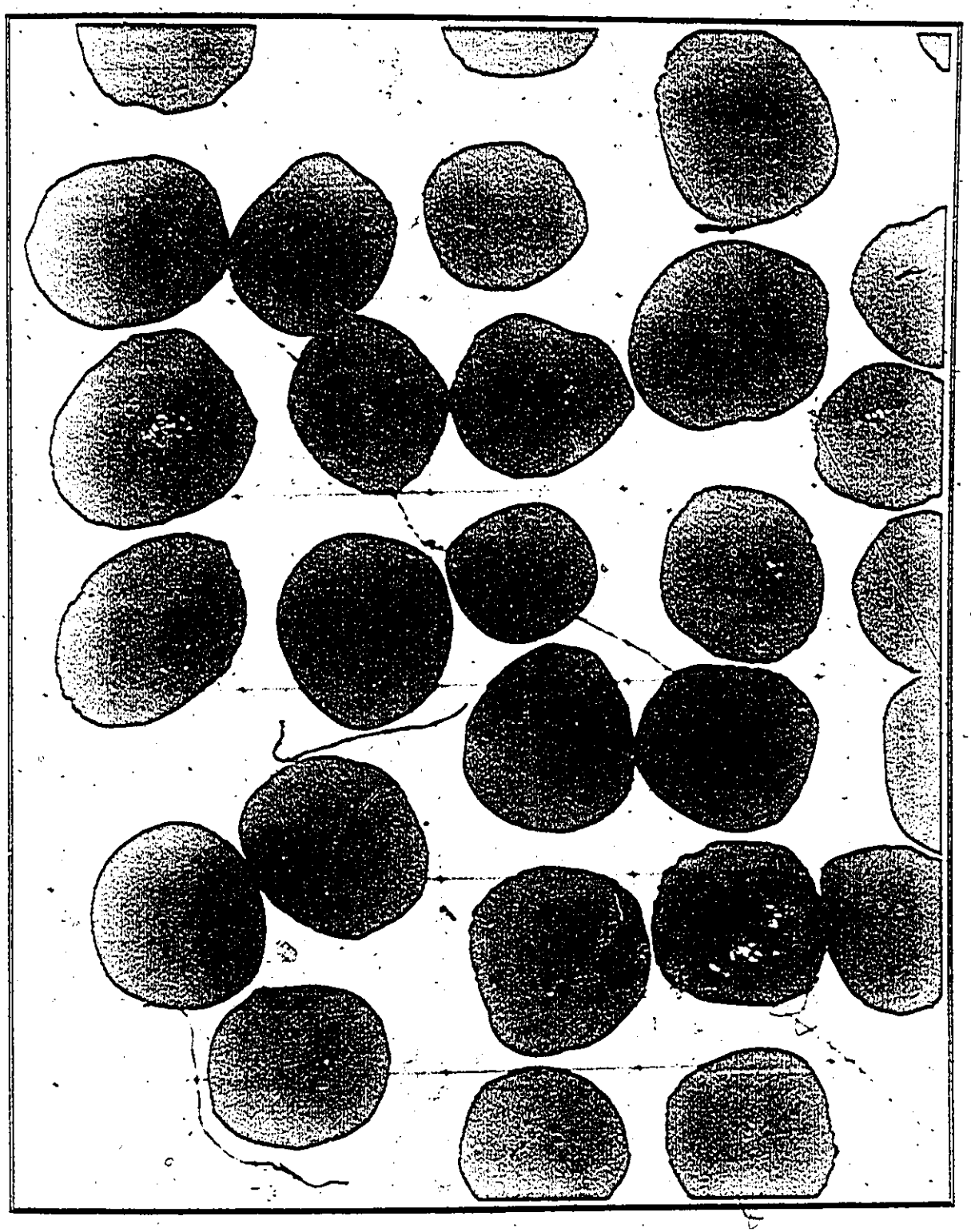

FIG. 2 20-30 OTTAWA SAND PARTICLES.
MESH SIZE: 1 mm SQUARE

of Ottawa. The results of analysis are presented in Fig. 3. As can be seen from this figure, the sample is very uniformly graded, diameter of about 80 per cent of the particles lying in the range from 0.75 to 0.85 mm. In general, the uniformity of a granular material is expressed by the uniformity coefficient, which is a ratio of D_{60} to D_{10}, where D_{60} is the particle diameter at which 60 per cent of the material weight is finer and D_{10} is the corresponding value at 10 per cent finer. A material having uniformity coefficient smaller than about 2 is considered uniform (Lambe and Whitman, 1969). The uniformity coefficient of our sand, calculated with the help of Fig. 3 is very close to unity, which suggests that our sand is very uniform in size.

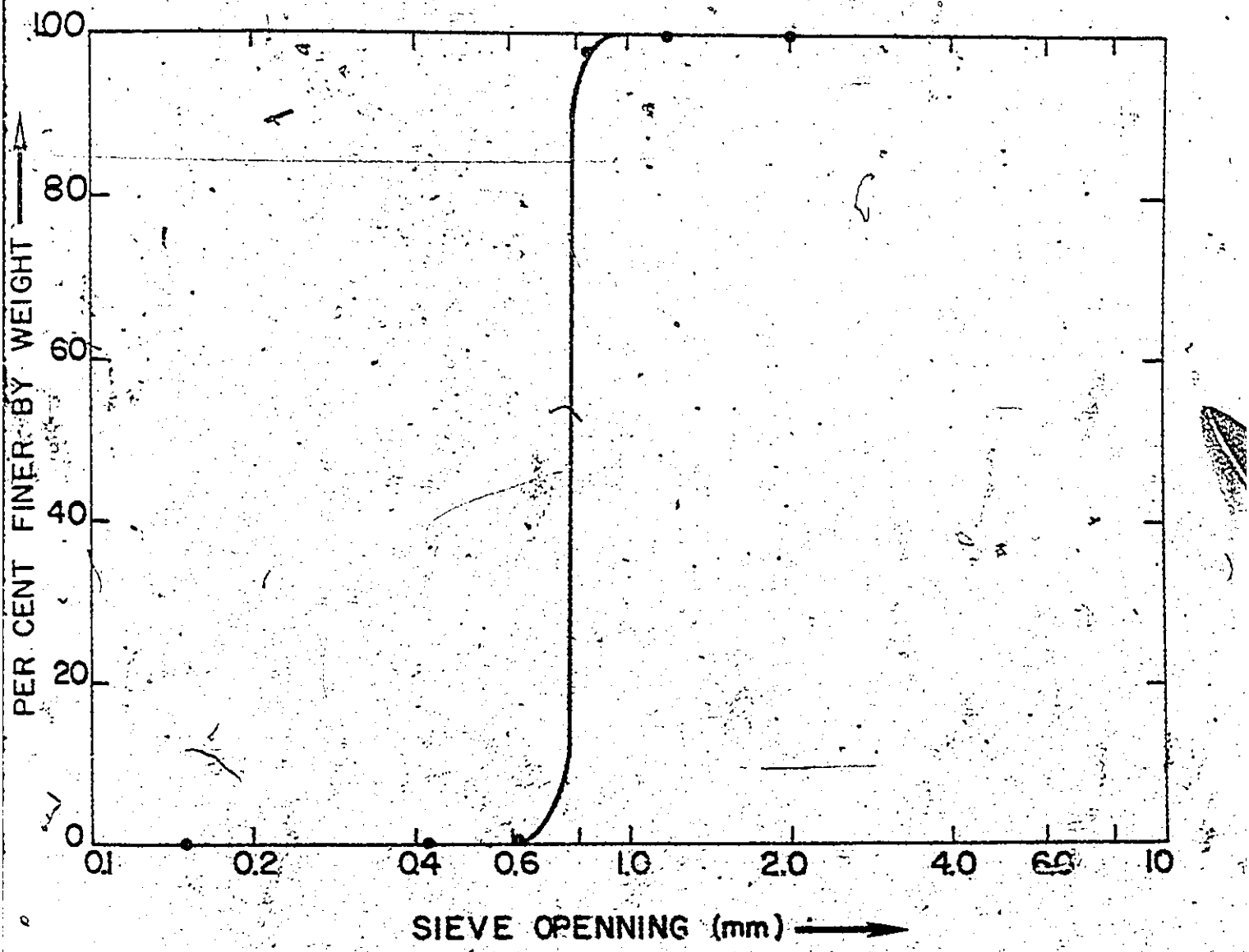

FIG. 3 GRAIN-SIZE DISTRIBUTION OF OUR 20-30 OTTAWA SAND

4. POROSITY AND DENSITY

Between the packed particles of granular material is an interstitial space which is continuous, that is, a path can be drawn from any point in it to any other point without leaving the space. This is a very different state of affairs from the discrete bubble nature of the air spaces in such materials as pumice or foam, which are known as cellular or porous materials. It is, however, a common practice to refer to the space between the particles in granular materials as the *pore space*, mainly because of the nature of these spaces -- consisting of caverns interconnected by narrower channels. Hence, the words, like pore, pore space, porous, porosity, etc. will be used hereafter with reference to granular materials. This is in accordance with usual practice, (cf.Childs, 1969).

The *porosity* P of a granular material is defined as a ratio of pore volume Vp, to the total volume V, or

$$P = V_p/V, \qquad (1)$$

and the *dry density* ρ of a granular material is defined as a ratio of weight of granular material W_s to the total volume V, or

$$\rho = W_s/V. \qquad (2)$$

The values of both porosity and density depend on packing of material particles. Dense packing gives large value of density and small value of porosity. These two values are also affected by the range of particle size. The smaller the range of particle size present (i.e., the more nearly uniform the soil), the smaller the particles, and the more angular the

particles, the smaller the dry density and larger the porosity (i.e., the greater the opportunity for building loose arrangement of particles). The greater the range of particle size present, the greater the dry density (i.e., the pores among the larger particles can be partially filled with smaller particles) and, thus, the smaller the porosity.

The processes of packing the material in our experimental cell and of obtaining the volume of the cell have been explained in Chapter III, Section 3.2. The volume of the cell is 1135 cm^3 and the weight of the sand packed in it is 1971 g. Hence, the dry density of the sand used is

$$\rho = 1.736 \text{ g/cm}^3. \tag{3}$$

The density of quartz is 2.65 g/cm^3, as taken from the Thermophysical Properties Research Center Handbook (Touloukian, 1966). The volume occupied by dry sand particles V_s, is, therefore

$$V_s = 743.8 \text{ cm}^3, \tag{4}$$

and that occupied by the pores is

$$V_p = V - V_s = 391.2 \text{ cm}^3. \tag{5}$$

Hence, the porosity of the sand in the cell is

$$p = 391.2/1135 = 0.345,$$

or

$$p = 34.5 \text{ per cent}. \tag{6}$$

5. CAPILLARITY

A liquid surface is capable of resisting a certain amount of tensile stress because of intermolecular attraction. We talk in this connection about *surface tension*. Similar attraction exists between molecules of the liquid and any solid surface with which it happens to be in contact. The magnitude of the latter may be greater or smaller than the former, and we shall be then faced with the phenomena of *wettability* or *non-wettability*, respectively. Thus, e.g., a drop of water will not spread on a non-wettable surface and will adopt the form shown in Fig. 4. The ratio of the diameter, D, of the drop to its height, H, for a given mass will depend primarily on the magnitude of its density versus its surface tension (though to some degree also on the actual weakness of the attraction between the solid and the liquid molecules). On the other hand, the same drop placed on a highly wettable surface will spread into a very thin layer.

Similar things could be said about the contact between two non-miscible liquids. Thus, in case of the surface tension being weak in relation to the mutual attraction between the molecules of the two liquids, e.g., a drop of lubricating oil placed on the surface of water, the oil will spread until its layer reaches a thickness of only a few molecules. By contrast, a drop of melted fat on the surface of a bowl of soup will form a lense which will not spread.

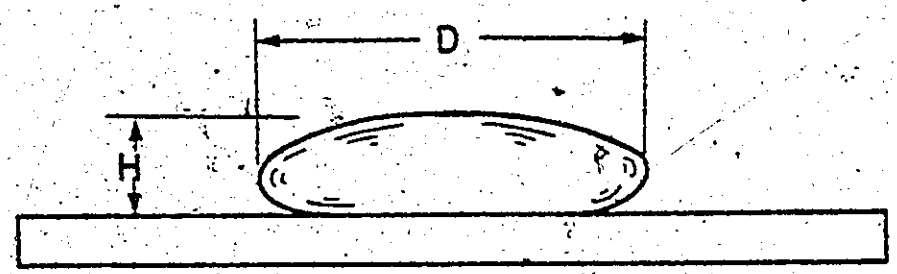

FIG. 4 A DROP OF WATER

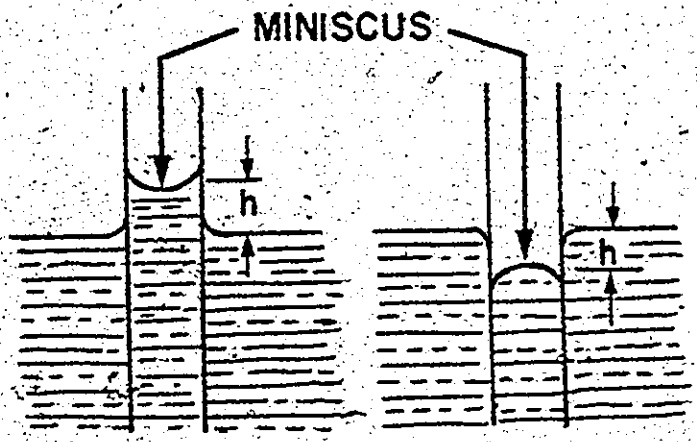

FIG. 5 CAPILLARY RISE & CAPILLARY DEPRESSION

The well-known phenomenon of *capillarity* is due to the surface tension combined with wettability or non-wettability, as the case may be. Fig. 5 shows what happens in the two cases.

Experiments have shown that water *wets* the surfaces of our granulated material and has, therefore, a tendency to climb in the pores. In other words, capillarity enables a dry sand to draw water to elevations above the free water surface; it also enables a draining sand mass to retain water above the free water surface. The height of water column which can be supported by any sand is dependent on the pore sizes besides being a function of some properties of the liquid, as explained before. In sand, unlike in fine bore tubes, the capillary walls form sharp angles and consequently the water creeps far above the normal capillary height (Carman, 1941). The time required for equilibrium to be reached greatly depends on the nature of sand as well as on the temperature to which it is subjected. The maximum height for which water is uniformly distributed when it is either allowed to rise or is drained out of sand similar to ours has been found by Lane and Washburn (1946) to be equal to about 6 cm. It, therefore, seemed reasonable at first to assume that the water will become uniformly distributed throughout the specimen of our sand, which is only 3.4 cm in height, if it were injected in several places and the whole specimen kept warm for a certain number of days. As already stated in Chapter II, Section 4, this has proved not to be the case in the numerous experiments performed within our temperature range.

6. UNFROZEN MOISTURE CONTENT

It is known that all the water in soils and other porous systems does not freeze at the same temperature and that the ice content gradually increases as the temperature is lowered (Lovell, 1957; Penner, 1963; Williams, 1964). Freezing of water in finely porous materials may take place over a range of temperatures reaching down to as far as 25 deg. C below zero. The greatest depression of the freezing point below zero occurs in water that is most firmly held and is closest to the grains. The main factors thought to control the amount of liquid water in frozen porous materials are mineral type, kind of exchangeable ions and pore size distribution. Naturally, the salt conteht of the pore water has a major influence on its freezing point irrespectively of any other factors. In general, fine-grained materials contain more unfrozen water at a given temperature below 0 deg. C than do coarse-grained materials.

Since some experiments with the specimen material were performed at different moisture levels and below freezing point of water, it seemed interesting to know the relationship between the temperature and the amount of unfrozen moisture. If the amounts of unfrozen moisture proved to be significant, this would be important for the analysis of the experimental results as well as for the analytical study of the heat-flow mechanism in the specimen, because the conductivity values of ice and water are widely different. The thermal conductivity of water increases with temperature, whereas that of ice decreases with increasing temperature, and at 0 deg. C the conductivity of ice is nearly four times greater than

that of water.

A dry sample of 20-30 Ottawa sand was sent to the Department of Geography and Geotechnical Science at Carleton University, Ottawa to determine the temperature of initial ice formation (freezing point) and unfrozen water content versus temperature relationship for the overall moisture contents of 1, 3, and 5 per cent by dry weight. Dr. P.J. Williams had these tests performed, and using his pressure plate technique, described in Properties and Behaviour of Freezing Soils (Williams, 1967) and in Richards and Fireman (1943), produced results in the form of graphs shown in Figs. 6, 7, and 8, for 1, 3, and 5 per cent moisture content, respectively. The graphs are drawn for unfrozen water content versus temperature (below 0 deg. C). The difference between the unfrozen water content and the initial water content is the ice content at a given temperature.

The conclusion of Dr. Williams' experiments on the 20-30 Ottawa sand was that because of its coarse porous nature this sand has extremely small quantities of water remaining unfrozen at temperatures lower than a few thousandths of a degree below zero. For all practical purposes, almost all the water in our sand at its various moisture levels can be said to freeze at 0 deg. C. Negative outcome of such investigations is as important as a positive one in the sense that it shows that a particular consideration has not been overlooked.

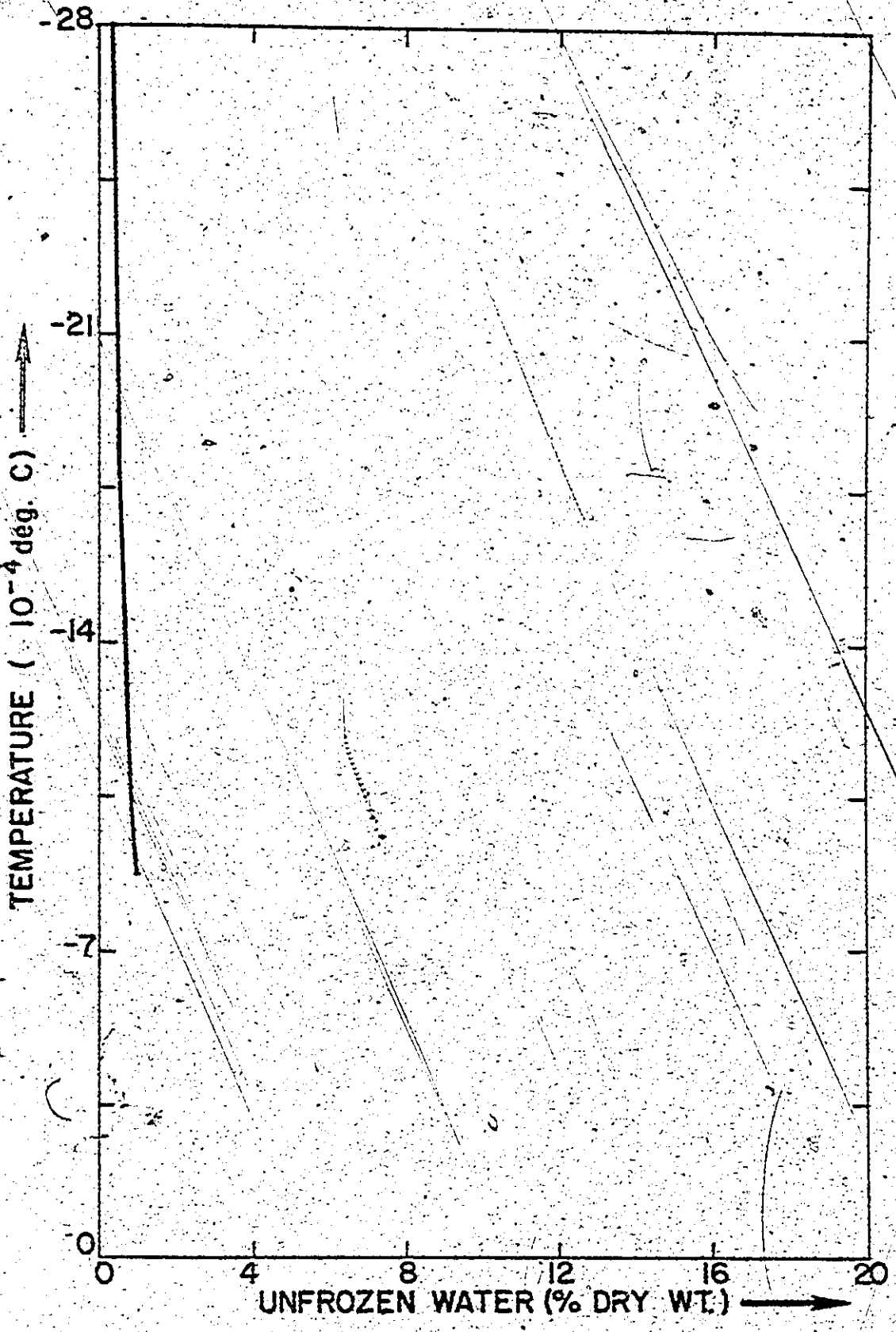

FIG. 6 UNFROZEN WATER CONTENT FOR <M> = 1 %

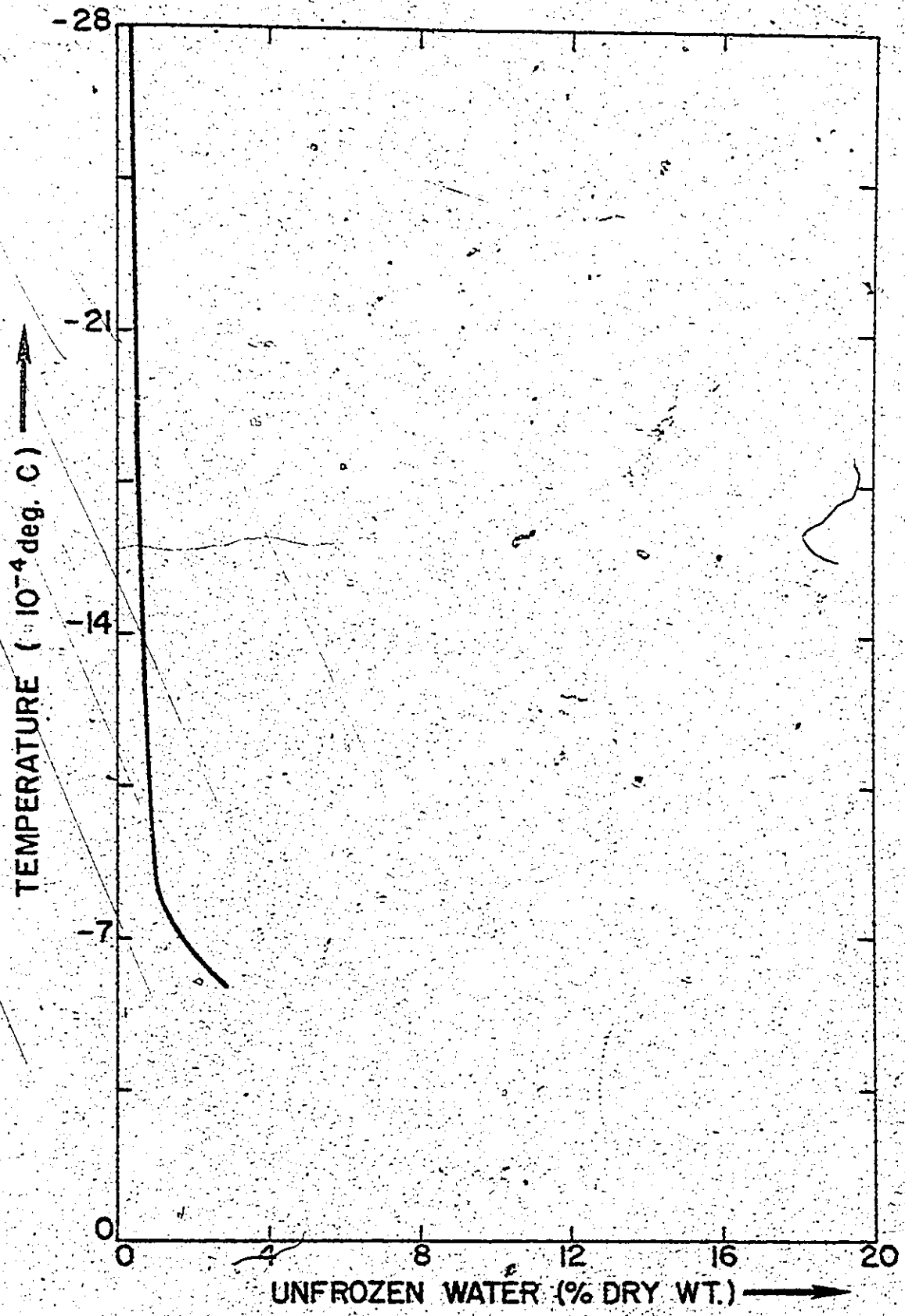

FIG. 7 UNFROZEN WATER CONTENT FOR <M> = 3%

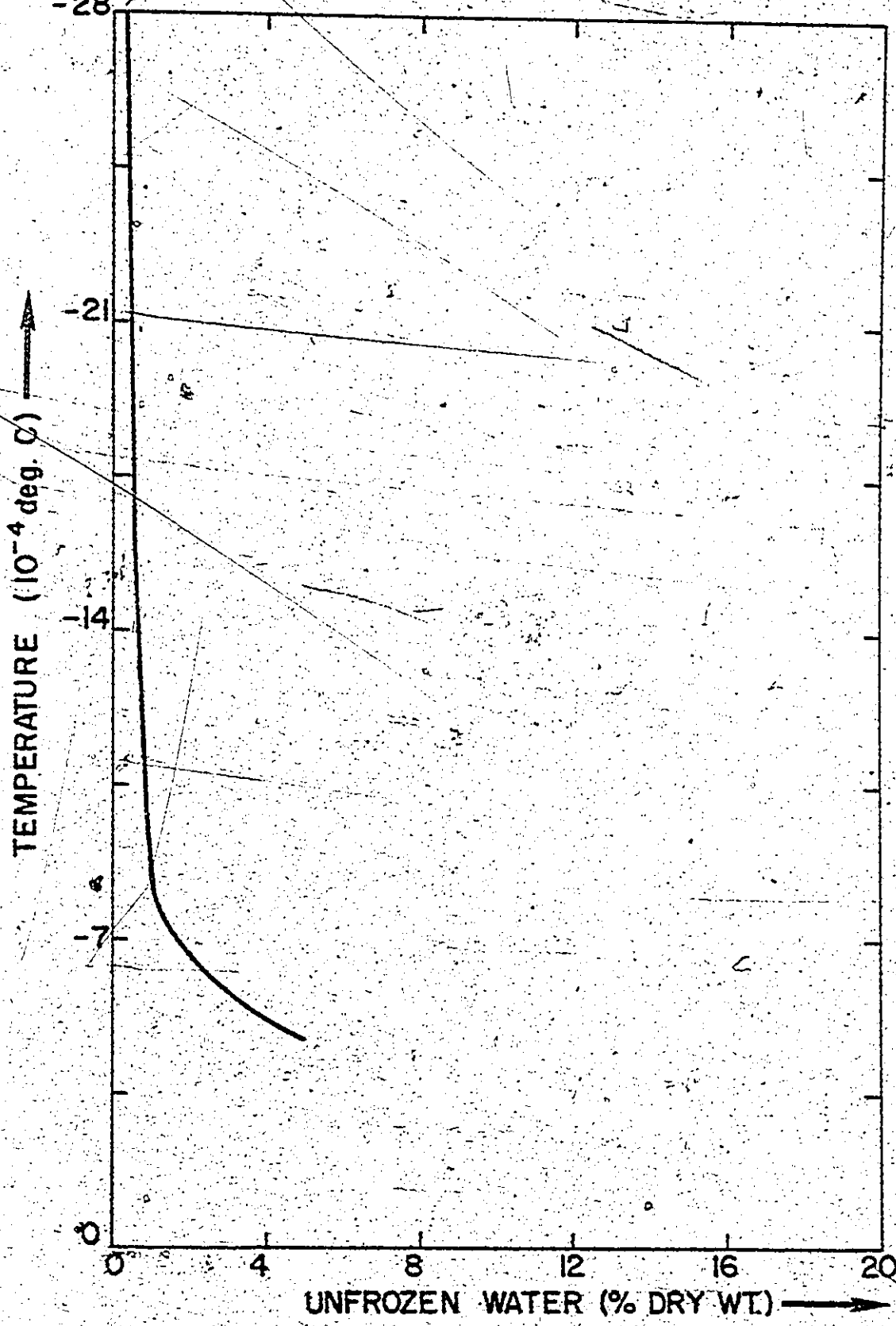

FIG. 8 UNFROZEN WATER CONTENT FOR <M> = 5 %

Chapter V

EXPERIMENTAL RESULTS AND ANALYSIS

1. CONDUCTIVITY CALCULATIONS

Measurements of ΔT_o and ΔT_q were performed as explained in Chapter II on page 21. In every case these values were calculated separately for the upper and the lower part of the specimen, i.e. between the upper and the middle wire and between the middle and the lower wire, respectively. These temperature differences, therefore, in addition to the subscripts o or q will have to carry subscripts 1 for the upper and 2 for the lower part of the specimen.

Experiments performed for 0, 1, 3 and 5 per cent moisture content, yielded two base lines for each, one for the upper and one for the lower part of the specimen. The equations of these eight base lines are tabulated in Table 1. These lines were fitted between experimental points by the least square method (see Appendix D, Section 2).

Gradient tests, performed on the sample, gave the temperature differences, ΔT_{q_1} and ΔT_{q_2}, for the upper and the lower part of the specimen.

These were obtained, as were ΔT_{o1} and ΔT_{o2}, for the various moisture contents and within the temperature range of our interest. The temperature differences, ΔT, to be used in the calculations of the conductivities, were obtained by subtracting ΔT_o from ΔT_q at the same mean temperature.

With fixed values of the area of cross-section of the specimen of 8.107 (10^{-3}) m^2 and the separation of the sensors of 8.763 (10^{-3}) m. (same for both, the upper and the lower parts of the specimen), as mentioned on page 18, and with the values of the heat flows as obtained from the gradient tests, the thermal conductivity of the specimen was calculated for each test. A step-by-step procedure of these calculations in form of a typical example, is given, in Appendix D, Section 3.

The results of calculations of thermal conductivity are presented in Tables 2, 3, 4, and 5 in Appendix D for overall moisture contents of 0, 1, 3, and 5 per cent, respectively. The thermal conductivities of the specimen, only those with 0 per cent moisture content are plotted here in Fig. 1. The figure shows a variation of λ_1 and λ_2 versus temperature for the dry specimen in a temperature range from -15 to 40 deg. C. The results show that the conductivity within this range varies linearly with temperature, the slope being about 14 mW/m-K^2.

The conductivities of the specimen with 1, 3, and 5 per cent moisture contents could not be plotted in a similar manner since the local moisture contents to which these conductivities correspond had not been known at this stage. Equation (17) on page 33 was used to calculate these

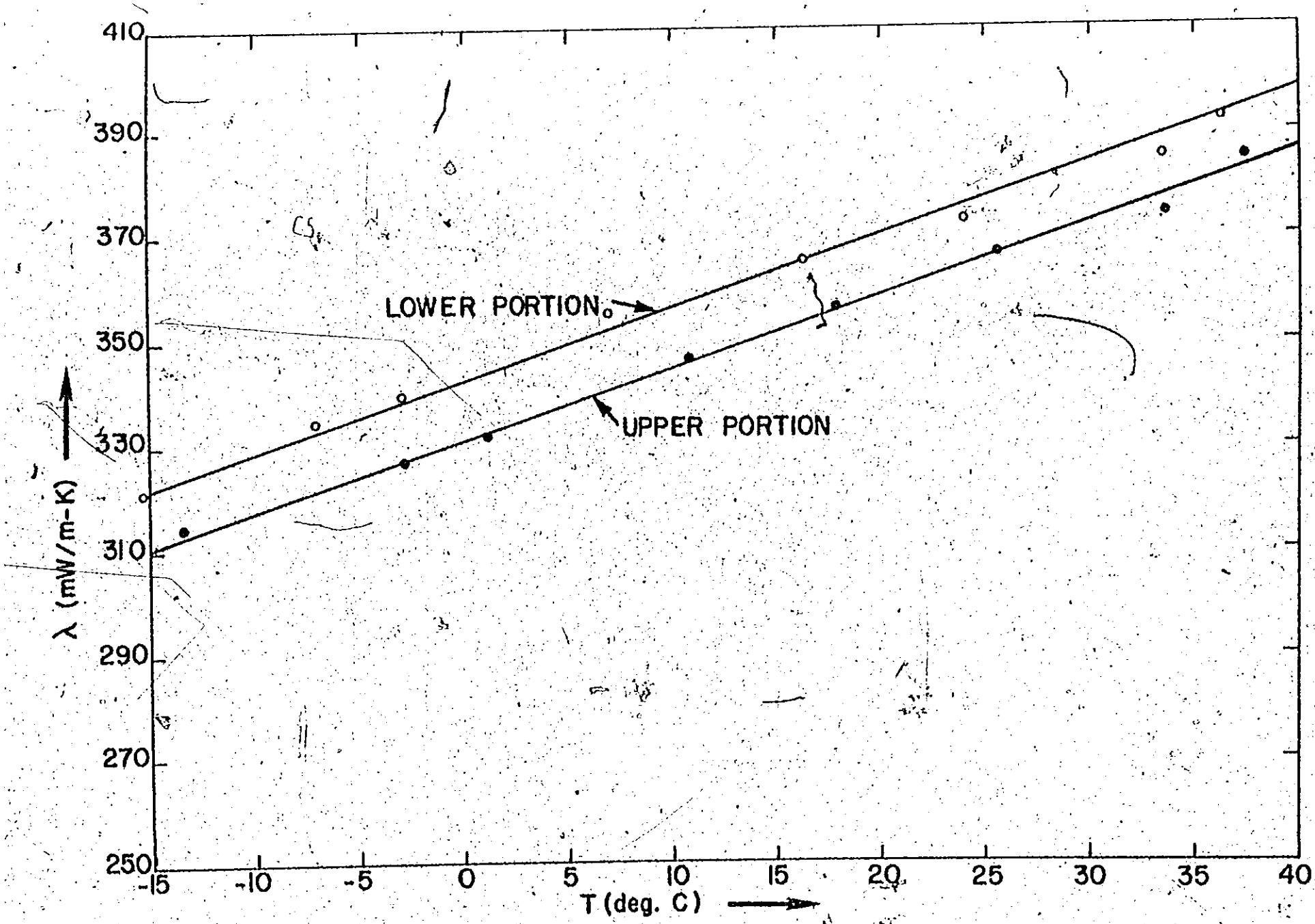

FIG. 1 THERMAL CONDUCTIVITY VERSUS TEMPERATURE OF THE DRY SPECIMEN

unknown local moisture contents. The unknowns b, d, and n, appearing in that equation had to be evaluated before putting the equation to this use. The following section deals with the evaluation of these constants. In doing so, the distributions of moisture contents under isothermal conditions are also obtained.

TABLE 1

Equations of the base lines

Moisture content, <M>	Equations of the base lines
0	$\Delta T_{o_1} = -0.08834 - 0.00196\ T$
	$\Delta T_{o_2} = -0.12467 - 0.00143\ T$
1	$\Delta T_{o_1} = -0.02674 - 0.00037\ T$
	$\Delta T_{o_2} = -0.09640 - 0.00035\ T$
3	$\Delta T_{o_1} = -0.03107 - 0.00024\ T$
	$\Delta T_{o_2} = -0.12046 - 0.00116\ T$
5	$\Delta T_{o_1} = -0.04022 - 0.00120\ T$
	$\Delta T_{o_2} = -0.12673 - 0.00121\ T$

2. MOISTURE CALIBRATION ANALYSIS

From the self-heating responses of the copper wires under isothermal conditions at various combinations of temperature and overall moisture content, the values of C, which as explained on page 24 is one of the parameters describing a self-heating response of a copper wire, were obtained. Three plots, similar to Fig. 5 in Chapter II, were obtained for the three copper wires. The experimental points along with the best straight lines drawn through them are shown in Figs. 2, 3, and 4, for the top, middle, and bottom copper wires, respectively.

As mentioned in Chapter II, page 29 originally it was thought that at every isothermal temperature of the specimen a uniform condition of moisture in the specimen would prevail. But later, from the study of Figs. 2, 3, and 4, it was concluded that this was not the case. This conclusion followed from the fact that for identical copper wires under identical condition of the surrounding material, it is reasonable to expect a very similar, if not identical, behavior of the copper wires on their self heating. Variation of C from wire to wire by order of magnitude suggested that the wires were not subjected to identical surrounding conditions.

The actual distribution of moisture was evaluated with the help of Eq.(17) developed in Chapter II and repeated here for convenience,

$$M(x) = \left[\frac{-b + \sqrt{b^2 - 4d\left[C(x)/CD(x) - 1\right]}}{2d}\right]^{1/n} \qquad \text{(17 rep.)}$$

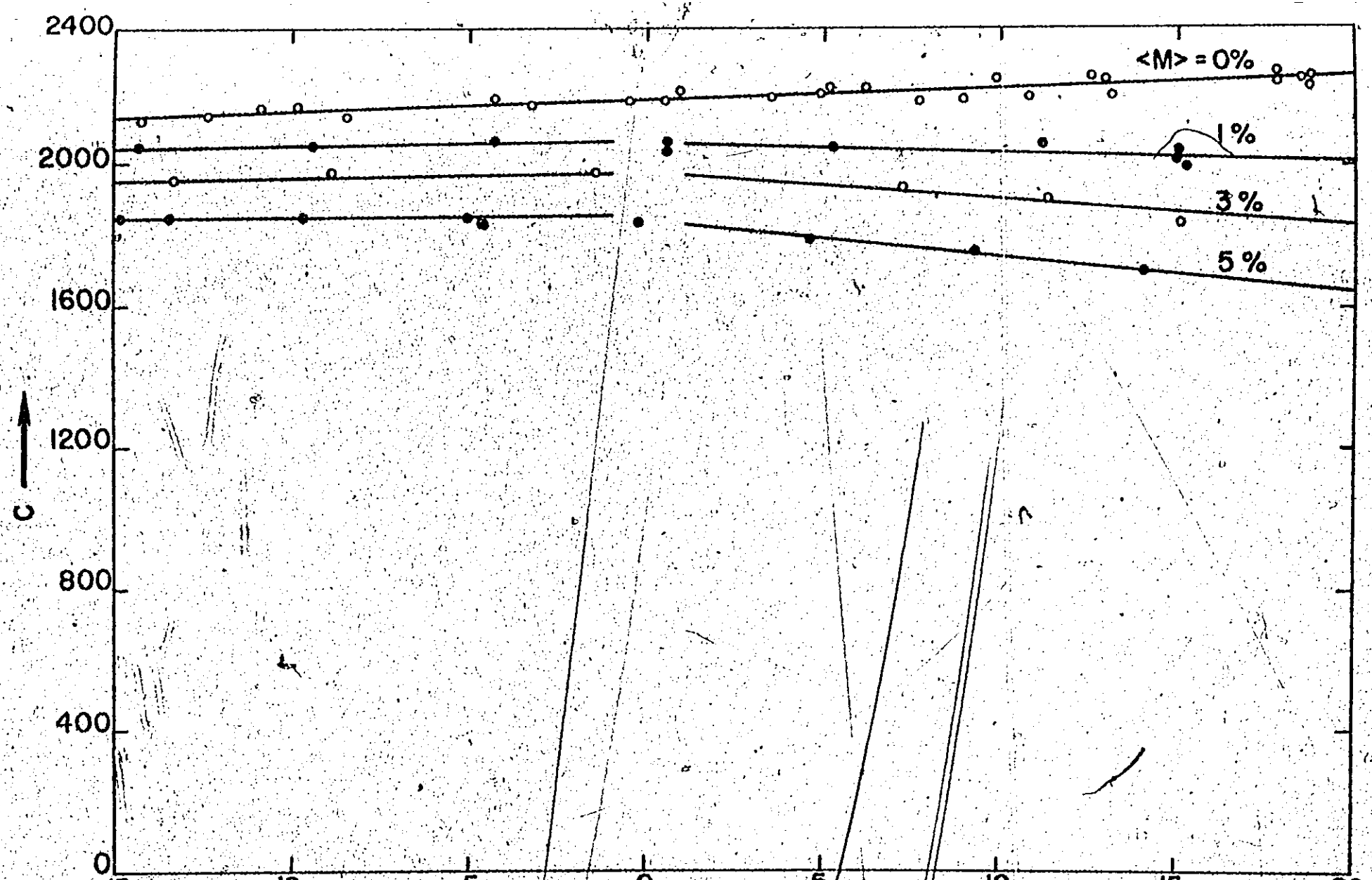

FIG. 2 PARAMETER C AS A FUNCTION OF T AND <M> : TOP COPPER WIRE

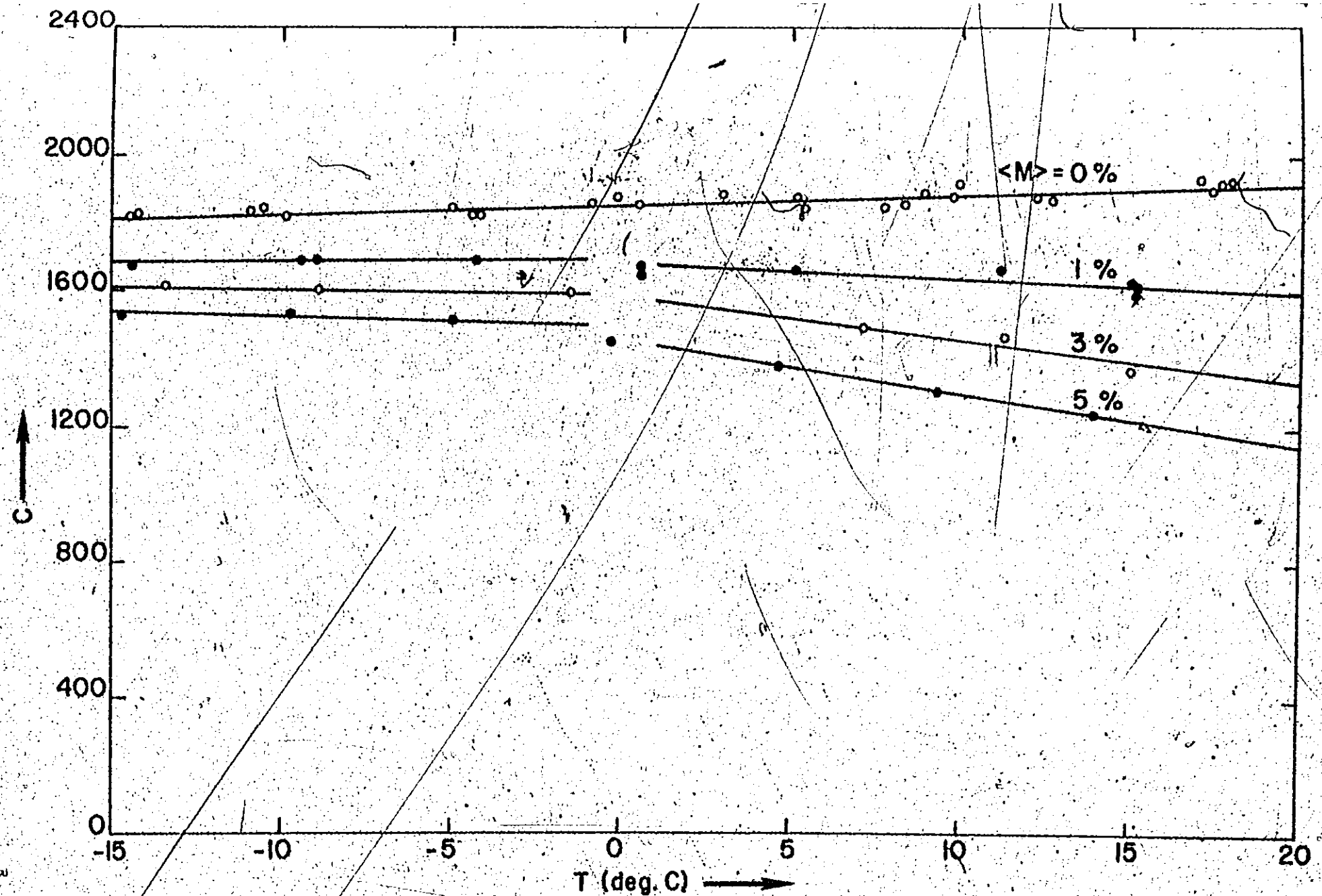

FIG. 3 PARAMETER C AS A FUNCTION OF T AND $\langle M \rangle_o$: MIDDLE COPPER WIRE

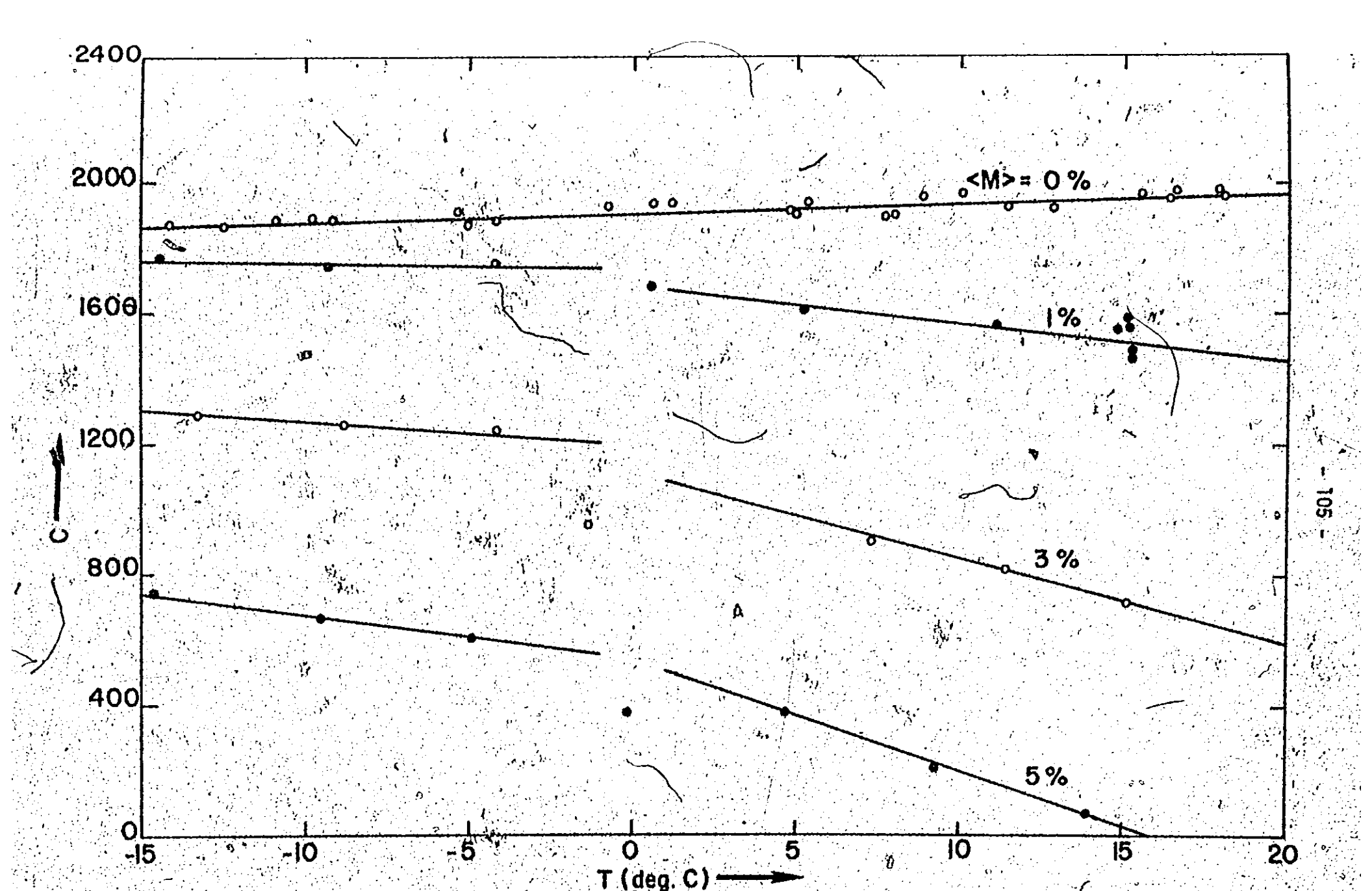

FIG. 4 PARAMETER C AS A FUNCTION OF T AND <M> : BOTTOM COPPER WIRE

For this evaluation the values of the parameters, C(x) and CD(x), to be used in the above equation were obtained from Figs. 2, 3, and 4, and are shown in Table 2. By the procedure explained in the analysis in Chapter II on page 34, the values of the constants b, d, and n were determined. With these, the values of M(x) for the three levels in the specimen were calculated. The analysis was tested by computing the values of <M> (Eq.(24), Chapter II) at various temperatures and comparing them with the known values of the overall moisture contents. The minimum error, δ, defined by Eq.(25), on page 34, was also calculated.

The results of the above computation are presented in Table 3. The maximum value of the error δ, in most cases is less than 0.008, and in two cases it is about 0.03. As can be seen from the results of this analysis, the overall moisture content was predicted with an accuracy of better than 0.1 per cent of moisture in majority of the cases.

The values of b, d, and n in Table 3 were expressed as a function of temperature in the following manner:

For T below 0 deg. C:

$$b = 0.065 + 0.0015\ T\ , \qquad (1)$$

$$d = 0.0009 - 0.0001\ T, \qquad (2)$$

$$n = 1.2. \qquad (3)$$

For T above 0 deg. C:

$$b = 0.074 + 0.0060\ T, \qquad (4)$$

$$d = 0.0095 - 0.0006\ T, \qquad (5)$$

$$n = 0.9. \qquad (6)$$

TABLE 2

Parameters C(x) and CD(x) under isothermal conditions

Isothermal Temperature (deg. C)	Known <M>	Parameter C	Location of the copper wires		
			Top x=1	Middle x=0	Bottom x= -1
-15	0	CD(x):	2140	1820	1860
	1	C(x):	2060	1700	1760
	3		1960	1620	1300
	5		1850	1550	740
-10	0	CD(x):	2150	1830	1870
	1	C(x):	2060	1700	1750
	3		1960	1620	1260
	5		1850	1540	680
- 5	0	CD(x):	2160	1840	1890
	1	C(x):	2060	1700	1740
	3		1970	1600	1230
	5		1850	1520	600
- 1	0	CD(x):	2180	1860	1900
	1	C(x):	2060	1700	1740
	3		1970	1600	1200
	5		1850	1510	550
1	0	CD(x):	2180	1860	1910
	1	C(x):	2060	1680	1670
	3		1970	1580	1100
	5		1830	1460	510
5	0	CD(x):	2200	1870	1920
	1	C(x):	2050	1660	1620
	3		1940	1520	980
	5		1790	1380	370
10	0	CD(x):	2220	1880	1930
	1	C(x):	2040	1640	1570
	3		1910	1460	850
	5		1740	1300	200
15	0	CD(x):	2240	1900	1940
	1	C(x):	2020	1620	1510
	3		1880	1400	720
	5		1690	1220	60

TABLE 3

Results of analysis for moisture distribution under isothermal conditions

Isothermal Temperature (deg. C)	b	d	n	δ	Known <M>	Calculated <M>	Calculated M(x)		
							M(1)	M(0)	M(-1)
-15	0.0425	0.0024	1.2	0.0335	1	0.89	0.86	1.15	1.35
					3	3.15	1.63	1.99	4.09
					5	5.00	2.33	2.49	6.41
-10	0.0500	0.0019	1.2	0.0213	1	0.92	0.84	1.19	1.29
					3	3.12	1.53	1.87	4.08
					5	4.96	2.18	2.40	6.46
- 5	0.0575	0.0014	1.2	0.0013	1	0.99	0.82	1.23	1.27
					3	3.00	1.38	1.90	4.06
					5	4.97	2.05	2.38	6.60
- 1	0.0635	0.0010	1.2	0.0009	1	0.99	0.88	1.24	1.27
					3	3.00	1.39	1.88	4.05
					5	4.97	2.00	2.38	6.65
1	0.0800	0.0089	0.9	0.0046	1	0.99	0.61	1.09	1.41
					3	3.05	1.08	1.68	4.33
					5	4.96	1.79	2.36	6.83
5	0.1040	0.0065	0.9	0.0081	1	1.02	0.60	1.02	1.43
					3	3.08	1.07	1.72	4.41
					5	4.97	1.72	2.42	6.94
10	0.1340	0.0035	0.9	0.0029	1	0.99	0.56	0.92	1.39
					3	3.05	1.02	1.69	4.41
					5	5.00	1.63	2.38	7.06
15	0.1640	0.0005	0.9	0.0023	1	1.01	0.56	0.89	1.39
					3	3.02	0.97	1.68	4.40
					5	4.96	1.56	2.36	7.06

3. CONDUCTIVITY AS A FUNCTION OF TEMPERATURE AND MOISTURE

From the self-heating responses of the three copper wires under gradient conditions the values of the parameter C, described in Chapter II, page 24, were calculated at various combinations of temperature and overall moisture contents. The tests on the dry specimen gave the values of $CD(x)$ for $x = 1$, $x = 0$, and $x = -1$ as a function of temperature. Similarly, the tests on the wet specimen gave values of $C(x)$ for $x = 1$, $x = 0$, and $x = -1$ as a function of temperature at each of the known values of $\langle M \rangle$. With these values, the corresponding local moisture contents, $M(x)$, were calculated using Eq.(17), as discussed in Chapter II, page 30. Results of these calculations appear in Tables 6, 7, and 8 in Appendix D. These tables also show the values of temperatures, T_1 and T_2, and moisture contents, M_1 and M_2, which were obtained simply by taking arithmatic means of the adjacent $T(x)$ and $M(x)$, respectively.

The results of the calculations of conductivity as a function of temperature, and moisture content as a function of temperature were combined together and are presented in Table 4. Subscript 1 refers to the values for the upper part of the specimen and 2 to the lower, as already mentioned earlier. The values of T and M in this table are rounded up to one digit after the decimal point.

Formulation of an empirical relation correlating λ with T and M was attempted by plotting these values and fitting appropriate curves through them. Such plots are shown in Figs. 5 and 6, for the upper and

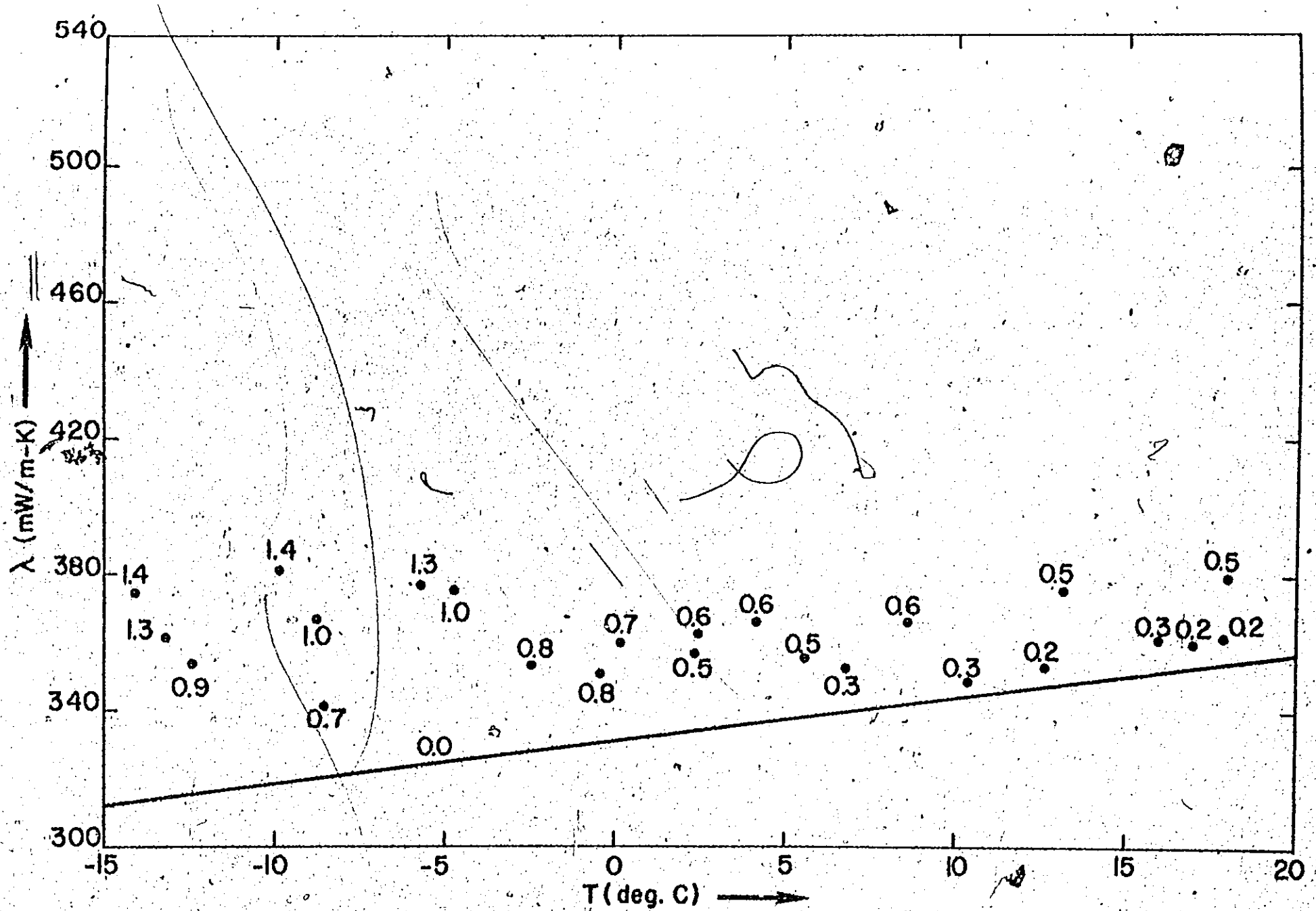

FIG. 5 EXPERIMENTAL VALUES OF CONDUCTIVITY AS A FUNCTION OF T & M: UPPER PART

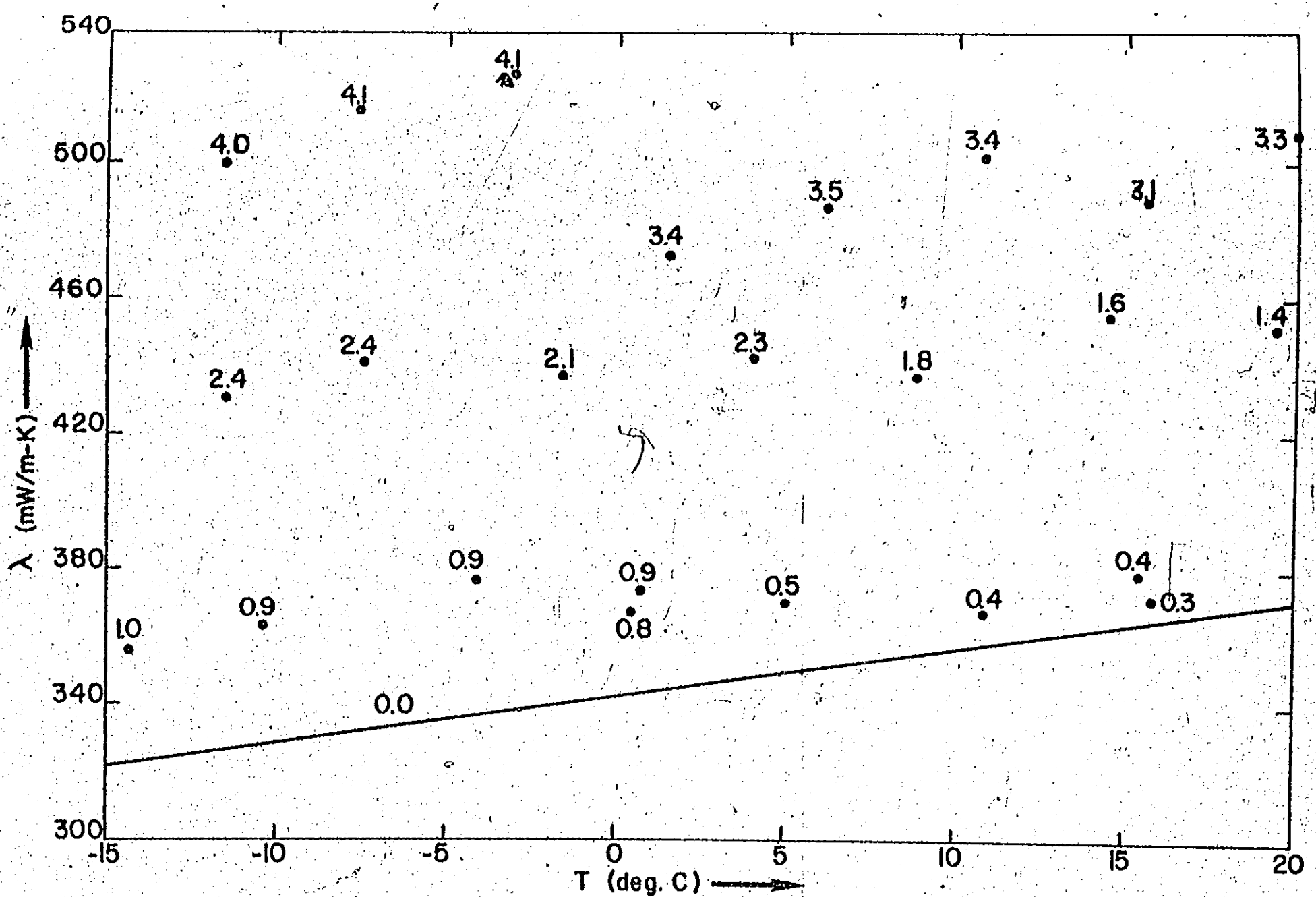

FIG. 6 EXPERIMENTAL VALUES OF CONDUCTIVITY AS A FUNCTION OF T & M: LOWER PART

TABLE 4

Conductivity as a function of temperature and moisture content

Overall Moisture Content (%)	No.	T (deg. C)		λ (mW/m-K)		M (%)	
		T_1	T_2	λ_1	λ_2	M_1	M_2
0	1	37.4	36.2	385	392	0	0
	2	41.9	40.8	391	401	0	0
	3	33.6	32.3	373	385	0	0
	4	48.1	44.7	393	407	0	0
	5	10.9	6.9	347	356	0	0
	6	-1.3	- 3.0	332	340	0	0
	7	- 2.7	- 7.1	327	336	0	0
	8	-13.4	-15.4	315	321	0	0
	9	17.9	16.2	356	365	0	0
	10	25.5	23.9	366	371	0	0
1	1	17.0	15.4	360	379	0.2	0.4
	2	12.6	10.9	354	369	0.2	0.4
	3	6.8	5.0	354	371	0.3	0.5
	4	- 2.4	- 4.1	354	377	0.6	0.9
	5	- 8.5	-10.4	342	364	0.7	0.8
	6	-12.4	-14.3	354	357	0.9	1.0
	7	2.5	0.7	364	375	0.6	0.9
	8	17.8	15.9	363	372	0.2	0.3
	9	2.4	0.5	358	368	0.5	0.8
3	1	-14.1	-15.8	375	423	1.4	2.4
	2	- 9.8	-11.5	382	431	1.4	2.4
	3	- 5.7	- 7.4	377	442	1.3	2.4
	4	0.2	- 1.6	361	439	0.7	2.1
	5	5.6	4.0	357	443	0.5	2.3
	6	10.4	8.8	350	437	0.3	1.8
	7	16.0	14.4	362	455	0.3	1.6
	8	20.9	19.3	364	451	0.3	1.4
5	1	22.5	20.2	374	508	0.4	3.3
	2	13.2	10.7	370	502	0.5	3.4
	3	8.6	6.1	368	488	0.6	3.5
	4	4.1	1.5	367	473	0.6	3.4
	5	- 0.4	- 3.1	352	427	0.8	4.1
	6	-13.1	-15.8	362	490	1.3	4.2
	7	- 8.7	-11.5	367	500	1.0	4.2
	8	- 4.8	- 7.6	377	516	1.0	4.1
	9	18.0	15.5	381	489	0.5	3.1

the lower part of the specimen, respectively. It was observed in these figures that the variation of λ with T for any particular M could be approximated by a straight line. Such straight lines appeared to have different slopes and different intercepts on ordinate at $T = 0$ for various values of M. The differences of slopes and intercepts of these lines with respect to the corresponding values for the dry specimen were obtained and expressed as functions of M. Thus, a simple empirical relation aimed at, was of the form

$$\lambda_{moist} = \left[\lambda_{dry} + \lambda(M)\right]_{at\ T=0} + \left[\left(\frac{d\lambda}{dT}\right)_{dry} + \frac{d}{dT}\lambda(M)\right] T. \quad (8)$$

Two expressions of the form similar to Eq.(8) were obtained; one for the temperatures below 0 deg. C and the other above zero. They are

$$\lambda_{moist} = \left[\lambda_{dry_{at\ T=0}} + 46M\right] + \left[\left(\frac{d\lambda}{dT}\right)_{dry} + 0.25\ M\right]T\ ,\ T< 0 \quad (9)$$

$$\lambda_{moist} = \left[\lambda_{dry_{at\ T=0}} + 40M\right] + \left[\left(\frac{d\lambda}{dT}\right)_{dry} + \arctan M\right]T,\ T> 0 \quad (10)$$

There is a discontinuity in the values of λ_{moist} at $T = 0$. This could be due to a discontinuity in the thermal conductivity values of water at the freezing point.

As shown in Fig. 1, we have a slight difference in the magnitudes between the thermal conductivities for the upper and the lower part of the dry specimen. This could be due to the error in the distances between the copper wires. The two values of λ_{dry} at $T = 0$ thus obtained were

$\lambda_{dry} = 332$ mW/m-K, for the upper part, (1)

$\lambda_{dry} = 344$ mW/m-K, for the lower part, (2)

In order to eliminate this discrepancy and to be able to present the results for the specimen as a whole, an arithmatic average of the two values of λ_{dry} was used in Eqs.(9) and (10). The value of $d\lambda/dT$ for the dry specimen, for both, the lower and the upper parts, is 1.34 mW/m-K^2. With these, Eqs.(9) and (10) were rewritten as

$$\lambda_{moist} = (338 + 46M) + (1.34 + 0.25M)T, \quad T<0 \tag{13}$$

$$\lambda_{moist} = (338 + 40M) + (1.34 + \arctan M)\,T, \quad T>0 \tag{14}$$

where λ is in mW/m-K, T is in degree Celsius, and M is the percentage of moisture by weight.

Chapter VI

DISCUSSION OF THE RESULTS

1. DRY SPECIMEN

The overall average thermal conductivity of our dry specimen, as a function of the mean overall temperature is shown in Fig. 1. These results, beside being comparable to those available in the literature, indicated an improved precision of the variation of the thermal conductivity with the average temperature of the specimen. The variation of temperature here is from -15 to 40 deg. C. The thermal conductivity in this range varies linearly with the temperature. The slope is about 14 $mW/m\text{-}K^2$, which agrees with the slope of the line shown beside the experimental line and obtained by substituting appropriate values in De Vries' equation. De Vries had found that when dry soil thermal conductivities calculated from an equation derived originally by Maxwell and Rayleigh were multiplied by a correction factor of 1.2, they agreed fairly well with the experimental data on dry soils. The magnitude of our results is also in agreement with De Vries (1952b).

The thermal conductivity values, obtained experimentally by Woodside and Cliffe (1959), Moench (1969), and Williams (1973) on dry

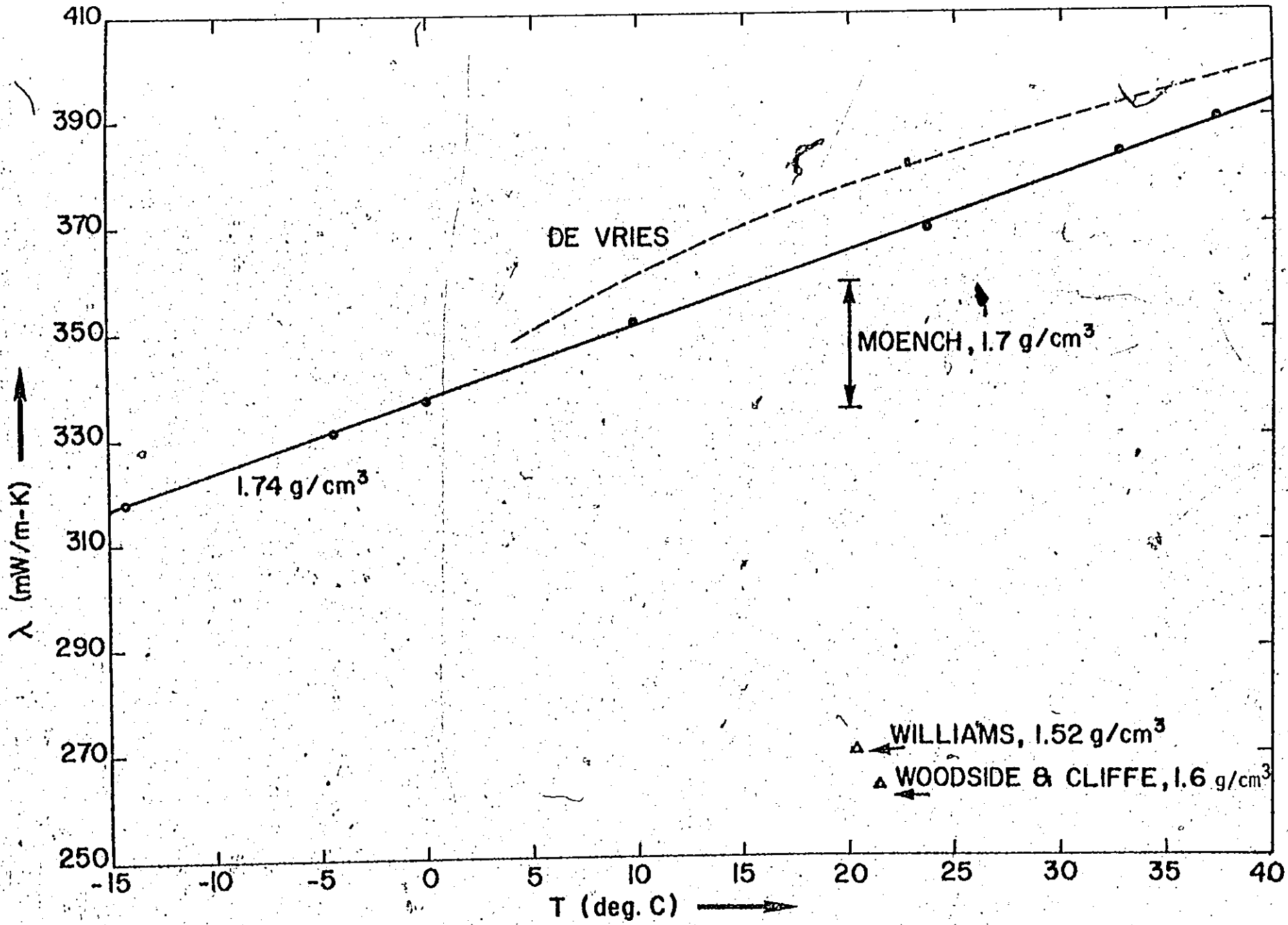

FIG. 1 CONDUCTIVITY VERSUS TEMPERATURE OF THE DRY SPECIMEN; A COMPARISON

specimens of 20-30 Ottawa sand are also plotted in Fig. 1. Taking into account the variation in the dry density of the specimen, these values compare fairly well with our findings.

As shown in Fig. 1 of the previous chapter, two different lines were originally obtained, one for the upper part and the other for the lower part of the dry specimen. This was contrary to the expectation. The two lines should really have coincided with each other since they represent the conductivity of exactly the same material. Departure of the two values of the conductivity from each other did not appear to vary with the temperature of the specimen. This constant error could have been neither due to the values of ΔT or q, which were measured with at least four digits of accuracy, nor due to any possible inexactitude of the value of A which would affect both conductivities equally. The only possible cause of the discrepancy that could be thought of is the fact that the theoretically equal distances between the wires could not be duplicated in practice.

Even in an empty specimen container and even with the supports mentioned on page 17, the theoretical distance $\Delta x_1 = \Delta x_2 = 8.763(10^{-3})$ m could not be maintained throughout. During the filling and later when the supports were being removed every precaution was taken to avoid disturbing the wires. This notwithstanding, some minor disturbances have in all probability occurred.

These are thought to be the reasons for the constant error of about 4 per cent in the computation of the conductivities.

It was thought that this error could be partially eliminated if for each temperature an arithmetic average between the calculated conductivity values for the upper and the lower parts of the specimen was taken to represent the true conductivity. These average values were used in plotting the line representing conductivity changes with temperature for the dry specimen (Fig. 1). The line itself is a straight segment obtained by the least square method.

The deviation of our experimental points from the line in Fig. 1 is well within ± 1%. Standard error, given by

$$\varepsilon = \frac{1}{n}\sqrt{\sum_{i=1}^{n} (y - y_i)^2} ,$$

shows the degree of scatter of the experimental points about the best fitted curve passing through these points. The standard error in our case was only 1.7 mW/m-K, which corresponds to about 0.5%.

2. MOISTURE UNDER ISOTHERMAL CONDITIONS

Contrary to our original assumption, that the moisture becomes uniformly distributed in the specimen under isothermal conditions, the moisture distribution was found to vary along the thickness of the specimen. The local moisture content increased towards the bottom of the specimen for any given overall moisture content.

It, therefore, became necessary to find a way to determine the variation of the local moisture content. An analytical approach was developed to express the local moisture content as a function of the position along the thickness of the specimen, the isothermal temperature, and the overall moisture content of the specimen. Figures 2 and 3 show the moisture distributions obtained by the said analysis for the overall moisture contents of 1, 3, and 5 per cents at various isothermal temperatures. As can be seen from these figures, at a low overall moisture content of 1 per cent the moisture is distributed fairly uniformly in the specimen. But at overall moisture contents of 3 and 5 per cents, the distribution curves appear to have a hyperbolic shape. Migration of moisture from the upper end of the specimen to the lower appears to be slightly more in case of higher temperatures than in case of lower.

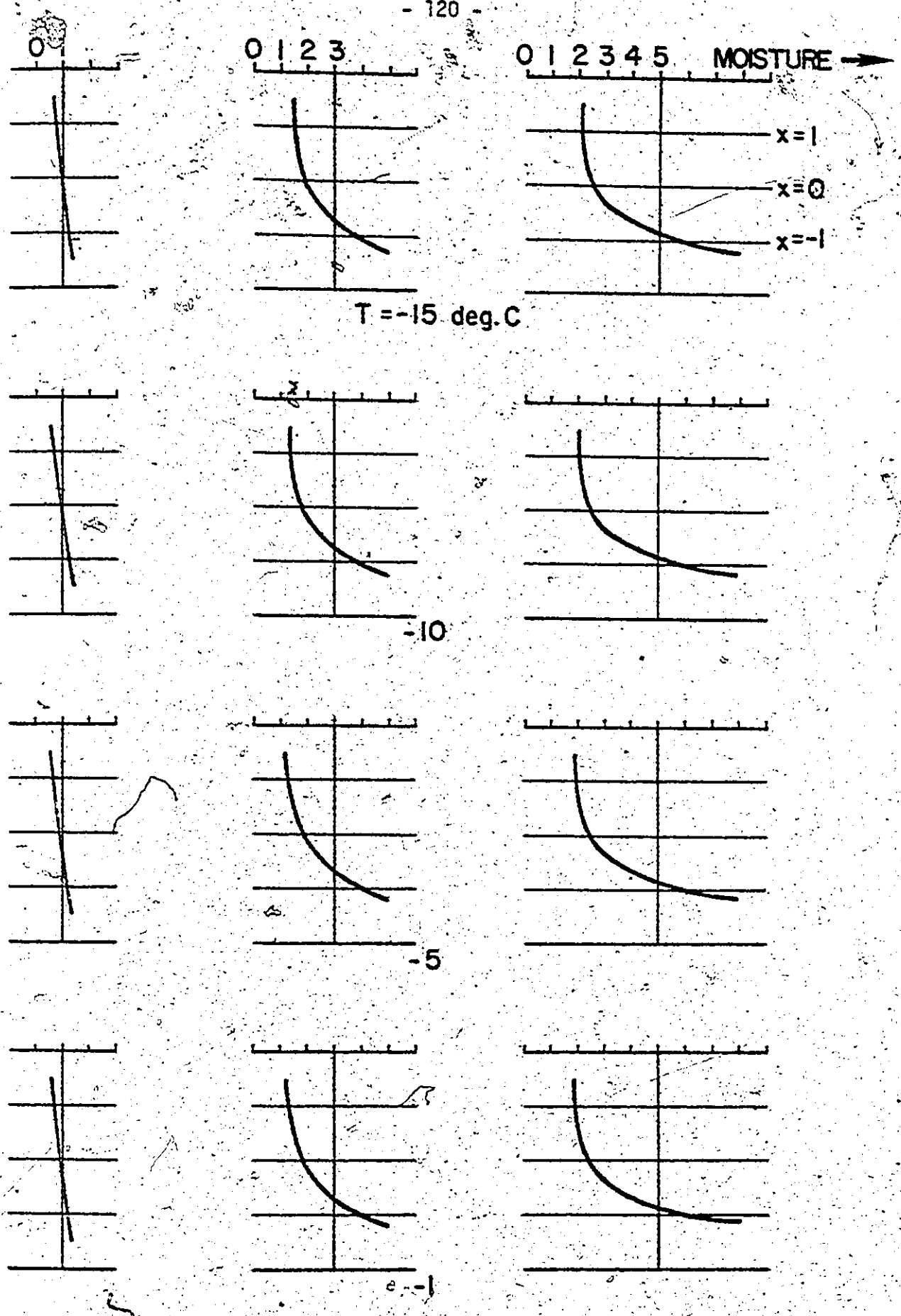

FIG. 2 MOISTURE DISTRIBUTION UNDER ISOTHERMAL CONDITION.
T < 0 deg. C

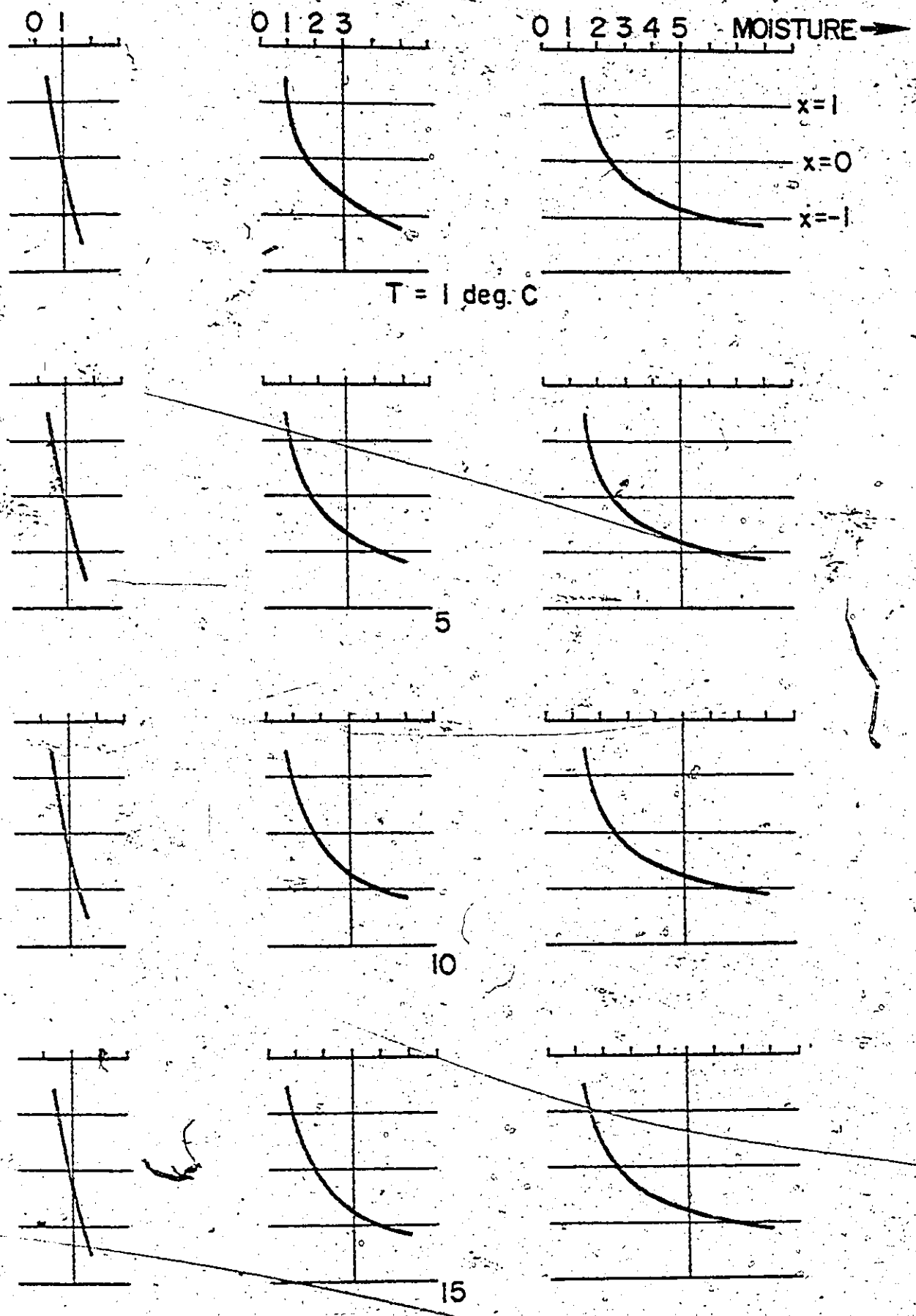

FIG. 3 MOISTURE DISTRIBUTION UNDER ISOTHERMAL CONDITION.
T > 0 deg. C

3. THERMAL CONDUCTIVITY OF MOIST SPECIMEN

The thermal conductivity of our specimen is plotted in Fig. 4 as a function of temperature and moisture content. The calculated values, obtained from Eqs.(13) and (14) on page114, are shown by solid lines, whereas the experimental values are shown by solid circles. There seem to be a fair agreement except in the region from -1 deg. C to + 1 deg. C.

The prediction of the conductivity of moist granular material was attempted in three different ways, as described in detail in Appendix E. These three approaches to a simplified model are: (1) approximate analysis, (2) improved analysis, and (3) nonanalytical approach. The results of the approximate analysis are presented in Table 1 in Appendix E. Comparison of these results with our experimental findings show that the predicted values of conductivity give a positive λ-T slope and indicate an abrupt change in magnitude at the freezing point of water, as do the experimental values. But there is a wide difference in the magnitudes of the predicted and the observed values. The assumptions of looser packing arrangement of the particles, and of the concentration of the moisture around the contact points of the spheres, in the approximate analysis, were thought to be the main causes of this discrepancy. Several appropriate suggestions are made in the improved analysis for obtaining better results. The calculations performed in the manner suggested in the nonanalytical approach were found to yield results closer to the observed values than those obtained by the ap-

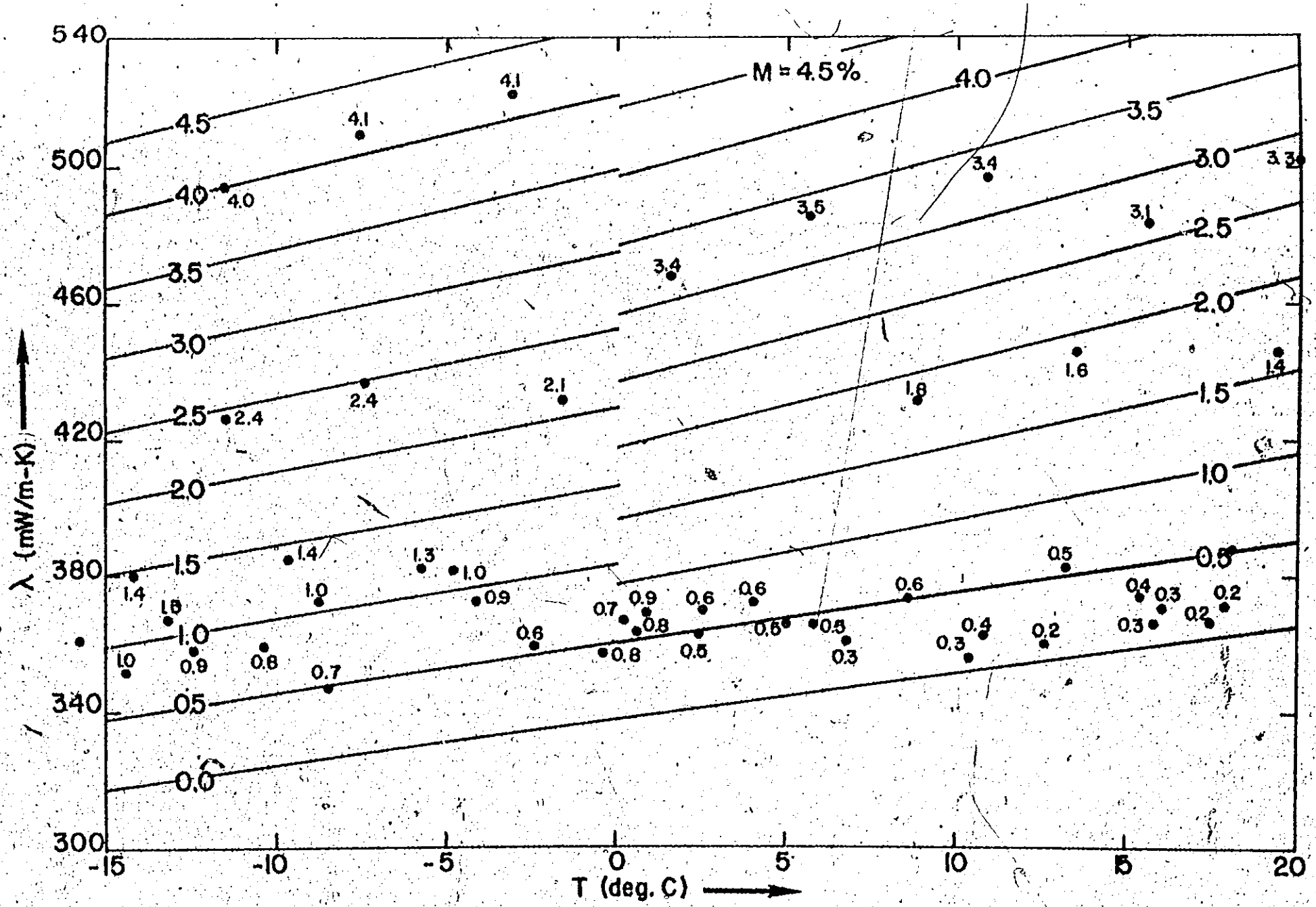

FIG. 4 CURVE-FITTING FOR CONDUCTIVITY AS A FUNCTION OF TEMP. AND MOISTURE

proximate analysis.

The thermal conductivities of our specimen were also obtained by a transient method, as discussed in detail in Appendix F. These values were about 20 per cent lower than those obtained from the steady-state method, for the dry specimen. The scatter of the transient values was much larger than that of steady-state values. These discrepancies were found to be larger in case of moist specimen.

Woodside and Cliffe's results (1959) on a specimen of 20-30 Ottawa sand are shown in Fig. 5. Though their specimen material is of the same description as ours, the density of their material is somewhat lower than ours, 1.6 as opposed to 1.74 g/cm^3. Woodside and Cliffe performed their experiments only at one particular value of the overall mean temperature, that is, 24 deg. C. Even though our results are available only up to 20 deg. C., we can attempt to compare them with Woodside and Cliffe by extrapolating them to 24 deg. C.

Woodside and Cliffe's values turn out to be quite different from ours. This difference could be attributed to various reasons. The main ones seem to be: (1) Different specimens were used by Woodside and Cliffe for tests at each moisture content, (2) the overall thermal conductivity — and not the local thermal conductivity — was measured by these authors at each overall moisture content as a function of the temperature difference across the specimen, and then the limiting value of the conductivity for zero temperature difference was obtained by

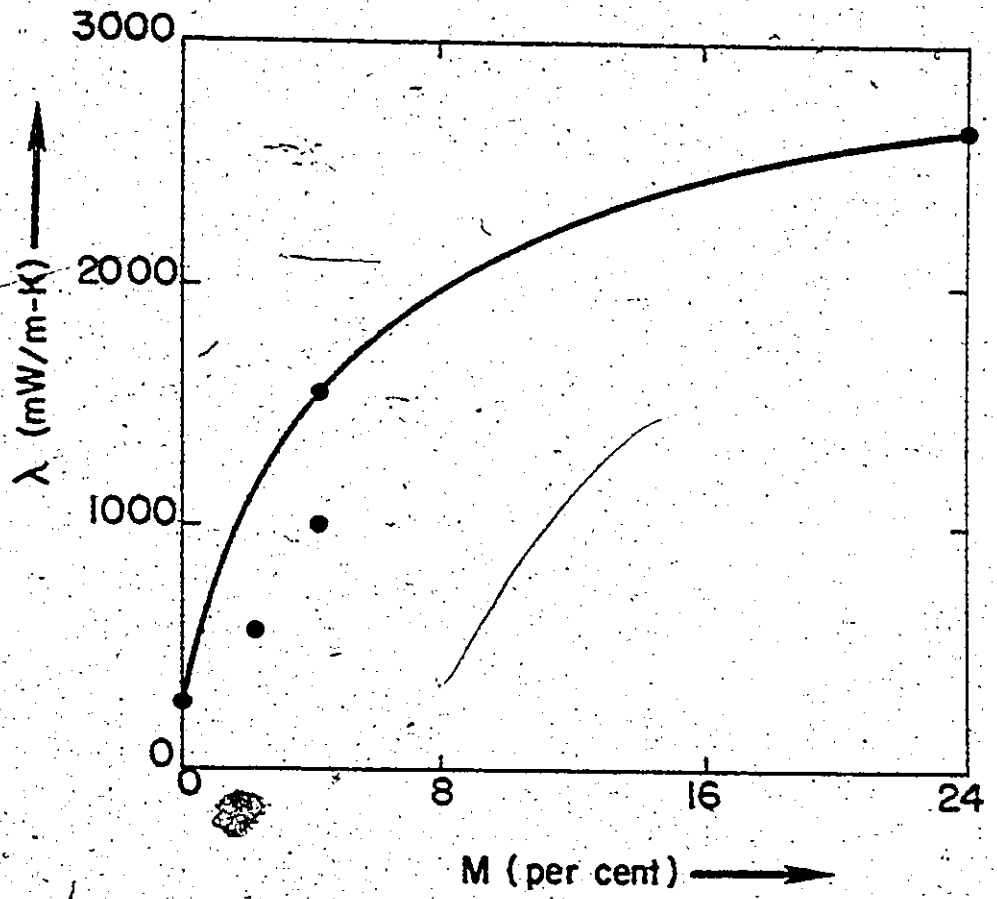

FROM WOODSIDE AND CLIFFE (1959)

FIG. 5 CONDUCTIVITY AS A FUNCTION OF MOISTURE

extrapolation. The moisture, in this limiting case, was assumed to be uniformly distributed in the specimen. Hence, the extrapolated value of the conductivity was assumed to represent the conductivity of the specimen at that particular moisture content.

Be that as it may, their experimental points rather than the solid line drawn in Figure 5, are closer to our results.

The limited number of sensors used in our specimen to measure local moisture and local conductivity is sufficient to indicate the existence and perhaps the trend of the variation of the moisture with the specimen-thickness, but may not be sufficient to give a precise measure of this variation.

Finally, a few suggestions that could be made here for achieving better results from the use of this technique are: (1) construction of a bigger cell to accommodate more sensors could help determine the λ, T, and M distributions more accurately, and hence, could further improve the precision of the correlation of λ, T, and M, and (2) prolonged heating of the cell above 100 deg. C, after the moisture is injected into the specimen material, could help the moisture spread uniformly in the specimen under isothermal conditions, keeping in mind, however, that only a limited amount of moisture can be suspended in the interstices between grains through capillary action. The gravity will drain the surplus to the bottom of the sample.

Appendix A

BASIC EXPERIMENTAL UNIT

The basic unit available for the experimentation was a standard research unit for measuring the thermal conductivity of low conducting materials, built by the Dynatech Corporation of Cambridge, Massachusetts. This unit, designed according to the ASTM specifications (1963), employs a *guarded hot-plate technique* for measuring thermal conductivity of materials available in form of a flat circular slab and having conductivity somewhere in the range from 20 to 2000 mW/m-K. As the name indicates, a guarded hot-plate apparatus consists of a flat main heater (hot plate) which is surrounded by a guard heater. Both heaters are independently maintained at the same temperature so that ideally no heat leakage occurs from the edges of the main heater. The specimen to be examined is made large enough to extend over the joint surfaces of the main and the guard heater. It could be viewed as consisting of two portions. The central portion under the main heater forms the actual sample with respect to which the measurements are taken, while the surrounding remaining portion of the specimen under the guard heater acts as a thermal guard. The ASTM specifications allow for either square or circular main and guard heater

assembly. The Dynatech unit has a circular one.

The principle of operation of this unit is shown by a schematic diagram in Fig. 1. Two identical samples of the test material are placed on either side of a flat circular guarded hot plate. The main heater produces a heat flux necessary to maintain a desired temperature gradient across the main test section of the sample within which the measurements take place. The function of the guard heater is to eliminate radial heat losses, thus forcing the heat generated in the main heater to flow unidirectionally through the two test samples. The assembly is held under moderate pressure between two liquid-cooled heat sinks. The temperature difference across the sample resulting from a uniform heat flow through it is directly proportional to the thickness and inversely proportional to the coefficient of thermal conductivity of the material. The heat transfer process may include the various modes of heat transfer depending on type of material and test temperature. For higher temperature operation, auxiliary heaters are inserted between the samples and the heat sinks. In this way, the sample temperature can be raised to any value merely by adjusting the power input to the auxiliary heaters. The entire test assembly is surrounded by a liquid-cooled shroud, and the space between the shroud and the test stack is filled with insulating material.

The guarded hot-plate method for measurement of thermal conductivity is based on the assumption that isotherms in the central area of the test specimens are planes parallel to the hot and cold-plates, that is, that the heat flow is perpendicular to the faces of the sample. This assumption

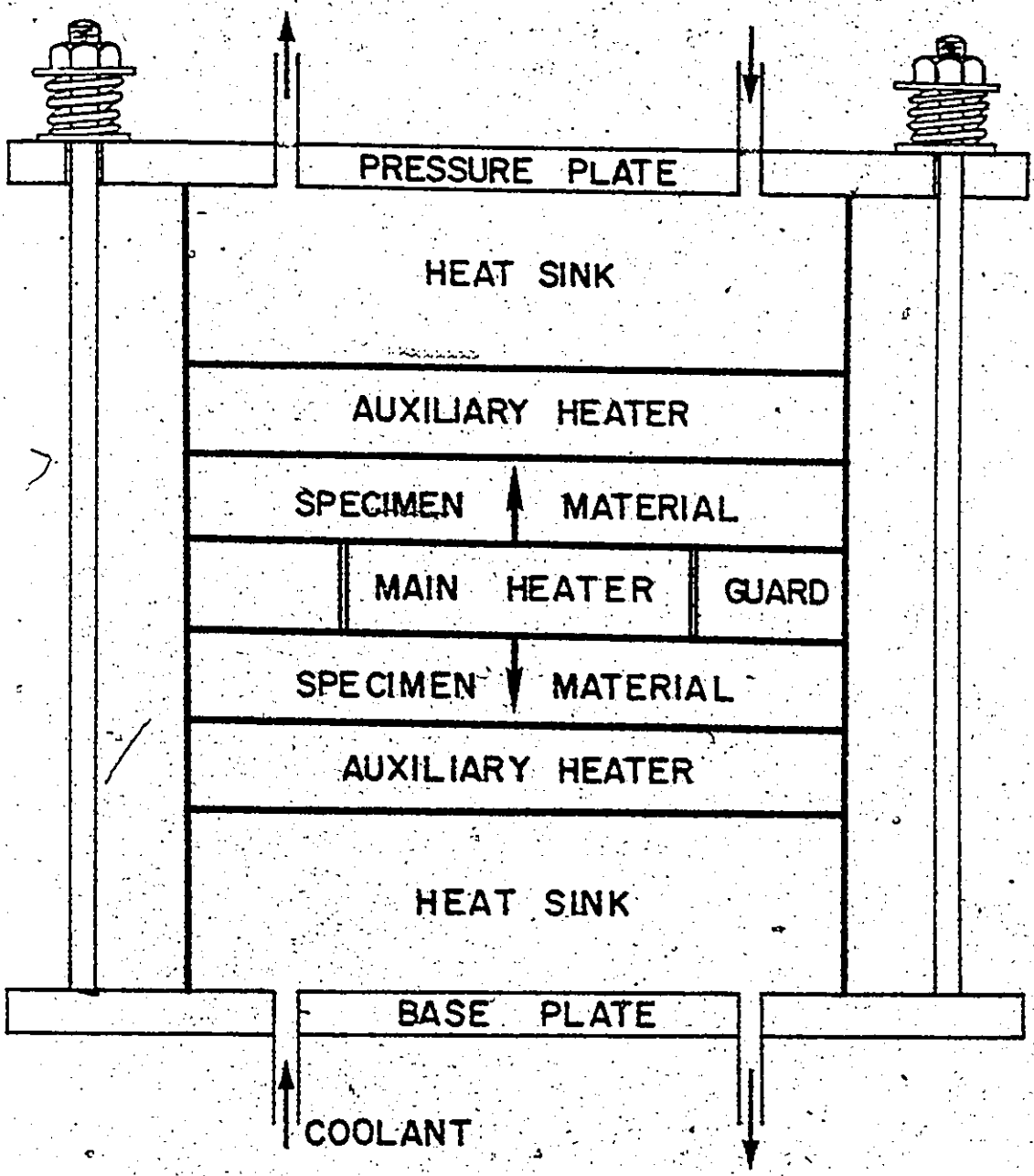

FIG. 1 SCHEMATIC DIAGRAM OF A STACK ASSEMBLY OF GUARDED HOT-PLATE APPARATUS

of unidirectional heat flow works well for thin specimens where the end effects are relatively small. Otherwise the edge of the sample would somehow have to be maintained at a temperature profile similar to the one developing in the central portion of the sample. On the other hand if a specimen is very thin, contact resistances may become dominant. In case of porous or granular materials, very thin specimen may not even accurately represent the original material because the open pores on its exposed surface may influence heat transfer differently from similar, but closed, pores existing elsewhere. Such open pores will, of course, exist also on the outer face of a thicker sample, but their relative effect will be smaller when compared with the total sample resistance. Errors due to radial heat losses are minimized in guarded hot-plate apparatus, but they are not completely eliminated due to unbalance between the main and the guard heaters. These are discussed by Woodside and Wilson (1957), Woodside (1957a), Woodside (1957b), and Orr (1967).

The above factors have limited the thickness of specimens that may be tested by the guarded hot-plate apparatus to approximately one third of the diameter of the central section of the heating unit. The central section of the hot plate of the available unit is 4 in. (10.16 cm) in diameter, with 2 in. (5.08 cm)-wide annular guard ring surrounding it. This limits the allowable specimen thickness to 1-1/3 in. (≈ 3.4 cm). Figure 2 shows the actual view of the test-stack assembly of this unit.

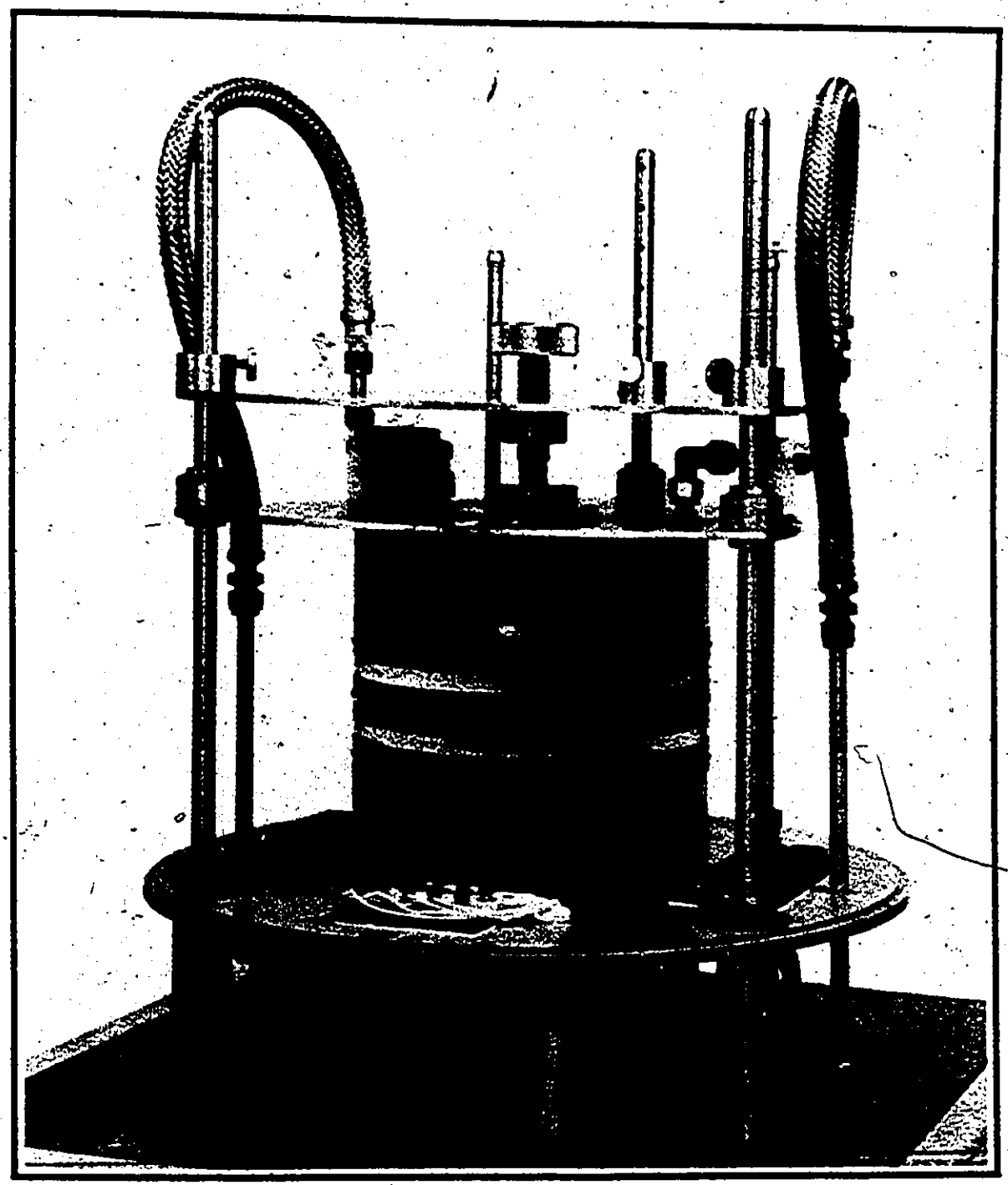

FIG. 2 TEST-STACK ASSEMBLY OF THE DYNATECH UNIT

The idea of having two samples, two heat sinks, etc., one on each side of the heat source, stems from the necessity of properly accounting for the heat generated in the main heater. It is reasonable, everything else being equal, that this rate of heat generation divides equally between the two samples. Had only one sample been used, we would have to account for any heat loss which may occur from the other side of the heater.

The flow is produced by potentiometrically measured d.c. power being dissipated in the main heater. The guard heater, separated from the main heater by a narrow gap, is operated at the same temperature as the main heater to eliminate radial heat flow to or from the main heater.

The instruments necessary for the functioning of the Dynatech unit are dealt with in Appendix C.

Appendix B

ANALYTICAL DERIVATION OF A SELF-HEATING RESPONSE

1. TEMPERATURE RESPONSE OF AN IDEAL LINE HEAT SOURCE

The idea of an instantaneous point source, that is, of a finite quantity of heat instantaneously liberated at a given point and time in an infinite region forms a base for the development of an expression for temperature distribution in an infinite region due to a continuous line heat source. The solution for temperature distribution due to an instantaneous point source, considered to be a fundamental solution (Carslaw and Jaeger, 1959), is integrated with regard to an appropriate space variable to give a solution for temperature distribution due to an instantaneous line heat source. Further integrating this solution with respect to time yields the solution for temperature distribution due to a continuous line heat source.

Let a quantity of heat Q be generated instantaneously at time $t=t_o$ at a point $A(x', y', z')$, shown in Fig. 1, in an infinite region initially at temperature T_i. The temperature of the point source at A at the instant $t=t_o$ will be infinite. Let P be any

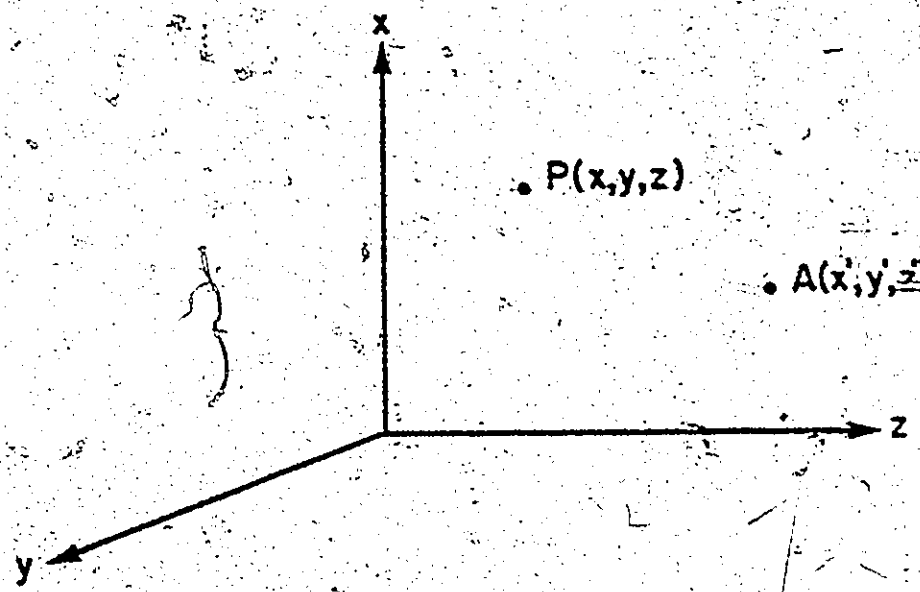

FIG. 1 AN INSTANTANEOUS POINT HEAT SOURCE, A, & AN ARBITRARY POINT, P, IN AN INFINITE REGION

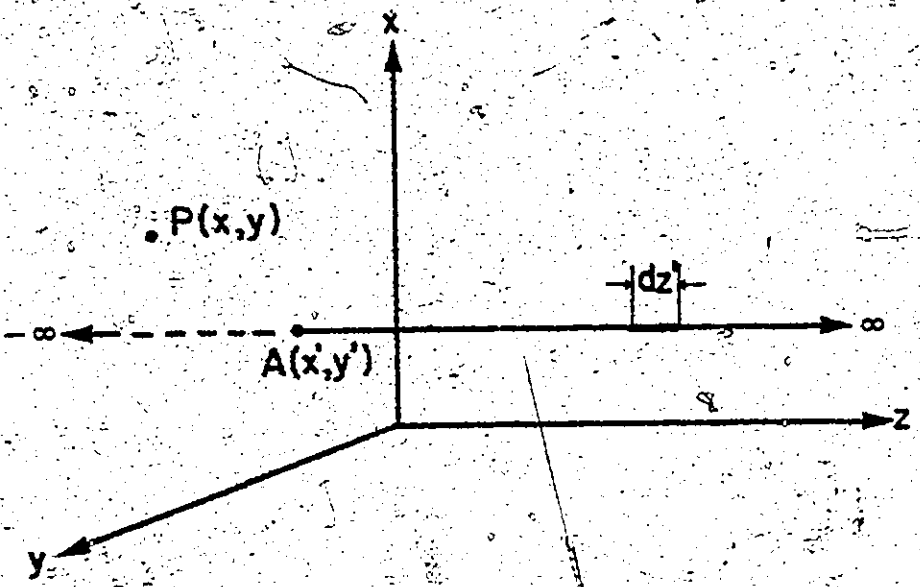

FIG. 2 AN INSTANTANEOUS LINE HEAT SOURCE PASSING THROUGH POINT A, AND AN ARBITRARY POINT, P, IN AN INFINITE REGION

point in the region having variable space coordinates x, y, and z. The differential equation governing the temperature in the region is

$$\frac{\partial^2 T}{\partial x^2} + \frac{\partial^2 T}{\partial y^2} + \frac{\partial^2 T}{\partial z^2} = \frac{1}{\alpha}\frac{\partial T}{\partial t}, \qquad (1)$$

which is satisfied by the solution

$$T - T_i = \frac{Q}{8\rho c[\pi\alpha(t-t_o)]^{3/2}} e^{-[(x-x')^2 + (y-y')^2 + (z-z')^2]/4\alpha(t-t_o)}. \qquad (2)$$

where $\alpha = \lambda/\rho c$, is thermal diffusivity of the region,

ρ is the density and c is the specific heat.

Solution (2) satisfies the following initial and boundary conditions:

at $t=t_o$, $T=T_i$ (except at point A), (3)

and

at $t=t_o$, $T=\infty$ at point A. (4)

Uniformly distributed instantaneous point heat sources along a line constitute an instantaneous line heat source. Let a quantity of heat per unit length, Q', be generated instantaneously at time $t=t_o$ by a line heat source parallel to z-axis passing through a point $A(x', y')$ in an infinite region initially at temperature T_i (Fig. 2). The heat generated by a portion dz' of the line source is $dQ = Q'dz'$. The temperature distribution due to this line heat source is obtained by replacing Q by dQ in Eq.(2) and integrating it over the entire length z', from $-\infty$ to ∞. Thus,

$$T - T_i = \int_{-\infty}^{\infty} \frac{Q'dz'}{8\rho c[\pi\alpha(t-t_o)]^{3/2}} e^{-[(x-x')^2 + (y-y')^2 + (z-z')^2]/4\alpha(t-t_o)}$$

$$= \frac{Q'}{8\rho c[\pi\alpha(t-t_o)]^{3/2}} e^{-[(x-x')^2 + (y-y')^2]/4\alpha(t-t_o)} \int_{-\infty}^{\infty} e^{-(z-z')^2/4\alpha(t-t_o)} dz'$$

$$= \frac{Q'}{4\rho c[\pi\alpha(t-t_o)]} e^{-[(x-x')^2 + (y-y')^2]/4\alpha(t-t_o)} \quad (5)$$

Let $(x-x')^2 + (y-y')^2 = d^2$, then

$$T-T_i = \frac{Q'}{4\pi\rho c\alpha(t-t_o)} e^{-d^2/4\alpha(t-t_o)} \quad (6)$$

Now, in order to obtain a solution for temperature distribution due to a continuous line heat source, let a quantity of heat per unit time and per unit length, $q(\tau)$, be liberated continuously by the line source of Fig. 2. If the supply of heat starts at time $t=t_o$ when the region is at temperature T_i, the temperature at any time t is obtained by letting $dQ' = q(\tau)d\tau$ in Eq.(6) and integrating it after appropriate substitutions. Thus,

$$T-T_i = \int_{t_o}^{t} \frac{q(\tau)d\tau}{4\pi\rho c\alpha(t-\tau)} e^{-d^2/4\alpha(t-\tau)}$$

In Eq.(6) t_o is replaced by a variable time τ which is now the starting time for the supply of the differential heat $dQ' = q(\tau)d\tau$. Rewriting the above equation, we have

$$T-T_i = \frac{1}{4\pi\rho c\alpha} \int_{t_o}^{t} \frac{q(\tau)}{t-\tau} e^{-d^2/4\alpha(t-\tau)} d\tau. \quad (7)$$

If the heat is liberated at a constant rate, then $q(\tau) = q$, and

$$T-T_i = \frac{q}{4\pi\rho c\alpha} \int_{t_o}^{t} \frac{e^{-d/4\alpha(t-\tau)}}{t-\tau} d\tau. \quad (8)$$

In order to simplify the expression, let the starting time t_o be equal to zero, and let $d^2/4\alpha(t-\tau) = u$.

Then,

$$T-T_i = \frac{q}{4\pi\lambda} \int_{d^2/4\alpha t}^{\infty} \frac{e^{-u}}{u}\, du, \qquad (9)$$

where $\lambda = \rho c \alpha$ and u is an arbitrary variable. Equation (9) represents a solution for a temperature distribution in an infinite region due to a continuous line heat source. This equation contains a definite integral which does not seem to have a closed form solution. In terms of an exponential integral, Eq.(9) is rewritten as

$$T-T_i = -\frac{q}{4\pi\lambda} E_i\left(-\frac{d^2}{4\alpha t}\right). \qquad (10)$$

In this, $E_i(-x) = -\int_x^{\infty} \frac{e^{-u}}{u}\, du$ is known as an *exponential integral*. This integral is expressable in terms of an infinite series (Jahnke, 1960) as follows:

$$E_i(-x) = \gamma + \ell n\, X + \sum_{n=1}^{\infty} (-1)^n \frac{X^n}{n \cdot n!}$$

$$= \gamma + \ell n\, X - X + \frac{1}{4}X^2 - \frac{1}{18}X^3 + \ldots \qquad (11)$$

where $\gamma = 0.577215665$, is *Euler's constant*. Substituting Eq.(11) into Eq.(10), we get

$$T-T_i = -\frac{q}{4\pi\lambda}\left(\gamma + \ell n X - X + \frac{1}{4}X^2 - \frac{1}{18}X^3 + \ldots\right) \qquad (12)$$

where,

$$X = d^2/4\alpha t.$$

Thus, Eq.(12) represents a temperature distribution in an infinite region due to an ideal line heat source.

2. PARAMETERS DESCRIBING A NON-IDEAL SELF-HEATING RESPONSE

A temperature rise in any material due to a flow of an electric current in a thin wire of finite diameter can be approximated by an equation [1]

$$T-T_i = -\frac{q}{4\pi\lambda}\left(\gamma + \ell n \frac{d^2}{4\alpha t}\right) \qquad (13)$$

provided that $4\alpha t$ is much larger than d^2. This equation is obtained from Eq.(12) by neglecting the series of X for small value of X. As explained in the previous section, T_i in Eq.(13) is the initial temperature of the material, T is the temperature measured at a distance d from the wire as a function of time t, γ is the Euler's constant and is equal to 0.5772, q is the constant rate of heat liberated by the wire, λ is the conductivity and α is the diffusivity of the material. As such, this equation does not take into account either the error due to finite dimensions of the wire and the surrounding material or the error due to the contact resistance between the wire and the material.

In our experimental situation a self-heating response of a copper wire was obtained by measuring change in voltage, ΔV, across the two measuring points on the wire, as a function of time t, as explained in Chapter III, Section 3.6. The relation between ΔV and $\delta T(= T-T_i)$ was obtained as shown by Eq.(10) in Chapter III. This relation is

$$\delta T = T-T_i = (250\ \Delta r_{cal}/r.\Delta V_{cal})\Delta V . \qquad (14)$$

Comparing Eqs.(13) and (14), and rearranging, we get

$$(\Delta r_{cal}/\Delta V_{cal})\Delta V = (qr/10^3\pi\lambda)\ell nt + qr\{\ell n(4\alpha/d^2) - \gamma\}/10^3\pi\lambda, \qquad (15)$$

or

$$y = B\,\ell nt + C, \qquad (16)$$

where

$$y = (\Delta r_{cal}/\Delta V_{cal})\Delta V, \qquad (17)$$

$$B = qr/10^3\pi\lambda, \qquad (18)$$

$$C = qr\{\ell n(4\alpha/d^2) - \gamma\}/10^3\pi\lambda. \qquad (19)$$

A self-heating response, obtained experimentally, was, thus expressible by an equation of a line of the form in Eq.(16), when plotted on $y - \ell nt$ coordinates.

Appendix C

INSTRUMENTATION

Various types of instruments and circuits employed in this investigation can be considered under two separate headings; on the one hand, what was available to us as an integral part of the Dynatech unit, and on the other, what had to be designed and manufactured to complete the experimental set-up for simultaneous temperature and moisture measurement.

The functions of the instruments covered under the first heading are:

(a) to provide a known amount of heat flowing through the main test-section of the specimen,

(b) to maintain the temperatures of the guard and the top auxiliary heaters closely at the level of the main-heater temperature,

(c) to provide temperature limit control for the system,

(d) to provide cooling for the system,

(e) to monitor temperature at different locations in the system.

In some cases an instrument was designed to perform a specific function, in others — the stipulated function was performed jointly by

two or more instruments.

The main features of all these instruments are described below.

1. HEATER ASSEMBLY

The dimensions of the main and guard heater are given in Appendix A. The surface plates of these heaters are made of anodized aluminum, and the assembly is suitable for use between -180 to 230 deg. C. The main heater supplied a measurable heat flow, which was produced by the d.c. power being dissipated in the main heater having resistance of about 8 Ω.

2. POWER SUPPLY

The d.c. power to the main heaters was supplied by Lambda Regulated Power Supply, model LK-342 A, manufactured by Lambda Electronics Corp., Melville, L.I., N.Y. The input to this power supply is 105-132 V a.c. at 57-63 cycles, and 340 W. The d.c. output of this supply is adjustable from 0 to 36 V and from 0 to 5.2 A, The input voltage to this supply is regulated to 0.015 per cent or 1.0 mV, whichever is greater for input variations between 105 and 132 V a.c., and the input current is regulated to 0.1 per cent or 10 mA, whichever is greater for input variations between 105 and 132 V a.c. The output voltage is regulated to 0.015 per cent or 1.0 mV, whichever is greater for load variations from zero to full load, and the output current is regulated to 0.1 per cent or 10 mA, whichever is greater for load voltage-changes between zero and the rated d.c. voltage. This power supply is equipped with external overload protection in form of an adjustable, automatic, electronic

current-limiting circuit, settable to 105 per cent of rated current. Its object is to prevent output current from exceeding a preset limit for protection of load and power supply when external overloads and short circuits occur.

The output voltage has a dual control consisting of a coarse adjustment potentiometer, which varies the d.c. voltage over a range 0-35 V, and a fine adjustment potentiometer, which varies the d.c. voltage over a one-volt range. Similarly, the current limiter has a dual control consisting of a coarse adjustment potentiometer, which varies the d.c. current over 90 per cent of the rated current range and a fine adjustment potentiometer, which varies the d.c. current over 10 per cent of the rated current range. This power supply functions as a constant voltage source as long as the load current does not equal the current value set by the current limiter control. As soon as the load current exceeds this limit, the supply crosses over automatically and operates as a constant current source. Further decrease in the load resistance decreases the voltage across the load while current remains regulated to the limiting value. The output voltage and current were monitored by d.c. voltmeter and d.c. ammeter, respectively. Since the voltage and current at the output terminals of the power supply may not be the same as the voltage and current at input to the load, the precise values of the load voltage and current were obtained from the measurements of the signals coming out of the voltage and current leads.

3. HEATER POWER MEASUREMENT

The voltage and current leads coming out of the heater are connected to a precision resistor network, and finally to a selector switch. The signals from the switch were taken to a potentiometer for a precise determination of their magnitudes. The resistors are such that 1 mV on the potentiometer corresponds to 1 V across the main heater for voltage measurement, and 1 mV on the potentiometer corresponds to 0.1 A through the main heater for current measurement. The resistor network is shown in Fig. 1. The potentiometer employed for measuring these signals is manufactured by Minneapolis-Honeywell Registered Co., Rubicon Instruments, Philadelphia, model 2732, and it has a resolution of 1 μV. The product of the voltage and current readings thus obtained gave the total power dissipated through the main heater.

4. GUARD HEATER TEMPERATURE CONTROL

The guard heater, separated from the main heater by a narrow gap of 1/16 in., was operated at the same temperature as the main heater to eliminate the radial heat flow to and from the main heater. The thermal balance was maintained by the use of a differential thermocouple shown in Fig. 2. The junctions of this thermocouple alternate between the main and guard heater surfaces so as to produce opposing electromotive force outputs from each junction. Thus, when the guard and main temperatures coincide, a net balance between the guard and main heater produce a null or zero signal from the thermocouple. A temperature unbalance between the main and guard produces a positive or a negative signal,

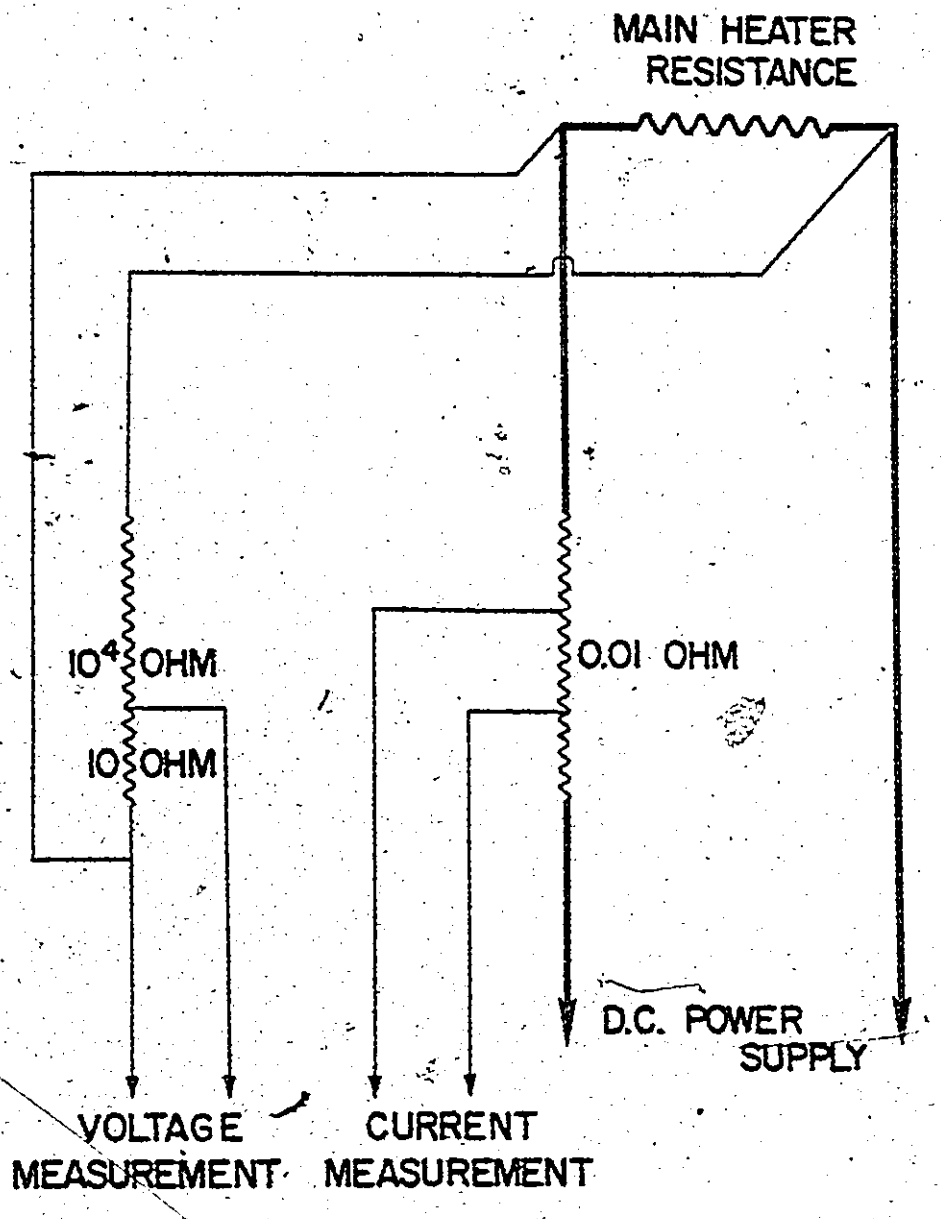

FIG. 1 VOLTAGE AND CURRENT MEASURING NETWORK FOR THE MAIN HEATER

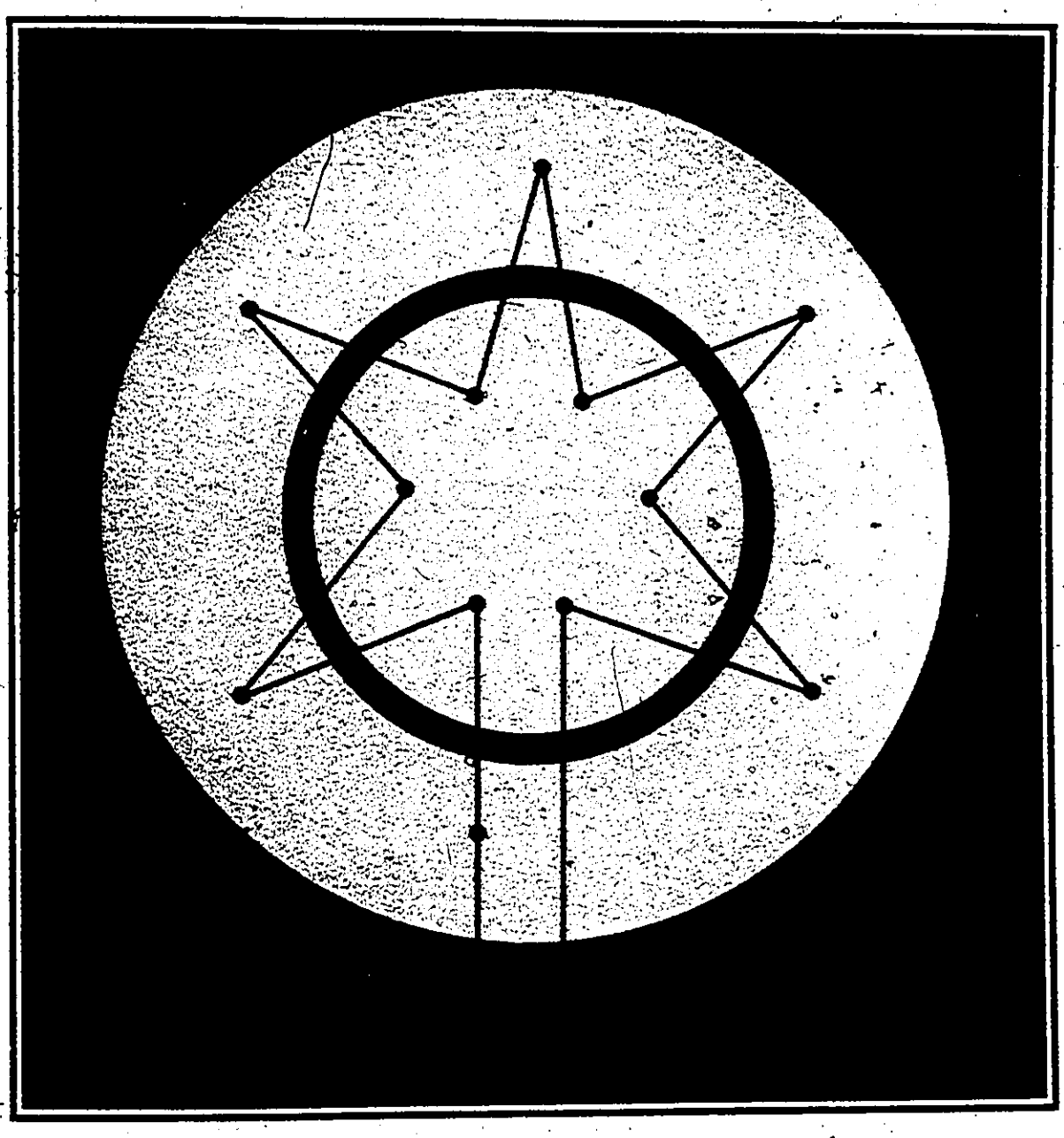

FIG. 2 A DIFFERENTIAL THERMOCOUPLE FOR THE MAIN AND GUARD HEATER ASSEMBLY

depending on the direction of unbalance. The signal from the thermocouple was fed into the zero-differential proportional controller for the guard heater.

The zero-differential proportional controller, API model 225, is a precision, thermocouple-actuated temperature controller. With automatic reset, temperature stays at set-point even if the thermal load changes. This controller is also capable of maintaining a biased balance, which was particularly useful since the true zero may sometimes be different from the zero set on the controller. Temperature difference between the guard and the main heaters were measured separately by means of thermocouples after the zero-differential proportional controller had produced a steady-state balance or unbalance between the guard and the main heater. If the temperatures of the guard and the main heaters differed by more than 0.025 deg. C from each other, then the controller was biased so as to bring the temperature difference within acceptable limits.

5. TOP AUXILIARY HEATER TEMPERATURE CONTROL

The top auxiliary heater-surface facing the main heater was accurately matched in temperature to the main heater by means of an automatic heater control. This instrument, API model 226, is a precision thermocouple-actuated, two-mode temperature controller with solid state circuitry and automatic reset. The controller can be set to give a desired temperature anywhere from -180 to 240 deg. C by adjusting a digital indicator setting on it. Appropriate digital indicator setting for a desired tempera-

ture is obtained from the graph provided with the control for this purpose. The controller has an indicating meter which displays the number of degrees deviation of the top auxiliary heater from the set point. The indicator pointer stays at null point when the top auxiliary heater attains the set temperature.

In case the top auxiliary automatic heater control should fail for any reason, an adjustable autotransformer was connected in parallel with it to provide a manual control for the heater. The autotransformer chosen is known by its proprietory name of Variac, model W10, manufactured by the General Radio Company of West Concord, Massachusetts. Of course, the manual control takes much longer time than the automatic control to bring the heater to the desired level of temperature and was only provided as stand by equipment.

6. TEMPERATURE LIMIT CONTROL

A thermocouple junction was attached close to the hottest point in the experimental unit, and the signal was fed to a temperature-limit control. This control protects the experimental unit from an accidental over heating. It has a built-in thermocouple break protection, and it switches off all the heaters of the unit as soon as the temperature of the thermocouple junction overshoots the set cut-off point on the control dial.

7. COOLING SYSTEM

As explained earlier in Appendix A in the operation of the guarded hot-plate apparatus, the heat generated in the main heater flows linearly

down the specimen to the heat sink, and is then carried away by coolant circulating in the heat sink; whereas, the heat from the main heater produces a desired temperature gradient across the specimen, the temperature of the heat sink or that of the bottom auxiliary heater, establishes a mean temperature of the specimen at which the tests are to be performed.

In the temperature range from -15 to 20 deg. C the desired test temperature was achieved by controlling the temperature of the curculating coolant in the heat sink by means of a refrigerating unit, COLORA Ultra-Kryostat, model KT 90S, eliminating the use of the bottom auxiliary heater. This unit, manufactured by Colora Messtechnik GmbH of West Germany, is capable of maintaining the temperature of its bath to an accuracy of ± 0.05 deg. C anywhere between its limits from 40 to -90 deg. C. Cooling rate and net refrigerating capacity of this model are shown in Figs. 3 and 4. The cooling time of this unit is quite short and the net refrigerating capacity is adequate within the temperature interval of interest to us.

A mixture of *Perma-fill*, a commercially available anti-freeze, normally used in automobiles during winter, and water was used as a coolant. In proper proportion, this mixture can be used for temperatures as low as -50 deg. C.

At various temperatures two sets of experiments were performed; a gradient test, and an isothermal test. For gradient test, the Colora unit was used to set the cold-side temperature of the specimen, while

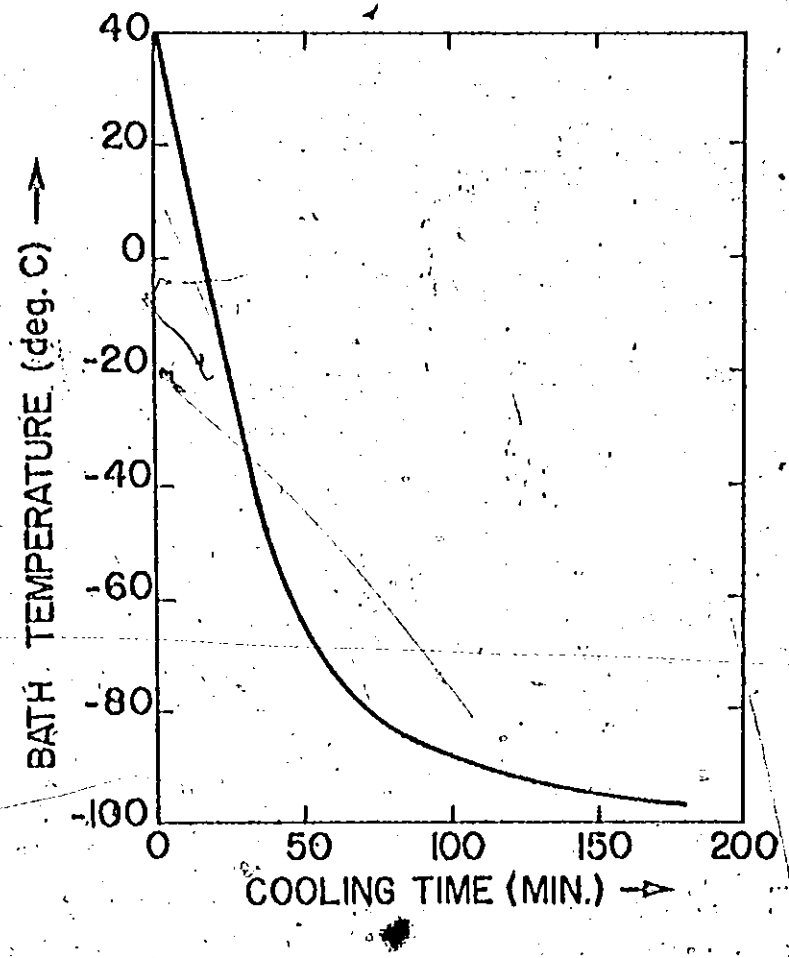

FIG. 3 COOLING RATE OF THE COLORA UNIT

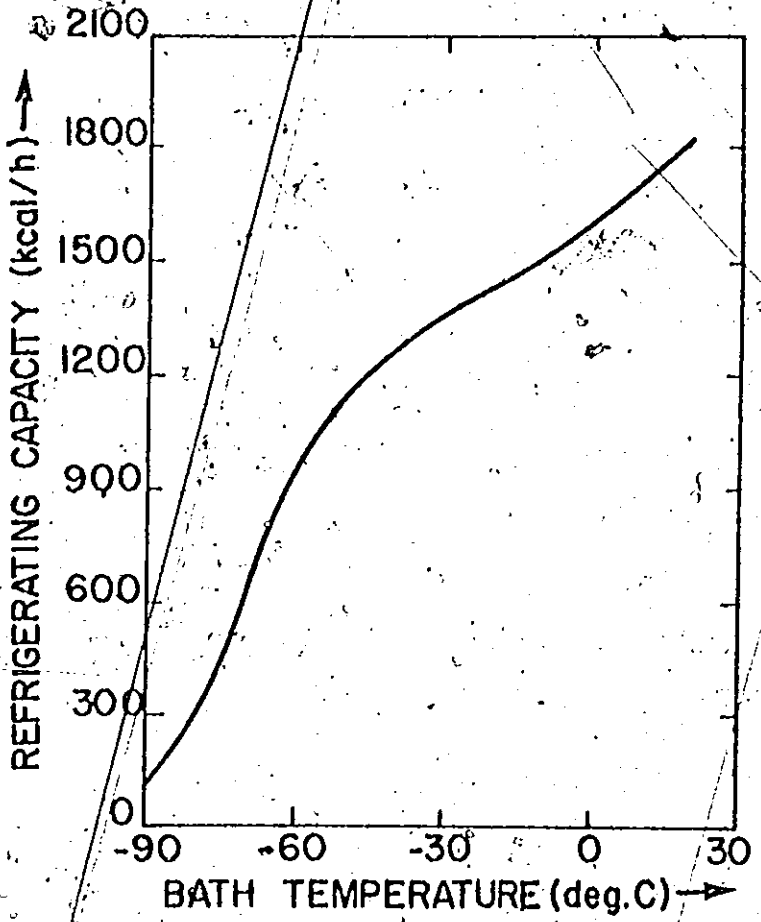

FIG. 4 NET REFRIGERATING CAPACITY OF THE COLORA UNIT

heat input to the hot side was provided by the heater. On the other hand, for isothermal test, the Colora unit alone was used to provide a uniform temperature in the specimen.

8. INSULATION

Insulation plays a vital role in almost all the heat transfer experiments. It is sometimes used simply to prevent the undesirable flow of heat to or from the object under consideration. On other occasions, judicious distribution of insulating material on certain outer surfaces of the objeet is used to govern the direction of heat flow through this object.

Two types of insulating materials were used in this experimental set up to achieve the desired degree of protection. *Styrofoam*, a cellular insulating material, was used to fill the space between the main heater and the top auxiliary heater to minimize any flow of heat in this region. A space between the cooling shroud and the cell was also filled with Styrofoam cut to size to minimize any heat flow to or from the cell wall. This assembly was then covered by a pyrex bell jar, making it airtight. To further reduce any heat flow to or from this set up, and particularly to avoid condensation of atmospheric water vapor on the bell jar at low temperatures, the bell jar was tightly covered by *Armstrong Armaflex*, a foamed plastic insulating material. Bags full of active Silica-Gel were placed inside the bell jar in order to prevent the condensation of water vapor on the test-stack assembly.

At lower temperatures, the condensation of the atmospheric water-vapor on the electrical connections also causes severe problems, leading sometimes to the failure of the experiment. Heavy insulation was also needed, therefore, for the base of the experimental unit which contains all the thermocouple leads and the electrical connections. Bags full of Silica-Gel were placed inside the base which was then sealed to make it airtight.

The coolant-carrying tubes, which connect the experimental unit to the coolant supplying unit, were heavily insulated by 1 in.-thick Armaflex pipe insulation, to minimize the change in temperature along the length of the tubes, and also to avoid atmospheric water vapor condensation on them at lower temperatures.

Let us now have a look at the instruments and the circuits that were designed to complete the experimental set up. The major circuit designed to measure temperature and moisture at three levels in the specimen is shown in Fig. 4 of Chapter III. The circuit had to suit the requirements of both low and high current intensity, always keeping in mind the following criteria necessary for any precision electrical measurements:

(a) negligible thermal electromotive force in the circuit,

(b) stable zero on the null detector,

(c) low and nearly constant resistance in the electromotive force circuit,

(d) low a.c. pick up,

(e) negligible thermal electromotive force and resistance changes in switches and resistors,

(f) a high degree of linearity of the resistance box,

(g) stable calibration,

Figure 7 in Chapter III shows the details of the electrical circuit which accommodates the above-mentioned criteria with the help of the instruments and the accessories described below:

9. CURRENT SOURCE

The two levels of current requirements, that is, 0.03 A for resistance measurement and 2 A for self-heating of copper wires, were met by DC

Power Supply, series MPB-3, model 6281A, manufactured by Hewlett Packard. There are coarse and fine voltage controls and coarse and fine current controls to set desired output voltage or current. This power supply can be operated on either constant voltage or constant current mode, and it has a provision for an automatic cross-over. Load regulation for constant voltage mode is less than 5 mV for a full load to no load change in output current, and load regulation for constant current mode is less than 0.01 per cent plus 250 μA for a zero to maximum change in output voltage.

10. REVERSING SWITCH

Thermal electromotive forces of the order of few microvolts are usually present in any circuit no matter how well it is designed. Reasonably stable electromotive forces in the measuring loop are reduced quite easily by the use of a neutral reversing switch. The reversing switch shown in Fig. 7 in Chapter III reverses the flow of current through the two resistances, one standard and the other unknown. It, thereby, not only eliminates the effect of thermal electromotive forces in the resistors and the galvanometer at balance, but it also doubles the sensitivity of the detector circuit.

11. STANDARD RESISTORS

A resistance of 0.1 Ω was connected permanently in series with the copper wires so that the same current flows through both of them. The resistance of the copper wires was determined by comparing the voltage

developed across the copper wires with that developed across the standard resistance. The standard resistance of 0.1 Ω was provided by a resistor, model 9222 of Guildline Instruments, to an accuracy of 0.00001 Ω over its complete rated current range of 0-22 A. The case of the resistor is filled with white mineral oil (medicinal paraffin) designed to maintain it at a constant and uniform temperature. This resistor was recalibrated before use at the Division of Physics, National Research Council of Canada, Ottawa, and according to the calibration report, its value was found to be 0.1000103 Ω when a d.c. measuring current of 4.0 A was used.

Another standard resistance of 0.01 Ω was used in place of the copper wires, in series with the standard resistance of 0.1 Ω at the time of calibration of the potentiometer. A standard resistor, model 1659 of Guildline Instruments was used having nominal value of 0.01 Ω and rated current of 30 A. Its calibrated value before use was found to be 0.0099974 Ω.

12. POTENTIOMETER

Precision Vernier Potentiometer, model 9180 of Guildline Instruments was used in the circuit only to function as a voltage divider. The voltage across the standard resistance of 0.1 Ω was divided by means of measuring dials on the potentiometer in such a way that it was equal to the voltage across the copper wires within six significant figures.

The potentiometer has three measuring dials giving voltage increments up to 2.10100 with smallest step being 0.00001 V. It also has a range dial by which the range of the voltage on the potentiometer could be reduced by factors of 10 or 100. The thermal electromotive force in the potentiometer is less than 0.1 μV and the components are well protected from external electrical signals. The components are enclosed in a copper box, which functions as a heat distributor and as an electrostatic shield. All switch contacts in the potentiometer are of copper construction with special emphasis on good reproducibility of contact resistance and on the reduction of thermal electromotive forces to a minimum. The potentiometer has four sensitivity keys to provide increasing galvanometer sensitivity.

13. CHOPPER

Low thermal chopper, model 9745, manufactured by Guildline Instruments, having three sections and double poles was used. It has contact arms made of gold-silver alloy and the contacts of solid gold blocks, which reduce thermal electromotive forces to a minimum of 0.1 μV under normal operating conditions. Tantalum condensers were used rather than paper or polystyrene ones because they have a much better performance. With these condensers the two voltages could be compared to an accuracy of 1 μV.

14. LOW THERMAL SWITCH

Thermal electromotive forces arise principally at three locations: (1) across resistance elements, if the end points are not maintained at the same temperature, (2) within switches, as a result of temperature gradients across contact interfaces and along switch brushes, and (3) at and around the terminals, as a result of temperature differences between inside and outside of the terminal base. Normally, the switches in various parts of a circuit generate heat and consequently electromotive forces as well as transients at contacts.

Low Thermal Selector Switch, model 9145 A of Guildline Instruments was employed in the circuit to keep these undesirable electromotive forces to an absolute minimum. The switch generates no more than 0.01 μV thermal electromotive forces. The switch has gold-silver alloy contacts and is mounted in a solid block of aluminum to minimize temperature gradients. Junctions of dissimilar metals are arranged to occur in pairs and excellent thermal contacts are achieved so that small thermal electromotive forces which may appear tend to be self cancelling.

15. GALVANOMETER

Detectors used with potentiometers are either, electronic or galvanometric. Each type has its own advantages and disadvantages, and the choice usually depends on the particular application. Electronic detectors are insensitive to mechanical disturbance, but are usually sensitive to a.c. pickup, circuit noise, and ground loop troubles.

Electronic detectors are not usually reversible and for low level measurements such reversibility is essential. Galvanometers may be either simple light beam instruments or may be preceded by a photocell galvanometer amplifier for extremely high sensitivity. Such detectors are sensitive to mechanical disturbance, but are almost completely immune to a.c. pickup and ground loop difficulties and are extremely simple in operation. They use only direct current and are usually reversible.

Galvanometer, type 9461A, and photocell galvanometer amplifier, type 9460, both manufactured by Guildline Instruments were used jointly as a null detector in our potentiometer circuit.

The amplifier is an extremely sensitive light-beam-coupled instrument which is capable of amplifying d.c. signals of nanovolt and nanoampere levels. Because of its high current sensitivity this set is ideally suited for use as a null detector. The amplifier was adjusted to have parallel feedback configuration so that it could be used as a current amplifier. The series feedback configuration is meant for voltage amplification. With a 6 V and 15 W lamp, typical current sensitivity of this amplifier is 13 mm/nA, that is, 7×10^{-3} nA/mm, with input resistance of 0.25 Ω. The amplifier is mounted in such a position that it is not subjected to vibration and is connected to a source capable of supplying up to 3 A at 6 V. The amplifier output is linear, and its input signal polarity may be reversed without

introducing errors due to hysteresis or input offset currents. This reversal capability is useful to balance out parasitic or thermal electromotive forces in the measured circuit. The input and output terminals are made from high purity copper and are electrically insulated from the front panel. Thermal electromotive forces are reduced by the front panel, which acts as a heat sink to equalize the terminal temperatures, and by the removable cover which eliminates drafts.

To give a visible indication of the amplifier output current, a Guildline galvanometer, type 9461A, was used. It is referred to as a secondary galvanometer since it is designed primarily for use with a photocell galvanometer-amplifier. The galvanometer has a switch which provides four scales of sensitivity increasing from 1/1000 to 1/1 for use in initial balancing operations. At the most sensitive position (1/1) sensitivity is 0.5 mm/nA, that is, 2 nA/mm. The nominal galvanometer resistance is 500 Ω. The galvanometer has two mechanical zero controls, a coarse control mounted atop the galvanometer suspension requiring adjustment at the time of installation, and a fine control on the front panel for adjustment at the time of experimentation.

16. RECORDER

Speedomax recorder, type G, and stabilized d.c. microvolt amplifier, type 9835-B, both manufactured by Leeds & Northrup Company were used to record the time change in voltage across the copper wires when they were heated by passing a current of 2 A through them.

The amplifier, which itself is a completely self-contained null-balance type instrument, is used as a preamplifier for the recorder. It has six ranges, from 50 μV to 2000 μV, to work with. It has three-position operation switch; the first position for non-linear meter response for the indicator, the second position for linear meter response, and the third position for output to recorder connector.

The recorder is an electronic null-balancing instrument. It has an adjustable zero and adjustable range switches. It is a strip-chart recorder with the chart speeds ranging from 1/4 in. per hour to 1 in. per second.

Appendix D

EXPERIMENTAL DATA AND ITS ANALYSIS

1. ICE-POINT RESISTANCE OF THE SENSORS

Resistance measurement of any wire by Ohm's law involves passing a small current through it and measuring a voltage drop across it. A current flowing through a wire generates heat, which is proportional to the square of the magnitude of the current. The heat generated in the wire increases the temperature of the wire, and in general the resistivity is a function of temperature. Keeping a wire in an ice-water bath does not, therefore, guarantee that the resistance measured corresponds to the ice point. For this reason the following procedure was adopted in accordance with the normal practice.

In order to calculate the ice-point resistance of the three copper wires, potentiometer readings r for various magnitudes of current were taken. These values are given in Table 1.

TABLE 1

Potentiometer reading r for ice-point resistance of the copper wires.

Copper wires \ Current (I) amps.	0.1	0.2	0.3	0.4
Top	163189	163192	163198	163202
Middle	159042	159043	159051	159059
Bottom	158823	158833	158843	158853

These values are plotted in Fig. 1 on r versus I^2 scale. Straight lines were drawn through these values using a least square curve fitting method. The results obtained on extrapolation for $I^2 = 0$ are

Copper wires	r
Top	163189
Middle	159040
Bottom	158824

Comparing these values of r with the first column in Table 1, it could be deduced that the current intensity of 0.1 A causes negligible heating of the wires. Hence, any current intensity up to this level could be safely used to obtain the resistances of the wires under other conditions as well.

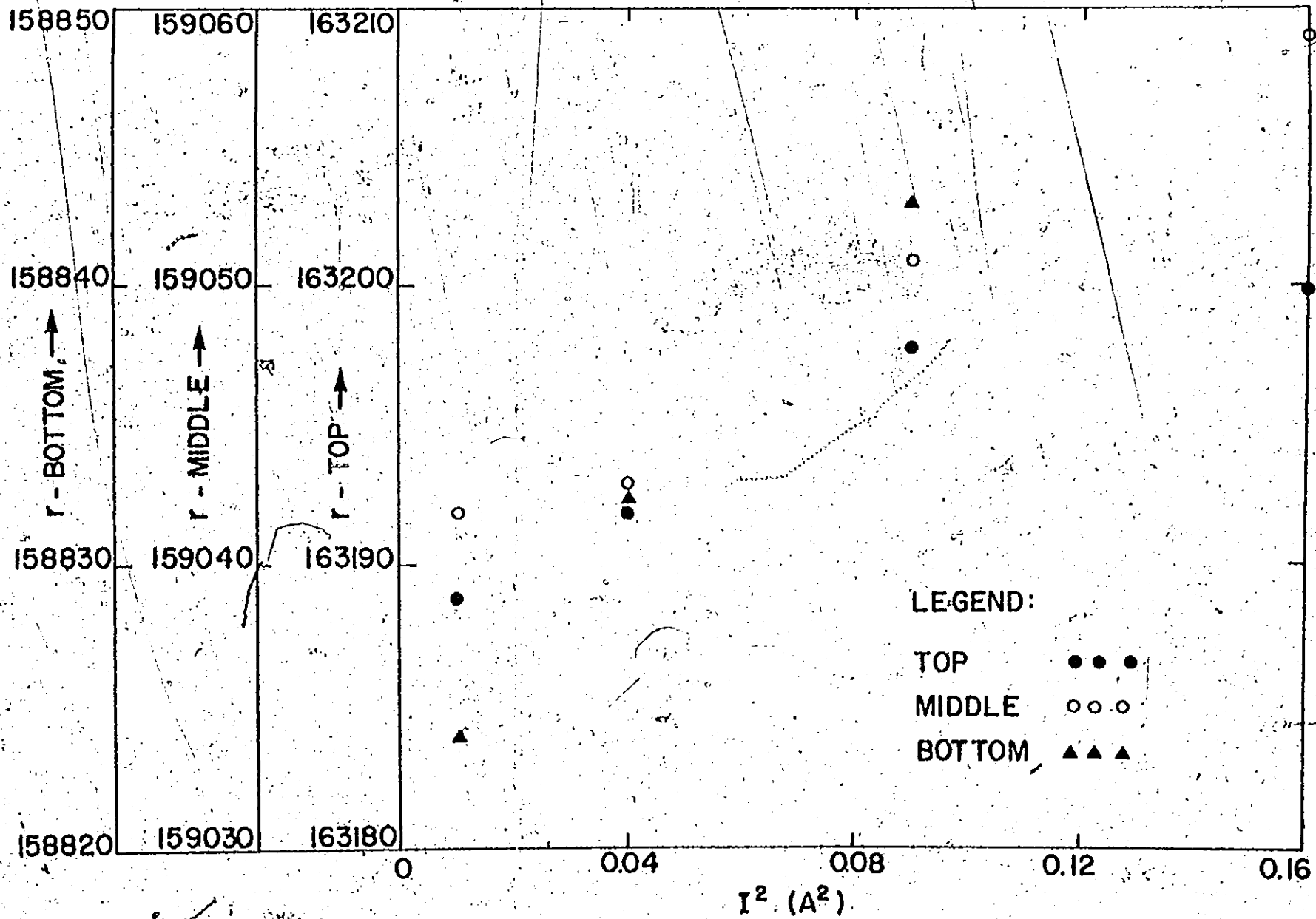

FIG.1 I VERSUS r PLOT FOR THE COPPER WIRES

With the above values, the ice-point resistance of the three copper wires was calculated using Eq.(2), Chapter III. Designating the resistance by a letter R and using subscript T, M, and B for top, middle, and bottom copper wires, respectively, the resistances are:

$$R_{To} = 0.0311586\ \Omega, \tag{1}$$

$$R_{Mo} = 0.0303664\ \Omega, \tag{2}$$

$$R_{Bo} = 0.0303252\ \Omega, \tag{3}$$

where subscript o is used to indicate that these are ice-point resistances.

2. BASE-LINES

As explained in Chapter II, on page 21, two kinds of tests were performed on the specimen at various mean temperatures for each moisture content; namely, a gradient test, and an isothermal test. We will recollect, that in isothermal tests the temperature difference ΔT_o was measured when only incidental heat flowed through the specimen, and in gradient tests the temperature difference ΔT_q was measured when the still present incidental heat as well as the heat from the main heater flowed through the specimen. The difference $\Delta T = \Delta T_q - \Delta T_o$ gave the correct value of the temperature difference to be used for the calculation of the thermal conductivity of the specimen [Eq.(5), page 21].

Since ΔT_o varies with temperature, the process of subtracting ΔT_o from ΔT_q is meaningful only when both of these have been obtained at the same mean temperature of the specimen. In practice it is very difficult to obtain identical mean temperatures for any two separate tests under different conditions. Hence, what was done here was, first a correlation between ΔT_o and the mean temperature for each moisture content was obtained, and then this correlation was used to estimate ΔT_o at the required mean temperature of gradient tests. It is now in order, to emphasize the difference between the overall mean temperature of the specimen from the section means for the upper and the lower parts. The overall mean temperature of the specimen is the arithmetic mean of the temperatures measured by the three copper wires, whereas the upper and the lower section mean temperatures are the averages of the top and the

middle and the bottom copper wires, respectively.

Calculations of ΔT_o, section mean temperatures, and overall mean temperature for a typical set of readings are illustrated here by the following example:

	Top	Middle	Bottom
Potentiometer reading (r)	169945	165696	165567
Resistance ($R=1.9105(10^{-7})r\Omega$)	0.0324684	0.0316567	0.0316320
Resistance ratio (R/R_o)	1.04206	1.04250	1.04311
Temperature (deg. C)	9.81607	9.91758	10.05995
ΔT_o (deg. C)		- 0.10151	- 0.14238
Section mean temperature (deg. C)		9.8668	9.9888
Overall mean temperature (deg. C)		9.9312	

Figures 2 to 5 show the variation of ΔT_o with temperature for moisture contents of 0, 1, 3, and 5 per cent, respectively. Straight lines were drawn through the experimental points using least square curve fitting method.

It should be observed that in all the experiments performed with the same sample there has always been a difference between ΔT_o for the lower and the upper portions of the sample. In fact, ΔT_o was always greater between the middle and the bottom wire than between the top wire and the middle. This may be due to a slight distortion in the distance separating the wires which may have occurred during the preparation of the sample, notwithstanding all the care which was taken to prevent it.

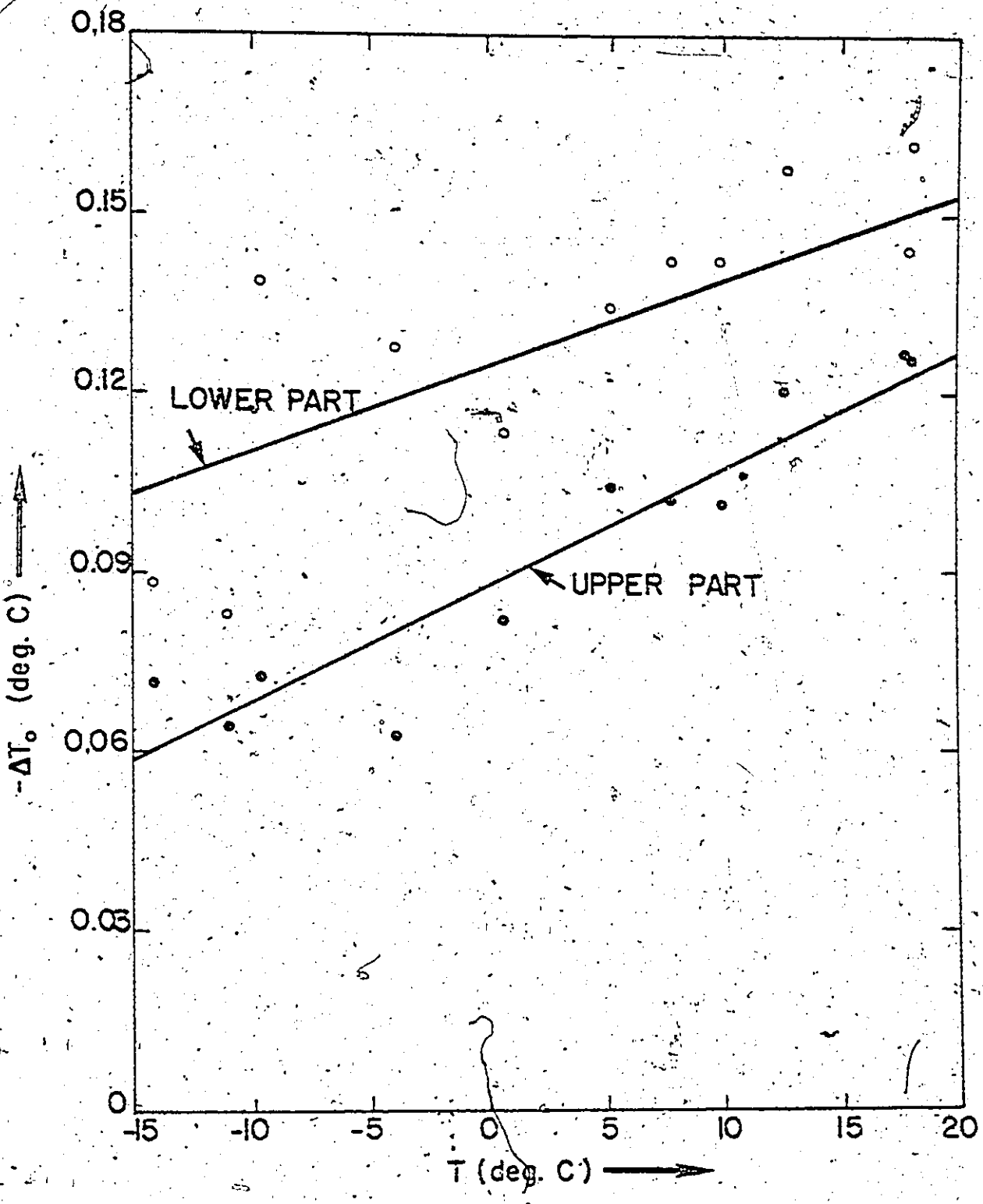

FIG. 2. VARIATION OF ΔT_o WITH T; <M> = 0 %

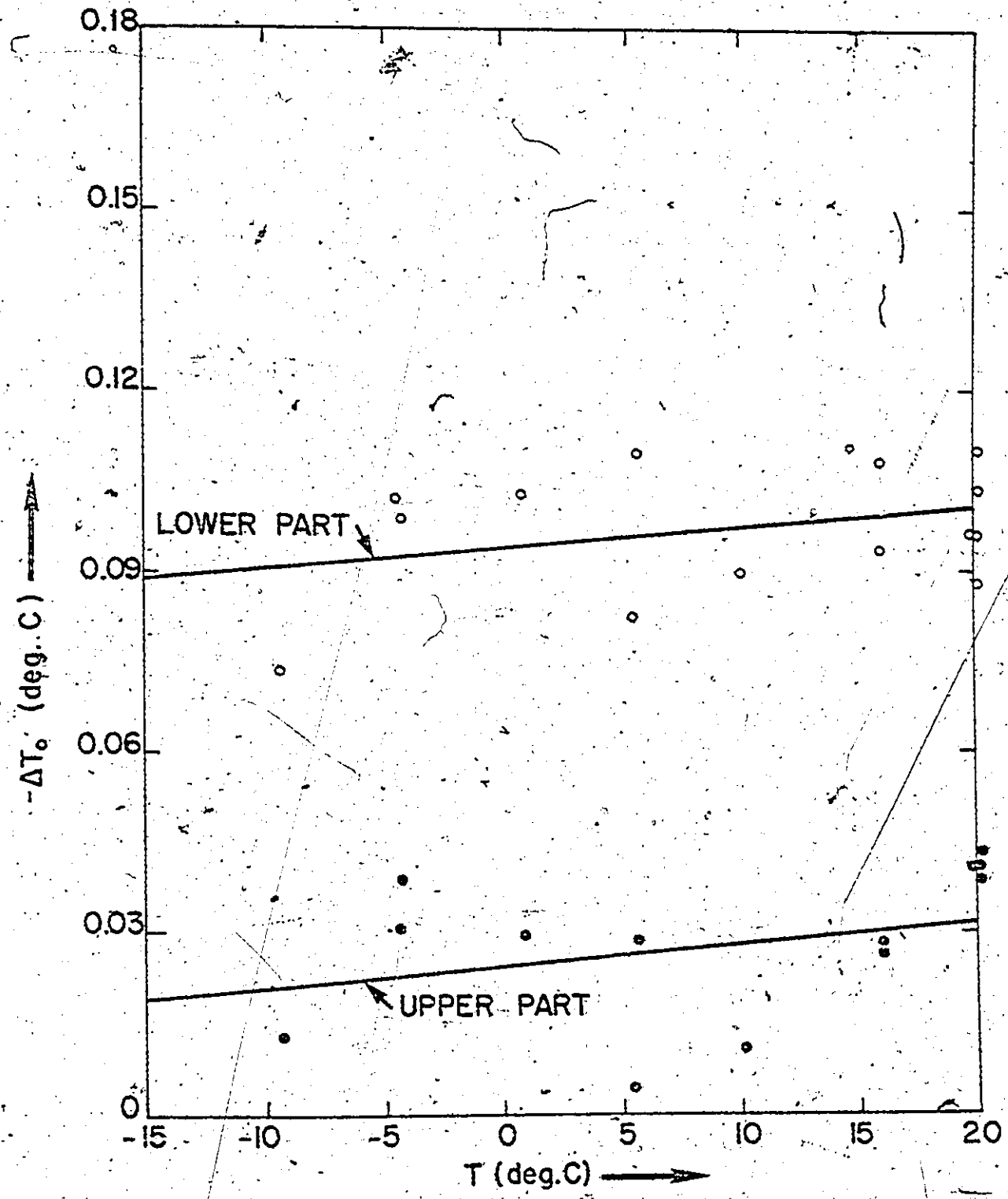

FIG. 3 VARIATION OF ΔT_0 WITH T; <M> = 1 %

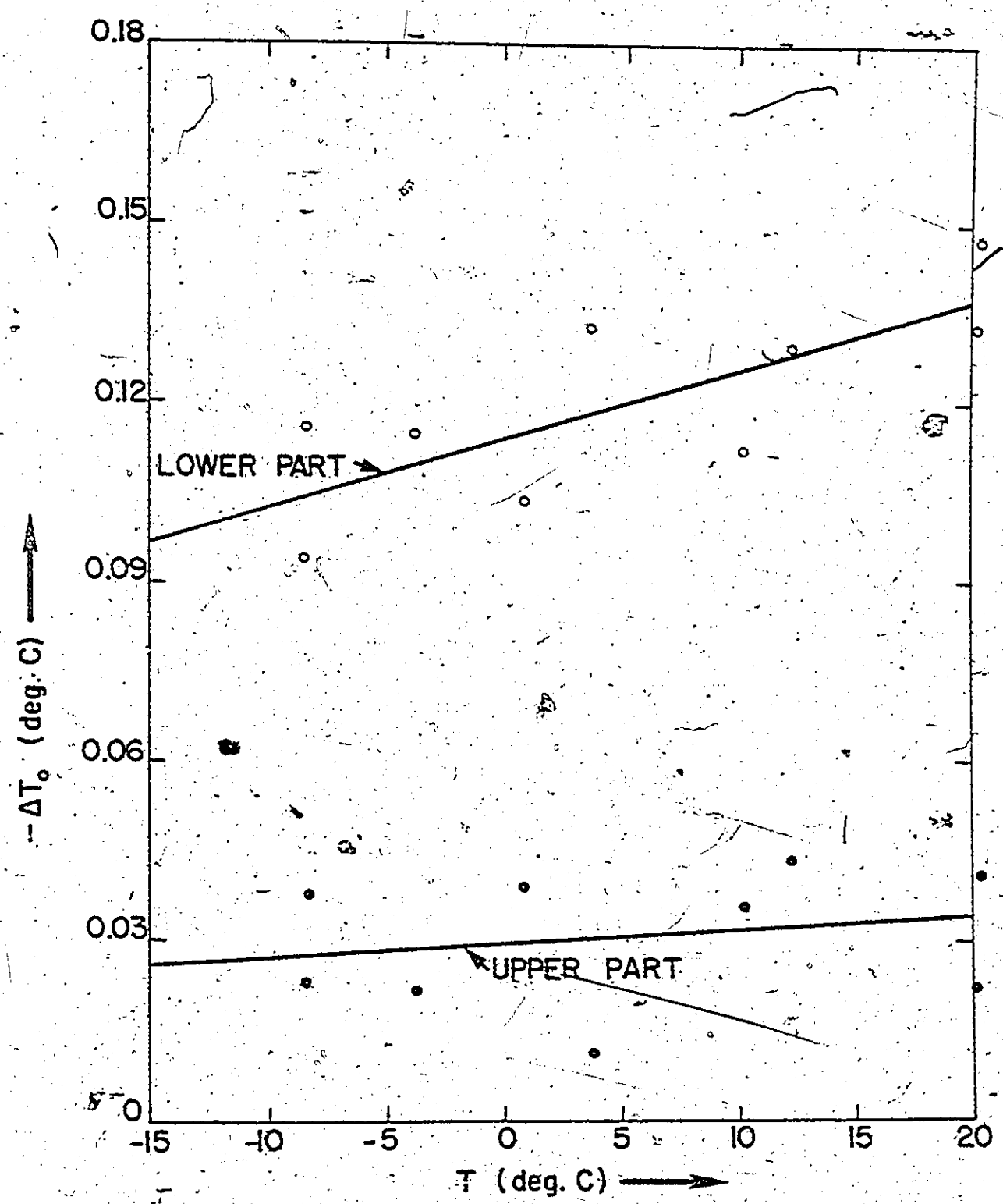

FIG.4 VARIATION OF ΔT_0 WITH T; $\langle M \rangle = 3\%$

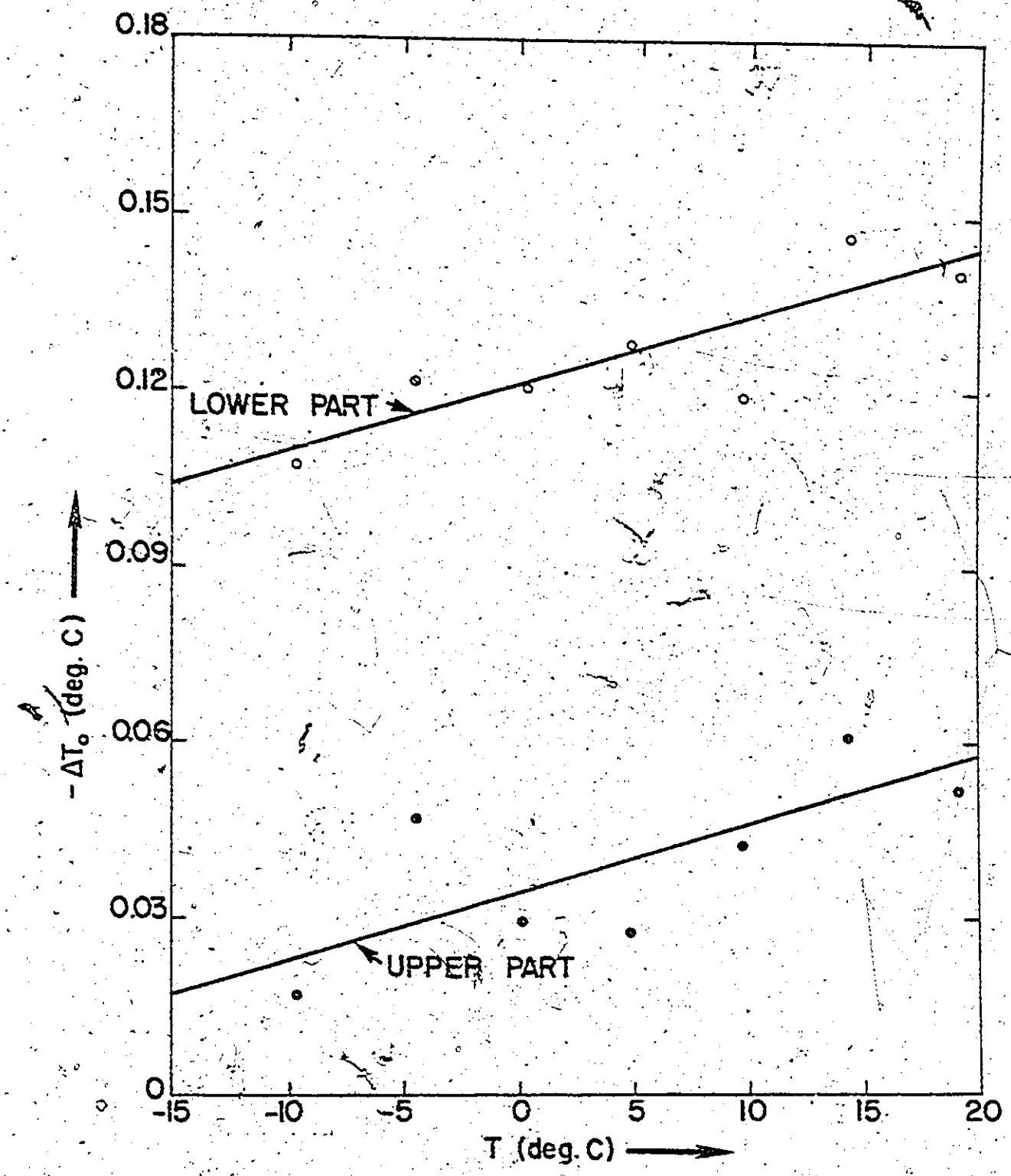

FIG. 5 VARIATION OF ΔT_o WITH T; <M> = 5 %

3. GRADIENT TESTS FOR CONDUCTIVITY

Gradient tests, described in Chapter II, page 21, yielded the values of ΔT_{q_1}, ΔT_{q_2}, and q for the various moisture contents and within the temperature range from -15 to 20 deg. C. The thermal conductivities for the upper and the lower part of the specimen were calculated according to the procedure discussed in Chapter II, Section 3.

A typical thermal conductivity calculation is shown in the following example:

Area of cross-section, $A = 8.107\ (10^{-3})\ m^2$

Distance between the sensors, $\Delta x = \Delta x_1 = \Delta x_2 = 8.763\ (10^{-3})\ m$

Voltage drop across the main heater = 3.001 V

Current through the main heater = 449.0 mA

The flow of heat through the specimen, $q = 3.001(449.0) = 1.3474\ (10^{3})\ mW$

	Top	Middle	Bottom
Potentiometer reading (r)	172160	165000	162080
Resistance ($R = 1.9105\ (10^{-7})r\ \Omega$)	0.0328916	0.0315237	0.0309658
Resistance ratio (R/R_o)	1.0556428	1.0381173	1.0211379
Temperature (deg. C)	12.983	8.896	4.935
Section mean temperature (deg. C)		10.942	6.916
Overall mean temperature (deg. C)		8.938	
ΔT_q (deg. C)		4.087	3.962
ΔT_o (from the base lines, page 101)		- 0.110	- 0.135
$\Delta T = \Delta T_q - \Delta T_o$ (deg. C)		4.197	4.096
Thermal conductivity ($\lambda = \frac{\Delta x}{A}\frac{q}{\Delta T}$ mW/m-K)		347	356

The results of this and other similar calculations are presented in Tables 2, 3, 4, and 5, for the overall moisture contents of 0 (dry specimen), 1, 3, and 5 per cent, respectively. The results are listed in the tables in the order in which the tests were performed.

TABLE 2

Conductivity as a function of temperature for the dry specimen

No.	T (deg. C)		λ (mW/m-K)	
	T_1	T_2	λ_1	λ_2
1	37.378	36.218	385	392
2	41.878	40.775	391	401
3	33.569	32.342	373	385
4	48.102	44.659	393	407
5	10.942	6.916	347	356
6	1.258	- 2.984	332	340
7	- 2.745	- 7.047	327	336
8	-13.406	-15.371	315	321
9	17.880	16.228	356	365
10	25.522	23.919	366	371

TABLE 3

Conductivity as a function of temperature for the specimen with <M> = 1

No.	T (deg. C)		λ (mW/m-K)	
	T_1	T_2	λ_1	λ_2
1	17.021	15.422	360	379
2	12.626	10.878	354	369
3	6.800	5.046	354	371
4	- 2.410	- 4.138	354	377
5	- 8.547	-10.387	342	364
6	-12.422	-14.282	354	357
7	2.496	0.678	364	375
8	17.756	15.934	363	372
9	2.350	0.542	358	368

TABLE 4

Conductivity as a function of temperature for the specimen with <M> = 3

No.	T (deg. C)		λ (mW/m-K)	
	T_1	T_2	λ_1	λ_2
1	-14.109	-15.824	375	423
2	- 9.792	-11.451	382	431
3	- 5.723	- 7.351	377	442
4	0.180	- 1.553	361	439
5	5.605	3.963	357	443
6	10.403	8.756	350	437
7	15.970	14.398	362	455
8	20.879	19.293	364	451

TABLE 5

Conductivity as a function of temperature for the specimen with <M> = 5

No.	T (deg. C)		λ (mW/m-K)	
	T_1	T_2	λ_1	λ_2
1	22.520	20.155	374	508
2	13.154	10.735	376	502
3	8.562	6.083	368	488
4	4.065	1.486	367	473
5	- 0.393	- 3.090	352	527
6	-13.075	-15.806	362	490
7	- 8.722	-11.535	367	500
8	- 4.840	- 7.575	377	516
9	18.038	15.527	381	489

4. GRADIENT TESTS FOR MOISTURE

Tables 6, 7, and 8 present the results of calculations for local moisture contents under temperature gradient conditions, for overall moisture contents of 1, 3 and 5 per cent, respectively. These tables also list the values of T_1, T_2, M_1, and M_2, which are simply the averages of the corresponding adjacent values of $T(x)$ and $M(x)$. The order in which the data are listed in the tables correspond to the sequence in which the tests were performed.

TABLE 6

Local temperature and moisture content under gradient conditions for <M>=1

No.	Location x=	C(x)	CD(x)	T(x)	M(x)	T_1 and T_2	M_1 and M_2
1	1	2190	2250	17.853	0.108	17.021	0.236
	0	1770	1900	16.189	0.363	15.422	0.407
	-1	1790	1950	14.656	0.451		
2	1	2180	2230	13.527	0.117	12.626	0.219
	0	1790	1890	11.725	0.322	10.878	0.373
	-1	1810	1930	10.031	0.423		
3	1	2140	2210	7.703	0.226	6.800	0.340
	0	1770	1870	5.896	0.455	5.046	0.501
	-1	1800	1920	4.195	0.546		
4	1	2120	2180	- 1.512	0.492	- 2.410	0.619
	0	1770	1850	- 3.308	0.746	- 4.139	0.865
	-1	1780	1890	- 4.969	0.984		
5	1	2100	2160	- 7.594	0.556	- 8.547	0.677
	0	1760	1830	- 9.501	0.798	-10.387	0.801
	-1	1800	1870	-11.273	0.804		
6	1	2050	2150	-11.466	0.908	-12.422	0.874
	0	1710	1820	-13.378	1.239	-14.282	1.046
	-1	1750	1860	-15.185	1.252		
7	1	2090	2200	3.438	0.453	2.496	0.610
	0	1730	1860	1.555	0.767	0.678	0.941
	-1	1760	1900	- 0.199	1.114		
8	1	2220	2250	18.697	0.049	17.756	0.160
	0	1800	1900	16.815	0.270	15.934	0.327
	-1	1810	1950	15.053	0.383		
9	1	2100	2200	3.285	0.409	2.350	0.530
	0	1750	1860	1.415	0.651	0.541	0.784
	-1	1790	1900	- 0.332	0.917		

TABLE 7

Local temperature and moisture content under gradient conditions for <M>=3

No.	Location x=	C(x)	CD(x)	T(x)	M(x)	T_1 and T_2	M_1 and M_2
1	1	2060	2140	-13.123	0.818	-14.109	1.365
	0	1630	1820	-15.094	1.911	-15.824	2.382
	-1	1280	1860	-16.553	4.253		
2	1	2020	2150	- 8.837	1.127	- 9.792	1.368
	0	1660	1830	-10.747	1.610	-11.451	2.389
	-1	1220	1870	-12.154	4.369		
3	1	2020	2170	- 4.780	1.121	- 5.723	1.304
	0	1670	1840	- 6.665	1.487	- 7.351	2.431
	-1	950	1880	- 8.036	5.375		
4	1	2080	2190	1.166	0.539	0.180	0.720
	0	1750	1860	- 0.805	0.901	- 1.553	2.124
	-1	1360	1900	- 2.300	3.348		
5	1	2080	2210	6.563	0.456	5.605	0.515
	0	1750	1880	4.646	0.574	3.963	2.296
	-1	1110	1910	3.280	4.017		
6	1	2140	2220	11.353	0.225	10.483	0.260
	0	1800	1880	9.454	0.295	8.756	1.751
	-1	1180	1930	8.059	3.207		
7	1	2130	2240	16.873	0.248	15.970	0.309
	0	1770	1900	15.066	0.370	14.398	1.641
	-1	1130	1940	13.730	2.913		
8	1	2130	2260	21.787	0.242	20.879	0.266
	0	1790	1910	19.971	0.289	19.293	1.377
	-1	1270	1960	18.616	2.064		

TABLE 8

Local temperature and moisture content under gradient conditions for <M>=5

No.	Location x=	C(x)	CD(x)	T(x)	M(x)	T_1 and T_2	M_1 and M_2
1	1	2220	2270	23.912	0.071	22.520	0.441
	0	1600	1910	21.128	0.810	20.155	3.304
	-1	250	1960	19.182	5.799		
2	1	2200	2230	14.564	0.072	13.154	0.539
	0	1610	1890	11.743	1.006	10.735	3.443
	-1	500	1930	9.726	5.881		
3	1	2180	2220	10.002	0.102	8.562	0.616
	0	1620	1880	7.121	1.130	6.083	3.487
	-1	640	1920	5.045	5.845		
4	1	2170	2200	5.561	0.111	4.065	0.624
	0	1800	1870	2.568	0.337	1.486	3.353
	-1	640	1900	0.405	6.370		
5	1	2140	2190	1.145	0.227	-0.393	0.833
	0	1670	1850	- 1.931	1.439	-3.090	4.076
	-1	560	1890	- 4.249	6.713		
6	1	2040	2150	-11.530	0.984	-13.075	1.326
	0	1660	1820	-14.619	1.668	-15.806	4.139
	-1	700	1860	-16.992	6.610		
7	1	2100	2160	- 7.137	0.562	- 8.722	1.046
	0	1670	1830	-10.307	1.530	-11.535	4.041
	-1	680	1870	-12.763	6.553		
8	1	2110	2170	- 3.308	0.539	- 4.840	1.011
	0	1670	1840	- 6.371	1.484	- 7.575	4.098
	-1	600	1880	- 8.778	6.712		
9	1	2170	2250	19.591	0.156	18.038	0.450
	0	1650	1900	16.485	0.744	15.527	3.096
	-1	470	1940	14.568	5.447		

5. ERROR IN ABSOLUTE VALUE OF CONDUCTIVITY

Despite all precautions and sophistication in the design of an apparatus and in the process of taking readings, it is never possible to completely suppress all the sources of errors. It is always good to have some idea of the uncertainties encountered in the measurements due to these sources of errors. A method for estimating such uncertainties, suggested by Kline and McClintock (1953), is based on deciding how likely it is for the maximum uncertainty to occur in any given primary measurement. According to this method, if w_R is the uncertainty to be calculated of the result R, where R is a given function of the independent variables $x_1, x_2, \ldots x_n$, and $w_1, w_2, \ldots w_n$ are the known uncertainties in the independent variables, then

$$w_R = \left[\left(\frac{\partial R}{\partial x_1} w_1 \right)^2 + \left(\frac{\partial R}{\partial x_2} w_2 \right)^2 + \ldots + \left(\frac{\partial R}{\partial x_n} w_n \right)^2 \right]^{1/2}, \qquad (4)$$

if the odds are the same for all measurements.

Applying this method in our case, where the conductivity is given by

$$\lambda = - \frac{q}{A} \frac{\Delta T}{\Delta x},$$

we have,

$$\frac{\partial R}{\partial x_1} = \frac{\partial \lambda}{\partial q} = - \frac{1}{A} \frac{\Delta T}{\Delta x},$$

$$\frac{\partial R}{\partial x_2} = \frac{\partial \lambda}{\partial \Delta T} = - \frac{q}{A} \frac{1}{\Delta x},$$

$$\frac{\partial R}{\partial x_3} = \frac{\partial \lambda}{\partial \Delta x} = \frac{q}{A} \frac{\Delta T}{(\Delta x)^2},$$

$$\frac{\partial R}{\partial x_4} = \frac{\partial \lambda}{\partial A} = \frac{q}{A^2} \frac{\Delta T}{\Delta x},$$

Substituting these values in Eq.(4) and dividing both sides of the equation by λ, we get

$$\left(\frac{W_\lambda}{\lambda}\right)^2 = \left(\frac{W_q}{q}\right)^2 + \left(\frac{W_{\Delta T}}{\Delta T}\right)^2 + \left(\frac{W_{\Delta x}}{\Delta x}\right)^2 + \left(\frac{W_A}{A}\right)^2 \quad (6)$$

But $q = IV$. where I is current and V is voltage. Therefore, Eq.(6) may also be written:

$$\left(\frac{W_\lambda}{\lambda}\right)^2 = \left(\frac{W_I}{I}\right)^2 + \left(\frac{W_V}{V}\right)^2 + \left(\frac{W_{\Delta T}}{\Delta T}\right)^2 + \left(\frac{W_{\Delta x}}{\Delta x}\right)^2 + \left(\frac{W_A}{A}\right)^2 \quad (7)$$

Considering the values of the independent variable from a typical set of readings, we have

$I = 0.1988 \pm 0.0001$ A

$V = 1.331 \pm 0.001$ V

$\Delta T = 0.6856 \pm 0.0005$ deg. C

$\Delta x = 8.763(10^{-3}) \pm 0.0004$ m

$A = 8.107(10^{-3})$ m^2

These values, when substituted in Eq.(7), give

$$\frac{W_\lambda}{\lambda} = 0.045.$$

The error in Δx is dominant in the calculations of the overall error in the value of λ. It is obvious that this procedure of error-estimation is meaningful only if the percentage error or uncertainty is of the same order of magnitude for all the independent variables.

Appendix E

SIMPLIFIED MODEL

1. APPROXIMATE ANALYSIS

1.1 REPRESENTATION OF THE SYSTEM:

In principle the problem of expressing the thermal conductivity of a granular material as a function of the conductivities and volume fractions of its constituents can be solved if the shape of the granules and their mode of packing are known. But in practice, this cannot be achieved because of the innumerable difficulties that come in the way. One of the major difficulties is that the exact geometry of the pore system in sequence along the flow path should be known in detail, which normally is not the case. The irregularity of the shape and distribution of the granules makes it virtually impossible to produce a rigorous analysis of the problem. Appropriate simplifications must therefore be made to be able to formulate an approximate solution of this problem.

The following was an attempt at doing precisely this. Certain assumptions were made regarding the size, shape, and distribution of the granules, the location of the moisture present in it, and the mode of

heat transfer.

The granular material was assumed to be composed of identical and uniform solid spherical particles of radius R, though in reality the granules are more likely to be oblate spheroids rather than spheres. The arrangement of the spheres was assumed such that each sphere touches six neighbors only. This arrangement, known as a cubic lattice of uniform spheres, gives a porosity of 47.64 per cent, though in reality the spheres would be packed tighter than that. The moisture present, owing to capillarity, was assumed to be located only around the contact points of the spheres, occupying a wedge-shaped ring. The curvature of the meniscus was taken as zero.

For the calculation of the thermal conductivity of a composite system of solid, liquid, and gas, it is sufficient to consider a flow of heat through a representative portion of this composite system. Such a representative portion may consist of a cube in which is enclosed a solid sphere of radius R. Six wedge-shaped rings of water are located at the contact points of the sphere and the cube wall, and the rest of the cube is filled with still air. For sake of simplicity, it is sufficient to consider one half of our cube, as shown in Fig. 1. The base of the hemisphere is perpendicular to the direction of the flow of heat. The value of R was taken as unity.

The cross-section of the wedge-shaped ring of water located around point N in Fig. 1 is shown by the cross-hatched area PQN. The volume

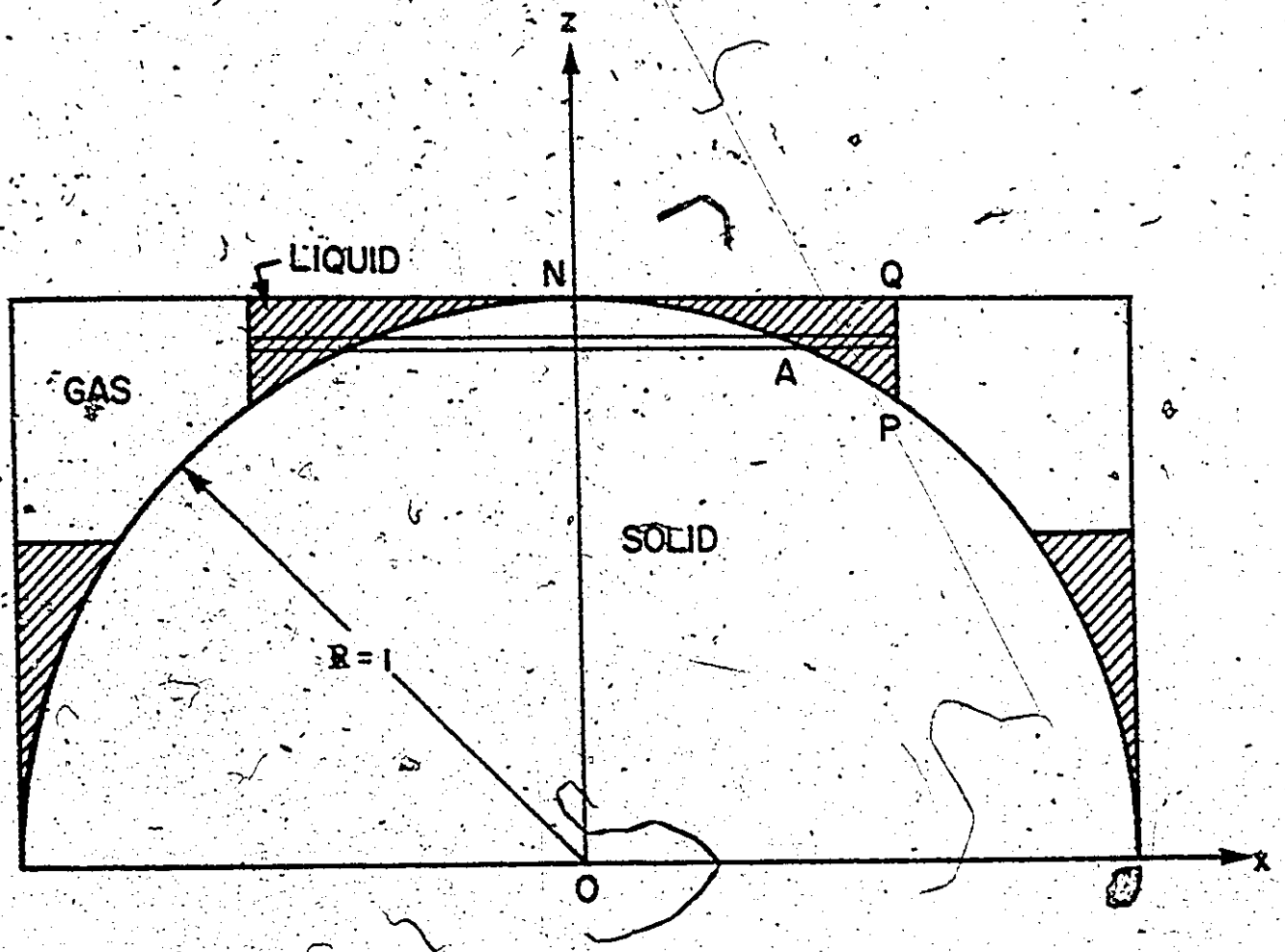

FIG. 1 A COMPOSITE SYSTEM OF SOLID, LIQUID, & GAS

of this ring increases with the increasing moisture content of the system. If the moisture content by volume, that is, the ratio of water volume to the total volume of the system, is designated by H, then

$$H = \frac{\text{(Volume of one ring) x (number of rings)}}{\text{(volume of the cube)}}$$

or the volume of the ring PQN equals 4H/3.

With reference to Fig. 1, we shall designate by u and v the coordinates of point P, and by x and z those of any arbitary point A lying on arc NP. The dependence of v on H was obtained as follows:

The volume of an infinitesimal ring-shaped layer is $\pi(u^2 - x^2)dz$, and the volume of the total ring of water is given by

$$\pi \int_v^1 (u^2 - x^2)dz. \qquad (1)$$

Substituting $(z^2 - v^2)$ for $(u^2 - x^2)$ since $x^2 + z^2 = 1$, we can write

$$\int_v^1 (z^2 - v^2)dz = \pi\left(\frac{1}{3} - v^2 + \frac{2}{3}v^3\right). \qquad (2)$$

Hence,

$$\frac{4H}{3} = \pi\left(\frac{1}{3} - v^2 + \frac{2}{3}v^3\right), \qquad (3)$$

or

$$H = \frac{\pi}{4}(1 - 3v^2 + 2v^3). \qquad (4)$$

The minimal value of v is $1/\sqrt{2}$ (see Fig. 1), since there will be an overlapping of the neighbouring ring of water below this value of v.

This sets an upper limit of the value of H to about 0.16 for a valid use of this model which fortunately did not concern us here because our values of H do not range above about 0.1.

For a given value of the moisture content, H, Eq.(4) is a cubic equation in v. The appropriate value of v was obtained in the following manner.

Equation (4) was rewritten as

$$y^3 + py^2 + qy + r = 0, \tag{5}$$

where $y = v$, $p = -3/2$, $q = 0$, $r = 1/2 - 2H/\pi$.

Substituting $x - p/3$ for y, Eq.(5) was reduced to the form

$$x^3 + ax + b = 0, \tag{6}$$

where $a = (3q - p^2)/3 = -3/4$,

$$b = (2p^3 - 9pq + 27r)/27 = (\pi - 8H)/4\pi.$$

Three kinds of solutions are available for this equation depending on the value of $b^2/4 + a^3/27$ being greater than, equal to, or smaller than zero.

In our case

$$\frac{b^2}{4} + \frac{a^3}{27} = \frac{H(4H - \pi)}{4\pi^2} < 0,$$

because the value of H was always less than about 0.1. Accordingly, Eq.(6) has three real and unequal roots, namely:

$$x_o = 2\sqrt{-a/3}\,\cos(\phi/3),$$

$$x_1 = 2\sqrt{-a/3}\,\cos(\phi/3 + 2\pi/3),$$

$$x_2 = 2\sqrt{-a/3}\,\cos(\phi/3 + 4\pi/3),$$

where

$$\cos \phi = \pm\sqrt{b^2/4 \div (-a^3/27)},$$

negative sign being applicable in front of the square root when b is positive. In our case b is positive, since $H < 0.1$. Therefore,

$$\cos \phi = -\sqrt{b^2/4 \div (-a^3/27)}$$
$$= 8H/\pi - 1,$$

and

$$x_o = \cos\left[\frac{1}{3}\arccos(8H/\pi - 1)\right],$$
$$x_1 = \cos\left[\frac{1}{3}\arccos(8H/\pi - 1) + 2\pi/3\right],$$
$$x_2 = \cos\left[\frac{1}{3}\arccos(8H/\pi - 1) + 4\pi/3\right].$$

Recalling that $y = x - p/3$, the three real roots of Eq. (5) are;

$$y_o = 0.5 + \cos\left[\frac{1}{3}\arccos(8H/\pi - 1)\right],$$
$$y_1 = 0.5 + \cos\left[\frac{1}{3}\arccos(8H/\pi - 1) + 2\pi/3\right],$$
$$y_2 = 0.5 + \cos\left[\frac{1}{3}\arccos(8H/\pi - 1) + 4\pi/3\right].$$

Which of these three roots was suitable for the problem in question had to be decided by substituting various values of H in them and selecting the one whose value remained within the limits $0 < y < 1$. This condition was satisfied only by y_2.

Hence,

$$v = 0.5 + \cos\left[\frac{1}{3}\arccos(8H/\pi - 1) + 4\pi/3\right]. \qquad (7)$$

In our experimental investigation we have used the ratio of weight of water to the weight of dry sand, <M>, rather than the ratio of the

water volume to the total volume, H. The relationship between H and <M> is:

$$H = \frac{\text{water volume}}{\text{total volume}}$$

$$= \frac{\text{weight of water}}{\text{density of water}} \frac{1}{\text{total volume}}$$

$$= \frac{\langle M \rangle \text{ (weight of sand)}}{\text{density of water}} \frac{1}{\text{total volume}} .$$

In our case, weight of sand = 1971 g,

total volume = 1135 cm^3,

density of water = 1 g/cm^3,

Thus,

$$H = 1.736 \langle M \rangle . \qquad (8)$$

We now have v as a function of <M>:

$$v = 0.5 + \cos\left[\frac{1}{3} \arccos(13.888 \langle M \rangle/\pi) + 4\pi/3\right] . \qquad (9)$$

1.2 COMPUTATION OF THERMAL RESISTANCE AND THERMAL CONDUCTIVITY:

Because of a large difference between the conductivities of the constituent phases of the system shown in Fig. 1, the heat flow lines are not parallel to each other. But for simplicity, in this approximate analysis, the heat-flow lines are assumed to be parallel.

In the first stage of our calculations we shall disregard the four water rings located around the four points on the equator of our sphere. An appropriate correction will be introduced subsequently.

Thus, in that first approximation the system in Fig. 1 is divided in three sections, as shown in Fig. 2. Section 1 is a right circular cylinder of radius u, composed of water and solid. Section 2 is a hollow cylinder of outer radius of unity and composed of air and solid. Section 3 consists of four corners of the model containing air only.

The Fourier equation of uni-directional heat conduction with constant cross-sectional area, A, is

$$\frac{q}{\Delta T} = \frac{A}{\sum \ell_i/\lambda_i}, \tag{10}$$

where q is the heat-flow rate, ΔT is the temperature difference, and ℓ_i and λ_i are respectively the thickness and the conductivities of different layers of materials.

Consider an elemental cylinder of unit height, radius r, and thickness dr (Fig. 2). The value of $dq/\Delta T$ for this cylinder is

$$\frac{dq}{\Delta T} = \frac{2\pi r\, dr}{\ell_s/\lambda_s + \ell_f/\lambda_f}, \tag{11}$$

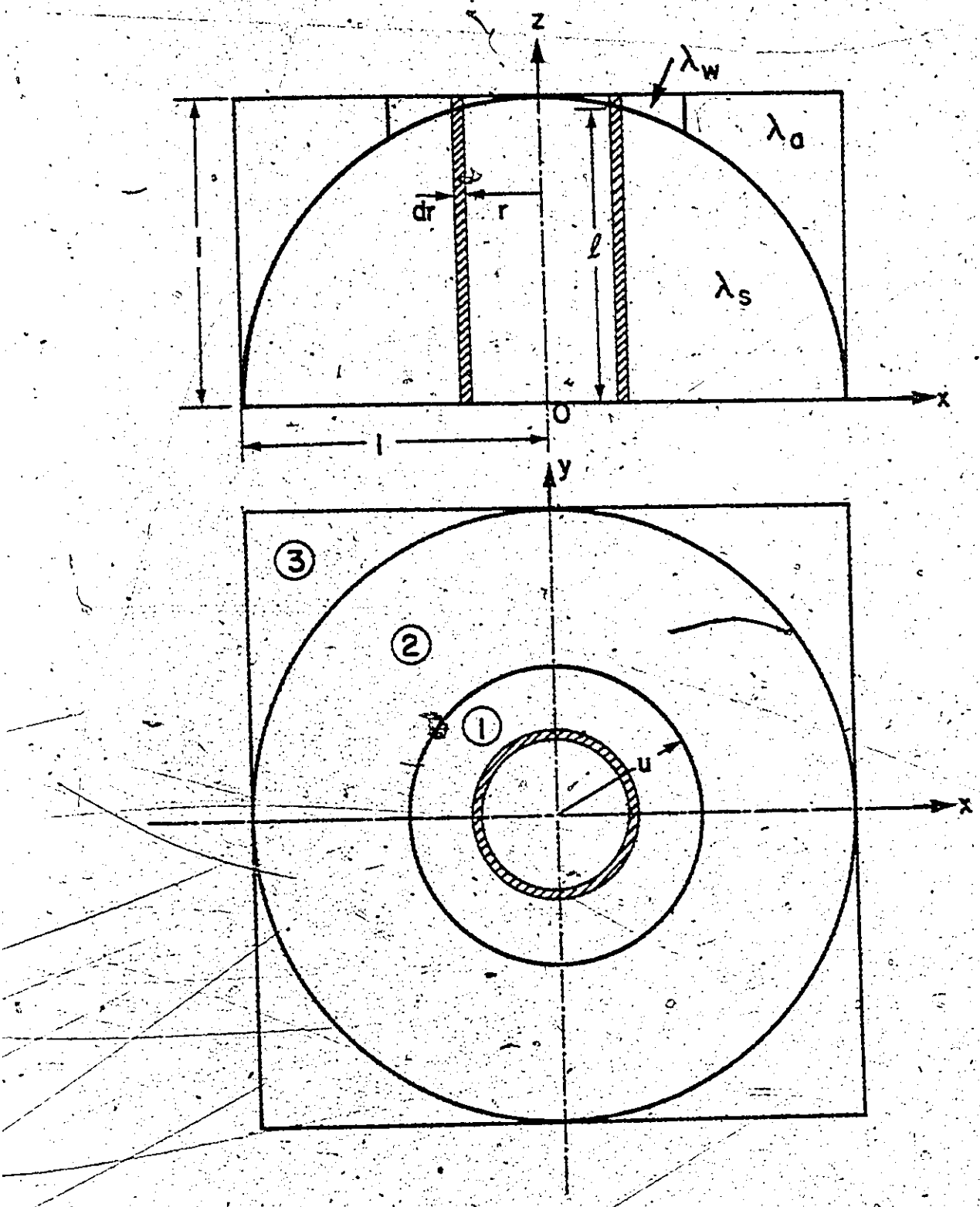

FIG. 2 THREE SECTIONS OF THE COMPOSITE SYSTEM

where ℓ_s and λ_s refer to the solid and ℓ_f and λ_f to the fluid. For section 1 we shall write ℓ_w and λ_w (w signifying water) and for section 2 — ℓ_a and λ_a (a signifying air).

Let q_1 and q_2 be the heat-flow rates in sections 1 and 2 respectively. Then,

$$\frac{q_1}{\Delta T} = \int_0^u \frac{2\pi r\, dr}{\ell_s/\lambda_s + \ell_w/\lambda_w}$$

$$= 2\pi\, \lambda_s\lambda_w \left[\frac{1 - v}{\lambda_w - \lambda_s} + \frac{\lambda_s}{(\lambda_w - \lambda_s)^2} \ell n \frac{(\lambda_w - \lambda_s)v + \lambda_s}{\lambda_w} \right], \quad (12)$$

$$\frac{q_2}{\Delta T} = \int_u^1 \frac{2\pi r\, dr}{\ell_s/\lambda_s + \ell_a/\lambda_a}$$

$$= 2\pi\, \lambda_s\lambda_a \left[\frac{v}{\lambda_a - \lambda_s} + \frac{\lambda_s}{(\lambda_a - \lambda_s)^2} \ell n \frac{\lambda_s}{(\lambda_a - \lambda_s)\, v + \lambda_s} \right], \quad (13)$$

where $v = 1 - u^2$.

Section 3, consisting of the four corners, has a total cross-sectional area

$$A_3 = 4 - \pi.$$

Thus,

$$\frac{q_3}{\Delta T} = \frac{\lambda_a(4 - \pi)}{1}. \quad (14)$$

The total rate of heat flow in this first approximation is

$$\frac{q}{\Delta T} = \frac{q_1}{\Delta T} + \frac{q_2}{\Delta T} + \frac{q_3}{\Delta T}$$

$$= -2\pi\,\lambda_s\lambda_w\left[\frac{1 - v}{\lambda_w - \lambda_s} + \frac{\lambda_s}{(\lambda_w - \lambda_s)^2}\ln\frac{(\lambda_w - \lambda_s)v + \lambda_s}{\lambda_w}\right]$$

$$- 2\pi\,\lambda_s\lambda_a\left[\frac{v}{\lambda_a - \lambda_s} + \frac{\lambda_s}{(\lambda_a - \lambda_s)^2}\ln\frac{\lambda_s}{(\lambda_a - \lambda_s)v + \lambda_s}\right]$$

$$+ (4 - \pi)\lambda_a . \qquad (15)$$

In order to correct for the four water rings at the equator, we must concern ourselves only with areas m and n in Fig. 3. There are eight identical pairs of such areas. The correction consists of subtracting the heat flow calculated with respect to these areas with the previous assumptions and substitute for it the heat flow existing in the presence of the equatorial water rings.

Consider an enlarged quarter of Fig. 3. The heat flows through columns perpendicular to the plane of the figure. Let dA_m and dA_n, shown in Fig. 4, be generic cross-sections of such columns in areas m and π, respectively.

Area m was previously considered to include air only. Its area is

$$A_m = u(1 - v) - \left(\frac{1}{2}\arctan\frac{u}{v} - \frac{1}{2}uv\right).$$

The previously calculated heat flow through this area is

$$\frac{q_m}{\Delta T} = \frac{\lambda_a A_m}{1 -} . \qquad (16)$$

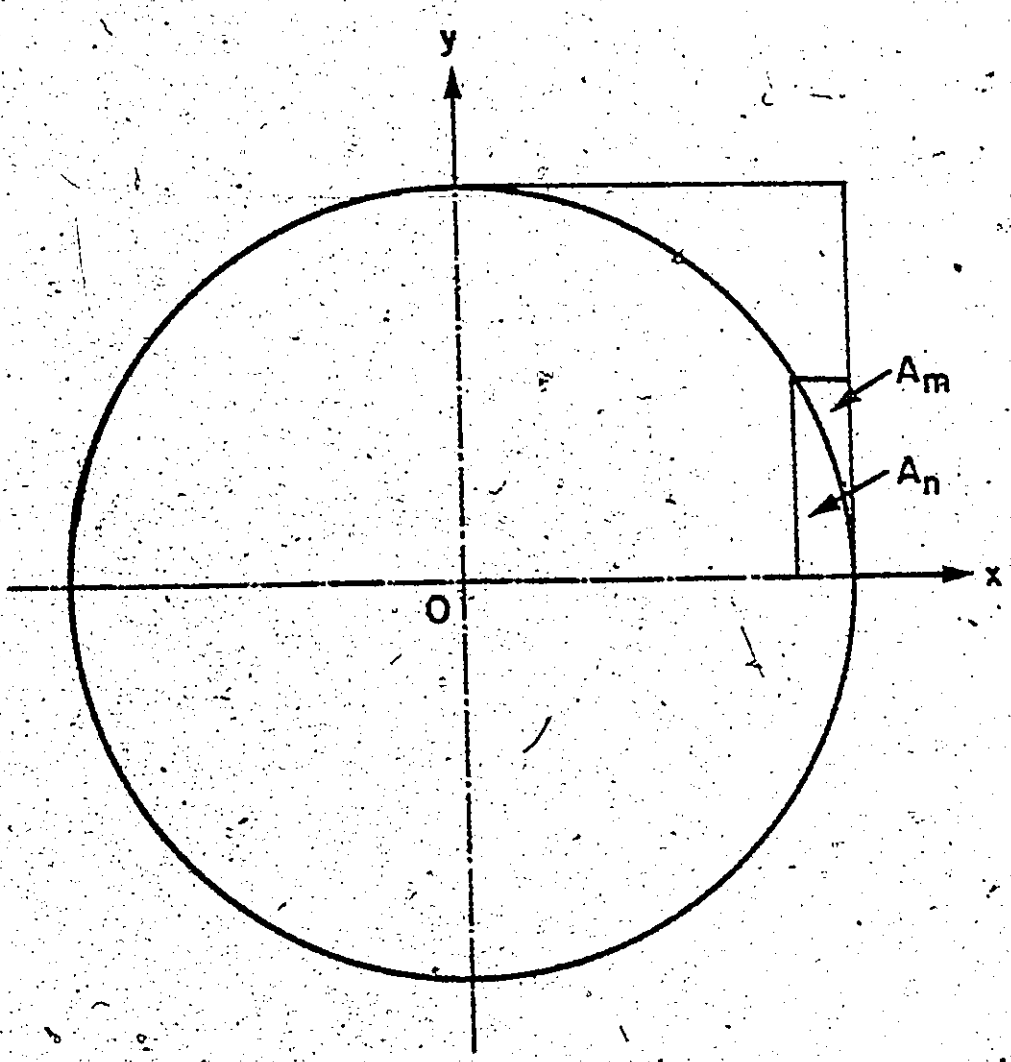

FIG. 3 AREAS UNDER CONSIDERATION

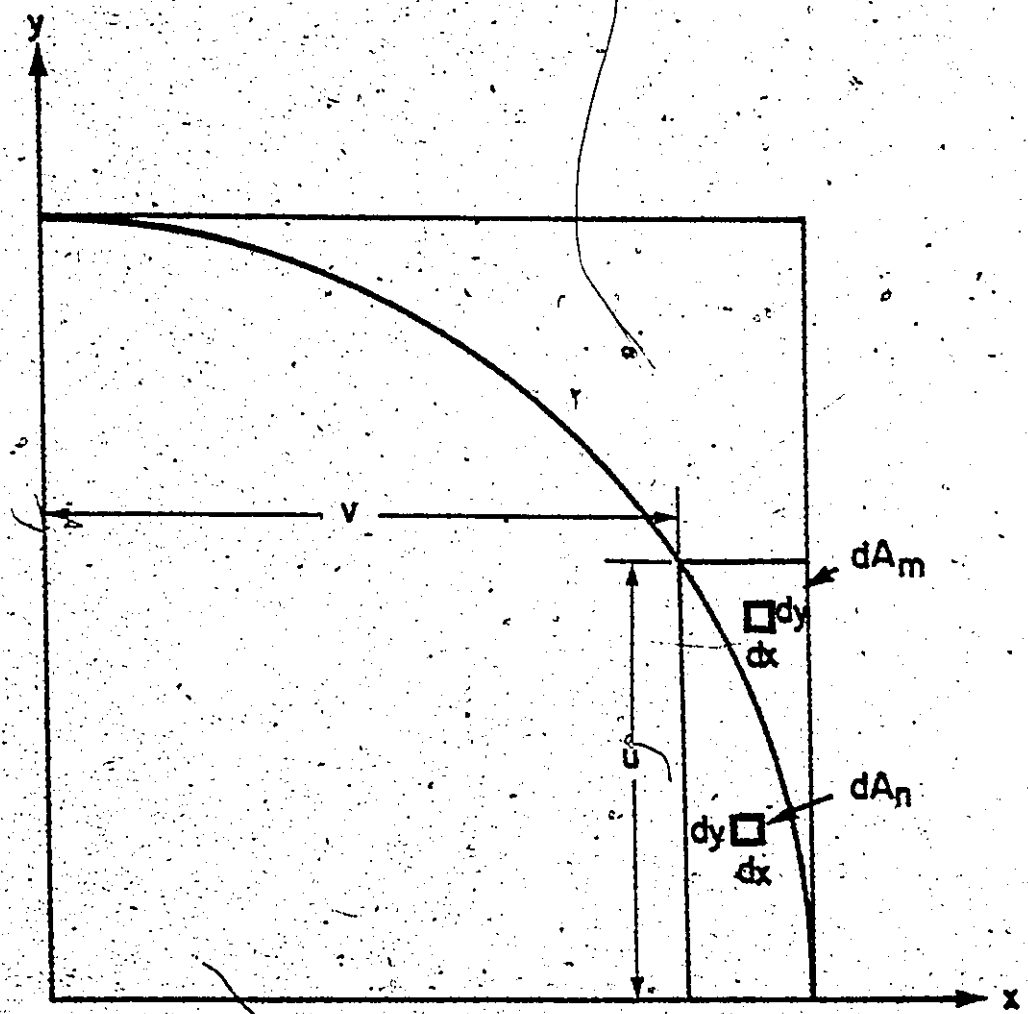

FIG. 4 AN ENLARGED QUARTER OF FIG. 3

For it we must now substitute

$$\frac{q'_m}{\Delta T} = \int_v^1 dx \int_{\sqrt{1-x^2}}^{u} \frac{dy}{(1 - \sqrt{u^2 - y^2})/\lambda_a + \sqrt{u^2 - y^2}/\lambda_w} \qquad (17)$$

Thus, the correction for the area m is

$$\frac{q'_m}{\Delta T} - \frac{q_m}{\Delta T} = \int_v^1 dx \int_{\sqrt{1-x^2}}^{u} \frac{dy}{(1 - \sqrt{u^2 - y^2})/\lambda_a + \sqrt{u^2 - y^2}/\lambda_w} - \lambda_a A_m \qquad (18)$$

Similarly, the correction for the area n is

$$\frac{q'_n}{\Delta T} - \frac{q_n}{\Delta T} = \int_v^1 dx \int_0^{\sqrt{1-x^2}} \frac{dy}{(1 - \sqrt{u^2 - y^2})/\lambda_a + (\sqrt{u^2 - y^2} - \sqrt{1-x^2-y^2})/\lambda_w + \sqrt{1-x^2-y^2}/\lambda_s}$$

$$- \int_v^1 dx \int_0^{\sqrt{1-x^2}} \frac{dy}{(1 - \sqrt{1-x^2-y^2})/\lambda_a + \sqrt{1-x^2-y^2}/\lambda_s} \qquad (19)$$

For half a cube

$$\frac{q_c}{\Delta T} = \frac{4\,\lambda_{moist}}{1}$$

where λ_{moist} is the required conductivity of moist material and $q_c/\Delta T$ is the corrected rate of heat flow through the model element consisting of half a cube:

$$\frac{q_c}{\Delta T} = \frac{q}{\Delta T} + 8\left[\frac{q'_m}{\Delta T} - \frac{q_m}{\Delta T}\right] + 8\left[\frac{q'_n}{\Delta T} - \frac{q_n}{\Delta T}\right] \qquad (21)$$

Hence,

$$\lambda_{moist} = \frac{\pi}{2}\lambda_s\lambda_w\left[\frac{1-v}{\lambda_w-\lambda_s} + \frac{\lambda_s}{(\lambda_w-\lambda_s)^2}\ell n\,\frac{(\lambda_w-\lambda_s)v+\lambda_s}{\lambda_w}\right]$$

$$+ \frac{\pi}{2}\lambda_s\lambda_a\left[\frac{v}{\lambda_a-\lambda_s} + \frac{\lambda_s}{(\lambda_a-\lambda_s)^2}\ell n\,\frac{\lambda_s}{(\lambda_a-\lambda_s)v+\lambda_s}\right]$$

$$+ \frac{1}{4}(4-\pi)\,\lambda_a$$

$$+ 2\int_v^1 dx \int_{\sqrt{1-x^2}}^{u} \frac{y}{(1-\sqrt{u^2-y^2})/\lambda_a + \sqrt{u^2-y^2}/\lambda_w}$$

$$- 2\,\lambda_a\left[u(1-v) - \left(\frac{1}{2}\arctan\frac{u}{v} - \frac{1}{2}uv\right)\right]$$

$$+ 2\int_v^1 dx \int_0^{\sqrt{1-x^2}} \frac{dy}{(1-\sqrt{u^2-y^2})/\lambda_a + (\sqrt{u^2-y^2}-\sqrt{1-x^2-y^2})/\lambda_w + \sqrt{1-x^2-y^2}/\lambda_s}$$

$$- 2\int_v^1 dx \int_0^{\sqrt{1-x^2}} \frac{dy}{(1-\sqrt{1-x^2-y^2})\lambda_a + \sqrt{1-x^2-y^2}/\lambda_s} \qquad (22)$$

Equation (22) represents the conductivity of the system in terms of the conductivities of the constituent phases. The conductivities of two special cases are also obtained from the same equation by appropriate substitutions. Conductivity of dry model is obtained by letting $\lambda_w = \lambda_a$. Thus,

$$\lambda_{dry} = \frac{\pi}{2}\lambda_a\lambda_s\left[\frac{1}{\lambda_a-\lambda_s} + \frac{\lambda_s}{(\lambda_a-\lambda_s)^2}\ell n\,\frac{\lambda_s}{\lambda_a}\right] + (1-\frac{\pi}{4})\lambda_a \qquad (23)$$

Replacing λ_a by λ_w in Eq.(23) we get the conductivity of the model completely saturated with water. Thus,

$$\lambda_{sat} = \frac{\pi}{2} \lambda_w \lambda_s \left[\frac{1}{\lambda_w - \lambda_s} + \frac{\lambda_s}{(\lambda_w - \lambda_s)^2} \ln \frac{\lambda_s}{\lambda_w} \right] + \left(1 - \frac{\pi}{4}\right) \lambda_w . \qquad (24)$$

1.3 CONDUCTIVITY OF THE CONSTITUENT PHASES:

For the numerical calculations of the thermal conductivity of granular material of varying moisture content by means of Eq.(22), the numerical values of the thermal conductivity of solid, liquid, and gaseous phases involved are required. Besides being able to calculate the dependence of the thermal conductivity of the system on its moisture content, the variation of the thermal conductivity with average temperature of the system could also be obtained, provided the variation of the thermal conductivity of the constituent phases with temperature was also known.

The constituent phases involved in our problem are pure crystalline quartz, water, and air, and the temperature range of interest to us is from -15 to 20 deg. C. The conductivities in this temperature range were obtained as follows:

Conductivity of quartz:

The thermal conductivities of pure quartz at various temperatures were obtained from Touloukian, Powell, Ho, and Klemens (1970). In this reference, the values are given for two configurations. Some selected values are:

Thermal conductivity of SiO_2 (High-purity single quartz crystal)

T (K)	λ_1(W/cm-K) Heat flow parallel to C-axis	λ_2(W/cm-K) Heat flow perpendicular to C-axis
250	0.127	0.075
273	0.116	0.0684
300	0.104	0.0621

A body of crystalline quartz will normally consist of a large number of crystals of random orientation. A mean value of λ must be weighted 1 for parallel and 2 for perpendicular orientation, giving

$$\lambda = \frac{\lambda_1 + 2\lambda_2}{3}$$

So weighted, the values of λ are:

T(deg. C)	λ_{quartz}(W/cm-K)
-- 23	0.0923
0	0.0843
27	0.0761

The relation between λ and T seems approximately linear in this range of temperature, and may be expressed as

$$\lambda_{quartz} = 0.0843 - 0.00032\ T \quad (W/cm\text{-}K), \qquad (25)$$

where T is in deg. C.

Conductivity of water:

The selected values of thermal conductivity of saturated water were obtained from Touloukian, Lilely, and Saxena (1970);

They are

T(deg. C)	λ(W/cm-K)
- 3	0.005551
7	0.005818
17	0.005918

The relation between λ and T is approximately linear in the given temperature range, expressible as

$$\lambda_{water} = 0.00571 + 0.000015\ T \quad (W/cm\text{-}K) \tag{26}$$

where T is in deg. C.

Conductivity of ice:

It is found that the thermal conductivity of ice is rather difficult to measure with any accuracy. According to Pounder (1965) the best data for pure ice are probably those of Jakob and Erk, as is also confirmed by Fletcher (1970). They found the variation of λ_{ice} with temperature to be approximately linear, and represented it by

$$\lambda_{ice} = 5.35(10^{-3})\left[1 - 4.8(10^{-3})T\right] \quad Cal/cm\text{-}sec\text{-}C$$

where T is a centigrade temperature. On changing the units, the above equation becomes

$$\lambda_{ice} = 0.0224 - 0.00011\ T \quad (W/cm\text{-}K) \tag{27}$$

where T is in deg. C. This expression is not valid for ice temperatures below about 100 K, which does not concern us.

Conductivity of air:

The conductivity values for dry air were adopted from Touloukian, Lilely, and Saxena (1970). Some selected values are

T(deg. C)	λ_{air}(W/cm-K)
-23	0.0002226
-13	0.0002305
-3	0.0002385
7	0.0002461
17	0.0002538

which can be approximated by a relation

$$\lambda_{air} = 0.00024 + 0.000001\ T \quad (W/cm\text{-}K) \tag{28}$$

where T is in deg. C.

1.4 COMPARISON OF RESULTS:

The values of λ_{moist} were calculated using Eq.(22) at various temperatures and various overall moisture contents. Conductivities of solid quartz, water, ice, and dry air were obtained from Eqs.(25), (26), (27), and (28), respectively. The values of v, appearing in Eq.(22) were obtained from Eq.(9) for the various values of the overall moisture content <M>. The results of calculations are presented in Table 1. The table contains the values of λ_{moist} for <M> varying from 1 to 5 per cent by weight in steps of 1 per cent, and for T varying from -15 to 20 deg. C in steps of 5 deg. The values of the two limiting cases of Eq.(22), that is, the dry system and the saturated system, are also given in the same table.

TABLE 1

Predicted values of thermal conductivity of moist sand

T (deg. C)	-15	-10	-5	-1	1	5	10	15	20
Quartz:	8910	8750	8590	8462	8398	8270	8110	7950	7790
Water:	2405	2350	2295	2251	572	578	586	593	601
Air:	23	23	23	24	24	24	25	25	26
Dry Sand:	182	184	187	189	190	192	194	197	199
Sat. Sand:	4624	4528	4433	4357	1939	1941	1944	1945	1946
<M> = 1:	1099	1112	1125	1135	876	897	922	946	970
<M> = 2:	1464	1465	1465	1464	1036	1052	1072	1092	1110
<M> = 3:	1723	1714	1705	1698	1137	1151	1168	1184	1200
<M> = 4:	1927	1912	1896	1883	1210	1223	1237	1251	1265
<M> = 5:	2098	2076	2054	2036	1268	1278	1291	1303	1315

Comparison of the results of this computation with our experimental findings given on page 123 helped us to draw the following conclusions. The predicted values give a positive λ-T slope, as do the experimental values, both for the dry specimen as well as for the moist. Both, the predicted and the experimental values, indicate an abrupt change in their magnitude at the freezing point of water. The predicted values for the dry sand are lower than the experimental ones by a factor of about 1.8. This could, most probably, be due to the assumption of looser packing arrangement of the particles in this approximate analysis of the model. The predicted values for the moist sand on the other hand are much higher than those obtained experimentally, and the ratio of the predicted to the observed values increases slightly with increasing

moisture content. The assumption that all the moisture is concentrated around the contact points of the spheres exaggerates its influence on conductivity and is the most likely cause for the high values predicted by the model.

Another possible reason for the discrepancy in magnitudes is that the computation of the thermal resistance in this approximate analysis was based on a very crude assumption of parallel heat-flow lines. The next section deals with a way of obtaining the thermal resistance with a better approximation. It also incorporates other suggestions to improve this analysis.

2. IMPROVED ANALYSIS

2.1 BETTER ASSUMPTIONS:

There are several problems in analyzing heat flow in a moist granular material. One of these problems, as already mentioned, is the constant movement of moisture, giving rise to an additional heat-flow mechanism besides straight conduction. Even if only conduction is considered, a number of improvements can be made in our previously described analysis.

Shape and size of particles:

It seems not unreasonable to assume that our material is composed of identical and uniform solid spherical particles, and that the surface of these particles is smooth for all practical purposes. This assumption is supported by an examination of an enlarged photograph of some randomly selected sand particles, shown in Fig. 2 in Chapter IV. Thus we do not propose to modify this assumption which has the virtue of relative simplicity.

Packing arrangement:

The closest possible packing arrangement of uniform spheres gives a porosity value of 26 per cent. Looser systems of packing can be obtained by carefully constructing arches within the packing, but the loosest of the stable packing arrangement gives a porosity value of 47.6 per cent. The porosity value of unsystematic stable packing of uniform spheres lies somewhere between these two values. The porosity value of our sample is about 35.5 per cent, which is far from close to 47.6 per cent that has been assumed for the model in the previous section. The assumption of cubic lattice arrangement of spheres is highly idealized and most unlikely to occur in practice. Webb (1956) attributed the discrepancies between the experimental and predicted values of thermal conductivity of dry granular materials, to the idealised packing of the particles. De Vries (1956) also confirmed that the inadmissible simplification regarding the arrangement of spheres is to be blamed for errors in the predicted conductivity values for dry granular materials. It is reasonable to suggest that similar discrepancies must arise in the case of moist granular materials. For a better model, a packing arrangement which has a porosity value closer to reality, should be considered. Several packing arrangements of uniform spheres are shown in Fig. 5, and the porosity, density, volume of unit prism, spacing of layers, and number of points of contact for each such arrangement are listed in Table 2.

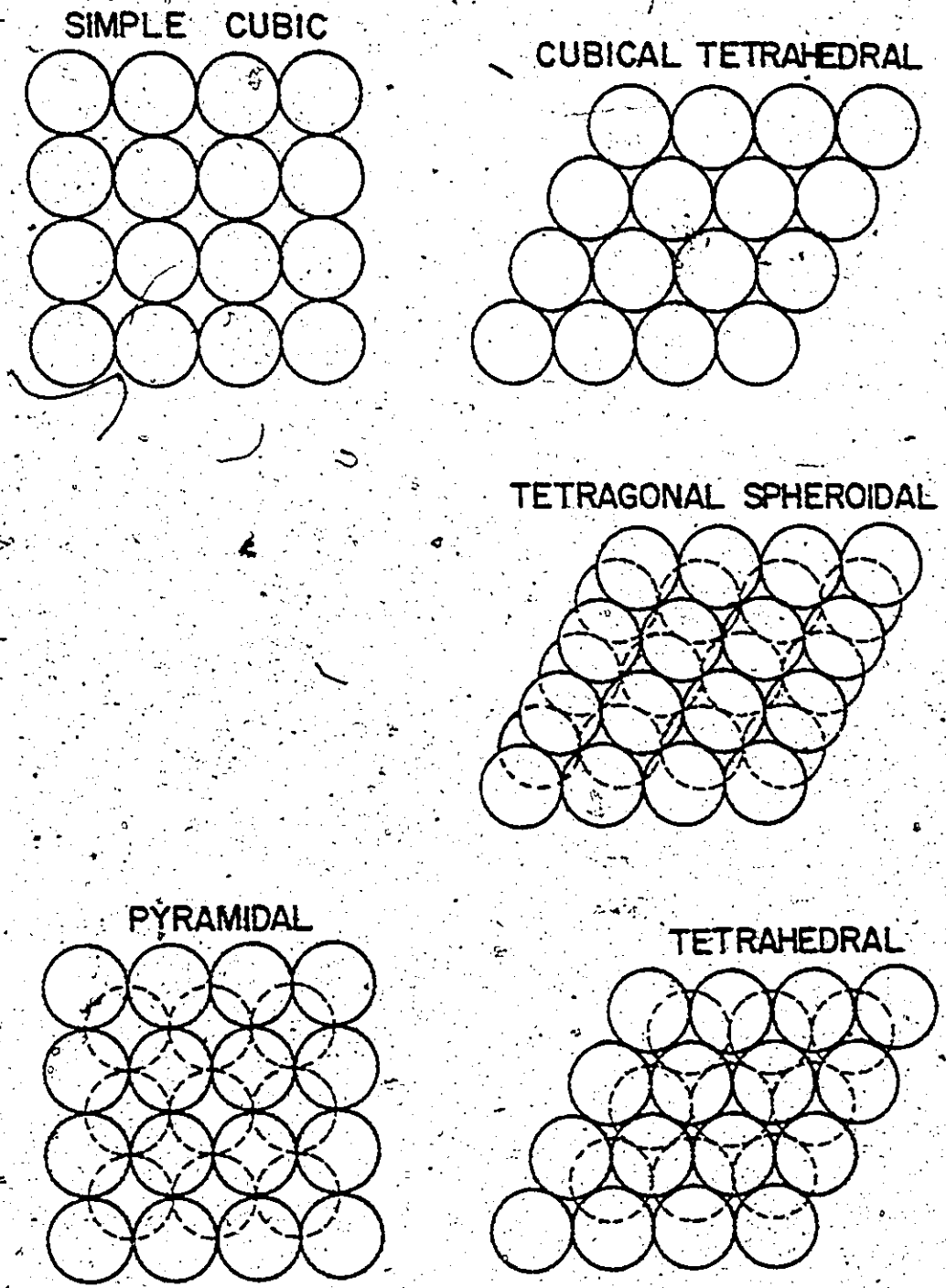

FIG. 5 PACKING ARRANGEMENT OF UNIFORM SPHERES

It would appear that calculations should be performed with cubic-tetrahedral and tetragonal-spheroidal arrangements and an average value of conductivities thus obtained may be thought of being more representative of our sand.

TABLE 2

Packing arrangements

Type of packing	Number of Contact points	Spacing of layers	Volume of unit prism	Density	Porosity (per cent)
Simple cubic	6	$2R$	$8R^3$	$\pi/6$	47.64
Cubical-tetrahedral	8	$2R$	$4\sqrt{3R^3}$	$\pi/3\sqrt{3}$	39.54
Tetragonal-spheroidal	10	$R\sqrt{3}$	$6R^3$	$2\pi/9$	30.19
Pyramidal	12	$R\sqrt{2}$	$4\sqrt{2R^3}$	$\pi/3\sqrt{2}$	25.95
Tetrahedral	12	$2R\sqrt{2/3}$	$4\sqrt{2R^3}$	$\pi/3\sqrt{2}$	25.95

In the above table, R is the radius of sphere. The details of these packings can be found in Deresiewicz (1958). It should be noted that the density and porosity is independent of the common diameter of the spheres, provided that the packing is extended over a very large region so that the boundary effect is negligible. The problem of packing of spheres in a finite region is considerably more difficult. Packing in a circular cylinder has been discussed by Suphik (1949), and inside a hollow sphere by Hadwiger (1952). When, as in our case, the diameter of the particles is very small compared to the overall dimensions of the sample, this aspect of the problem is quite unimportant. Deresiewicz (1958) also discusses problem of packing of a system having particles of different

sizes, as well as a packing of non-spherical particles.

Location of moisture and its influence on conductivity of air:

Lacking better information, one would presumably continue to consider liquid moisture to be concentrated in rings around the contact points. It is, however, more likely that the air in the pores is water-vapor saturated rather than dry. The mass of this vapor should be subtracted from the mass used in the calculation of ring dimensions. Also, rather than using the conductivity of dry air, we could use *effective thermal conductivity* of saturated air (after Krisher, 1941). This latter value includes the effects of evaporation, vapor diffusion and condensation.

2.2 PROCEDURE:

The assumption of unidirectional heat flow and mutually parallel heat flow lines is justifiable in a case when the conductivities of solid, liquid, and gaseous phases of a composite system do not depart much from each other. But in a case like ours, where the conductivities of the constituent phases differ from each other by orders of magnitude, such an assumption is bound to lead to sizeable errors, as was shown by Feingold (1966).

In order to provide a mathematically correct solution, consideration of a three-dimensional flow of heat is unavoidable. Because of the symmetry in any of the packing arrangements listed in Table 2, parallel isothermal planes can be identified so that the geometry and the pattern

of heat flow be repeated between each pair of such consecutive planes. We need, therefore, to concern ourselves only with what happens in one such discrete layer. Generally, other isothermal surfaces will not be plane. If the shape of a number of them were known, we could draw heat-flow lines perpendicularly through them; each line extending from one isothermal plane of symmetry to the next. These heat-flow lines would identify channels and the heat flux could be calculated for each such channel. These, in turn, would be added to provide the total rate of heat flow.

To illustrate this principle, let us consider the simplified representative model of the system shown in Fig. 1 on page 182. The hemisphere is redrawn in Fig. 6. In this figure, the system is bounded between two parallel isothermal planes, A-A' and B-B'. These planes could be identified easily, because of the symmetry of the model about these planes. The isothermal and the heat-flow lines are schematically shown in only half the portion of the figure. These lines could be obtained in the following manner.

The model could be divided into a number of small cubes, and the temperatures in the corners of these cubes could be obtained by usual numerical procedures. Isothermal surfaces, such as C-C' and D-D' in Fig. 6, could then be identified by interpolation. Two heat-flow lines perpendicular to these surfaces are marked as E-E' and F-F'. The whole model can be filled up with such isothermal surfaces and as

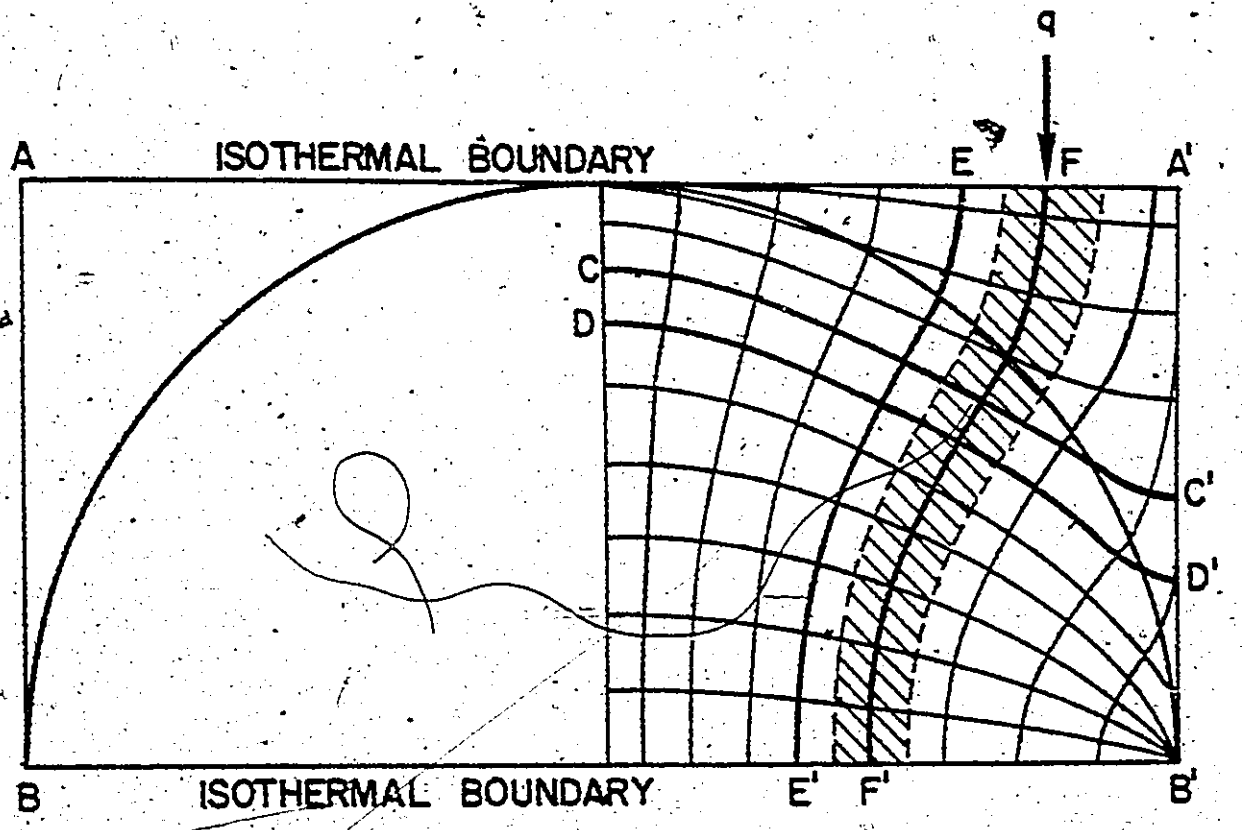

FIG. 6 ISOTHERMAL AND HEAT-FLOW LINES

many equidistant heat-flow lines as is found convenient.

Considering a particular heat-flow line, say F-F', the thermal resistance in the path of q could be computed. The cross-section of such a path is shown by the shaded area in the figure. This thermal resistance may be composed of the resistances due to solid, liquid and gaseous phases in different combinations depending on where the particular path is located.

The accuracy of the numerical method for the determination of temperature distribution depends theoretically on the number of points used. In practice this is not quite so simple because the linear system resulting from our numerical equations is not solved with unlimited accuracy and an unlimited computer storage capacity. Thus, a happy medium has to be found beyond which further increase in the number of points will be counter producing.

Interpolation will have to be resorted to at the curved boundaries between the phases and the entire enterprise is very tedious but not impossible.

3. NONANALYTICAL APPROACH

As discussed on page 115 in Chapter VI, the equation proposed by De Vries (1952) was used to predict the conductivity of our dry sand. The comparison between the predicted and the experimental values was shown to be good (see Fig. 1, page 117). De Vries' equation is

$$\lambda = 1.2 \frac{\lambda_f v_f + \lambda_s v_s F}{v_f + v_s F}, \tag{29}$$

where

$$F = \frac{1}{3} \sum_{i=1}^{3} \frac{1}{1 + (\lambda_s/\lambda_f - 1) g_i}, \tag{30}$$

with

$$\sum_{i=1}^{3} g_i = 1 . \tag{31}$$

In this, λ_f and λ_s are the fluid (gas or liquid) and solid conductivities, respectively. The fluid and the solid volume fractions are represented by v_f and v_s, respectively. De Vries selected $g_1 = g_2 = 0.125$ and $g_3 = 0.75$, which corresponds to particles having the shape of an ellipsoid of revolution.

Equation (29) is modified here to predict the conductivity of moist sand for low overall moisture contents. We are attempting to replace the conductivity of dry air (λ_f in Eq.(29)) by a value which would take into account the conductivity of dry air and that of water. This effective conductivity of air could be expressed as a function of volume fractions of air and water. Thus, Eq.(29) would read

$$\lambda_{moist} = 1.2 \frac{\lambda_{ea} v_a + \lambda_s v_s F}{v_a + v_s F}, \tag{32}$$

$$F = \frac{1}{3} \sum_{i=1}^{3} \frac{1}{1 + (\lambda_s/\lambda_{ea} - 1) g_i}, \tag{33}$$

where λ_{ea} stands for the effective conductivity of air. The expressions similar to Eqs.(32) and (33) would be used to evaluate λ_{ea}, such that

$$\lambda_{ea} = \frac{\lambda_a v_a + \lambda_w v_w B}{v_a + v_w B}, \tag{34}$$

$$B = \frac{1}{3} \sum_{i=1}^{3} \frac{1}{1 + (\lambda_w/\lambda_a - 1) g_i}. \tag{35}$$

where subscripts a and w stand for air and water, respectively.

There is, of course, no real physical basis for this extension of De Vries' procedure. However, when the calculations were performed in the manner suggested, they were closer to our experimental results than those obtained from Eq.(22).

Appendix F

PROBE TECHNIQUE FOR CONDUCTIVITY DETEMINATION

1. DESCRIPTION

The guarded hot-plate instrument is considered to be a *Standard Lab* apparatus, in which the emphasis is on accuracy rather than on reducing the duration of tests. All steady-state methods for that matter demand careful experimentation, and involve rather long durations of time.

It is, therefore, natural for scientists to try to obtain similar information more rapidly by transient methods. One of the nonsteady-state methods for the measurement of thermal conductivity, known as a *heated probe technique*, utilizes time-temperature relationship of a line heat source embedded in the material. The temperature rise of such a line heat source, as a function of time, as already derived in Appendix B, is

$$T - T_i = \frac{q}{4\pi\lambda} \left(\ln \frac{4\alpha t}{d^2} - \gamma\right). \tag{1}$$

For a time interval $t_2 - t_1$, the rise in temperature at a point in the medium is given by

$$T_1 - T_2 = \frac{q}{4\pi\lambda} \ln \left(\frac{t_2}{t_1}\right). \tag{2}$$

A plot of temperature rise versus the logarithm of time should give a straight line with a slope of $q/4\pi\lambda$. With the knowledge of this slope and of the power applied per unit length, λ can be obtained from Eq.(2). This simple equation does not always give the correct indication of the conductivity when used in this technique. The reason is that Eq.(2) is applicable only in a case when an infinitely large medium is heated by an infinitely thin line heat source for a sufficiently large duration of time. The factors that are thought to affect the accuracy, are:

(1) Finite probe dimensions;
(2) Thermal properties of the probe material;
(3) Contact resistance at the probe-specimen interface;
(4) Location of temperature measuring device;
(5) Finite specimen dimensions;
(6) Conduction heat losses through temperature measuring leads;
(7) Initial temperature difference between the probe and the specimen.

Improvements in the design and the theory of probes have taken care of most of the above factors but not all. With modifications, the probe method of determining thermal conductivity of dry granular material has been found reasonably satisfactory (Mann and Forsyth, 1956; De Vries and Peck, 1958; Woodside, 1958; Haupin, 1960; etc.). In most of the cases the test results were reproducible and were in good agreement with similar results obtained from the tests on guarded hot-plate apparatus. In spite of this, it was thought that "this method will not supersede

the "standard" methods" — Mann and Forsyth.

While this method works reasonably well on dry granular materials, it encounters severe shortcomings when employed to calculate thermal conductivity of non-granular materials, like wood, concrete, fibrous insulation, etc. This method is also unsuitable for determining thermal conductivity of moist granular materials. Drying of the material near the line heat source causes a lowering of thermal conductivity, and the value of λ obtained by the use of Eq.(2) with a reasonable degree of accuracy, represents some kind of an average thermal property of the moist material (De Vries and Peck, 1958; Woodside, 1958; Woodside and Bruyn, 1959; Pratt, 1969; Moench and Evans, 1970).

Even with the knowledge of the shortcoming of the probe technique, specially in our experimental set up, an attempt was made to evaluate the conductivity of our specimen using this method. The following section deals with the calculation of conductivity from the temperature rise versus time curves of our sensors embedded in the specimen, and also with the comparison of these results with our steady-state results.

2. CALCULATION AND COMPARISON

The temperature-rise versus time curves, that is, the self-heating responses of our copper wires, were used to calculate the conductivity of our specimen material. All the self-heating responses, obtained under various temperature and moisture conditions of our specimen, were plotted on a semi-log scale as discussed on page 24 in Chapter II. The slope of the lines (parameter B in Eq.(6) on page 24, Chapter II) were calculated, which represent the value of $q/4\pi\lambda$ appearing in Eq.(2) of this appendix to a certain scale. The values of the power applied per unit length, q, were available to us from our gradient tests. The values of λ were calculated for our dry specimen as well as our moist specimen for the three given overall moisture contents, in the temperature range from -15 to 20 deg. C.

Each experimental set gave us three values of thermal conductivity at the three levels in the specimen. To see how these values compare with those obtained using the steady-state method, the conductivities of the dry specimen — obtained by the two methods — are plotted in Fig. 1. The line in the upper part of the figure is for the steady-state method, and is the same as the one appearing in Fig. 1 in Chapter VI. The two lines appearing in the lower part of the figure are those for the bottom and top portions of the specimen, obtained using nonsteady state method. All the three lines were obtained by the method of least squares. The actual experimental points are also shown in the figure.

As can be seen from the figure, the transient method yielded the conductivities which are about 20 per cent lower than those obtained from steady-state method. The difference between the conductivities for the top and the bottom portions of our specimen, obtained by the use of the former method diminishes with increasing temperature. Lastly, as can be observed, the scatter of the experimental points about the respective lines is much larger in case of transient method than that in case of steady-state. These discrepancies were found to be larger in case of moist specimen.

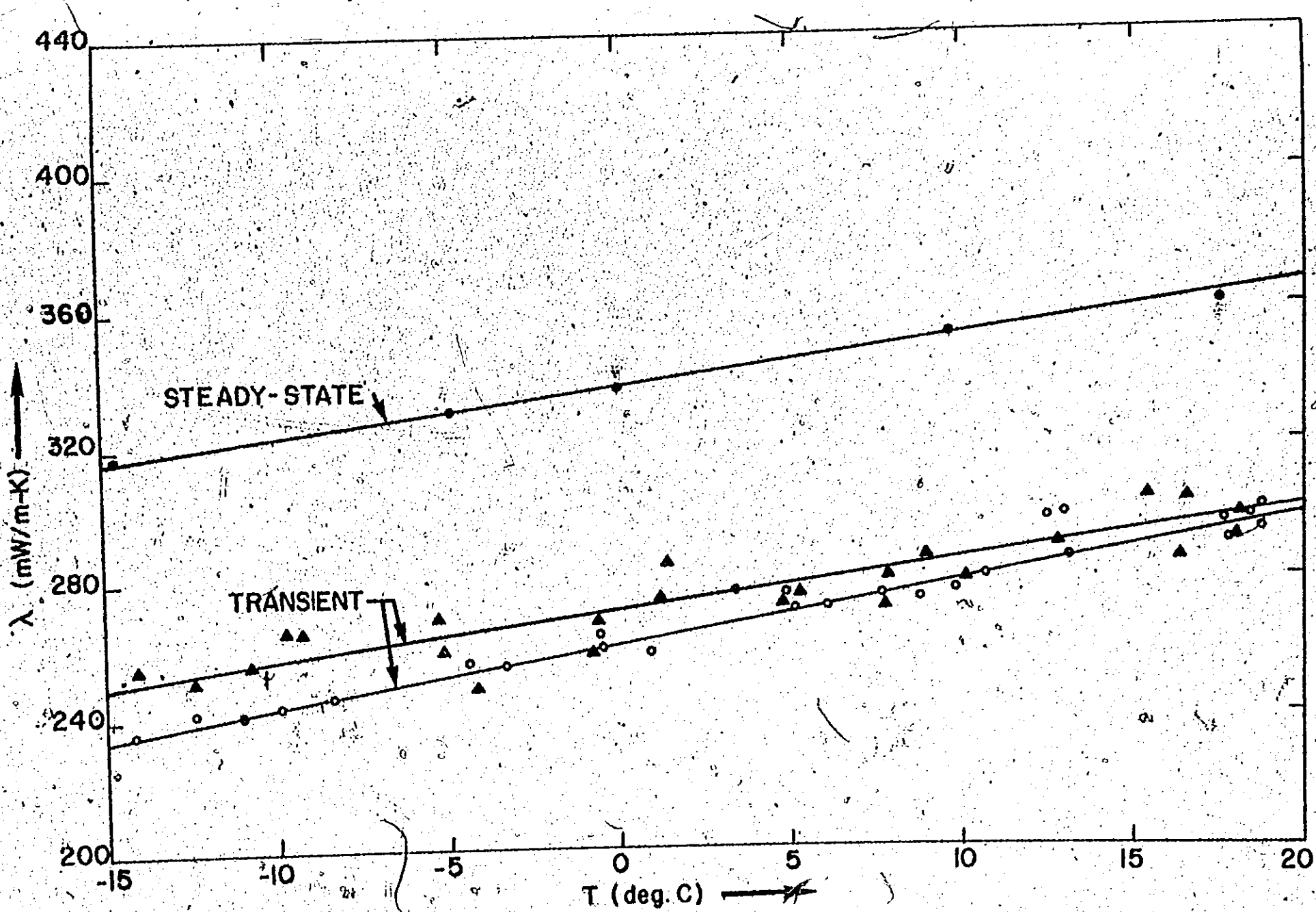

FIG. 1 COMPARISON OF TRANSIENT & STEADY-STATE RESULTS

Appendix G

A REVIEW OF THEORIES REGARDING FLOW OF MOISTURE IN RESPONSE TO TEMPERATURE GRADIENT

The heat flow through dry granular materials involves a rather complex combination of conduction, convection, and radiation with different degree of importance to be attached to each of these modes according to circumstances. Several hypotheses have been suggested to explain the mechanisms of heat flow in dry granular materials, and calculations performed in accordance with these hypotheses agree fairly well with measured values. But as soon as moisture is associated with the dry granular materials, the heat-flow mechanism changes and becomes far more complicated. A thorough understanding of the flow of moisture becomes a prerequisite to any successful heat transfer theory.

Moisture movement in granular materials is a complex phenomenon. Although the movement of moisture due to a temperature gradient through granular materials has been studied by many workers, the mechanism by which moisture moves through such materials remains a point of controversy. An attempt has been made, therefore, in this appendix, to bring together and study various existing hypotheses.

It is observed that moisture moves in granular material ordinarily because of body-forces, such as gravity, capillary forces, and vapor transfer. Some of these body forces are altered by thermal influences. Capillary forces and vapor movements are sensitive to thermal influences, whereas gravity is not. Moisture migration under the influence of temperature gradient in granular material was first observed by Bouyoucos (1915, 1915a), who in his pioneer paper in 1915 described experimental work in which he indicated that soil-moisture moved from a warm and moist soil to a cold and dry soil. This observation was later confirmed in greater detail by Smith (1939, 1943), MacLean and Gwatkin (1946), Croney and Coleman (1947), and many others. It was found in all cases, that in the liquid phase, the flow is being caused by change of water affinity of soil with temperature. Bouyoucos concluded from his experiments that the vapor-transfer in soils was negligible and capillary movement was solely responsible for the process of liquid-transfer. Lewis (1937) and Winterkorn (1947) supported the hypothesis of Bouyoucos and his experimental findings.

The second theory postulates, that the moisture moves from warm to cold regions in the vapor phase and the driving potential is the vapor-pressure difference which corresponds to the temperature difference. Smith (1939) criticized Bouyoucos' findings on the basis that only a small portion of the soil column was affected by the temperature gradient in the latter's experiments and this would account for the small water movement observed. Based on the arguments that the temperature does not

affect the surface tension of water to the extent which would cause the observed water transfer, Smith suggested that transfer took place by means of vapor convection. This mechanism was also proposed by Maclean and Gwatkin, and by Hutchison, Nixon, and Denbigh (1948). But the concept of moisture transfer in vapor phase was disregarded by many workers on the grounds that the experimentally observed rate of movement is about ten times as large as the calculated rate based on vapor diffusion (e.g. Bouyoucos, 1915; Winterkorn, 1947).

Smith abandoned his theory of vapor movement in his later paper in 1943, and instead, proposed a mechanism of liquid flow, from the hotter to the colder part of the material, initiated by small amounts of vapor condensation in capillary pores. In his modified theory, Smith proposed that there exists another flow-mechanism in the material before equilibrium has been established. On the application of the temperature difference across the material, the equilibrium of the capillary bodies close to the warmer side is disturbed. The capillary bodies evaporate and the excess vapor condenses on the adjacent capillary bodies towards the colder side. Two such bodies are shown in Fig. 1 at locations A and B. These bodies will be brought into contact by vapor-condensation, and consequently they will coalesce. This disturbs the equilibrium of the resulting body forcing it to move by ordinary capillary towards the next body. What is left behind is a ring of liquid around the contact-point. Thus, vapor-condensation serves here as a trigger to start the process. The process would continue until all the liquid, except that left around

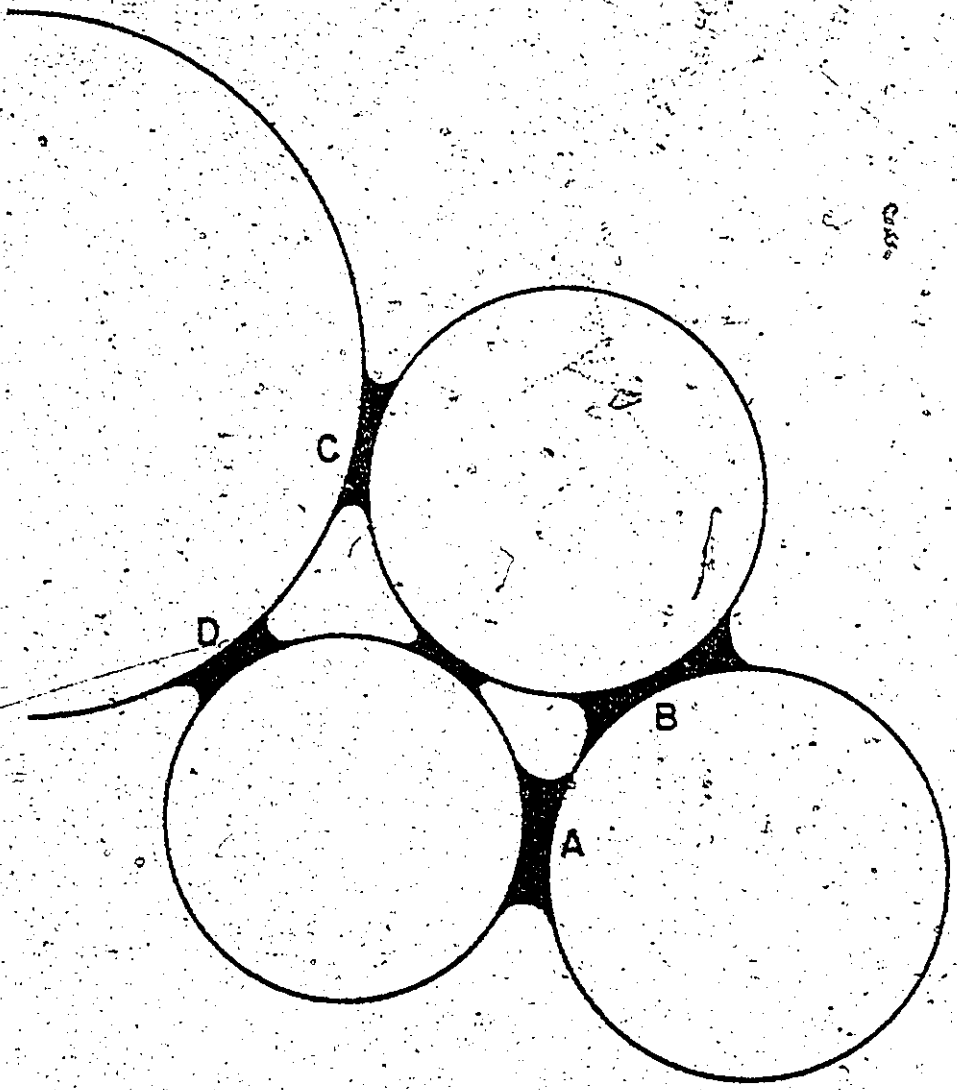

FIG. I CAPILLARY BODIES

the contact points, has moved to the cooler side of the material. According to Smith, if the two bodies are too far apart, as are C and D in Fig. 1, the above mentioned process will not start, and instead, the capillary bodies around the contact points will merely grow in size and then evaporate when the advancing heat-front reaches them. This latter process will result in only a slight adjustment of the water-distribution that is necessary for equilibrium under the temperature gradient. Any large water-distribution will only occur under the former process.

Yet another hypothesis was proposed by Krischer and Rohnalter (1940), who have shown that the vapor moves from the warmer to the colder side in an enclosed porous material, while the liquid flow occurs from the wetter to the drier side, which is usually from the colder to the warmer. Gurr, Marshall, and Hutton (1952), independently confirmed this theory by a different technique. According to this approach to the water-flow mechanism, the liquid flow is in the direction of cold to warm, contrary to the earlier hypothesis. The moisture transfer will take place, initially in the vapor phase, from the warmer to the colder end, on the application of the temperature gradient across the material. The condensation of water vapor on the colder side increases the water pressure and consequently the liquid flows in the direction opposite to that of the vapor flow. The conducting films govern the path and the extent of the liquid flow in that direction. Thus, a circulating system comes into existence in which vapor moves in the direction of decreasing temperature and liquid moves in the opposite direction. The flow in each direction becomes equal within the

closed system under equilibrium conditions, and is governed by the temperature and pressure gradients and the permeability for the liquid and vapor phases, respectively. The above hypothesis does not hold good for either very wet or only slightly wet granular materials.

Taylor and Cavazza (1954) agreed with this hypothesis and with the help of their experimental investigation confirmed that considerable amount of moisture moves in the material by both the processes of air convection and vapor diffusion accompanied by a return flow of liquid. Evaporation in warmer regions and condensation in colder ones play an important part in the flow-mechanism. Liquid flow is affected by the temperature gradient only in an indirect manner.

The phenomenon of moisture transfer under a temperature gradient in an unsaturated porous medium, when the cold region is below freezing, was investigated by Hoekstra (1966). Dirksen (1964), as quoted by Hoekstra, had already shown the existence of moisture movement in frozen soils. Dirksen indicated that the presence of ice in porous materials changes the process of moisture movement. The water in the unfrozen films was also shown by Hoekstra and Chamberlain (1964) to be quite mobile. In 1966, Hoekstra attempted to show that the presence of an ice phase in granular materials under temperature gradient greatly enhances the amount of moisture transfer. The moisture transfer by the flow of liquid through the films of unfrozen water was also found to be accompanied by the flow of vapor, but not to a significant degree. Thus, the major part, in the

transfer of moisture in frozen materials, is played by the process of liquid flow. The unfrozen-water-film-thickness decreases with decreasing temperature, and hence, the rate of liquid flow also decreases rapidly with decreasing temperature below 0 deg. C.

Further attempts to bring the theories closer to the observed amounts of moisture transferred are continuously being made. Philip and De Vries (1957) suggested that the ratio of the temperature gradient in air voids to the over-all temperature gradient in the system is of the order of two to three. This increased temperature gradient in air voids was thought to be responsible for the observed increase of vapor transfer.

Woodside and Kuzmak (1958), noting that there was a big discrepancy between the observed and the calculated moisture flow rates through porous materials under temperature gradient, the observed rates being many times the calculated rates based on vapor diffusion equations, applied a temperature gradient across a large scale model of high-quartz wet sand and measured the temperature distribution within the pore spaces. They found that the ratio of the temperature gradient in the pore spaces to the over-all applied gradient was as large as six. They suggested that approximately the same ratio exists between the respective vapor pressure gradients. According to the hypothesis proposed by Woodside and Kuzmak, the flow mechanism consists of multiple vapor-diffusion and liquid-flow steps. The liquid-flow rate is governed by the pressure gradients and it encounters very little resistance in its flow-path.

The fact that the temperature and consequently the pressure gradients are of the order of six times the over-all gradients previously used to calculate the flow rate, according to these investigators, at least, partially explained the discrepancy.

Appendix H

A REVIEW OF THEORIES REGARDING TRANSFER OF HEAT BY MOISTURE IN RESPONSE TO TEMPERATURE GRADIENT

At the time when it was first established that moisture migrates to the colder region in response to temperature gradient, very few workers accepted the suggestion that the increase in the heat transmission process in moist materials might be partly, at least, due to the heat carried by the migrating vapor. Later on, as investigators were trying to postulate the mechanism of moisture-migration in porous materials under temperature gradient, and were suggesting different hypothesis, the fact that the moisture-migration contributes to the heat-transmission process in porous materials, gradually became accepted. It was concluded from the experiments that the heat-transmission process was not only influenced by the amount of moisture present, but also by the rate of moisture-movement.

Moisture increases the thermal conductivity of the porous materials mainly in two ways. Firstly, the sensible heat which is transferred by conduction and which finds water paths more conductive than air (Joy, 1957), and secondly, the latent heat carried through the porous material by water vapor movement under the influence of differences in

vapor pressure. According to Joy, these two processes are essentially independent of each other, but an interchange from one mechanism to the other is possible along the path. The operating temperature, the temperature gradient, and the vapor permeability of the material govern the latent heat mechanism, whereas, the arrangement of the solid or the liquid forms of the moisture present in the material govern the sensible heat component of the over-all heat transfer process.

Cammerer (1964), in his survey of the international literature up to 1957 on the influence of humidity on the heat transfer process in porous materials, has credited Krischer and his co-worker (Krischer, 1934; Krischer and Rohnalter, 1937; Krischer and Rohnalter, 1940; Krischer, 1941) with clarifying the physical reasons for the increase in the heat conductivity of porous materials with increasing moisture content. Krischer has shown that among the various kinds of heat transfer processes occurring in a particular air-filled pore in a moist material, the process of vapor diffusion plays the most important part. Some of the other heat transfer processes taking place in air-filled pores of moist materials, as suggested by Krischer, are: (1) molecular heat conduction by the air, (2) air convection in the pores, (3) radiation between pore walls, (4) replacement of some of the pore air by water (a better conductor), and (5) formation of bridges on the surface of contact between the solid components by the water.

Considering the molecular heat conduction and the heat transfer due to vapor diffusion, Krischer (1941) calculated the equivalent coefficient of thermal conductivity of the pore air. The latent heat of evaporation of water is transferred by the diffusion of the water vapor in the air in the pore space. This movement of moisture is defined by Stefan's diffusion law

$$W_v = -\frac{\mu_{air}}{R_v T} \frac{p}{p-p_v} \frac{dp_v}{dx} , \qquad (1)$$

where W_v is the rate of water vapor diffusing per unit of cross-sectional area of the pore, $[kg_m/m^2h]$,

μ_{air} is the diffusion coefficient of water vapor in air, $[m^2/h]$,

p is the air pressure, $[kg/m^2]$,

p_v is the partial pressure of water vapor, $[kg/m^2]$,

R_v is the gas constant for water vapor, $[m\ kg/kg_m\text{-}k]$,

T is the absolute temperature, $[K]$,

and x is the length coordinate, $[m]$.

An assumption was made at this stage that the vapor pressure is equal to the normal saturation vapor pressure. In reality, this condition is generally fulfilled to a good approximation if the moisture content is not very low. If the walls of the pores are assumed to be wet so that saturation pressure exists, then the saturation pressure can be expressed as function of the temperature, and the expression for W_v could be rewritten as

$$W_v = -\frac{\mu_{air}}{R_v T} \frac{p}{p-p_v} \frac{dp_v}{dT} \frac{dT}{dx} . \qquad (2)$$

Krischer experimentally studied the diffusion between the wetted walls of a greatly enlarged model of a pore, under the influence of temperature gradients. From his experiments, the following value of the diffusion coefficient resulted,

$$\mu_{air} = \frac{239}{p} \left(\frac{T}{273}\right)^{2.3} \quad cm^2/sec, \tag{3}$$

where p is in g/cm^2,

or

$$\mu_{air} = 0.086 \left(\frac{T}{273}\right)^{2.3} \frac{10000}{p} \quad m^2/h, \tag{4}$$

where p is in kg/m^2.

Denoting the amount of heat transferred by diffusion of the water vapor in air by Q_v, and the latent heat of evaporation of water by L, the expression for heat flux is written as

$$Q_v = -\frac{\mu_{air}}{R_v T} \frac{p}{p - p_v} L \frac{dp_v}{dT} \frac{dT}{dx}, \tag{5}$$

or

$$Q_v = -\lambda_v \frac{dT}{dx}, \tag{6}$$

where

$$\lambda_v = \frac{\mu_{air}}{R_v T} \frac{p}{p - p_v} L \frac{dp_v}{dT}. \tag{7}$$

Thus, λ_v represents the equivalent heat conductivity of a moist pore due to the transfer of latent heat. The overall conductivity λ_1 of the moist pore air may therefore be expressed as the sum of the diffusion component, λ_v, and the thermal conductivity of the air, λ_a. Krischer

plotted on a λ-T scale, the rapid increase in λ_1 due to water vapor diffusion in air with rise in temperature as is shown in Fig. 1. The corresponding values for water and air were also included by Krischer in his plot. The thermal conductivities of air and water increase with temperature but not as much as the diffusion component. At 0 deg. C the diffusion component is more or less equal to the conductivity of air. At 59.3 deg. C, λ_1 equals λ_w, that is, the rate of heat transfer through wetted pores is as great as if these spaces were completely filled with water. This particular temperature point, according to Cammerer (op. cit.), is found to vary somewhat in the international literature, depending on the coefficient of diffusion of the water vapor. However, for all practical purposes, it could be said that at approximately 60 deg. C, the coefficient of thermal conductivity of a moist porous material is independent of the magnitude of the water content and equal to that for complete pore saturation. Above this temperature heat is transferred at a higher rate in the pores of a moist material filled with air than if completely filled with water.

The increase in the water content above 60 deg. C will cause the conductivity to fall by diminishing the volume fraction of air space, whereas the increase in the water content below 60 deg. C will cause the conductivity to rise toward a value at 60 deg. C. Figure 2 shows the variation in the coefficient of thermal conductivity with the moisture content below, at, and above 60 deg. C. The figure shows that at low moisture contents the conductivity changes more rapidly with temperature

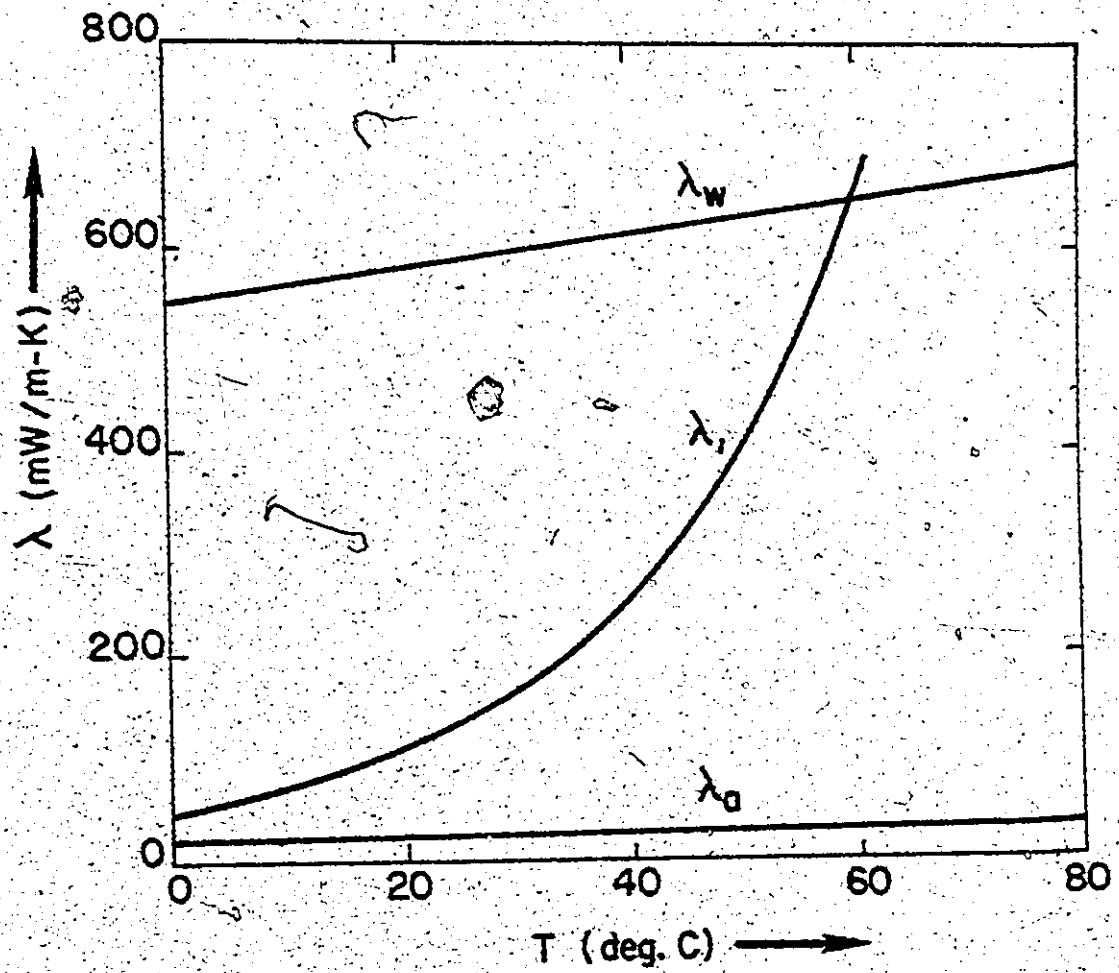

FIG. 1 CONDUCTIVITY OF MOIST PORE AIR

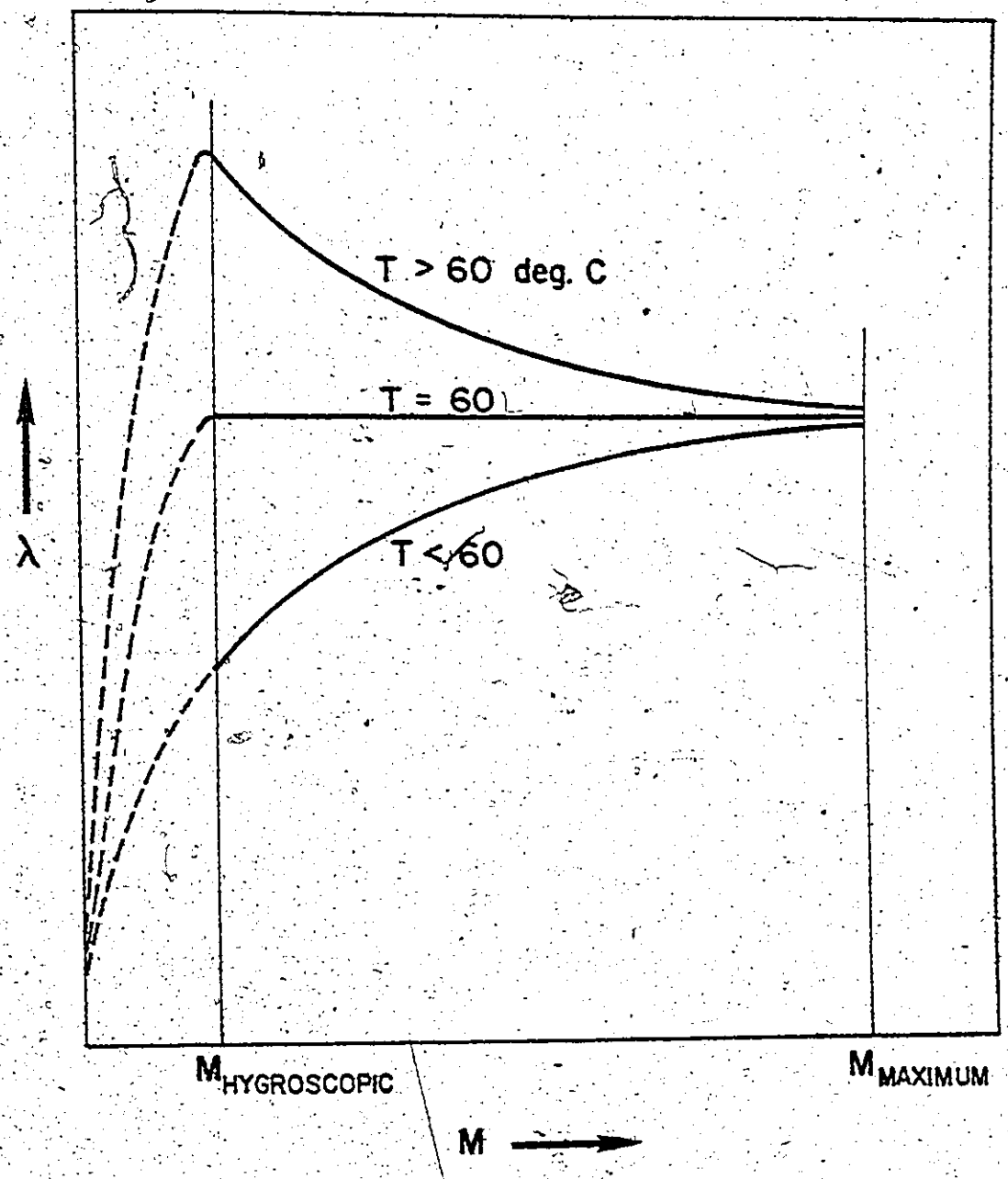

FIG. 2 DEPENDENCE OF CONDUCTIVITY ON TEMPERATURE & MOISTURE CONTENT

than at high moisture content. At very low moisture contents every pore wall is no longer coated with a film of water, and the diffusion component of the heat transfer does not retain its full value. Hence, for fully dry state, the curves in Fig. 2 must descend from the limiting moisture content to the dry state as shown by the dotted lines. The limiting moisture content, according to Krischer, is equal to the hygroscopic moisture content, and it is affected by the nature of the capillaries in the material.

De Vries (1952a) also seemed to have arrived at similar conclusions regarding the effect of the moisture content on the coefficient of thermal conductivity. This was illustrated by him by the experimental values for sand at different temperatures, as reported here in Fig. 3. According to De Vries, Krischer's theory is not valid at low moisture contents, because of the decrease of vapor pressure with decreasing moisture content.

In the last few pages, so far, the phenomenon of heat transfer due to diffusion of water vapor in pore spaces only has been discussed. There is yet another angle through which the phenomenon of heat transfer due to water vapor diffusion could be studied, and that is, to consider the behavior of the material as a whole rather than that of only a particular pore in the material. The following few pages deal precisely with this aspect.

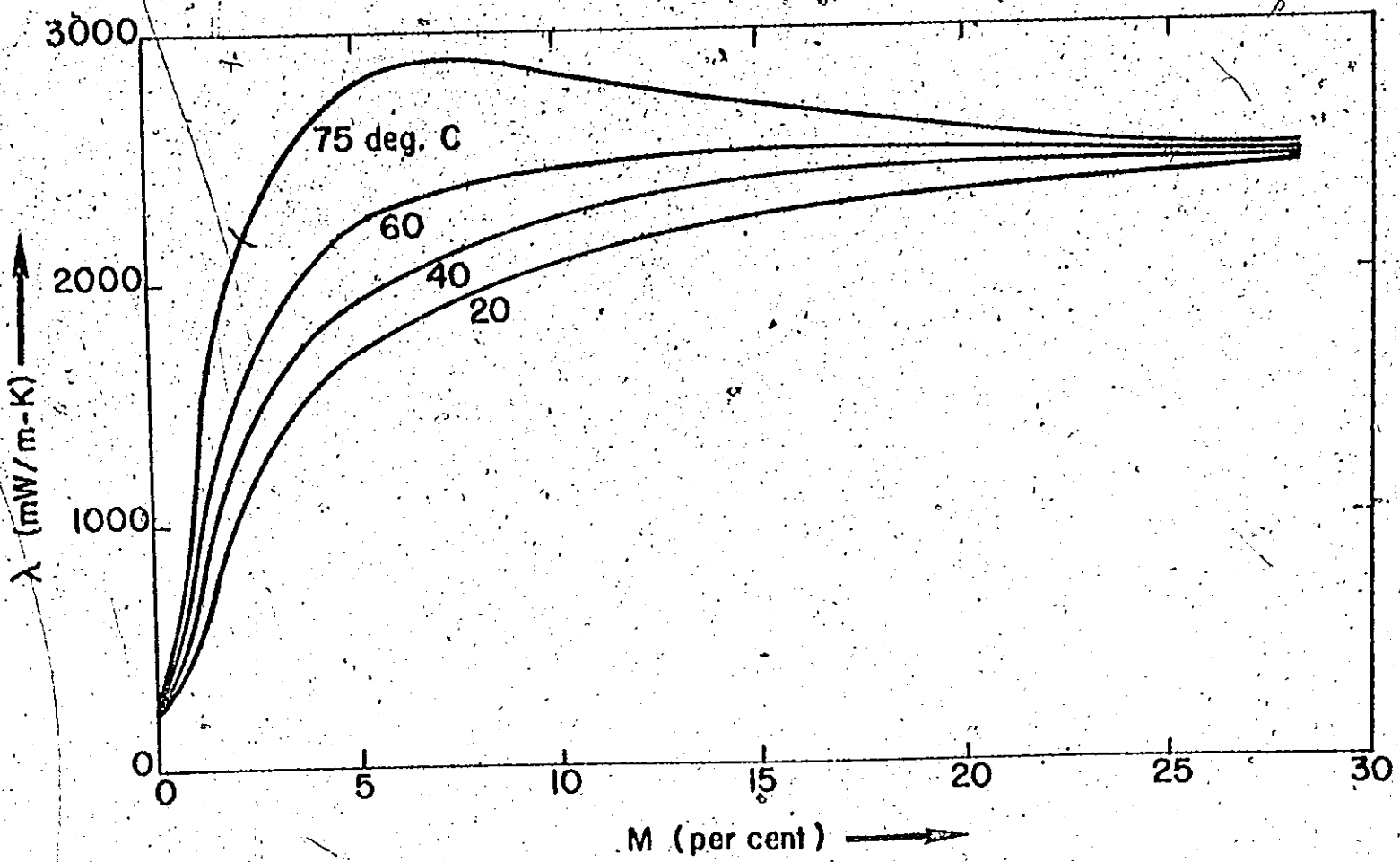

FIG. 3 VARIATION OF CONDUCTIVITY ON TEMPERATURE & MOISTURE

The transfer of moisture is a diffusion process and as such, according to some workers (e.g. Babbitt, 1939; Woodside and Cliffe, 1959; Sereda and Hutcheon, 1965) obeys the simple form of Fick's law, which is similar to Fourier's equation for the transfer of heat. Therefore, having found that Fick's law does satisfactorily explain the vapor diffusion process in granular materials, all the mathematical analysis developed for thermal applications becomes available for this study as well.

The equation used to describe the process of water vapor diffusion through materials, based on a simple form of Fick's Law, is

$$W_v = - \mu \frac{dp}{dx}, \qquad (8)$$

where W_v is the flow rate per unit area in unit time,

p is the vapor pressure,

x is the distance along the flow path,

dp/dx is the vapor pressure gradient,

and μ is the vapor permeability (diffusion coefficient) of the material.

This μ here is different from that appearing in Eq.(2). The water-vapor permeability of the material, μ, appearing here in Eq.(8) may be defined as the flow rate of vapor per unit area of the material when the material is subjected to a unit pressure gradient.

Assuming that the saturation vapor pressure conditions exist in the material, the vapor pressure gradient may be written as

$$\frac{dp}{dx} = \frac{dp}{dT} \frac{dT}{dx}, \qquad (9)$$

where dT/dx is the temperature gradient. Each unit of mass of diffusing vapor absorbs the latent heat L at the warmer end of the material where it evaporates and releases the same at the colder end where it condenses. This process acts in parallel to the heat transfer mechanism. If the amount of heat transferred by diffusion process is denoted by Q_v, then

$$Q_v = -\mu L \frac{dp}{dx}, \tag{10}$$

$$Q_v = -\mu L \frac{dp}{dT}\frac{dT}{dx}, \tag{11}$$

or

$$Q_v = -\lambda_v \frac{dT}{dx} \tag{12}$$

where $$\lambda_v = \mu L \frac{dp}{dT}. \tag{13}$$

The coefficient of diffusion, μ, can either be found experimentally for a moist material in question, or it could be calculated using the empirical relationships available in the literature. Penman's (1940) empirical relationship between vapor permeability and porosity P for dry or moist soils is

$$\mu = 0.66P\,\mu_{air}, \tag{14}$$

where μ_{air} is the diffusion coefficient for water vapor through air (same as that appearing in Eq.(2)), and P is the air-filled porosity, that is, the total porosity less the volumetric water content. Woodside (1959) has discussed the use of certain equations for the estimation of the water vapor permeability of porous media. The cup or dish method is generally used for the experimental determination of the average value of

the permeability.

In reality, the phenomenon of water vapor transfer in porous media is much more complicated than a simple diffusion process. Hence, the use of simple diffusion equations for the estimation of the heat transfer due to vapor movement in porous media could, in most of the cases, be considered to be a somewhat questionable procedure. But in order to obtain a working basis for the analysis of this problem, it becomes essential to treat the vapor-transfer as a simple diffusion phenomenon and to make use of the various equations that have been found to hold for such phenomena. For all practical purposes, the errors introduced in the estimation due to this assumption, according to Babbitt (1939), may be much smaller than those introduced by other unavoidable factors, such as variations in materials, packing arrangement, etc.

Philip and De Vries (1957) attempted to explain in detail the experimental data on vapor diffusion in terms of the mechanisms of vapor diffusion and liquid movement by capillary. Later, De Vries (1958) presented a generalized equation of simultaneous transfer of heat and moisture in porous media. He considered heat transfer by moisture movement in greater detail, and took into account the heat of wetting and transfer of sensible heat. De Vries' theory was based on the assumption that heat sources and sinks arising from evaporation - condensation and wetting-drying are distributed uniformly in the material, and thus the process of heat transfer takes place uniformly throughout the porous material.

However, in reality, De Vries admitted, that vapor transfer and liquid movement take place only in air-filled pore spaces and in the water-filled pore spaces, respectively, while evaporation and condensation take place at the water-air interfaces. A complete analytical treatment of these processes would have led him to a microscopic study of heat and moisture transfer in porous media. He found such an analysis extremely difficult and left it unattempted.

Analytical as well as experimental work on the heat and mass transfer in capillary-porous bodies has also been presented by Luikov (1964) in an attempt to enhance the understanding of the heat transfer processes in porous media under temperature gradient.

REFERENCES

American Society for Testing and Materials, "Standard Method of Test for Thermal Conductivity of Materials by Means of the Guarded Hot Plate", ASTM: C177-63, 1916 Race Street,Philadelphia 3, Pa., 1963. (I,II,A)*

Babbitt, J.D., "The Diffusion of Water Vapor Through Various Building Materials", *Canadian Journal of Research*, Vol. 17, pp. 15-32, February, 1939. (H)

Bouyoucos, G.J., "Effect of Temperature on Movement of Water Vapor and Capillary Moisture in Soils", *Journal of Agricultural Research*, Department of Agriculture, Washington, D.C., Vol. 5, No.4, pp. 141-172, October, 1915. (I,G)

Bouyoucos, G.J., "Effect of Temperature on Some of the Most Important Physical Processes in Soils", *Michigan Agricultural College Experimental Station, Technical Bulletin*, No.22, pp. 1-63, July, 1915a. (G)

* These refer to the chapters and appendices in which the particular reference is quoted.

Brailsford, A.D., and Major, K.G., *British Journal of Applied Physics*, Vol. 15, p. 313, 1964. (as quoted by Pratt, 1969). (I)

Burgers, H.C., *Physik. Z.*, Vol. 20, pp. 73-76. 1919. (as quoted by Laubitz, 1959). (I)

Cammerer, J.S., "The Influence of Humidity on the Thermal Conductivity Coefficients of Building Materials According to the International Literature", *NRC Technical Translation*, No. 1160, pp. 1-65, December, 1964. (H)

Carman, P.C., "Capillary Rise and Capillary Movement of Moisture in Fine Sands", *Soil Science*, Vol. 52, pp. 1-14, 1941. (IV)

Carslaw, H.S. and Jaeger, J.C., *Conduction of Heat in Solids*, 2nd Edition, Oxford University Press, London, 1959. (II,B)

Cheng, S.C. and Vachon, R.I., "Thermal Conductivity of Packed Beds and Powder Beds", *International Journal of Heat and Mass Transfer*, Vol. 12, pp. 1201-1206, 1969a. (I)

Cheng, S.C. and Vachon, R.I., "The Prediction of the Thermal Conductivity of Two and Three Phase Solid Heterogeneous Mixtures", *International Journal of Heat and Mass Transfer*, Vol. 12, pp. 249-264, 1969b. (I)

Childs, E.C., An Introduction to the Physical Basis of Soil Water Phenomena, John Wiley & Sons Ltd., 1969. (IV)

Croney, D. and Coleman, J.D., "Moisture Movements in Road Subgrades Associated with Fluctuations of the Pavement Temperature", *Road Research Laboratory, DSIR, England*, Note RN/842, 1947. (as quoted by Gurr et al., 1952). (G)

Cullity, B.D., *Elements of X-Ray Diffraction*, 3rd Edition, Addison-Wesley, Chapter 6, 1967. (IV)

Dauphinee, T.M., "An Isolating Potential Comparator", *Canadian Journal of Physics*, Vol. 31, pp. 577-591, May, 1953. (III)

Dauphinee, T.M. and Mooser, E., "Apparatus for Measuring Resistivity and Hall Coefficient of Semiconductors", *The Review of Scientific Instruments*, Vol. 26, No.7, pp. 660-664, July, 1955. (III)

Dauphinee, T.M. and Preston-Thomas, H., "A Copper Resistance Temperature Scale", *The Review of Scientific Instruments*, Vol. 25, No.9, pp. 884-886, September, 1954. (II)

Dauphinee, T.M. and Preston-Thomas, H., "A D.C. and Square Wave A.C. Resistance and Voltage Comparator", *Journal of Scientific Instruments*, Vol. 35, pp. 21-23, January, 1958. (III)

De Vries, D.A., "The Thermal Conductivity of Granular Materials", (Laboratorium voor Natuur - en Weerkunde, Wageningen), *Bulletin of The International Institute of Refrigeration*, XXXII, No.4, pp. 115-130, 1952a. (I,H)

De Vries, D.A., "The Thermal Conductivity of Soil", *Mededelingen van de Landbouwhogeschool te Wageningen/Nederland*, Vol. 52, No.1, pp. 1-73, 1952b. (I,VI,E)

De Vries, D.A., "Thermal Conductivity of Soil", *Nature*, Vol. 178, p. 1074, November, 1956. (E)

De Vries, D.A., "Simultaneous Transfer of Heat and Moisture in Porous Media", *Transactions, American Geophysical Union*, Vol. 39, No.5, pp. 909-916, October, 1958. (H)

De Vries, D.A., "Thermal Properties of Soils", *Physics of Plant Environment*, Editor — W.R. Van Wijk, North-Holland Publishing Company, Amsterdam, 1963. (E)

De Vries, D.A. and Peck, A.J., "On the Cylindrical Probe Method of Measuring Thermal Conductivity with Special Reference to Soils, Part I: Extension of Theory and Discussion of Probe Characteristics", *Australian Journal of Physics*, Vol. II, pp. 255-270, 1958. (E)

Deresiewicz, H., "Mechanics of Granualr Matter", *Advances in Applied Mechanics*, Volume V, Editors — H.L. Dryden and Th. Von Kármán, Academic Press Inc., Publishers, New York, N.Y., 1958. (E)

Dirksen, C., "Water Movement and Frost Heaving in Unsaturated Soil Without an External Source of Water", *Ph.D. Thesis, Cornell University*, 1964. (as quoted by Hoekstra, 1966). (G)

Feingold, A., "A Criticism of the Use of Electrical Analogy in Evaluating the Rate of Heat Transfer by Conduction in Composite Walls", *Bulletin, Mechanical Engineering Education*, Vol. 5, pp. 225-227, 1966. (E)

Fletcher, N.H., *The Chemical Physics of Ice*, Cambridge at the University Press, 1970. (E)

Gemant, A., "The Thermal Conductivity of Soils", *Journal of Applied Physics*, Vol. 21, pp. 750-752, August, 1950. (I)

Gupta, K.G., Laubitz, M.J., and Feingold, A., "A Technique for Simultaneous Measurement of Thermal Conductivity and Moisture Content of Granular Materials", *XII International Conference on Thermal Conductivity*, Birmingham, Alabama, September, 1972. (I)

Gurr, C.G., Marshall, T.J., and Hutton, J.T., "Movement of Water in Soil due to a Temperature Gradient", *Soil Science*, Vol. 74, No.5, pp. 335-345, November, 1952. (G)

Hadwiger, H., "Einlagerung kongruenter Kugeln in eine Kugel", *Elemente der Mathematik*, Vol. VII, No.5, pp. 97-103, September, 1952. (E)

Haupin, W.E., "Hot Wire Method for Rapid Determination of Thermal Conductivity", *Ceramic Bulletin*, Vol. 39, No.3, pp. 139-141, 1960. (F)

Hokestra, P. and Chamberlain, E., "Electro-Osmosis in Frozen Soil", *Nature*, Vol. 203, pp. 1406-1407, September, 1964. (G)

Hokestra, P., "Moisture Movement in Soils Under Temperature Gradients with the Cold-Side Temperature Below Freezing", *Water Resources Research*, Vol. 2, No.2, pp. 241-250, 2nd Quarter, 1966. (G)

Hutchison, H.P., Nixon, I.S., and Denbigh, K.G., "The Thermo-Osmosis of Liquids Through Porous Materials", *Discussions of the Faraday Society*, No. 3, pp. 86-94, 1948. (G)

Jahnke, E., *Tables of Higher Functions*, 6th Edition, Revised by Friedrich Lösch, McGraw-Hill, N.Y., 1960. (B)

Jakob, M., *Heat Transfer*, Volume 1, John Wiley & Sons, Inc., N.Y., 1957. (IV)

Joy, F.A., "Thermal Conductivity of Insulation Containing Moisture", *Symposium on Thermal Conductivity Measurements*, ASTM STP 217, ASTM Standards, pp. 65-80, 1957. (I,H)

Kersten, M.S., "Thermal Properties of Soils", *Bulletin of the University of Minnesota*, Institute of Technology, Engineering Experiment Station, Bulletin No.28, June, 1949. (IV)

Kline, S.J. and McClintock, F.A., "Describing Uncertainties in Single-Sample Experiments", *Mechanical Engineering*, pp. 3-8, January, 1953. (D)

Krischer, O., "Der Einflub von Feuchtigkeit, Körnung und Temperatur auf die Wärmeleitfähigkeit körniger Stoffe", *Beihefte zum Gesundheits-Ingenieur*, Reiche I, Nr.33, München und Berlin, 1934. (H)

Krischer, O., "Wärmeleitung und Dampfdiffusion in Kälteschutzstoffen", *Wärme-und Kältetechnik*, Bd.43, pp.1-6, January, 1941. (H,E)

Krischer, O. and Esdorn, H., "Die Wärmeübertragung in feuchten, porigem Stoffen verschiedener Struktur", *Forschung, auf dem Gebiete des Ingenieurwesens*, Bd.22, Nr.1, pp. 1-8, 1956. (I)

Krischer, O. and Rohnalter, H., "Die Wärmeübertragung durch Diffusion des Wasserdampfes in den Poren von Baustoffen unter Einwirkung eines Temperaturgefälles", *Gesundheits-Ingenieur*, Bd.60, pp. 621-627, October, 1937. (H)

Krischer, O. and Rohnalter, H., "Wärmeleitung und Dampfdiffusion in feuchten Gütern", *V.D.I.-Forschungsheft 402*, pp. 1-18, 1940. (G,H)

Lambe, T.W. and Whitman, R.V., *Soil Mechanics*, John Wiley & Sons, Inc., 1969. (IV)

Lane, K.S. and Washburn, D.E., "Capillarity Tests by Capillarimeter and by Soil Filled Tubes", *Proceedings, Highway Research Board*, 1946. (IV)

Laubitz, M.J., "Thermal Conductivity of Powders", *Canadian Journal of Physics*, Vol. 37, pp. 798-808, 1959. (I)

Laubitz, M.J. and McElory, D.L., "Precise Measurement of Thermal Conductivity at High Temperatures (100-1200 K)", *International Journal of Scientific Metrology*, Vol. 7, No.1, pp. 1-15, January, 1971. (II)

Lewis, M.R., "Rate of Flow of Capillary Moisture", *United States Department of Agriculture*, Technical Bulletin No. 579, pp. 1-29, October, 1937. (G)

Lovell, C.W. Jr., "Temperature Effects on Phase Composition and Strength of Partially-Frozen Soil", *Highway Research Board*, Bulletin No.168, pp. 74-95, 1957. (IV)

Luikov, A.V., "Heat and Mass Transfer in Capillary-Porous Bodies", *Advances in Heat Transfer*, Volume 1, Editors -- T.F. Irvine and J.P. Hartnett, Academic Press, New York, 1964. (H)

Maclean, D.J. and Gwatkin, R.M., "Moisture Movements Occurring in Soil Due to the Existence of a Temperature Gradient", *Road Research Laboratory, Department of Scientific and Industrial Research, England*, Note RN/761, May 1946. (G)

Mann, G. and Forsyth, F.G.E., "Measurement of Thermal Conductivity of Samples of Thermal Insulating Materials and of Insulation in situ by the Heated Probe Method", *Modern Refrigeration*, pp. 188-191, June, 1956. (F)

Maxwell, J.C., *Treatise on Electricity and Magnetism*, Volume I, 3rd Edition, Clarendon Press, Oxford, England, 1904. (I,VI)

Monech, A.F., "An Evaluation of Heat Transfer Coefficients in Moist Porous Media", *Ph.D. Thesis, University of Arizona*, 1969. (VI)

Monech, A.F. and Evans, D.D., "Thermal Conductivity and Diffusivity of Soil Using a Cylindrical Heat Source", *Soil Science Society of America Proceedings*, Vol. 34, pp. 377-381, 1970. (F)

Orr, H.W., "A Study of the Effects of Edge Insulation and Ambient Temperatures on Errors in Guarded Hot-Plate Measurements", *Proceedings of the Seventh Conference on Thermal Conductivity*, Washington, D.C., NBS Special Publication No. 302, pp. 521-526, 1967. (A)

Penman, H.L., "Gas and Vapor Movements in the Soil", *The Journal of Agricultural Science*, Vol. 30, pp. 438-462 and 570-581, 1940. (H)

Penner, E., "Frost-Heaving in Soils", *International Conference on Permafrost, Proceedings*, pp. 197-202, November, 1963. (IV)

Philip, J.R. and De Vries, D.A., "Moisture Movement in Porous Materials Under Temperature Gradients", *Transactions, American Geophysical Union*, Vol. 38, pp. 222-232, April, 1957. (I,G,H)

Pounder, E.R., *The Physics of Ice*, Pergamon Press, 1965. (E)

Pratt, A.W., "Heat Transmission in Low Conductivity Materials", *Thermal Conductivity*, Volume 1, Editor — R.P. Tye, Academic Press, 1969. (I,E)

Rayleigh, L., "On the Influence of Obstacles Arranged in Rectangular Order Upon the Properties of a Medium", *Philosophical Magazine and Journal of Science*, Vol. 34, Series 5th, pp. 481-502, 1892. (I;VI)

Richards, L.A. and Fireman, M., "Pressure-Plate Apparatus for Measuring Moisture Sorption and Transmission by Soils", *Soil Science*, Vol. 56, pp. 395-404, 1943. (IV)

Russell, H.W., "Principles of Heat Flow in Porous Insulators", *American Ceramic Society, Journal*, Vol. 18, No.1, pp. 1-5, 1935. (I)

Sereda, P.J. and Hutcheon, N.B., "Moisture Equilibrium and Migration in Building Materials", *ASTM Special Technical Publication*, No. 385, pp. 3-18, 1965. (H)

Smith, W.O., "Thermal Conductivities in Moist Soils", *Soil Science Society of America, Proceedings*, Vol. 4, pp. 32-40, 1939. (G)

Smith, W.O., "Thermal Transfer of Moisture in Soils", *American Geophysical Union, Transactions*, Vol. 2, pp. 511-524, 1943. (G)

Supnik, F., "On the Dense Packing of Spheres", *Transactions American Mathematical Society*, Vol. 65, pp. 14-26, January, 1949. (E)

Taylor, S.A. and Cavazza, L., "The Movement of Soil Moisture in Response to Temperature Gradients", *Soil Science Society of America, Proceedings*, Vol. 18, No.4, pp. 351-358, October, 1954. (I,G)

Touloukian, Y.S., "Recommended Values of the Thermophysical Properties of Eight Alloys, Major Constituents and Their Oxides", *Thermophysical Properties Research Center, Purdue University*, Lafayette, Indiana, February, 1966. (IV)

Touloukian, Y.S., Powell, R.W., Ho, C.Y., and Klemens, P.G., "Thermal Conductivity (Nonmetallic Solids)", *Thermophysical Properties of Matter*, Volume 2, IFI/Plenum, New York, Washington, 1970. (E)

Touloukian, Y.S., Liley, P.E., and Saxena, S.C., "Thermal Conductivity (Nonmetallic Liquids and Gases)", *Thermophysical Properties of Matter*, Volume 3, IFI/Plenum, New York, Washington, 1970. (E)

Tye, R.P. and Hurley, J.R., "The Measurement of Thermal Conductivity with Particular Reference to Temperature Measurement", Paper Presented at the *Fifth Temperature Measurements Society Conference at Hawthorne Memorial Center*, Hawthorne, California, March, 1967. (III)

Tye, R.P., "The Art of Measuring Thermal Conductivity", *Instrumentation Technology*, Paper 68-523 presented at the 23rd Annual ISA Conference, New York, N.Y., 1968. (II)

Webb, J., "Thermal Conductivity of Soil", *Nature*, Vol. 177, p. 989, May, 1956. (E)

Williams, P.J., "Properties and Behaviour of Freezing Soils", *Norwegian Geotechnical Institute*, Publication No. 72, 1967. (IV)

Williams, P.J., "Unfrozen Water Content of Frozen Soils and Soil Moisture Suction", *Geotechnique*, Vol. 14, No.3, pp. 231-246, 1964. (IV)

Williams, P.J., *Private Communication*, 1973. (VI)

Winterkorn, H.F., "Fundamental Similarities Between Electro-Osmatic and Thermo-Osmatic Phenomena", *Highway Research Board, Proceedings*, Vol. 27, pp. 443-455, 1947. (G)

Woodside, W., "Analysis of Errors due to Edge Heat Loss in Guarded Hot Plates", *ASTM Symposium on Thermal Conductivity Measurements and Applications of Thermal Insulations*, Special Technical Publication No.217, pp. 49-62, 1957a. (A)

Woodside, W., "Deviation from One-Dimensional Heat Flow in Guarded Hot-Plate Measurements", *The Review of Scientific Instruments*, Vol. 28, No.12, pp. 1033-1037, December, 1957b. (A)

Woodside, W., "Probe for Thermal Conductivity Measurement of Dry and Moist Materials", *ASHAE Journal Section; Heating, Piping, and Air Conditioning*, pp. 3-10, September, 1958. (F)

Woodside, W., "Water Vapor Permeability of Porous Media", *Canadian Journal of Physics*, Vol. 39, No.4, pp. 413-416, 1959. (H)

Woodside, W. and Bruyn, C.M.A., "Heat Transfer in a Moist Clay", *Soil Science*, Vol. 87, No.3, pp. 166-173, March, 1959. (F)

Woodside, W. and Cliffe, J.B., "Heat and Moisture Transfer in Closed Systems of Two Granular Materials", *Soil Science*, Vol. 87, pp. 75-82, 1959. (I,IV,VI,H)

Woodside, W. and Kuzmak, J.M., "Effect of Temperature Distribution on Moisture Flow in Porous Materials", *Transactions, American Geophysical Union*, Vol.39, No.4, pp. 676-680, August, 1958. (G)

Woodside, W. and Wilson, A.G., "Unbalance Errors in Guarded Hot Plate Measurements", *ASTM Symposium on Thermal Conductivity Measurements and Applications of Thermal Insulations*, Special Technical Publication No.217, pp. 32-45, 1957. (A)